

Electronic Thesis and Dissertation Repository

7-25-2019 3:00 PM

Hydrodynamics Studies of Air Dense Medium Fluidized Bed with Binary Mixtures for Dry Coal Beneficiation

Zhijie Fu, *The University of Western Ontario*

Supervisor: Zhu, Jesse, *The University of Western Ontario*

Co-Supervisor: Barghi, Shahzad, *The University of Western Ontario*

Co-Supervisor: Zhao, Yuemin, *China University of Mining and Technology*

A thesis submitted in partial fulfillment of the requirements for the Doctor of Philosophy degree in Chemical and Biochemical Engineering

© Zhijie Fu 2019

Follow this and additional works at: <https://ir.lib.uwo.ca/etd>

 Part of the [Other Chemical Engineering Commons](#)

Recommended Citation

Fu, Zhijie, "Hydrodynamics Studies of Air Dense Medium Fluidized Bed with Binary Mixtures for Dry Coal Beneficiation" (2019). *Electronic Thesis and Dissertation Repository*. 6252.
<https://ir.lib.uwo.ca/etd/6252>

This Dissertation/Thesis is brought to you for free and open access by Scholarship@Western. It has been accepted for inclusion in Electronic Thesis and Dissertation Repository by an authorized administrator of Scholarship@Western. For more information, please contact wlsadmin@uwo.ca.

ABSTRACT

A systematic and comprehensive study of fluidization hydrodynamics and separation properties was conducted in a bench-scale and a semi-industrial Air Dense Medium Fluidized Bed (ADMFB) systems for dry coal beneficiation. In order to achieve the fluidized bed density adjustment required for efficient dry gravity separation, various types of binary mixtures of solid particles were tested and used as the medium materials in the ADMFB. Fluidization hydrodynamics including minimum fluidization velocity, fluidized bed expansion, solids mixing/segregation, and bed density distribution were carefully investigated. A series of continuous experiments studying raw coal dry beneficiation were successfully implemented in a semi-industrial ADMFB system with binary mixtures magnetite and fine coal particles.

The minimum fluidization velocity of binary mixtures of solid particles was experimentally studied while accounting for the effects of particle size ratio, particle density ratio, and mixture composition of solid materials. A new correlation has been developed for the accurate prediction of minimum fluidization velocity of binary mixtures used in ADMFB or other similar fluidized bed systems. In addition, an attempt was made to study the effects of bed inventory on the incipient fluidization, and the correlation proposed by Wen and Yu was modified to precisely predict the minimum fluidization velocity as a function of the bed inventory. Combining of these two correlations would significantly improve the accuracy of estimations for various binary systems.

Fluidized bed expansion behavior was carefully investigated in terms of the two-phase theory which predicts the distribution of gas flow in bubbling fluidized beds. Since the original two-phase theory was confirmed to overestimate the bubble flowrate in most cases, a correction factor (Y) was introduced for the modification. The expansions of fluidized beds containing single and binary mixtures of solid particles were inspected to reveal the influences of particle properties and operating conditions on the correction factor (Y). The contribution for estimating the parameter Y for Geldart Group B and D particles was formulated based on the available experimental data in literature and the present work.

The mixing and segregation behavior of ADMFB with binary mixtures were investigated to achieve a relatively uniform gas-solid suspension for efficient coal beneficiation. The effects of operating parameters on the mixing and segregation pattern were examined, including particle properties, mixture composition, superficial gas velocity, and fluidized bed height. Moreover, a mixing index was employed to evaluate the mixing and segregation performance for identifying the appropriate conditions for the ADMFB operations.

The distribution of bed density in an ADMFB with Geldart Group B and D particles was studied both theoretically and experimentally. A new correlation based on the modified two-phase theory was derived to predict the distribution of fluidized bed density, with consideration of particle properties and fluidization characteristics. An examination of the bed density distribution for fluidizing single and binary mixtures of Geldart Group B and/or D particles at various operating conditions has been made to validate the proposed correlation with a strong agreement.

The performance of dry coal beneficiation in a semi-industrial ADMFB with binary mixtures was evaluated using the variations of ash content and calorific value, considering the effects of feed coal size, operating gas velocity, and mixture composition of solid particles. These continuous operations of coal beneficiation are used to validate the ADMFB operation using binary mixtures of solid particles as medium materials.

Keywords: Air dense medium fluidized bed; Binary mixtures; Fluidization characteristics; Dry coal beneficiation; Two-phase theory; Fluidized bed density.

SUMMARY FOR LAY AUDIENCE

Suspension of solid particles by an upward gas flow generally leads to a gas-solid fluidized bed, characterized by particles suspension and bed expansion, while the upward gas flow travels through the void space (voidage) between solid particles. At a relatively lower gas flowrate, the fluidized bed exhibits lower bed expansion with the appearance of gas bubbles, like boiling water. This bubbling fluidized bed which is also called Air Dense Medium Fluidized Bed (ADMFB) has similar properties like a liquid, and thus the buoyancy effect can be utilized for the dry gravity separation of particulate materials of different densities, e.g. raw coal dry beneficiation. According to Archimedes principle, the clean coal of less density than the fluidized bed will float on top of the bed, whereas the gangue of heavier density will sink to the bottom and thus can be removed from raw coal. Therefore, control of the density of fluidized bed is crucial for dry coal beneficiation by the ADMFB technology.

The density of a fluidized bed is corresponding to the mass of solid particles per unit bed volume. In order to adjust the bed density for more efficient coal beneficiation, binary mixtures of solid particles of different densities are proposed to replace the single particles in ADMFB system. Consequently, the fluidized bed density can be easily manipulated by changing the composition of the solids mixture. The objectives of this work is to study the fundamental theory and underlying mechanism of the ADMFB with binary mixtures, including the followings: (1) The minimum requirement of gas velocity for fluidization of the binary mixtures; (2) The gas distribution between the bubbles and emulsion phase; (3) Axial distribution of two types of solid particles in the fluidized bed; (4) Prediction of the fluidized bed density at different operating conditions; (5) Performance of coal beneficiation in a semi-industrial ADMFB with binary mixtures of solid particles.

CO-AUTHORSHIP

Title: Minimum Fluidization Velocity of Binary Mixtures of Medium Particles in the Air Dense Medium Fluidized Bed

Authors: Zhijie Fu, Jesse Zhu, Shahzad Barghi, Yuemin Zhao, Zhenfu Luo, Chenlong Duan

Zhijie Fu designed and performed the experiment and carried out data analysis under the guidance Dr. Jesse Zhu and Dr. Shahzad Barghi. All the experimental work was conducted by Zhijie Fu and the draft of this manuscript was written by Zhijie Fu. Revisions were carried out under the close supervision of Drs. Jesse Zhu, Shahzad Barghi, Yuemin Zhao, Zhenfu Luo and Chenlong Duan. The final version of this article has been published in the Chemical Engineering Science, 2019, 207: 194-201.

Title: Minimum Fluidization Velocity Growth due to Bed Inventory Increase in an Air Dense Medium Fluidized Bed

Authors: Zhijie Fu, Jesse Zhu, Shahzad Barghi, Yuemin Zhao, Zhenfu Luo, Chenlong Duan

Zhijie Fu designed and performed the experiment and carried out the data analysis under the guidance Dr. Jesse Zhu and Dr. Shahzad Barghi. All the experimental work was conducted by Zhijie Fu and the draft of this manuscript was written by Zhijie Fu. Revisions were carried out under the close supervision of Drs. Jesse Zhu, Shahzad Barghi, Yuemin Zhao, Zhenfu Luo and Chenlong Duan. The final version of this article has been published in the Chemical Engineering Journal, 2019, 359:1372-1378.

Title: On the Two-phase Theory of Fluidization for Geldart B and D Particles

Authors: Zhijie Fu, Jesse Zhu, Shahzad Barghi, Yuemin Zhao, Zhenfu Luo, Chenlong Duan

Zhijie Fu designed and performed the experiment and carried out the data analysis under the guidance of Dr. Jesse Zhu and Dr. Shahzad Barghi. All the experimental work was conducted by Zhijie Fu and the draft of this manuscript was written by Zhijie Fu. Revisions were carried out under the close supervision of Drs. Jesse Zhu, Shahzad Barghi. The final version of this article has been published in the Powder Technology, 2019, 354: 64-70.

Title: Mixing and Segregation Behavior in an Air Dense Medium Fluidized Bed with Binary Mixtures for Dry Coal Beneficiation

Authors: Zhijie Fu, Jesse Zhu, Shahzad Barghi, Yuemin Zhao, Zhenfu Luo, Chenlong Duan

Zhijie Fu designed and performed the experiment and carried out the data analysis under the guidance of Dr. Jesse Zhu and Dr. Shahzad Barghi. All the experimental work was conducted by Zhijie Fu and the draft of this manuscript was written by Zhijie Fu. Revisions were carried out under the close supervision of Drs. Jesse Zhu, Shahzad Barghi, Yuemin Zhao, Zhenfu Luo and Chenlong Duan. The final version of this article has been submitted to the Powder Technology, POWTEC-S-19-1780.

Title: The Distribution of Bed Density in an Air Dense Medium Fluidized Bed with Single and Binary Mixtures of Geldart B and/or D Particles

Authors: Zhijie Fu, Jesse Zhu, Shahzad Barghi, Yuemin Zhao, Zhenfu Luo, Chenlong Duan

Zhijie Fu designed and performed the experiment and carried out the data analysis under the guidance of Dr. Jesse Zhu and Dr. Shahzad Barghi. All the experimental work was conducted by Zhijie Fu and the draft of this manuscript was written by Zhijie Fu. Revisions were carried out under the close supervision of Drs. Jesse Zhu, Shahzad Barghi, Yuemin Zhao, Zhenfu Luo and Chenlong Duan. The final version of this article has been submitted to the Minerals Engineering, MINE-S-19-00585.

Title: Dry Coal Beneficiation by the Semi-industrial Air Dense Medium Fluidized Bed with Binary Mixtures of Magnetite and Fine Coal Particles

Authors: Zhijie Fu, Jesse Zhu, Shahzad Barghi, Yuemin Zhao, Zhenfu Luo, Chenlong Duan

Zhijie Fu designed and performed the experiment and carried out the data analysis under the guidance of Drs. Yuemin Zhao, Zhenfu Luo and Chenlong Duan. All the experimental work was conducted by Zhijie Fu and the draft of this manuscript was written by Zhijie Fu. Revisions were carried out under the close supervision of Drs. Jesse Zhu, Shahzad Barghi. The final version of this article has been published in *Fuel*, 2019, 243: 509-518.

DEDICATION

This work is dedicated to everybody whose helped, supported, and encouraged throughout my education career.

仅以此文献给帮助、支持我的所有人!

ACKNOWLEDGMENTS

First of all, I would like to extend my sincere gratitude to my supervisor Dr. Jesse Zhu, for his constant encouragement and instructive guidance. He has walked me through all the stages including research proposal, experimental design, result discussion, and thesis writing with continuous enthusiasm and patience. His meticulous supervision not only ensures the successful fulfillment of this research work but also greatly improves my comprehensive skills, which is invaluable and significant to my future life.

I would also like to express my sincere appreciation to my co-supervisor Dr. Shahzad Barghi for his patient and instruction, constructive suggestions, and kind encouragement during the progress of this work, especially for the helpful discussions and careful revisions of manuscripts. Without his consistent and illuminating instruction, this thesis could not have reached its present form.

Much appreciations are extended to Dr. Yuemin Zhao, Dr. Zhenfu Luo, Dr. Chenlong Duan, Dr. Xuliang Yang, Dr. Liang Dong, Dr. Bo Zhang, Dr. Enhui Zhou, Dr. Haishen Jiang, Dr. Yong Zhang and Dr. Cheng Sheng at the China University of Mining and Technology for their helpful suggestions and consistent support to make this work more valuable.

Special appreciations are directed to the faculties and staffs in the research group, Mr. Jianzhang Wen, Dr. Hui Zhang, Dr. Yong Liu, Dr. Tang Li, Mr. George Zhang, Mrs. Danni Bao for their kind help and support.

My special thanks go to my friends in the research group, Xiaoyang Wei, Tian Nan, Zeneng Sun, Jiangshan Liu, Haolong Wang, Lin Wang, Chenyang Zhou, Yandaizi Zhou, Zhehao Jing, Jinbao Huang, Hanlin Wang, and Bowen Xie for their discussions, suggestions and friendship.

The financial assistance from the Natural Sciences and Engineering Research Council of Canada (NSERC) and the National Natural Science Foundation of China are gratefully acknowledged.

Finally, I devote and dedicate this research work to my parents, Mr. Jiahong Fu and Mrs. Yongxiang Yang, and my girlfriend Miss. Dora Liu. Without their consistent and unreserved support, I could not have done this work thus far a success. Thank you very much!

TABLE OF CONTENTS

ABSTRACT	ii
CO-AUTHORSHIP	v
ACKNOWLEDGMENTS	ix
TABLE OF CONTENTS	x
LIST OF TABLES	xv
LIST OF FIGURES	xvii
LIST OF APPENDICES	xxiii
CHAPTER 1 GENERAL INTRODUCTION	1
1.1 Background.....	1
1.2 Research objectives.....	4
1.3 Thesis structure	5
References	7
CHAPTER 2 LITERATURE REVIEW	8
2.1 Introduction.....	8
2.2 Evaluation of fluidized bed separation technology.....	9
2.3 Recent developments in fluidized bed separation technology	19
2.4 Conclusions and Outlook.....	28
References	29
CHAPTER 3 MINIMUM FLUIDIZATION VELOCITY OF BINARY MIXTURES OF MEDIUM PARTICLES IN AN AIR DENSE MEDIUM FLUIDIZED BED 35	
3.1 Introduction.....	35
3.2 Experimental.....	37
3.2.1 Experimental setup.....	37
3.2.2 Experimental materials	38

3.2.3	Characterization of binary mixtures.....	39
3.3	Results and discussion	41
3.3.1	Minimum fluidization velocity of binary mixtures.....	41
3.3.2	Comparison of the correlations for binary mixtures.....	44
3.3.3	Modify the Cheung equation with the experimental data.....	47
3.3.4	Error analysis of the proposed correlation	50
3.4	Conclusion	51
	References.....	54

CHAPTER 4 MINIMUM FLUIDIZATION VELOCITY GROWTH DUE TO BED INVENTORY INCREASES IN AN AIR DENSE MEDIUM FLUIDIZED BED 59

4.1	Introduction.....	59
4.2	Theory.....	61
4.3	Experimental.....	64
4.3.1	Experimental setup.....	64
4.3.2	Experimental materials	65
4.4	Results and discussion	66
4.4.1	The effect of bed inventory on the minimum fluidization.....	66
4.4.2	The correlation for estimating minimum fluidization velocity.....	68
4.4.3	Error analysis of the correlation for minimum fluidization velocity	71
4.4.4	Comparison with the experimental data	72
4.5	Conclusion	73
	References.....	77

CHAPTER 5 ON THE TWO-PHASE THEORY OF FLUIDIZATION FOR GELDART GROUP B AND D PARTICLES 81

5.1	Introduction.....	81
5.2	Theory.....	84

5.3	Experimental	86
5.3.1	Experimental setup.....	86
5.3.2	Experimental materials	87
5.4	Results and discussion	88
5.4.1	The effects of particle property and excess gas velocity	88
5.4.2	The correlation for estimating the correction factor Y	90
5.4.3	Comparison with the experimental data	92
5.4.4	Further discussion of the correlation for correction factor Y	94
5.5	Conclusion	95
	References	98
CHAPTER 6 MIXING AND SEGREGATION BEHAVIOR IN AN AIR DENSE MEDIUM FLUIDIZED BED WITH BINARY MIXTURES FOR DRY COAL BENEFICIATION		102
6.1	Introduction.....	102
6.2	Experimental.....	105
6.2.1	Experimental setup.....	105
6.2.2	Experimental materials	106
6.2.3	Mixing and segregation evaluation.....	107
6.3	Results and discussion	108
6.3.1	Effect of particle density ratio.....	108
6.3.2	Effect of particle size ratio.....	109
6.3.3	Effect of mixture composition	112
6.3.4	Effect of superficial gas velocity	114
6.3.5	Effect of fluidized bed height	117
6.3.6	Mixing index of binary mixtures	119
6.4	Conclusion	123

References	126
CHAPTER 7 THE DISTRIBUTION OF BED DENSITY IN AN AIR DENSE MEDIUM FLUIDIZED BED WITH GELDART GROUP B AND/OR D PARTICLES	130
7.1 Introduction.....	130
7.2 Theory.....	133
7.3 Experimental.....	137
7.3.1 Experimental apparatus.....	137
7.3.2 Experimental materials	138
7.4 Results and discussion	139
7.4.1 Effect of particle size and density.....	139
7.4.2 Effect of excess gas velocity.....	141
7.4.3 Effect of mixture composition	143
7.4.4 Comparison with the experimental data	147
7.5 Conclusion	149
References	152
CHAPTER 8 DRY COAL BENEFICIATION BY THE SEMI-INDUSTRIAL AIR DENSE MEDIUM FLUIDIZED BED WITH BINARY MIXTURES OF MAGNETITE AND FINE COAL PARTICLES	157
8.1 Introduction.....	157
8.2 Experimental.....	160
8.2.1 Air Dense Medium Fluidized Bed system.....	160
8.2.2 The properties of medium materials and feed coal samples.....	162
8.2.3 Experimental procedure	164
8.3 Results and discussion	165
8.3.1 The effect of operating gas velocity.....	165
8.3.2 The effect of feed coal size	167

8.3.3	The effect of particle composition of binary mixtures.....	171
8.3.4	The performance of coal beneficiation in semi-industrial ADMFB.....	173
8.3.5	Comparison with the literature data.....	175
8.4	Conclusion	177
	References	180
	CHAPTER 9 CONCLUSIONS AND RECOMMENDATIONS	184
9.1	Conclusions.....	184
9.2	Recommendations.....	187
	Appendix A1. Curves for the improved Cheng Equation.....	188
	Appendix A2. Modified two-phase theory for binary mixtures.	189
	Appendix A3. Flow sheet of industrial ADMFB system.....	194
	Curriculum Vitae	195

LIST OF TABLES

Table 3.1. The properties of experimental materials.	39
Table 3.2. Literature summary of the minimum fluidization velocity of binary mixtures.	45
Table 3.3. Summary of the error analysis of various correlations for binary systems.	46
Table 4.1. The properties of experimental materials.	65
Table 4.2. The properties of binary mixtures of solid particles.	65
Table 4.3. Literature summary of minimum fluidization velocity in the case of bed inventory. .	69
Table 5.1. The particle properties of magnetite samples.	87
Table 5.2. The particle properties of glass bead samples.	87
Table 5.3. The particle properties of sand samples.	88
Table 5.4. The particle properties of gangue samples.	88
Table 5.5. Literature summary of experimental data on the correction factor (Y).	91
Table 6.1. The properties of experimental materials.	106
Table 7.1. The particle properties of magnetite samples.	138
Table 7.2. The particle properties of glass bead samples.	138
Table 7.3. The particle properties of river sand samples.	139
Table 7.4. The particle properties of fine coal samples.	139
Table 8.1. The mass distribution of binary medium A.	163
Table 8.2. The mass distribution of binary medium B.	163

Table 8.3. The properties of coal samples.	163
Table 8.4. Mass distribution and ash content of the classified coal samples.....	164
Table 8.5 Literature summary of dry coal beneficiation by different Air Dense Medium Fluidized Bed systems.	176

LIST OF FIGURES

Figure 2.1 The schematic diagram of first fluidized bed separator by Fraser et al.....	9
Figure 2.2 The schematic drawing of fluid separating medium apparatus by Levin et al.	10
Figure 2.3 The schematic representation of fluidized bed coal cleaner by Kendall et al.	11
Figure 2.4 The schematic diagram of fluidized bed dry separator by Weintraub et al.	12
Figure 2.5 The schematic drawing of fluidized bed separation apparatus by Eveson et al.	13
Figure 2.6 The schematic diagram of inclined trough separator by Eveson et al.	14
Figure 2.7 The schematic diagram of Warren Spring fluidized bed separator by Walsh et al.	15
Figure 2.8 The schematic drawing of counter-current fluidized cascades by Beeckmans et al. ..	16
Figure 2.9 The schematic diagram of agricultural fluidized bed separator by Zaltzman et al.	18
Figure 2.10 The schematic drawing of agricultural fluidized bed device by Zaltzman et al.....	18
Figure 2.11 The schematic diagram of fluidized bed medium separation by Oshitani et al.....	19
Figure 2.12 The fluidized bed apparatus for iron/copper beneficiation by Oshitani et al.	21
Figure 2.13 The Air Dense Medium Fluidized Bed for dry coal beneficiation by Sahu et al.	22
Figure 2.14 The schematic view of fluidized bed device for coal beneficiation by Azimi et al. .	24
Figure 2.15 The schematic drawing of Air Dense Medium Fluidized Bed by Chen et al.....	25
Figure 2.16 The pilot scale Air Dense Medium Fluidized Bed system by Chen et al.....	26
Figure 2.17 The first commercial ADMFB plant at the Qitaihe Coal Co.....	26
Figure 2.18 The commercial modularized Air Dense Medium Fluidized Bed by Zhao et al.....	27

Figure 3.1 The schematic diagram of experimental apparatus.	38
Figure 3.2 A typical pressure-drop-velocity curve of the M232-S485-45% mixture.....	41
Figure 3.3 The minimum fluidization velocity of binary mixtures of magnetite and sand particles.	42
Figure 3.4 The minimum fluidization velocity of binary mixtures of magnetite and gangue particles.	43
Figure 3.5 The minimum fluidization velocity of binary mixtures of magnetite and coal particles.	43
Figure 3.6 Comparison of the U_{mf} calculated by Equation (3.9) with the experimental data in the present work.....	48
Figure 3.7 Comparison of the U_{mf} calculated by Equation (3.9) with the experimental data in the literature.	49
Figure 3.8 Comparison of the U_{mf} calculated by Equation (3.9) with all available experimental data.....	50
Figure 4.1 The schematic diagram of the minimum fluidization state.	61
Figure 4.2 The schematic diagram of experimental apparatus.	64
Figure 4.3 Dependence of Reynolds number on the bed pressure drop.	67
Figure 4.4 Relations between the variation ratio of Reynolds number and bed pressure drop. ...	70
Figure 4.5 Error analysis of the proposed correlation for the available experimental data.	71
Figure 4.6 Comparison of the U_{mf} calculated using Equation (4.18) with the experimental data.	72
Figure 5.1 The schematic diagram of the two-phase theory of fluidization.	84
Figure 5.2 The schematic diagram of experimental apparatus.	86

Figure 5.3 Plot of Y value against the excess gas velocity for different types of solid particles. .	89
Figure 5.4 Effect of Archimedes number and excess gas velocity on parameter Y	91
Figure 5.5 The summary of Y values of all available data in literature and the present work.....	93
Figure 5.6 Comparison of Y values calculated using Equation (5.14) with all the available experimental data.....	93
Figure 5.7 A generalized description of the proposed correlation for predicting the correction factor (Y).	94
Figure 6.1 The schematic diagram of experimental apparatus.	105
Figure 6.2 The effect of particle density ratio on axial solids distribution of binary mixtures. .	109
Figure 6.3 The effects of particle size ratio on the axial solids distribution of M-S mixtures at lower and higher volume fractions.	111
Figure 6.4 The effects of particle size ratio on the axial solids distribution for M-G mixtures at lower and higher volume fractions.	111
Figure 6.5 The effects of particle size ratio on the axial solids distribution for M-C mixtures at lower and higher volume fractions.	112
Figure 6.6 Axial solids distribution of fluidized bed with M232-S368 mixtures at different mixture compositions.....	113
Figure 6.7 Axial solids distribution of fluidized bed with M232-G372 mixtures at different mixture compositions.....	114
Figure 6.8 Axial solids distribution of fluidized bed with M232-C396 mixtures at different mixture compositions.....	114
Figure 6.9 Axial solids distribution of fluidized bed with M232-S368 mixtures at various excess gas velocities ($U - U_{mf}$).	116

Figure 6.10 Axial solids distribution of fluidized bed with M232-G372 mixtures at various excess gas velocities ($U - U_{mf}$).....	116
Figure 6.11 Axial solids distribution of fluidized bed with M232-C396 mixtures at various excess gas velocities ($U - U_{mf}$).....	117
Figure 6.12 Axial solids distribution of fluidized bed with M232-S368 mixtures at different initial bed heights.....	118
Figure 6.13 Axial solids distribution of fluidized bed with M232-G372 mixtures at different initial bed heights.....	118
Figure 6.14 Axial solids distribution of fluidized bed with M232-C396 mixtures at different initial bed heights.....	119
Figure 6.15 The mixing index (I_m) of binary mixtures of magnetite and coal particles.	120
Figure 6.16 The mixing index (I_m) of binary mixtures of magnetite and gangue particles.	121
Figure 6.17 The mixing index (I_m) of binary mixtures of magnetite and sand particles.	121
Figure 6.18 The effect of excess gas velocity on the mixing index (I_m).....	122
Figure 6.19 The effect of initial bed height on the mixing index (I_m).	122
Figure 7.1 The schematic diagram of an Air Dense Medium Fluidized Bed.	133
Figure 7.2 The schematic diagram of experimental apparatus.	137
Figure 7.3 The distribution of bed density for different single particles of various size fractions.	141
Figure 7.4 The distribution of bed density for Geldart Group B particles at various excess gas velocities.	142
Figure 7.5 The distribution of bed density for Geldart Group D particles at various excess gas velocities.	143

Figure 7.6 Axial mass distribution of fluidized beds with binary mixtures of magnetite and sand particles.	145
Figure 7.7 Axial mass distribution of fluidized beds with binary mixtures of magnetite and coal particles.	145
Figure 7.8 Effect of mixture composition on the bed density distribution for binary mixtures of magnetite and sand particles.	146
Figure 7.9 Effect of mixture composition on the bed density distribution for binary mixtures of magnetite and coal particles.	146
Figure 7.10 Comparison of fluidized bed densities with various single particles calculated by Eq. (7.11) with the experimental data.	148
Figure 7.11 Comparison of fluidized bed densities with various binary mixtures of solid particles calculated by Eq. (7.11) with the experimental data.	148
Figure 8.1 The schematic diagram of dry coal beneficiation process in Air Dense Medium Fluidized Bed system.	161
Figure 8.2 A semi-industrial Air Dense Medium Fluidized Bed system for dry coal beneficiation.	161
Figure 8.3 The partition curves of sunk products of Lijiahao coals at various excess gas velocities.	166
Figure 8.4 The effect of excess gas velocity on the separation density.	167
Figure 8.5 The effect of excess gas velocity on the probable error.	167
Figure 8.6 The effect of feed coal size on partition curves of sunk products.	169
Figure 8.7 The effect of feed coal size on the separation density and probable error.	170
Figure 8.8 The partition coefficients of + 2.0 g/cm ³ and – 1.3 g/cm ³ coal as a function of feed coal size.	170

Figure 8.9 The partition curves of sunk products of Hecaogou coal by two types of binary mixtures of solid particles. 172

Figure 8.10 Comparison of the separation density and probable error by two types of binary mixtures of solid particles. 173

Figure 8.11 The variation of ash content of different feed coals with different coal size. 174

Figure 8.12 The variation of calorific value of different feed coals with different coal size. 175

LIST OF APPENDICES

Appendix A1. Curves for the improved Cheng Equation.....	188
Appendix A2. Modified two-phase theory for binary mixtures.	189
Appendix A3. Flow sheet of industrial ADMFB system.....	194

CHAPTER 1

GENERAL INTRODUCTION

1.1 Background

Coal is the second largest primary and available energy source in the world, which plays a major role in the economic development of many countries, e.g. China, India, Australia, South Africa. In 2018, the world production of coal was 7.54 billion ton occupying 27.6% of the world's energy structure, and the proven world coal reserves are 1552.5 billion tons and are currently sufficient to meet 134 years of global production which is much higher than that of oil and gas (BP statistical review of world energy, 2018). The run-of-mine coal is a complex mixture of organic and inorganic matters, generated by decaying and compression of organic plant under prolonged geological and environmental processes. This fossil energy source is generally used for power generation and as a critical substance in many industries through coal combustion, e.g. cement production, steel manufacturing. In order to reduce the environmental impact of emissions using coal combustion, the associated inorganic impurities such as ash-forming matter and pyritic sulfur should be first removed by coal beneficiation methods which can also upgrade the coal carbon concentration and reduce the transportation weight (Cooper et al., 1991; Gui et al., 2015). Therefore, the beneficiation process is of great importance for coal utilization.

Coal beneficiation process is a series of operations that remove the ash-forming and sulfur-containing inorganic impurities from raw coal. Generally, the run-of-mine coal needs to be crushed into the size range of smaller than 50 *mm* before the beneficiation operation, because the crushing process is required to dissociate the combining organic and inorganic materials in large coal ores. After coal crushing, raw coal will be sieved into different size ranges, which adequate to different coal beneficiation methods. For 1 ~ 50 *mm* raw coal, gravity-based physical separation processes, e.g. heavy medium cyclone, wet jigging, are generally used to achieve the ash removal and sulfur reduction, as the mineral matters are much denser than the clean coal material. Sulfur reduction by the separation process is reached due to the removed ash-forming matter contains pyritic sulfur. These gravity-based separation processes have the significant advantages of simple equipment, low operation cost, and good separation efficiency, which are

the desired methods for the beneficiation of relatively coarse coal. For the raw coal of smaller than 1 mm, froth floatation and triboelectrostatic separation processes based on chemical surface properties are usually employed to upgrade the quantity of fine raw coal.

In general, coal beneficiation processes can be divided into wet methods and dry methods. Currently, majority of coal beneficiation is carried out using wet methods (Noble and Luttrell, 2015), such as heavy medium cyclone, wet jigging, and froth floatation, due to the advantages of sharp separation and high product recovery. However, these hydraulic techniques suffer from coal slurry processing and wastewater treatment (Lockhart, 1984, Houwelingen and Jong, 2004), and the availability of large quantities of water for coal beneficiation is becoming an increasingly important problem in many parts of the world with dry climates weather and frozen area e.g. South Africa, Australia, Indian, and China (Dwari and Rao, 2007). Considering the aforementioned issues of hydraulic process and the recent progresses of dry beneficiation technologies, such as the air dense medium fluidized bed, air table, dry jigging, magnetic separator, and triboelectrostatic separator, the utilization of dry methods for the beneficiation of run-of-mine-coal seems to be inevitable in coal industries.

Air Dense Medium Fluidized Bed (ADMFB) as an efficient dry coal beneficiation method has been investigated in bench and industrial scale separation systems for many years (Chen et al., 2003; Sahu et al., 2009). It utilizes the pseudo-fluid behavior of gas-solid fluidized bed to create a uniform suspension of solid particles for dry coal separation as per their densities. So that the light component (clean coal) of feed coal can float on the top surface of the fluidized bed, and heavier ones (gangue and pyrite) would settle towards the bottom and thus can be removed. Thus, the fluidized bed density is the key factor for dry gravity separation in an ADMFB system. In order to achieve bed density adjustment and much better fluidization, binary mixtures of solid particles were frequently used as medium materials in the ADMFB for efficient gravity separation (Beeckmans et al., 1982; Chen et al., 2003; Sekito et al., 2006; Yoshida et al., 2008). Some basic principles and separation properties of the ADMFB can be found in earlier works (Luo et al., 2001; Mohanta et al., 2011). The ADMFB method is primarily used for dry gravity separation of relative coarse coal (> 6 mm), which targets the conventional wet processes of heavy medium cyclone and wet jigging (Zhao et al., 2011; Sahu et al., 2011). It has the intrinsic advantages of no water usage, lower construction and operating costs, comparable separation

efficiency as conventional hydraulic techniques, etc. In addition, an ADMFB also offers significant benefits in eliminating the needs for coal product dewatering and coal slurry thickening. Clearly, developing the ADMFB technology which has huge potential for efficient dry coal beneficiation is of great importance for the preparation and utilization of run-of-mine-coal in arid, water-deficient, and frozen areas.

Extensive investigations have been carried out by previous researchers to understand and practice the ADMFB technology for dry gravity *separation* (Luo et al., 2003; Sahu et al., 2009; Mohanta et al., 2013). However, there are still many challenges and difficulties, mainly due to the wake of understanding in fluidization hydrodynamics and separation mechanism of ADMFB. In addition, few research work on the fundamental theory and underlying principles of an ADMFB of binary mixtures has been conducted, and the knowledge related to binary systems for efficient dry coal separation is very limited. Therefore, systematical and fundamental studies are required to be undertaken for fully understanding the ADMFB with binary mixtures for efficient dry coal beneficiation and other similar applications.

1.2 Research objectives

The objectives of this research work are to comprehensively study the fluidization characteristics and basic theory of the Air Dense Medium Fluidized Bed (ADMFB) containing both single and binary mixtures of solid particles for efficient dry coal beneficiation. The present research work consists of the following parts:

- (1) Develop a model to accurately predict the minimum fluidization velocity of binary mixtures of solid particles used in the ADMFB system.
- (2) Identify the effect of bed inventory on the minimum fluidization velocity of solid particles in the ADMFB system with consideration of industrial practices.
- (3) Modify the two-phase theory model for both single and binary mixtures of solid particles (Geldart Group B and/or D particles) and understand the distribution of gas flow in the ADMFB.
- (4) Investigate the mixing and segregation behavior of binary mixtures of solid particles for determining appropriate operating conditions for ADMFB operation.
- (5) Analyze the distribution of bed density in the ADMFB with single and binary mixtures of solid particles for efficient dry coal beneficiation.
- (6) Verify the fundamental research results found by continuous experiments of dry coal beneficiation using the semi-industrial ADMFB system.

1.3 Thesis structure

This thesis follows the “Integrated-Article Format” as outlined in the UWO thesis regulation.

Chapter 1 gives a general introduction of the present research background and specific research objectives.

Chapter 2 gives a detailed literature review mainly on the evolution and development of the Air Dense Medium Fluidized Bed (ADMFB) technology.

Chapter 3 provides detailed experimental results on the minimum fluidization velocity of binary mixtures of medium particles. The influences of particle size, particle density, and mixture composition of medium particles on the incipient fluidization are investigated. A comparison of various correlations for estimating the minimum fluidization velocity of binary mixtures of solid particles reported in the literature and the present work is discussed. A modified correlation based on the Cheung equation has been developed for predicting the minimum fluidization velocity of binary mixtures of medium particles in ADMFB system.

Chapter 4 determines the bed inventory effect on the minimum fluidization velocity of single and binary mixtures of medium particles. An attempt has been made to develop an appropriate correlation for estimating the minimum fluidization velocity while considering the effect of bed inventory. The correlation proposed by Wen and Yu has been modified to predict the minimum fluidization velocity with the function of bed pressure drop. This correlation is very simple and is in reasonable agreement with almost all available experimental data in the literature and the present work.

Chapter 5 improves the two-phase theory model for the single and binary mixtures of medium particles (Geldart Group B/D particles). The original two-phase theory has been proved to be an overestimation in most cases, and therefore a correction factor (Y) has been introduced for the modification. The contribution for accurately predicting the parameter Y for the single and binary mixtures of Geldart Group B and/or D particles is formulated based on the available experimental data in the literature and the present work. And then, the distribution of gas flow between the bubble phase and dense phase in ADMFB is clear.

Chapter 6 investigates the mixing and segregation behavior of binary mixtures of medium particles in an ADMFB system. The effects of particle density ratio, particle size ratio, mixture composition, superficial gas velocity, and fluidized bed height on the mixing and segregation pattern are examined in terms of axial solids distribution. The mixing index proposed by Chiba et al. is employed to evaluate the mixing and segregation performance, and the appropriate operating conditions for efficient dry coal beneficiation in ADMFB are identified.

Chapter 7 exhibits the axial distribution of bed density in an ADMFB with single and binary mixtures of medium particles. The effects of particle size, particle density, superficial gas velocity, and mixture composition of medium particles on the bed density distribution are examined. An equation based on the modified two-phase theory has been derived to predict the axial density distribution of the fluidized bed, and this correlation successfully accounts for the estimation of density distribution in the ADMFB involving both single and binary mixtures of Geldart Group B and/or D particles.

Chapter 8 reports the continuous operation of dry coal beneficiation in the semi-industrial ADMFB system with binary mixtures of magnetite and fine coal particles. The influences of feed coal size, operating gas velocity, and mixture composition of medium particles on the coal separation performance are investigated. The variation of ash content and calorific value of the separated coal samples are examined. These semi-industrial experiments of continuous dry coal beneficiation are used to validate the ADMFB with binary mixtures of medium particles.

References

- BP statistical review of world energy 2018, <http://www.bp.com>.
- Beeckmans J. M., Goransson M., Butcher S. G., 1982. Coal cleaning by counter-current fluidized cascade. *Can. Min. Metall. Bull.* 75, 184-191.
- Chen Q. R., Wei L. B., 2003. Coal dry beneficiation technology in China: The state-of-the-art. *China Part.* 1(2), 52-56.
- Cooper B. R., Ellingson W. A., 1991. *The science and technology of coal and coal utilization.* Springer, Boston, United States.
- Dwari R. K., Rao K. H., 2007. Dry beneficiation of coal – A review. *Min. Process. Extra. Metall. Rev.* 28, 177-234.
- Gui X., Liu J., Gao Y., 2015. Coal preparation technology: Status and development in China. *Energy Environment.* 26, 997-1013.
- Houwelingen J. A., Jong T. P. R., 2004. Dry cleaning of coal: Review, fundamentals and opportunities. *Geol. Bel.* 7, 335-343.
- Lockhart N. C., 1984. Dry beneficiation of coal. *Powder Technol.* 40, 17-42.
- Luo Z. F., Chen Q. R., 2001. Dry beneficiation technology of coal with an air dense-medium fluidized bed. *Int. J. Min. Process.* 63, 167-175.
- Luo Z. F., Zhao Y. M., Tao X. X., Fan M. M., Chen Q. R., Wei L. B., 2003. Progress in dry coal cleaning using air-dense medium fluidized beds. *Coal Prep.* 23, 13-20.
- Mohanta S., Chakraborty S., Meikap B. C., 2011. Influence of coal feed size on the performance of air dense medium fluidized bed separator used for coal beneficiation. *Ind. Eng. Chem. Res.* 50, 10865-10871.
- Mohanta S., Rao C. S., Daram A. B., Chakraborty S., Meikap B. C., 2013. Air dense medium fluidized bed for dry beneficiation of coal: Technological challenges for future. *Part. Sci. Technol.* 31, 16-27.
- Noble A., Luttrell G. H., 2015. A review of state-of-the-art processing operations in coal preparation. *Int. J. Min. Sci. Technol.* 25(4), 511-521.

Sahu A. K., Biswal S. K., Parida A., 2009. Development of air dense medium fluidized bed technology for dry beneficiation of coal – A review. *Int. J. Coal Prep. Util.* 29, 216-241.

Sahu A. K., Tripathy A., Biswal S. K., Parida. A., 2011. Stability study of an air dense medium fluidized bed separator for beneficiation high-ash Indian coal. *Int. J. Coal Prep. Util.* 31, 127-148.

Zhao Y., Liu. J., Wei X., Luo Z., Chen Q., Song S., 2011. New progress in the processing and efficient utilization of coal. *Min. Sci. Technol.* 21, 547-552.

CHAPTER 2

LITERATURE REVIEW

2.1 Introduction

Gas-solid fluidized bed technologies have achieved many industrial applications (Kunii and Levenspiel, 1991; Rhodes, 2008), including fluid catalytic cracking, coal combustion, biomass gasification, mixing and drying, mineral beneficiation, etc. One of the most significant properties of gas-solid fluidized bed in the bubbling fluidization regime is connected with the uniform and stable density of gas-solid suspension (Davidson et al., 1985), which can be utilized for the dry gravity separation of particulate materials such as raw coal, lump iron, copper ores, etc. Fluidized bed separation also named Air Dense Medium Fluidized Bed (Chen et al., 2003(a)) has various advantages including high separation efficiency, less construction and operating costs, no water usage, and environmentally friendly, providing a better solution for mineral beneficiation and other similar applications (Mohanta et al., 2013). As one of the most important industrial practices, dry coal beneficiation using fluidized bed separation method has been extensively studied and exploited for decades (Lockhart et al., 1984), which creates a possible option for the preparation and utilization of coal resource in arid, water-deficient, and frozen areas. The first fluidized bed device for dry coal beneficiation was proposed occasionally by Fraser et al. in 1925 (Fraser and Yancey, 1925). Since then, a large number of relevant works and practices have been carried out by investigators in many countries and regions around the world e.g. United States, Canada, China, Israel, India, and South Africa.

In the present study, a review of the majority works conducted by different researchers has been summarized according to the evaluation and recent developments of fluidized bed separation technology. It is impractical and unnecessary to comprehensively cover all previous literatures; rather the important and meaningful progresses have been reported here. Much more attention has been paid to the continuous works and novel investigations made by these researchers, which will lead to a better understanding of the fluidized bed method. The objectives of this review are to comprehensively discuss and deeply analyze the fluidized bed separation for the efficient dry coal beneficiation and other similar industrial applications.

2.2 Evaluation of fluidized bed separation technology

In 1925, the dry coal separation process using fluidized bed technology was firstly proposed by Fraser et al., who applied for the first United States Patent of fluidized bed dry separator (U.S.1534346) (Fraser and Yancey, 1925). The river sand with a bulk density of 1.45 g/cm^3 was chosen as the medium material to achieve a uniform gas-solid suspension with a fluidized bed density of 1.20 g/cm^3 , and 10 ~ 50 mm coarse coal was successfully beneficiated in a bench scale fluidized bed dry separator (Fraser, 1926). The schematic diagram of this fluidized bed separator is shown in Figure 2.1. However, it has some apparent disadvantages. The most significant one is the insufficient separation efficiency, mainly due to the required bed density for coal separation is usually much higher than the density of fluidizing sand particles. A certain amount of clean coal may sink to the bottom of the fluidized bed and therefore be discharged mistakenly as tailings during the separation process. Another problem is that the final clean coal products could pollute the residual sand particles due to incomplete dense medium recycling. Although this fluidized bed technology has some shortcomings, the proposed method provides a potential way for efficient dry separation of raw coal or other particulate materials. Since then, extensive investigations of fluidized bed method for dry separation or sorting have been carried out in many countries, including the UK, USA, Germany, Canada, Russia, China, India, etc.

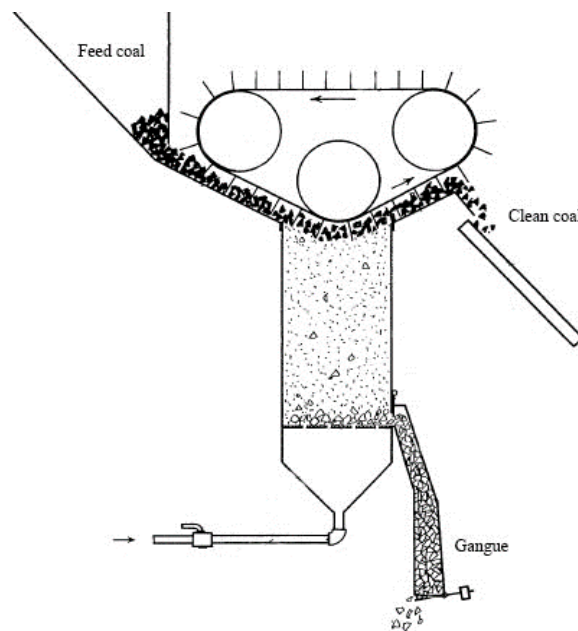


Figure 2.1 The schematic diagram of first fluidized bed separator by Fraser et al.

Soon after, more efforts have been made in the design and process control of fluidized bed dry separator, leading to an abundance of patents and articles. For example, the method of cleaning coal and fluid separating medium was proposed by Levin et al. (Levin and Yost, 1938), and the schematic drawing is shown in Figure 2.2. The most prominent aspect of this invention is that the inclined wheel conveyors are employed to transport separated coal products, providing a stable product delivery rate. However, the immersed mechanism conveyors may also disturb the gravity separation process and lower the separation efficiency. Another fluidized bed coal cleaner was developed by Kendall et al. (Kendall and Moore, 1942), and the schematic diagram is displayed in Figure 2.3. The objectives of this design are to speed up the coal separation process and reduce the construction and operating costs. This fluidized bed coal cleaner is relatively small and inexpensive, which can be nearly standard constructed to adapt a great variety of operating conditions. The separation process in the apparatus can be sped up by feeding the raw coal into a rapidly fluidizing of sand and air, which can quickly float the clean coal away and drop the gangue to the bottom. Then, the clean coal and heavy refuse products can be readily withdrawn very soon. Furthermore, many other types of fluidized bed dry separators were developed for industrial practices (Holmes, 1934; Dickerson, 1935; Svensson, 1958). Their inventions focus more on the design and operation of fluidized bed dry separators, and the development of the basic principle and theory for the fluidized bed separation method was not studied in detail.

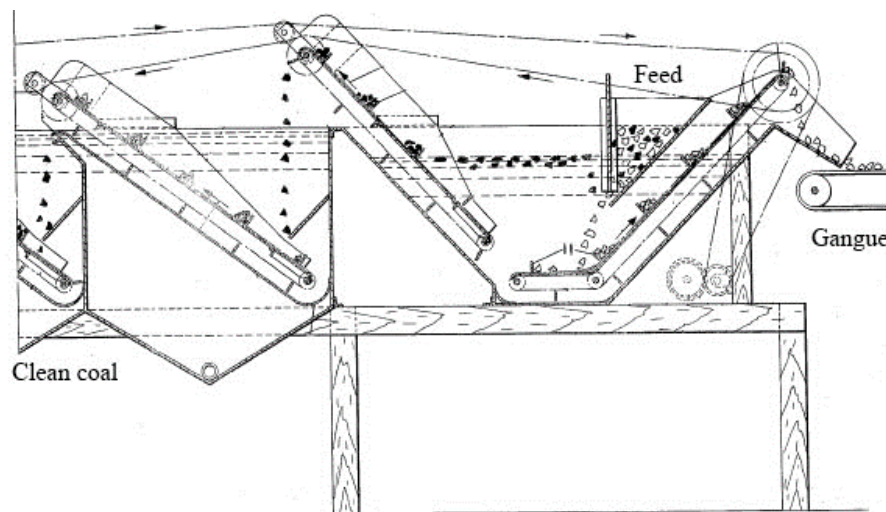


Figure 2.2 The schematic drawing of fluid separating medium apparatus by Levin et al.

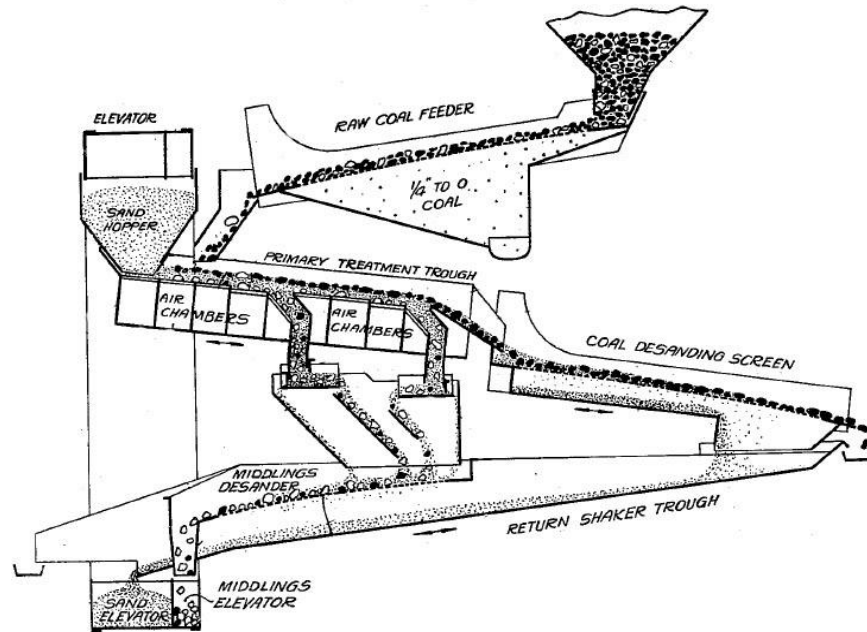


Figure 2.3 The schematic representation of fluidized bed coal cleaner by Kendall et al.

Weintraub et al. at the Pittsburgh Energy Technology Center in the United States proposed to use magnetite powder as the medium material in the fluidized bed separator for efficient dry coal beneficiation in 1979 (Weintraub et al., 1979). There are main three reasons: (1) magnetite powder has a good flowability which can achieve uniform and stable fluidization; (2) the bed density of fluidizing magnetite powder (around 2.0 g/cm^3) is close to the desired density for efficient coal separation; (3) the magnetic property of magnetite powder can be used to lower the consumption of medium particles through the magnetic recovery process. A large number of batch experiments were conducted in a cylindrical fluidized bed device with a diameter of 4-inches, and many process variables had been experimental explored, including the feed rate, residence time, feed size, and the size fraction of magnetite particles. The results demonstrated that all of these operating parameters were of significant effects and interacted with each other, resulting in complex design and operation problems. Moreover, the $0.55 \sim 9.5 \text{ mm}$ coarse coal particles can be separated effectively in 60 seconds, and the possible separation of finer coal particles will be up to 5 minutes. In addition, they also applied for a United States Patent for their fluidized bed separator (Weintraub and Deurbrouck, 1973), and the schematic drawing is shown in Figure 2.4. As can be observed that the design of this dry separator is very simple and the operation process is relatively easy.

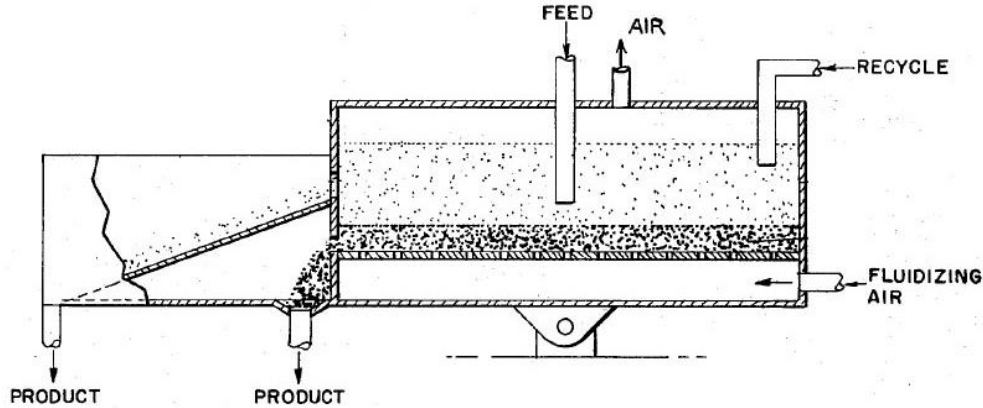


Figure 2.4 The schematic diagram of fluidized bed dry separator by Weintraub et al.

Researchers at Lehigh University in United States have focused on investigating fine coal dry cleaning using the shallow fluidized bed technology since 1987 (Levy et al., 1987). The segregation of different types of solid particles in the bubbling fluidized bed was utilized for fine coal dry beneficiation (Sahan, 1997). The shallow fluidized bed with different bed heights of 3 ~ 12 *cm* were tested, and the results demonstrated that the coal particles of 0.1 ~ 0.6 *mm* can be cleaned with a higher separation efficiency. For fine coal of smaller than 0.1 *mm*, slugging and channeling occurred in the fluidized bed mainly due to high interparticle cohesive forces, which would result in a poor beneficiation performance. Moreover, superficial gas velocity and feed weight ratio between raw coal and dense medium particles were proven to be the most important process variables, and their optimum ranges were successfully pointed out. Although the shallow fluidized bed separator was only validated in the bench scale, the proposed method provides a possible solution for the global issue of fine coal dry beneficiation. Sarunac et al., at Lehigh University combined the thermal drying and density segregation processes into one fluidized bed device for the efficient upgrading of low-rank coals in 2009 (Sarunac et al., 2009). There are mainly two stages. The first stage happened at the front of fluidized bed was used to segregate the higher density materials such as rocks and stones to the bottom of the fluidized bed. The second stage was used to evaporate the coal moisture by heating the fluidizing air through an in-bed heat exchanger. A low-temperature thermal drying were chosen to prevent the spontaneous combustion of the dried coal ores. Low-moisture and high-quality clean coal products were successfully produced, and the reduction in sulfur and mercury content were validated in this specially designed fluidized bed.

In Britain, researchers at the Wrightson Co. Ltd. have developed several fluidized bed dry separators since 1966, which were applicable to dry separation of raw coal and other similar particulate materials containing components of different densities (Eveson, 1966). A typical fluidized bed dry separator (Eveson and Thompson, 1969) is shown in Figure 2.5. In order to maintain a stable product delivery rate, the inclined conveyors immersed in the vessel are used to transport the separated clean coal and gangue products, and a series of turning baffles located at the top surface of the bed are designed to speed up the separated clean coal products. However, the immersed conveyors may impede the upward gas flow giving rise to a non-uniform gas-solid suspension, which would result in a relatively lower separation performance. Another fluidized bed separation apparatus was developed that comprised of an elongated vibratory trough for the treatment of fine coal dry cleaning (Eveson, 1968), as can be seen in Figure 2.6. The vibrated trough is constructed in the fluidized bed together with the air chamber and distributor, and a cleaning zone and a discharge zone are located at the same side of the fluidized bed. The fluidity of the bed in the discharge zone is manipulated to control the discharge rate of heavier product from the bottom of the fluidized bed, which is an innovative non-mechanism design for the discharge of separated products. Although the elongated vibratory trough in the fluidized bed separator may increase the energy consumption, this invention gives a possible solution to the global issues of fine coal dry beneficiation.

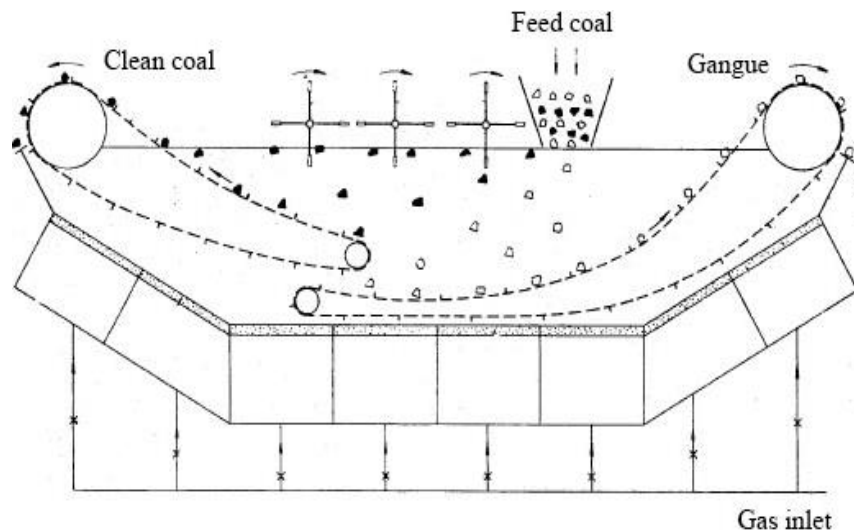


Figure 2.5 The schematic drawing of fluidized bed separation apparatus by Eveson et al.

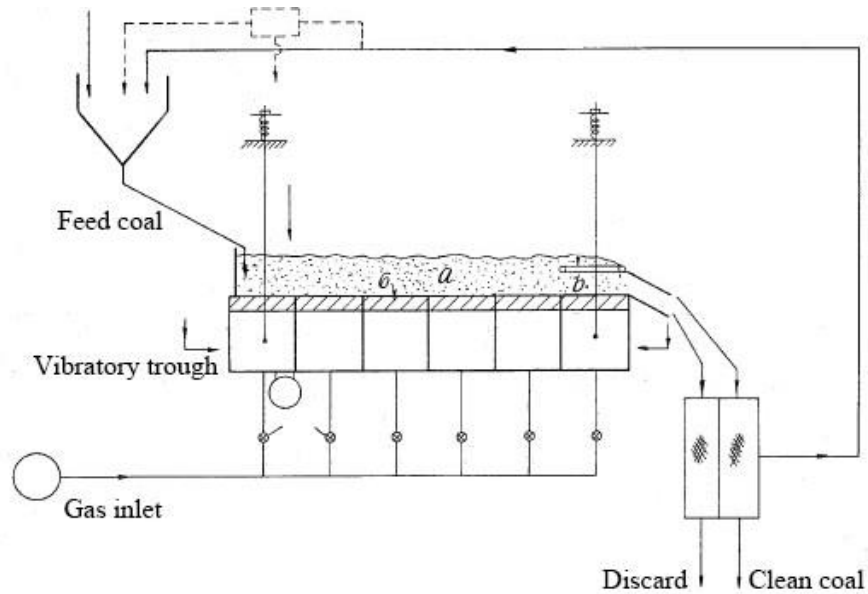


Figure 2.6 The schematic diagram of inclined trough separator by Eveson et al.

Douglas et al., at the Warren Spring Laboratory in the United Kingdom developed a novel fluidized bed apparatus with an inclined vibratory trough for the dry separation of particulate materials according to the different specific gravities (Douglas and Walsh, 1966), and the schematic diagram is illustrated in Figure 2.7. It should be noteworthy that this novel fluidized bed separator can be applicable to both the dry and wet gravity separation cases depending on the medium material used. In general, the used medium is a suspension of solid particles in an air flow, and the separating environment being a gas-solid fluidized bed. However, the medium can also be a slurry of solid particles kept suspended in the water flow by vibration or agitation, and then it becomes a wet heavy medium separation. In addition, this fluidized bed separator contains an inclined vibratory trough which designed to combine the particle fluidization along with the vibrating table and the transportation of separated products (Douglas et al., 1972). Raw coal in the size range of $-75 + 0.7 \text{ mm}$ was effectively beneficiated using the fluidizing sand particles. A commercial version of this fluidized bed separator was tested in the British Colliery (Sahu et al., 2009), but unfortunately the detail information of the separation process is not available. No more application of this separation process has been reported ever since, mainly due to the coal industry in United Kingdom gradual withdraw caused by the transformation of economic development and energy consumption structure.

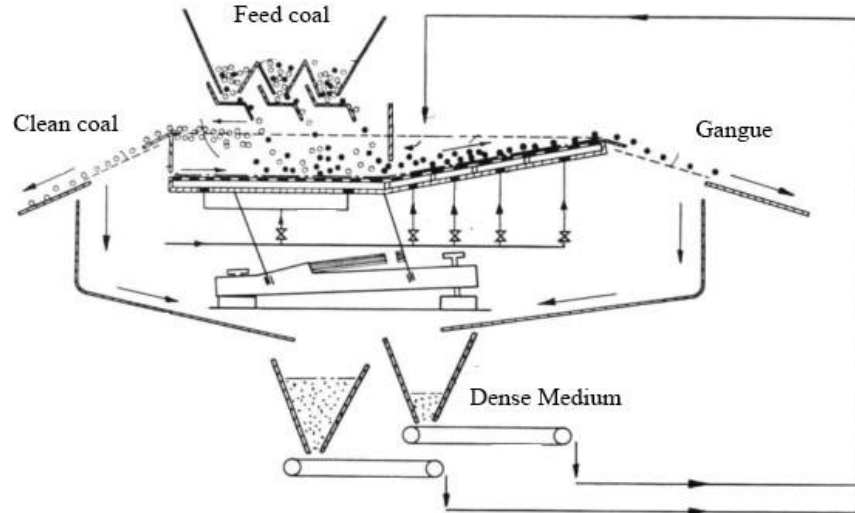


Figure 2.7 The schematic diagram of Warren Spring fluidized bed separator by Walsh et al.

In Canada, Beeckmans et al. at University of Western Ontario proposed and constructed a Counter-Current Fluidized Cascade (CCFC) system for dry gravity separation of particulate materials in 1977 (Beeckmans and Minh, 1977). Since then, several modifications have been made to this fluidized bed apparatus, and the original and three improved devices are addressed as CCFC-1, CCFC-2, CCFC-3, and CCFC-4 in this work, as can be seen in Figure 2.8. The authors mentioned that the fluidized bed cascade embodying the counter-current mass exchange principle was similar to those used in the chemical distillation or liquid-liquid extraction process. In a fluidized bed cascade system, the gravity separation performance can be enhanced by introducing two horizontal fluidized layers moving in the opposite directions, and the light and heavy components will segregate to upper and lower strata (Beeckmans, 1980), as displayed in Figure 2.8 (a). An endless baffled chain located at the upper surface of the bed is designed to create the fluidizing solids reflux and transport the separated products. The required gas velocity is only slightly above the minimum fluidization velocity for inducing the vertical segregation of solid particles according to density difference. The original fluidized bed cascade (CCFC-1) consists of a long rectangular trough (length \times width \times height = 2240 mm \times 203 mm \times 710 mm), and depth of the fluidized bed is approximately 300 mm. The CCFC-1 system was found to be a highly effective device for separating activated carbon (1330 μm) from sand particles (91 μm) (Beeckmans and Minh, 1977) and concentrating small quantities of coconut charcoal particles (342 μm) from salt particles (459 μm) (Muzyka et al., 1978). In 1982, the fluidized bed cascade device was modified for the removal of high-ash refuse from a run-of-mine coal (Beeckmans et

al., 1982), and the schematic drawing of CCFC-2 is shown in Figure 2.8 (b). In order to discharge the sunk objects at the bottom, the bed materials in the lower layer are conveyed by the motion of the endless baffled chain, and thus a return solids flow will occur in the upper layer and will be used for the transportation of floated products. The CCFC-2 system consists of an elongated shallow bed trough (length \times width \times height = 5487 mm \times 190 mm \times 609 mm), and raw coal of $-25 + 0.8$ mm was effectively separated by the fluidizing mixture of limestone and hematite particles. Another modified fluidized bed cascade (CCFB-3) was introduced by Chan et al. (Chan and Beekmans, 1982) and is presented in Figure 2.8 (c). The particle recycle system was developed and constructed for efficient gravity separation, and the concentration of pyrite and ash contents in the reject streams was achieved. Dong et al. developed another fluidized bed cascade (CCFC-4) with no moving parts and the solids reflux was induced by a current of air (Dong and Beekmans, 1990), as shown in Figure 2.8 (d). A continuous feed and withdrawal using carbon and magnetite particles in salt particles was experimentally tested.

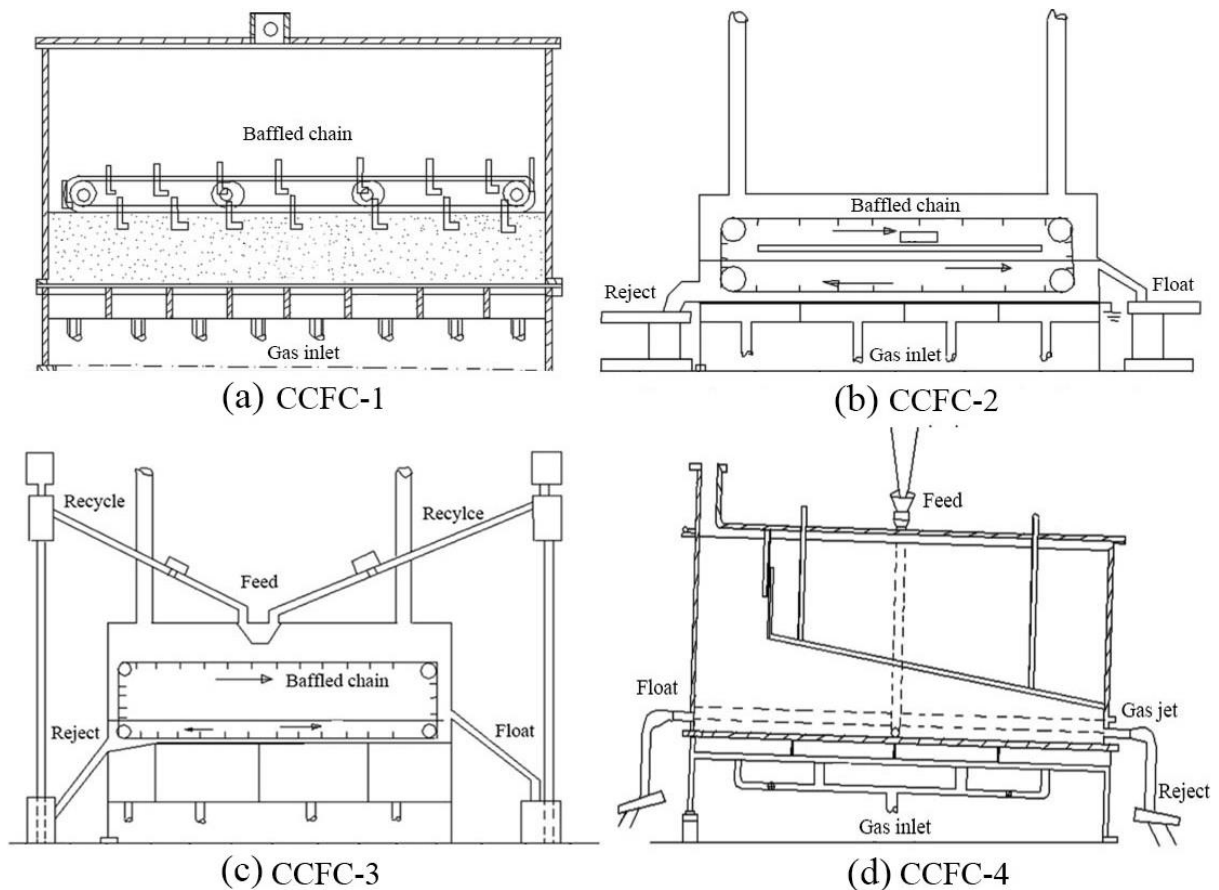


Figure 2.8 The schematic drawing of counter-current fluidized cascades by Beekmans et al.

In Israel, investigators at the Agricultural Research Organization have proposed and practiced the fluidized bed method for dry cleaning of agricultural products since 1983 (Zaltzman et al., 1983). As is known that wetting agricultural products may decay and fermentation quickly, and thus the dry method is preferred than the wet method in agricultural product cleaning areas. Compared with the traditional dry separation methods, e.g. pneumatic separation and X-ray based separation, the fluidized bed technology has the advantages of higher density-based separation efficiency and lower energy consumption, which is desirable for agricultural products cleaning. A pilot unit of agricultural fluidized bed separation system was developed by Zaltzman et al. in 1983 (Zaltzman et al., 1983), and the schematic drawing (Zaltzman et al., 1985) is shown in Figure 2.9. It is a continuous operation system and has been scale-up for industrial practice (Zaltzman and Schmilovitch, 1986). The dry separator comprises of two fluidized bed sections connected by an opening area, and the light and heavy products enter the different sections and will be discharged separately. A perforated conveyor is used to remove the floated (light) component, and the medium particles picked up by the conveyor will pass through the fine holes in the conveyor and return to the bed. A rotating drum and an outlet conveyor are used to transport the sunk (heavy) component. River sand is employed as the medium particles due to good flowability and the appropriate particle density, as well as almost no pollution affecting the final agricultural products. The dry separating or sorting of agricultural products including potatoes, crops, flower bulbs, fruits and vegetables were tested experimentally with very satisfactory results (Zaltzman et al., 1987). A separation effectiveness of 99.9% was achieved for the potato cleaning with the processing capacity of 20 - 22 t/h in field conditions (Zaltzman and Schmilovitch, 1986). For the flower bulbs, a separation effectiveness of 90-95% was completed with the processing capacity of 4 t/h, and only approximately 1% of the flower bulbs were lost by damage in the separator (Zaltzman et al., 1985). They also developed another agricultural fluidized bed separation apparatus by introducing the multi-stage inclined troughs in 1993 (Zaltzman, 1993), as can be seen in Figure 2.9. The fluidized bed is formed by forcing gas flow upwardly through the bottom of the trough and the medium particles, and feed materials can then be separated and transported in the inclined trough. Vertical oscillatory movement is imparted to the inclined trough to improve the density uniformity where a fluidization medium such as sand particles is suspended and fluidized. A series of inclined troughs can be combined to improve the separation effectiveness of the fluidized bed device.

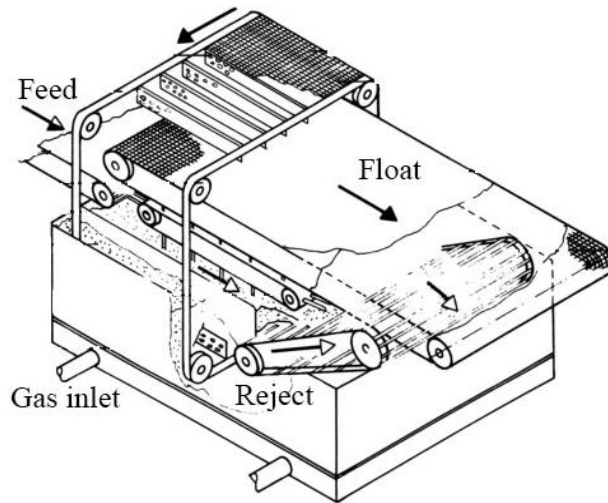


Figure 2.9 The schematic diagram of agricultural fluidized bed separator by Zaltzman et al.

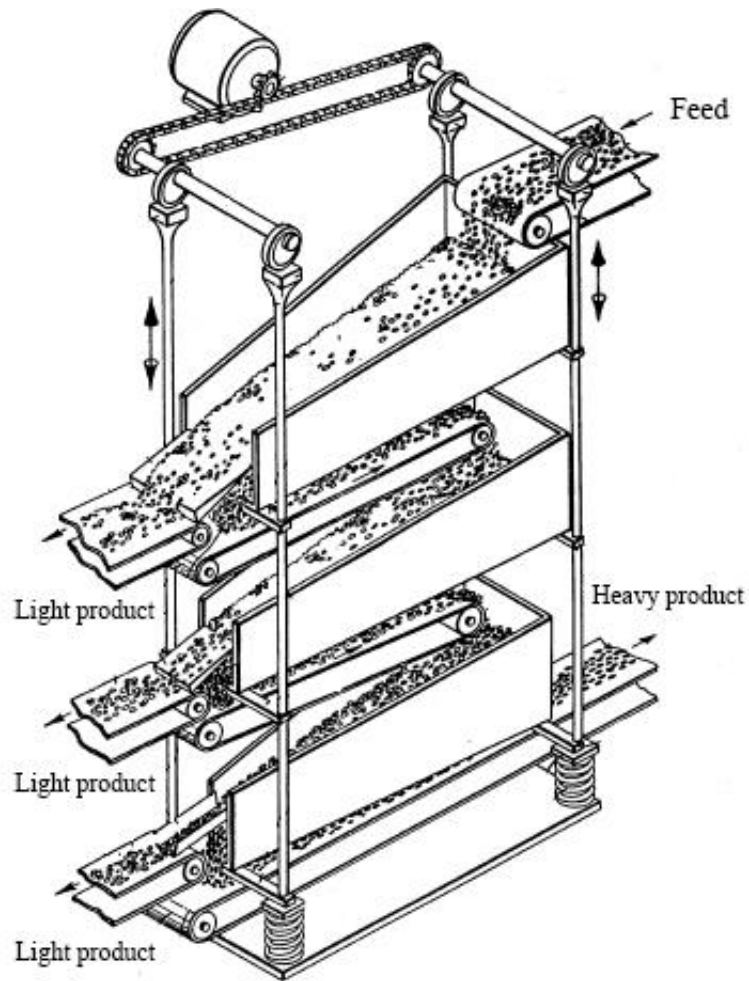


Figure 2.10 The schematic drawing of agricultural fluidized bed device by Zaltzman et al.

2.3 Recent developments in fluidized bed separation technology

In Japan, investigators at Okayama University have studied the fluidized bed medium separation for approximately 15 years (Oshitani et al., 2004), and a developed fluidized bed separator is displayed in Figure 2.11. This fluidized bed apparatus is a continuous separation system (length \times width \times height = 660 mm \times 450 mm \times 550 mm). An inclined rotating basket is utilized to collect the heavy product at the bottom of the bed, and a bucket elevator is used to remove the light product floated at the top surface. Solid mixtures of calcium carbonate (300 - 425 μm , 2.68 g/cm^3) and zircon sand particles (90 - 250 μm , 4.65 g/cm^3) were chosen as the medium material in the separation system for coarse coal dry cleaning. The continuous discharging of floating and sinking products in the fluidized bed system was achieved with a feed rate of 1000 kg/h . A clean coal product with the yield of 60 - 70% and the ash recovery of 60 - 80% was achieved with the probable error of 0.04 - 0.05 g/cm^3 . Soon after, Yoshida et al. at Okayama University studied the apparent specific gravity of gas-solid fluidized bed with binary particle systems (Yoshida et al., 2008). It was found that the apparent specific gravity of a fluidized bed can be changed by the mixing ratio of the binary system and superficial gas velocity. The fluctuation of specific gravity was proven to be determined by the extent of segregation of fluidized particles and fluidization intensity. After that, Firdaus et al. beneficiated the 5 ~ 31mm coarse coal ores in a fluidized bed medium separation system (Firdaus et al., 2012), and the coal separation efficiency had been proven to be affected strongly by the feed size and fluidized bed height.

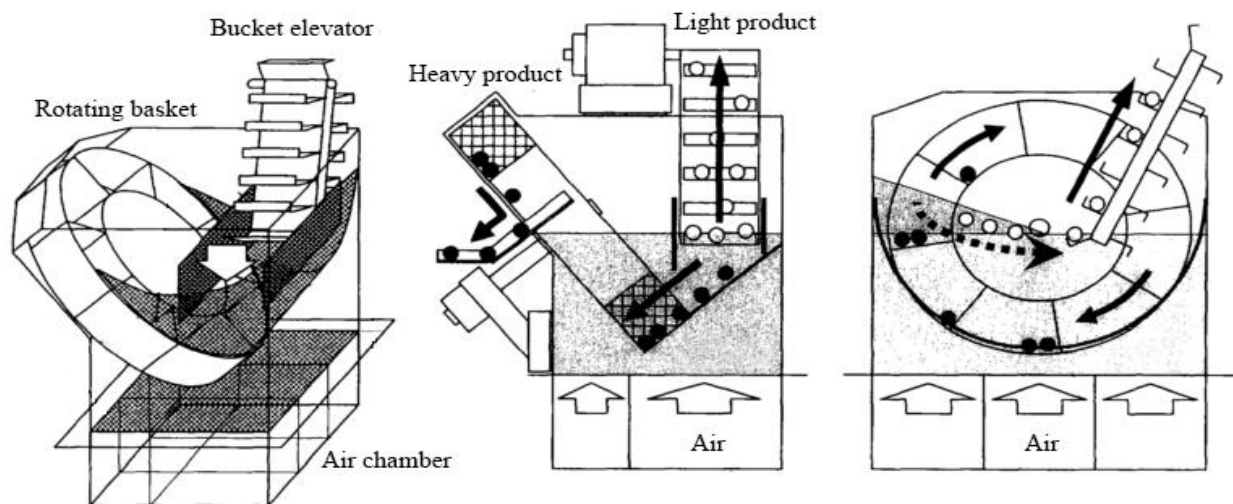


Figure 2.11 The schematic diagram of fluidized bed medium separation by Oshitani et al.

Oshitani et al. have attempted to extend the fluidized bed medium separation in other industrial applications including iron ore beneficiation, copper ore preparation, municipal waste separation, etc. A pilot unit of fluidized bed separation system was developed (Oshitani, et al., 2013), as shown in Figure 2.12. This particular separator is a continuous feeding and recovering system with a rectangular fluidized bed section (length \times width = 1600 mm \times 400 mm). In order to achieve a higher bed density for iron/copper ore beneficiation, binary mixtures of zircon sand and iron powder were selected as the medium particles. Continuous separation experiments were conducted for the 11.1 ~ 31.5 mm iron ore particles with a bed density of 2850 g/cm³ and a feed rate of 200 kg/h. The efficiency of iron ore separation was found to decrease with the decrease of feed ore size, and the iron ores with the particle density close to the bed density tend to scatter in the fluidized bed without floating or sinking (Oshitani et al., 2010). The fluidized bed separation of smaller sized particles (< 10 mm) can be improved as the fluctuations of fluidized bed surface are reduced by the decrease of fluidized bed height (Oshitani et al., 2012). Nearly perfect concentration of iron ore particles with a higher efficiency of 98.4% were attained, and the separation system produced an upgrade in iron content of 3.3 wt.% and reduced the Al and Si content by 44% (Oshitani et al., 2013), which shows a good beneficiation performance. In addition, the early rejection of gangue from copper ores was carried out by the fluidized bed medium separation with considerations of water and energy consumptions. Solid mixtures of iron powder, silica sand, and zircon sand particles were chosen as the medium materials for a wide bed density adjustment. Copper ores can be separated effectively at the bed density range of 2200 – 3700 kg/m³ with the probable errors below 0.06 g/cm³ (Franks et al., 2013). An economical and reasonable method with the combined separation processes was proposed for efficient copper ore beneficiation (Franks et al., 2015). In detail, the heavy product with a higher copper content collected from the bottom of the fluidized bed is sent to the wet grinding and flotation circuits, which would lead to significant reduction in energy and water usage. Less copper is lost in the flotation tails as the feed has been upgraded. The light product with a lower copper content rejected from the fluidized bed separation system can be treated by the inexpensive heap leaching process for the recovery of low-grade copper ores. The combined processes with fluidized bed medium separation, wet grinding and flotation, and heap leaching have many advantages and can result in significant reduction in energy and water consumption with minimal ore loss for copper ore beneficiation.

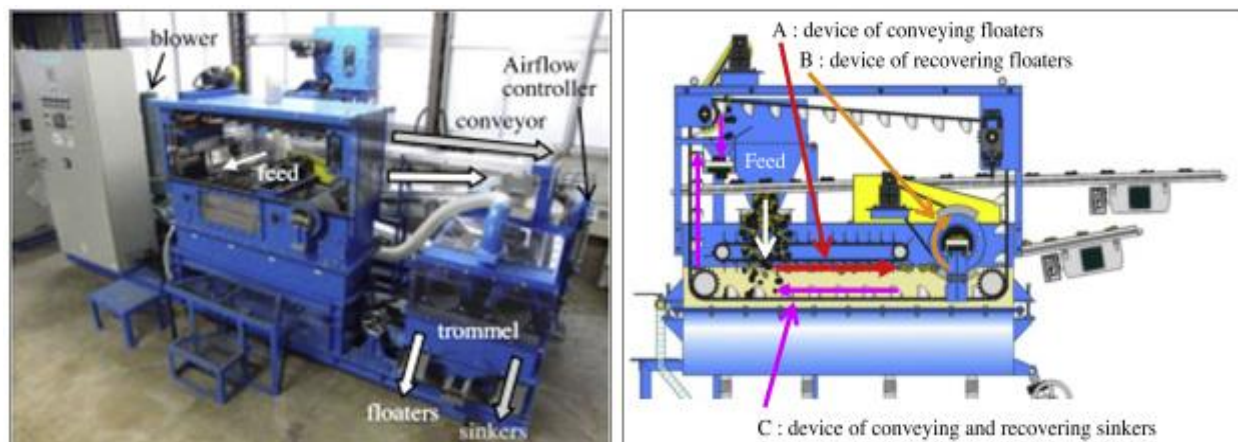


Figure 2.12 The fluidized bed apparatus for iron/copper beneficiation by Oshitani et al.

In addition, a rotating-type fluidized bed dry separator with silica sand as the dense medium was explored to decrease the Chlorine (Cl) content in municipal waste plastics (Yoshida et al., 2010). The waste plastics with Cl contents of 5.4 *wt.%* were used as the feedstock, and the Cl content of floated product was successfully decreased to 0.4 – 0.85 *wt.%* with an average recovery of 40~60% Cl-free plastics. The performance of waste plastics separation was affected by several parameters including operating air velocity, processing time, and the ratio of feed and medium particles. Sekito et al. at University of Miyazaki in Japan also attempted a batch separation of shredded municipal bulky waste by fluidized bed medium separation (Sekito et al., 2006 (a); Sekito et al., 2006 (b)). Glass beads with the particle size of 290 μm were employed as the bed material to form an apparent bed density of 1.5 g/cm^3 . The shredded bulky waste could be separated into combustibles (wood, paper, and plastics) and incombustibles (metals and glass) with an overall separation efficiency of 0.93. After that, binary mixtures of nylon shot and glass beads were used to manipulate the apparent bed density to be between 0.63 and 0.99 g/cm^3 , and wood and paper components were recovered while plastics remained in the fluidized bed with a final overall efficiency of 0.88. The accumulation of bulky waste material at the bottom of the fluidized bed was proven to decrease the separation efficiency dramatically, and a stable stirring can help to prevent this accumulation for improving the separation efficiency. In addition, the flexible sheet materials such as paper and film plastics were found to significantly decrease the separation efficiency, which indicates that the shape of the feedstock is an important factor influencing the performance of fluidized bed medium separation.

In India, the researchers at the Institute of Minerals and Materials Technology have started the investigation of fluidized bed separation technology for dry coal beneficiation since 2009 (Sahu et al., 2009). A pilot scale Air Dense Medium Fluidized Bed with a processing capacity of 600 kg/h was developed for the continuous processing of high-ash Indian coals (Sahu et al., 2011), as displayed in Figure 2.13. Magnetite powders of 7.26 and 21.7 μm were employed as the medium particles to create a uniform gas-solid fluidization with non-bubbling condition. A relatively lower bed density of 1.6 g/cm^3 was achieved mainly due to a larger bed expansion by fluidizing fine magnetite powders belonging to the Geldart A group. High-ash non-coking coal of 6 ~ 25 mm was beneficiated effectively with a separation density of 1.68 g/cm^3 and a probable error of 0.12 g/cm^3 , and the ash content of coal was reduced from 40% to 32% - 35.5% with a product yield of 60 - 72%. An attempt was made to study the stability of fluidized bed separator of different shapes (Sahu et al., 2013), and several parameters including the fluidization index, particulate expansion function, pressure drop of bed and distributor, and minimum fluidization and bubbling velocities were chosen and tested to characterize the operation stability. A fluidized bed of rectangular cross-sectional shape was found to provide a better stability than that of square or circular shape. To gain a better understanding of fluidized bed separation principle, the position of coal particles in the separator was investigated (Pallishree et al., 2015). The effective density of coal particles in the fluidized bed may increase as the additional weight due to the fine particles coating on the coal surface and the deposition at the dead zone area by medium particles.

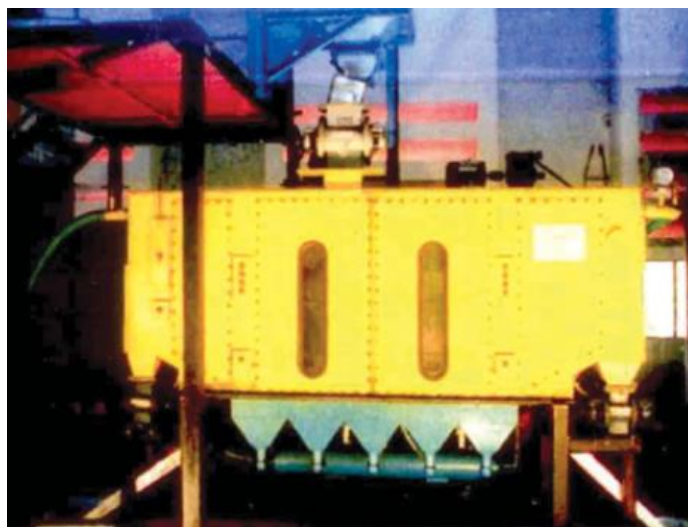


Figure 2.13 The Air Dense Medium Fluidized Bed for dry coal beneficiation by Sahu et al.

Recently, Mohanta et al. at the Indian Institute of Technology have studied the fluidized bed technology for the coal dry beneficiation from 2011 (Mohanta et al., 2011). The influence of feed coal size on the performance of gravity separation was carefully investigated in a bench scale fluidized bed separator. An attempt was made to quantify the optimum size range of feed coal over which the separation system can operate satisfactorily. Four coal samples from different Indian coal mines were used to verify the relation between the sharpness of separation and feed coal size, and the raw coal with the size range of 15 ~ 50 mm was proven to be beneficiated satisfactorily in the fluidized bed separator, regardless of the types of feed coals. The separation performance of different feed objectives of flat, blockish, and sharp-pointed prism shapes were tested in a batch fluidized bed separation system. It was found that feed materials of blockish shape that have the smallest surface area to volume ratio and thus are less subject to medium viscosity effects can be separated better than that of float and sharp-pointed shapes (Chikerma et al., 2012). Moreover, the minimum fluidization velocities of different magnetite powders used in the fluidized bed separation system were determined, and a semi-empirical correlation based on the basic particle properties was proposed for an accurate estimation without the knowledge of bed voidage and shape factors (Mohanta et al., 2012).

In Canada, Azimi et al. at University of Alberta carried out a comprehensive evaluation of the performance of low-ash coal dry beneficiation using fluidized bed separation technology in 2013 (Azimi et al., 2013 (a); Azimi et al., 2013 (b)). Response surface methodology was utilized to explore the effects of operating parameters including superficial gas velocity, residence time, and bed height on the beneficiation performance. The influences of the feed coal size and sample weight on the gravity separation were also discussed individually. It was revealed that the effectiveness of operating parameters is in the order of residence time > bed height > superficial gas velocity. A clean coal product with an ash content of 10.6 and a recovery rate of 95.63% was obtained at an optimum operating condition predicted by the proposed mathematical method. Several advanced techniques were utilized to analyze the performance of coal beneficiation in a fluidized bed separation system. The immigration behavior of hazardous elemental components and main clay mineral components during the fluidized bed processing was synthetically investigated by the Inductively Coupled Plasma-Mass Spectrometry and X-ray Fluorescence, respectively. The reactivity variation of clean coal product containing the max rate of weight loss

and the peak temperature was analyzed by Differential Thermogravimetry. In order to achieve a deeper understanding of the fluidized bed separation method, CFD simulation and statistical analysis were used to study the fluidization hydrodynamics and beneficiation performance of the continuous fluidized bed operation system (Azimi et al., 2015; Azimi et al., 2017), and the schematic view of the fluidized bed operation system is shown in Figure 2.14. Furthermore, Chong et al. at University of Albert examined the possibility of the fluidized bed separation method for dry beneficiation of fine coal particles (Chong et al., 2006). Magnetite particles of different size fractions including $45 - 75 \mu\text{m}$, $45 - 106 \mu\text{m}$, and $150 - 300 \mu\text{m}$ were selected to be the medium materials. It was confirmed that good separation efficiencies can be only accomplished with a feed coal size of down to 1 mm . To be exact, feed coal of $3.35 - 5.66 \text{ mm}$ can be beneficiated satisfactorily by fluidizing magnetite particles of $45 - 106 \mu\text{m}$ with a probable error of 0.03 g/cm^3 . Fine coal of $1 - 3.35 \text{ mm}$ could be separated in a fluidized bed with magnetite particles of $45 - 75 \mu\text{m}$, and the corresponding probable error was only 0.10 g/cm^3 . Mak et al. inspected the potential of mercury rejection through dry coal beneficiation by fluidized bed separation method (Mak et al., 2008). It was demonstrated that the mercury can be co-rejected with mineral matter from the gangue product by the fluidized bed separation, and a strong linear relation between the mercury and mineral matter contents in the heavy product was confirmed. A gangue product with the mercury rejection of 58% and the mineral matter rejection of 60% was obtained with a total combustible loss of 13%.

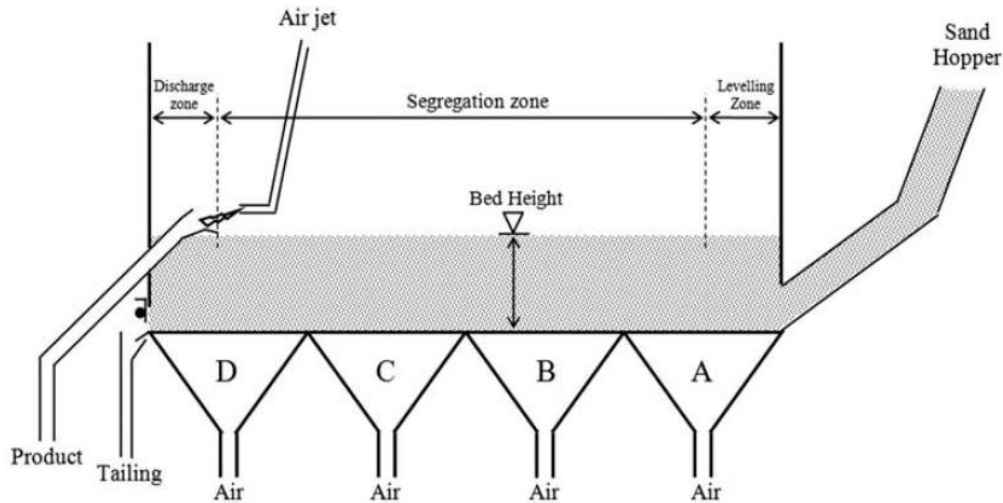


Figure 2.14 The schematic view of fluidized bed device for coal beneficiation by Azimi et al.

In China, the researchers in the Mineral Processing Research Centre at the China University of Mining and Technology focused on the dry coal beneficiation by fluidized bed technology for approximately 36 years (Chen et al., 1983). Continuous efforts have been made towards understanding the fluidization properties and separation mechanism of the fluidized bed separation system named Air Dense Medium Fluidized Bed (ADMFB). A schematic representation (Chen et al., 2003(a)) of ADMFB system is displayed in Figure 2.15. A trapezoidal shaped fluidized bed was employed as the gravity separation carrier, and an endless baffled chain was used to discharge both the heavy product at the bottom and the light product at the top surface. Magnetite particles of 150 – 300 μm were usually chosen as the medium material in the separation system with a bed height of 400 mm, and good separation efficiency can be achieved for feed coal of 6 ~ 50 mm with the probable error of 0.05 ~ 0.07 g/cm^3 (Chen et al., 2003(b)). It was also demonstrated that an efficient gravity separation in the ADMFB system requires a stable dispersion fluidization of medium particles with well distributed bed density, small bubbles, low viscosity, and high fluidity (Luo et al., 2001). A pilot scale ADMFB system was developed to exhaustively study the effects of operating parameters on the coal beneficiation performance in 1989, as can be seen in Figure 2.16. This continuous operation system contains the processes of raw coal pre-treatment, fluidized bed separation, medium solids recovery, air supply and dust collection. Magnetite particles were used in the separation system with a processing capacity of 5 – 10 t/h. An examination of ADMFB operation for 22 different raw coals from various Coal Mines was conducted with satisfactory results (Chen et al., 1993).

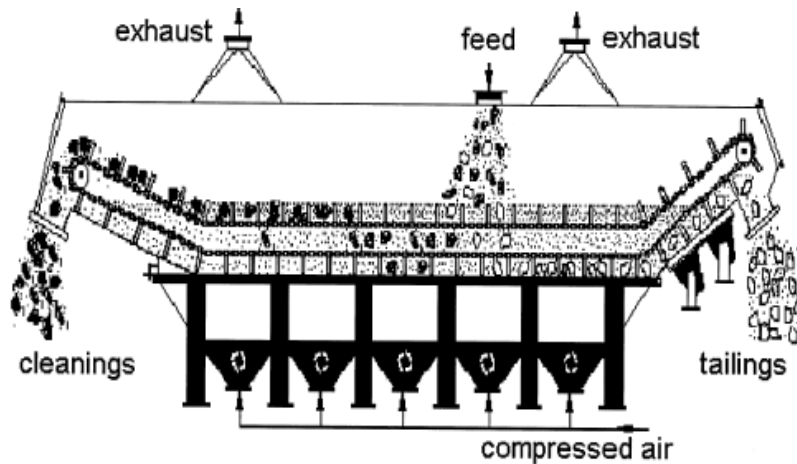


Figure 2.15 The schematic drawing of Air Dense Medium Fluidized Bed by Chen et al.

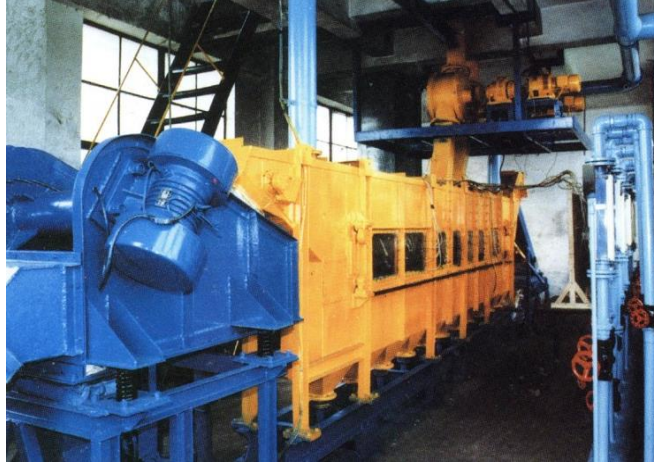


Figure 2.16 The pilot scale Air Dense Medium Fluidized Bed system by Chen et al.

The first commercial ADMFB plant was successfully constructed and operated at the Qitaihe Coal Co. in China since 1994 (Chen et al., 2005), as shown in Figure 2.16. The dimension of the fluidized bed separator was length \times width \times height = 660 mm \times 450 mm \times 550 mm, and the capacity of the separation system was 320, 000 t/a. Magnetite particles with the main size range of 150 – 300 μm were used as the medium material in the ADMFB system, and 6 ~ 50 mm raw coal from Qitaihe Coal Mine was beneficiated efficiently. It was found that the construction and operating costs of the ADMFB plant were only half of that of conventional wet preparation plant. Furthermore, the ADMFB system has the advantages of less energy consumption and without using water. Soon after, another ADMFB plant with the processing capacity of 700, 000 t/a was put into commercial application (Chen et al., 2003(a)).

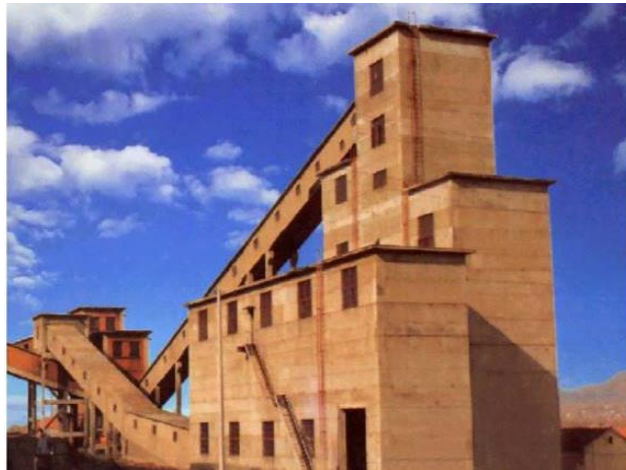


Figure 2.17 The first commercial ADMFB plant at the Qitaihe Coal Co.

Recently, Zhao et al. at China University of Mining and Technology developed a modularized industrial ADMFB system for efficient dry coal beneficiation in cooperation with the Tangshan Shenzhou Manufacturing Co. Ltd. in 2011 (Zhao et al., 2011). As can be observed in Figure 2.18, almost all the operation processes were integrated tightly in a modularized ADMFB unit, including raw coal pre-treatment, fluidized bed separation, separated product cleaning, medium particle circulation, air supply and dust collection, etc. Compared with the conventional ADMFB plant, the construction and labor costs required by the modularized ADMFB system have been reduced by 60% and 80%, respectively, which is also much less than that of the traditional wet preparation plant. An industrial modularized ADMFB plant was established and has been applied at the Xinjiang Energy Co. Ltd. in China since 2013 (Zhang et al., 2014; Zhao et al., 2017). The dimension of the modularized ADMFB system was length \times width \times height = 25 m \times 8 m \times 11 m, and the capacity of coal beneficiation was 40 – 60 t/h. Run-of-mine coal with the size range of 10 ~ 100 mm was beneficiated satisfactorily with a probable error of 0.055 g/cm³. The ash content of clean coal was decreased from 23.98% to 3.46% with an ash rejection of 85.57%, which can be used as the raw material of activated carbon. In addition, the medium particle consumption and operating cost were found to be less than 5 kg and \$2 per ton of coal product, respectively. Therefore, the modularized ADMFB has the advantages of high separation efficiency, low construction and operating costs, and environmental friendly, which provides a solution for dry coal beneficiation.



Figure 2.18 The commercial modularized Air Dense Medium Fluidized Bed by Zhao et al.

2.4 Conclusions and Outlook

The Air Dense Medium Fluidized Bed is well known to be one of the most efficient tools for dry gravity separation of particulate materials according to density differences, especially for the coal beneficiation process. The above literature review summarizes the development and present status of the fluidized bed separation technology, which provides a sufficient background knowledge for the current research work. As can be observed that most of the previous efforts have been devoted to experimental and industrial practices of specific materials separation, and the fundamental theory and separation mechanism of the ADMFB method have been rarely studied in detail. In order to freely adjust the bed density, binary mixtures of solid particles were frequently used as the dense mediums in ADMFB system for various applications. However, not much work has been made to study the basic theory of fluidized bed separation with binary medium particles, and the understanding of binary fluidization system for the gravity separation is very limited. The objective of this work is to comprehensively study the hydrodynamic characteristics and basic mechanism of ADMFB technology with dense medium of both single and binary mixtures of solid particles.

References

- Azimi E., Karimipour S., Nikrityuk P., Szymanski J., Gupta R., 2015. Numerical simulation of 3-phase fluidized bed particle segregation. *Fuel*. 150, 347-359.
- Azimi E., Karimipour S., Rahman M., Szymanski J., Gupta R., 2011(a). Evaluation of the performance of air dense medium fluidized bed (ADMFB) for low-ash coal beneficiation. Part 1: Effect of operating conditions. *Energy Fuels*. 27, 5595-5606.
- Azimi E., Karimipour S., Rahman M., Szymanski J., Gupta R., 2011(b). Evaluation of the performance of air dense medium fluidized bed (ADMFB) for low-ash coal beneficiation. Part 2: Characteristics of the beneficiated coal. *Energy Fuels*. 27, 5607-5616.
- Azimi E., Karimipour S., Xu Z., Szymanski J., Gupta R., 2017. Statistical analysis of coal beneficiation performance in a continuous air dense medium fluidized bed separator. *Int. J. Coal Prep. Util.* 37(1), 12-32.
- Beeckmans J. M., 1980. Method of sorting fluidized particulate material and apparatus therefor. U.S. Patent No. 4194971.
- Beeckmans J. M., Goransson M., Butcher S. G., 1982. Coal cleaning by counter-current fluidized cascade. *Can. Min. Metall. Bull.* 75, 184-191.
- Beeckmans J. M., Minh T., 1977. Separation of mixed granular solids using the fluidized counter current cascade principle. *Can. J. Chem. Eng.* 55, 493-496.
- Chan E. W., Beeckmans J. M., 1982. Pneumatic beneficiation of coal fines using the counter-current fluidized cascade. *Int. J. Min. Process.* 9, 157-165.
- Chen Q. R., 1983. Air dense medium separation technology. *Min. Sci. Technol. Info.* 3, 1-5.
- Chen Q. R., Yang Y. F., Liang C. C., Tao X. X., Luo Z. F., 1993. Air-dense medium fluidized bed dry beneficiation of coal: Results of 50 MTPH demonstration plant. *Coal Prep. 10th international coal preparation exhibition and conference*, Lexington.
- Chen Q. R., Yang Y. F., 2003(a). Development of dry beneficiation of coal in China. *Coal Prep.* 23, 3-12.

Chen Q. R., Wei L. B., 2003(b). Coal dry beneficiation technology in China: The state-of-the-art. *China Part. 1*(2), 52-56.

Chen Q. R., Wei L. B., 2005, Development of coal dry beneficiation with air-dense medium fluidized bed in China. *China Part. 3*, 1-2.

Chikerema P., Moys M., 2012. Effects of particle size, shape, and density on the performance of an air fluidized bed in dry coal beneficiation. *Int. J. Coal Prep. Util.* 32, 80-94.

Choung J., Mak C., Xu Z., 2006. Fine coal beneficiation using an air dense medium fluidized bed. *Coal Prep.* 26, 1-15.

Davidson J. F., Clift R., Harrison D., 1985. *Fluidization: 2nd Edition*. Academic Press, London.

Dickerson J. H., 1935. Method of and apparatus for cleaning coal. U.S. Patent No. 2022588.

Dong X., Beeckmans J. M., 1990. Separation of particulate solids in a pneumatically driven counter-current fluidized cascade. *Powder Technol.* 62, 261-267.

Douglas E., Joy A. S., Walsh T., Whitehead A., 1972. Development of equipment for the dry concentration of minerals. *Filtr. Sep.* 9, 532-544.

Douglas E., Walsh T., 1966. New type of dry heavy medium gravity separator. *Trans. Inst. Min. Metall.* 75, 226-232.

Eveson G. F., 1966. Pneumatic processes used in coal cleaning. *Coal Prep.* 4(8): 135-138.

Eveson G. F., 1968. Dry-cleaning of large or small coal or other particulate materials containing components of different specific gravities. U.S. Patent No. 3367501.

Eveson G. F., Thompson A., 1969. Fluidised-bed apparatus. U.S. Patent No. 3471016.

Firdaus M., Oshea J. P., Oshitani J., Franks G. V., 2012. Beneficiation of coarse coal ore in an air-fluidized bed dry dense-medium separator. *Int. J. Coal Prep. Util.* 32, 276-289.

Franks G. V., Firdaus M., Oshitani J., 2013. Copper ore density separations by float/sink in a dry sand fluidised bed dense medium. *Int. J. Min. Process.* 121, 12-20.

Franks G. V., Forbes E., Oshitani J., Batterham R. J., 2015. Economic, water and energy evaluation of early rejection of gangue from copper ores using a dry sand fluidised bed separator. *Int. J. Min. Process.* 137, 43-51.

Fraser T., 1926. Artificial storm of air-sand floats coal on its upper surface, leaving refuse to sink. *Coal Age*. 29, 325-327.

Fraser T., Yancey H. F., 1925. Process of separation loosely mixed materials. U.S. Patent No. 1534846.

Holmes C. W. H., 1934. Apparatus for separation of dry materials. U.S. Patent No. 1944643.

Kendall M. A., Moore C. C., 1942. Coal cleaner. U.S. Patent No. 2303367.

Kunii D., Levenspiel O., 1991. *Fluidization engineering: 2nd Edition*. Butterworth-Heinemann, United States.

Levin N. D., Yost S. H., 1938. Method of cleaning coal and fluid separating medium therefor. U.S. Patent No. 2108290.

Levy E. K., Kozanoglu B., Agostini M. D., 1987. Mechanical cleaning of coal in an air fluidized beds. *Coal Conference Proceedings, Pittsburgh, U.S.* 8(2), 11-16.

Lockhart N. C., 1984. Dry beneficiation of coal. *Powder Technol.* 40, 17-42.

Luo Z. F., Chen Q. R., 2001. Dry beneficiation technology of coal with an air dense-medium fluidized bed. *Int. J. Min. Process.* 63, 167-175.

Mak C., Choung J., Beauchamp R., Kelly D. J. A., Xu Z., 2008. Potential of air dense medium fluidized bed separation of mineral matter for mercury rejection from Alberta sub-bituminous coal. *Int. J. Coal Prep. Util.* 28, 115-132.

Mohanta S., Chakraborty S., Meikap B. C., 2011. Influence of coal feed size on the performance of air dense medium fluidized bed separator used for coal beneficiation. *Ind. Eng. Chem. Res.* 50, 10865-10871.

Mohanta S., Daram A. B., Chakraborty S., Meikap B. C., 2012. Characteristics of minimum fluidization velocity for magnetite powder used in an air dense medium fluidized bed for coal beneficiation. *Part. Part. Syst. Charact.* 29, 228-237.

Mohanta S., Rao C. S., Daram A. B., Chakraborty S., Meikap B. C., 2013. Air dense medium fluidized bed for dry beneficiation of coal: Technological challenges for future. *Part. Sci. Technol.* 31, 16-27.

Muzyka D., Beeckmans J. M., Jeffs A., 1978. Solids separation in a counter-current fluidized cascade: Jetsam-rich mixtures at total reflux. *Can. J. Chem. Eng.* 56, 286-291.

Oshitani J., Franks G. V., Griffin M., 2010. Dry dense medium separation of iron ore using a gas-solid fluidized bed. *Adv. Powder Technol.* 21, 573-577.

Oshitani J., Kajimoto S., Yoshida M., Franks G. V., Kubo Y., Nakatsukasa S., 2013. Continuous float-sink density separation of lump iron ore using a dry sand fluidized bed dense medium. *Adv. Powder Technol.* 24, 468-472.

Oshitani J., Kawahito T., Yoshida M., Gotoh K., Franks G. V., 2012. Improvement of dry float-sink separation of smaller sized spheres by reducing the fluidized bed height. *Adv. Powder Technol.* 23, 27-30.

Oshitani J., Tani K., Takase K., Tanaka Z., 2004. Fluidized bed medium separation (FBMS) for dry coal cleaning. *J. Soc. Powder Technol. Japan.* 41, 334-341.

Prusti P., Sahu A. K., Biswal S. K., 2015. Prediction of the position of coal particles in an air dense medium fluidized bed system. *Int. J. Min. Sci. Technol.* 25, 421-427.

Rhodes M. J., 2008. *Introduction to particle technology*, 2nd Edition. Wiley, England.

Sahan R. A., 1997. Coal cleaning performance in an air fluidized bed. *Energy Sources.* 19, 475-492.

Sahu A. K., Biswal S. K., Parida A., 2009. Development of air dense medium fluidized bed technology for dry beneficiation of coal – A review. *Int. J. Coal Prep. Util.* 29, 216-241.

Sahu A. K., Tripathy A., Biswal S. K., 2013. Study of particle dynamics in different cross sectional shapes of air dense medium fluidized bed separator. *Fuel.* 111, 472-477.

Sahu A. K., Tripathy A., Biswal S. K., Parida. A., 2011. Stability study of an air dense medium fluidized bed separator for beneficiation high-ash Indian coal. *Int. J. Coal Prep. Util.* 31, 127-148.

Sarunac N., Levy E. K., Ness M., Bullinger C. W., Mathews J. P., Halleck P. M., 2009. A novel fluidized bed drying and density segregation process for upgrading low-rank coals. *Int. J. Coal Prep. Util.* 29, 317-332.

Sekito T., Matsuto T., Tanaka N., 2006. Application of a gas-solid fluidized bed separator for shredded municipal bulky solid waste separation. *Waste Manage.* 26, 1422-1429.

Sekito T., Tanaka N., Matsuto T., 2006. Batch separation of shredded bulky waste by gas-solid fluidized bed at laboratory scale. *Waste Manage.* 26, 1246-1252.

Svensson K. J. V., 1958. Procedure and means for the separation of solid materials of different specific gravities according to the sink-and-float method. U.S. Patent No. 2850166.

Weintraub M., Deurbrouck A. W., 1973. Separation of particulate solids of varying densities in a fluidized bed. U.S. Patent No. 3774759.

Weintraub M., Deurbrouck A. W., Thomas R. H., 1979. Dry-cleaning coal in a fluidized bed medium. U.S. Government Report RI-PTMC-4 (79).

Yoshida M., Nakatsukasa S., Nanba M., Gotoh K., Zushi T., Kubo Y., Oshitani J., 2010. Decrease of Cl contents in waste plastics using a gas-solid fluidized bed separator. *Adv. Powder Technol.* 21, 69-74.

Yoshida M., Oshitani J., Ono Keiko., Ishizashi M., Gotoh K., 2008. Control of apparent specific gravity in binary particle systems of gas-solid fluidized bed. *Kona Powder Part. J.* 26, 227-237.

Zaltzman A., 1993. Apparatus and method for improving density uniformity of a fluidized bed medium, and/or for improved material fluidized bed sorting. U.S. Patent No. 5244099.

Zaltzman A., Feller R., Mizrach A., Schmilovitch Z. 1983. Separating potatoes from clods and stones in a fluidized bed medium. *Trans. A. S. A. E.* 26(4), 987-990.

Zaltzman A., Schmilovitch Z., Mizrach A., 1985. Separating flower bulbs from clods and stones in a fluidized bed. *Can. Agric. Eng.* 27 (2), 63-67.

Zaltzman A., Schmilovitch Z., 1986. Evolution of a potato, fluidized bed medium separator. *Trans. A. S. A. E.* 29(5), 1462-1469.

Zaltzman A., Verma B. P., Schmilovitch Z., 1987. Potential of quality sorting of fruits and vegetables using fluidized bed medium. *Trans. A. S. A. E.* 30(3), 823-831.

Zhang B., Zhao Y., Luo Z., Song S., Li G., Sheng C., 2014. Utilizing an air-dense medium fluidized bed dry separating system for preparing a low-ash coal. *Int. J. Coal Prep. Util.* 34, 285-295.

Zhao Y., Liu. J., Wei X., Luo Z., Chen Q., Song S., 2011. New progress in the processing and efficient utilization of coal. *Min. Sci. Technol.* 21, 547-552.

Zhao Y., Li G., Luo Z., Zhang B., Dong L., Liang C., Duan C., 2017. Industrial application of a modularized dry-coal-beneficiation technique based on a novel air dense medium fluidized bed. *Int. J. Coal Prep. Util.* 37(1), 44-57.

CHAPTER 3

MINIMUM FLUIDIZATION VELOCITY OF BINARY MIXTURES OF MEDIUM PARTICLES IN AN AIR DENSE MEDIUM FLUIDIZED BED

Minimum fluidization velocity of binary mixtures is one of the most important parameters when applying an Air Dense Medium Fluidized Bed (ADMFB) system for dry coal beneficiation. Measurements of minimum fluidization velocities were carried out for binary mixtures of magnetite and sand/gangue/coal particles. The experimental results showed that the minimum fluidization velocity of binary mixtures remained almost unchanged when the volume fraction of magnetite particles was above 50%, whereas it varied significantly when the volume fraction of magnetite particles was below 50%. A new correlation based on the Cheung equation has been developed for predicting the minimum fluidization velocity of binary mixtures in terms of particle size ratio, volumetric composition and incipient fluidization velocity of each component. The extended Cheung equation is in reasonable agreement with almost all the available experimental data in the present work and the literature, and it can be used to accurately estimate the minimum fluidization velocity of binary mixtures of solid particles for ADMFB and other similar fluidized bed operations.

3.1 Introduction

Air Dense Medium Fluidized Bed is well known to be one of the most efficient methods for dry coal beneficiation (Chen and Yang, 2003; Mohanta *et al.*, 2013; Sahu *et al.*, 2009; Zhao *et al.*, 2011), and this technology has been used extensively for iron/copper ore separation (Franks *et al.*, 2015; Oshitani *et al.*, 2011), agricultural products cleaning (Zaltman *et al.*, 1983), municipal solid waste classification (Sekito *et al.*, 2006; Yoshida *et al.*, 2010), etc. For efficient separation, the understanding of fluidization characteristics of the ADMFB is very important (Oshitani *et al.*, 2012; Zhao *et al.*, 2012), especially for modeling and operation purposes. Minimum fluidization velocity is one of the most crucial hydrodynamic parameters that strongly influences the behavior of ADMFB application, which reflects the lower limit of gas flowrate required for

fluidization. Moreover, an accurate prediction of the minimum fluidization velocity of medium particles is an essential prerequisite for the overall design and subsequent scale-up of the ADMFB applications (Choung *et al.*, 2006; Mohanta *et al.*, 2012).

In general, magnetite particles are used as the medium material in ADMFB system for dry coal beneficiation due to the good flowability and magnetic property, which can reduce the consumption of medium particles through the magnetic recovery process (Dwari and Rao, 2007; Mohanta *et al.*, 2011). However, the bed density of fluidizing magnetite particles is usually higher than expected for efficient dry coal beneficiation (Wei *et al.*, 2003; Yoshida *et al.*, 2008;), since the ADMFB is a gravity-based separation method. To obtain the desired bed density, various binary mixtures of solid particles have been processed as medium materials, which may achieve the adjustable bed density and more uniform fluidization for efficient separation performance (Firdaus *et al.*, 2012; Tang *et al.*, 2009; Wei *et al.*, 2003; Weintraub *et al.*, 1979). Therefore, the knowledge of fluidization characteristics, particularly the minimum fluidization velocity, of binary mixtures of medium particles is of great importance for the ADMFB applications.

There are mainly two types of approaches for estimating the minimum fluidization velocity of binary mixtures of solid particles (Asif, 2010; Chayang *et al.*, 1989). The first approach is to treat the binary mixture as mono-component system by developing an equivalent particle diameter and density (Formisani, 1991; Jena *et al.*, 2008; Li *et al.*, 2005; Noda *et al.*, 1986; Paudel and Feng, 2013; Renia *et al.*, 2000), and submit the substituting parameters into the generalized Ergun-type equations that were obtained from the integration of force balance and bed pressure drop relations for single particles (Ergun, 1952). However, for binary fluidization systems, the bed pressure drop may not be equal to the apparent weight of solid particles per unit cross-section area, since some particles only partially fluidized at the incipient fluidization state (Carsky *et al.*, 1987; Formisani *et al.*, 2013; Vaid and Gupta, 1978). Furthermore, unlike the mono-component particles, the bed voidage of binary systems vary significantly with the particle size ratio and size distribution of the two dissimilar solid materials involved (Asif, 2012; Stovall *et al.*, 1986; Yu and Standish, 1991). Unavoidably, there are always some discrepancies between the theory and experiment by this approach, which may result in large error for estimating the minimum fluidization velocity of binary mixtures. The second approach is the use of empirical

correlations which were developed directly from the experimental data. Several formulas have been proposed in the literature (Asif, 2011; Cheung *et al.*, 1974; Chiba *et al.*, 1979; Obata *et al.*, 1982; Rincon *et al.*, 1994), and most of these equations are all in good agreement with particular experimental data. Generally, empirical correlations have the advantage of being more accurate and considerably simpler. It is therefore better for the appropriate estimation of minimum fluidization velocity for binary mixtures of solid particles in limited range of involved variables. However, the validity of the empirical correlation for different binary particle systems needs to be further confirmed.

In the present work, a comprehensive analysis of the minimum fluidization velocity of binary mixtures of medium particles in ADMFB has been studied for dry coal beneficiation. Different existing correlations have been compared for various binary particle systems from both the literature and this work. An attempt has been made to develop a suitable and applicable correlation for predicting the minimum fluidization velocity of binary mixtures based on the Cheung equation (Cheung *et al.*, 1974), which is the most commonly used correlation so far. Almost all the available experimental data have been computed to enable this extended Cheung equation, and the calculated results have been compared with the experimental data in the literature and the present work.

3.2 Experimental

3.2.1 Experimental setup

All experiments were carried out in a gas-solid fluidized bed at ambient condition, as shown in Figure 3.1. The experimental apparatus consists of mainly four parts: (1) air supply; (2) cylindrical bed column with the diameter of 152.4 mm. (3) U-shaped water monometers for the pressure-drop measurement; (4) dust collection device. After being filtered and compressed, the ambient air was sent to fluidize the solid particles in the bed through the air chamber and perforated distributor. The orifice diameter of the perforated distributor is 1.5 mm with the total open area of 11%. The flow rate of inlet air was regulated by a rotameter. A ruler was attached on the outside wall of the bed column to determine the bed height of solid particles. The pressure drop across the fluidized bed was measured by the U-shaped water piezometric pipes connecting

to axial pressure taps mounted on the bed column with the interval of 5 cm. Fine dust generated during fluidization was blown away and gathered by the dust collection device.

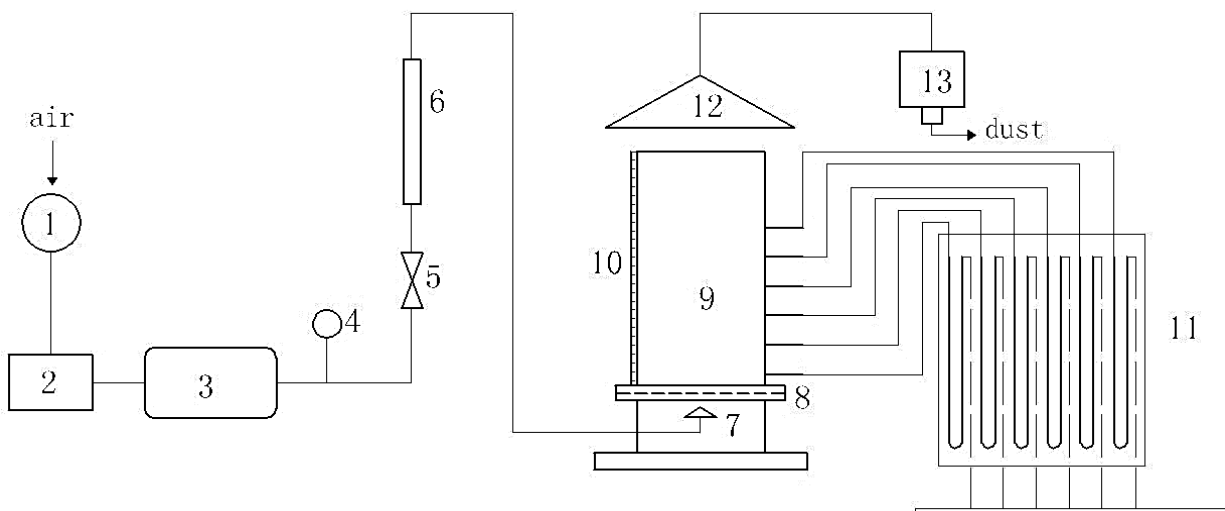


Figure 3.1 The schematic diagram of experimental apparatus: 1. Air filter; 2. Roots blower; 3. Tank; 4. Pressure gague; 5. Valve; 6. Rotameter; 7. Air chamber; 8. Perforated distributor; 9. Cylindrical bed column; 10. Ruler; 11. U-shaped manometer; 12. Dust cover; 13. Dust collector.

3.2.2 Experimental materials

Experiments were performed with binary mixtures of magnetite and sand/gangue/coal particles at various particle compositions. Magnetite particles with the size fraction of 150 – 300 μm which have been found to be the appropriate medium in the ADMFB system (Chen and Yang, 2003; Mohanta *et al.*, 2013; Sahu *et al.*, 2009; Weintraub *et al.*, 1979) were employed as the core material. To achieve the adjustable bed density for efficient coal beneficiation (Tang *et al.*, 2009; Wei *et al.*, 2003; Yoshida *et al.*, 2008), sand/gangue/coal particles with the size ranges of 150 – 300, 300 – 425, 425 – 590, 590 – 710, and 710 – 850 μm were mixed individually with the magnetite to form various binary medium particles in this study. For convenience, binary mixtures of magnetite and sand/gang/coal particles are named as M-S, M-G, and M-C mixtures, respectively. All the solid particles used in the experiment belong to Geldart Group B/D particles, and the properties of these experimental materials are shown in Table 3.1. It should be mentioned that 15 types of binary mixtures were prepared, and 10 different mixture compositions

between *vol.5%* and *vol.95%* with the interval of *vol. 10%* were chosen for each type of binary mixture. Therefore, the total 150 different binary mixtures of medium particles were tested in the present study.

Table 3.1. The properties of experimental materials.

Material	Size range (μm)	Mean diameter (μm)	Density (kg/m^3)	U_{mf} (cm/s)	AOR* ($^\circ$)	Ar	Re_{mf}	Notation
Magnetite	150-300	232	4600	9.5	36.1	2266	1.6	M232
Sand	150-300	224	2650	4.9	33.6	1175	0.8	S224
Sand	300-425	368	2650	12.4	34.5	5208	3.3	S368
Sand	425-590	485	2650	20.2	37.4	11923	7.1	S485
Sand	590-710	636	2650	33.5	38.1	26885	15.4	S636
Sand	710-850	807	2650	39.7	38.5	54924	23.1	S807
Gangue	150-300	215	2100	4	36.5	823	0.6	G215
Gangue	300-425	372	2100	10.9	39.3	4263	2.9	G372
Gangue	425-590	486	2100	18.7	40.2	9505	6.5	G486
Gangue	590-710	625	2100	24.6	41.7	20216	11.1	G625
Gangue	710-850	808	2100	34.1	43.6	43681	19.9	G808
Coal	150-300	245	1300	3.2	38.4	754	0.6	C245
Coal	300-425	396	1300	8	39.3	3182	2.3	C396
Coal	425-590	460	1300	13.5	40.1	4988	4.5	C460
Coal	590-710	617	1300	17.8	42.2	12036	7.9	C617

* Angle of repose (AOR) above 38° is considered cohesive.

3.2.3 Characterization of binary mixtures

The minimum fluidization point of gas-solid fluidized bed with binary mixtures represents the transition between the fixed and fluidized states, and the corresponding gas velocity is defined as minimum fluidization velocity (U_{mf}) which is generally measured by the bed pressure drop against superficial gas velocity curve method (Chiba *et al.*, 1979). A typical pressure-drop-velocity curve of the fluidized bed with a binary mixture (M232-S485-45%) is shown in Figure 3.2 together with the method for determining the minimum fluidization velocity of binary particle system. Compared with the single particle system, binary system has the other feature of incipient and total fluidization velocities (U_{if}/U_{tf}) which have been shown in Figure 3.2. Among these fluidization velocities, the minimum fluidization velocity is much more important for

characterizing a binary system, especially for the modelling and design of various fluidized bed operations.

In order to estimate the minimum fluidization velocity of a binary system, it is necessary to define its surface/volume average particle diameter and density, which are also important for characterizing a binary mixture. By giving the same total surface area per unit apparent weight of the binary system, the effective particle diameter and density can be defined as (Asif, 2011; Formisani *et al.*, 2013; Goossens *et al.*, 1971; Noda *et al.*, 1986),

$$\frac{1}{\bar{\rho}} = \frac{w_F}{\rho_F} + \frac{w_P}{\rho_P} \quad (3.1)$$

$$\frac{1}{\bar{d}_p} = \frac{w_F}{d_F \rho_F} + \frac{w_P}{d_P \rho_P} \quad (3.2)$$

where w is the weight fraction of each component of solid particles, and the subscripts, F and P , are used to distinguish the particle components which have the lower and higher minimum fluidization velocities, respectively. Based on the definitions of effective particle diameter and density, Archimedes number and Reynolds number of a binary mixture can be given by,

$$\bar{Ar} = \rho_g (\bar{\rho}_p - \rho_g) \bar{d}^3 / \mu^2 \quad (3.3)$$

$$\bar{Re}_{mf} = \rho_g U_{mf} \bar{d} / \mu \quad (3.4)$$

Since the binary system has two types of dissimilar particles, the minimum fluidization velocity of binary mixture is not only sensitive to the particle properties of each component, but also to the volumetric composition of binary mixtures. In a binary system, the volume fraction of each component of solid materials can be given by,

$$x_F = w_F \frac{\bar{\rho}}{\rho_F} \quad (3.5)$$

$$x_P = w_P \frac{\bar{\rho}}{\rho_P} \quad (3.6)$$

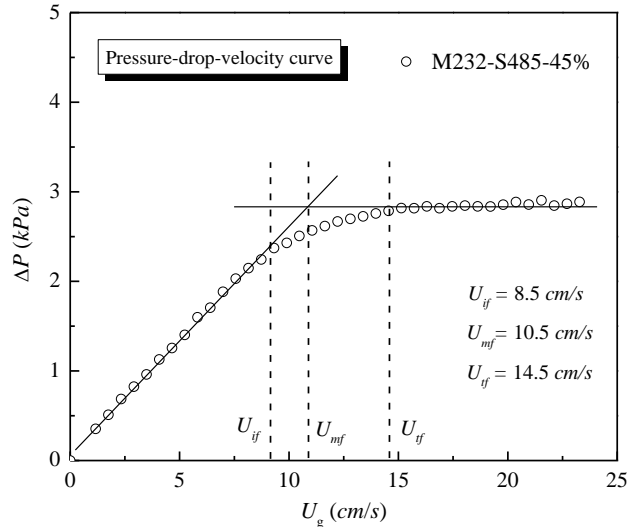


Figure 3.2 A typical pressure-drop-velocity curve of the M232-S485-45% mixture.

3.3 Results and discussion

3.3.1 Minimum fluidization velocity of binary mixtures

Measurements of the minimum fluidization velocity of binary mixtures have been conducted in a gas-solid fluidized bed with the initial bed height of 15 cm. The bed pressure drop against the decreasing superficial gas velocity curve was employed to determine the minimum fluidization velocity to avoid the wedging effect. Binary mixtures of magnetite and sand/gangue/coal particles with various particle compositions have been tested, and the corresponding minimum fluidization velocities are shown in Figures 3.3, 3.4 and 3.5, respectively. It should be noted that all the solid particles involved in this experiment belong to Geldart Group B/D particles.

The relation between the minimum fluidization velocity and the volume fraction of sand particles for M-S mixtures is illustrated in Figure 3.3. It can be seen that, when the volume fraction of sand particles is below *vol.50%*, the minimum fluidization velocity of M-S mixtures remains almost unchanged regardless of the size range of sand particles, and its value is very close to that of mono-component magnetite particles. However, above *vol.50%*, the minimum fluidization velocity of M-S mixtures varies significantly with increasing the volume fraction of sand particles and reaches the maximum/minimum value at pure sand particles. The same trend was

also observed for M-G and M-C mixtures, as can be seen in Figures 3.4 and 3.5, respectively. This is reasonable and can be attributed to the partial fluidization and bed voidage variation of binary systems at minimum fluidization state.

Since the particle size of magnetite is smaller than (or equal to) that of sand, gangue and coal, the magnetite particles will play a dominant role in achieving the minimum fluidization velocity when its proportion is higher than that of sand/gangue/coal particles. It can be explained by the larger/heavier solid particles only partially fluidized at the minimum fluidization state for binary mixtures. At the other extreme, magnetite particles with the relatively smaller size will fill the interparticle voidage formed by the sand/gangue/coal particles when the concentration of magnetite particles is very low, and the minimum fluidization velocity of binary mixtures will decrease as the void fraction reduces. For the design and operation purposes, it is necessary to calculate the minimum fluidization velocity of binary mixtures of solid particles, thus avoiding experimental measurements.

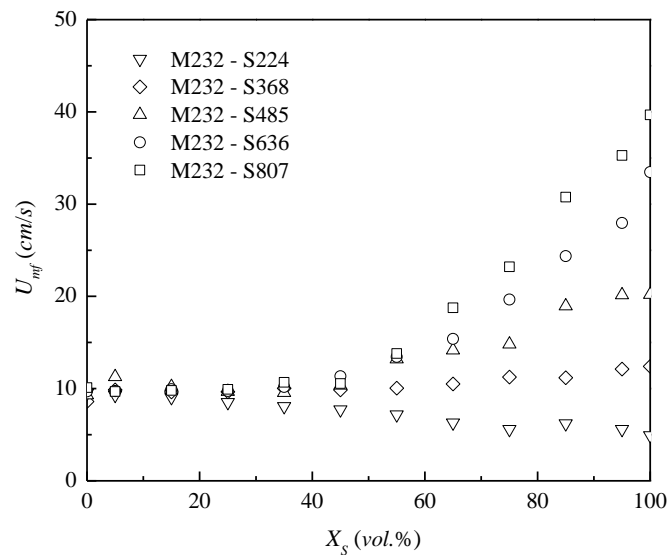


Figure 3.3 The minimum fluidization velocity of binary mixtures of magnetite and sand particles.

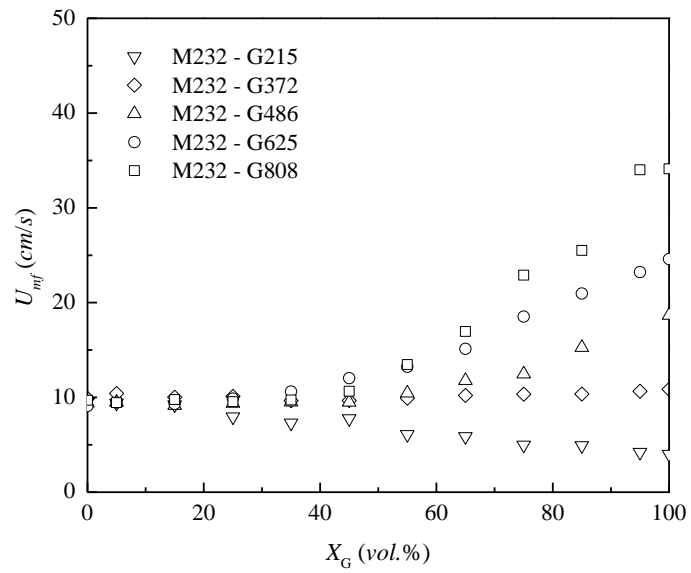


Figure 3.4 The minimum fluidization velocity of binary mixtures of magnetite and gangue particles.

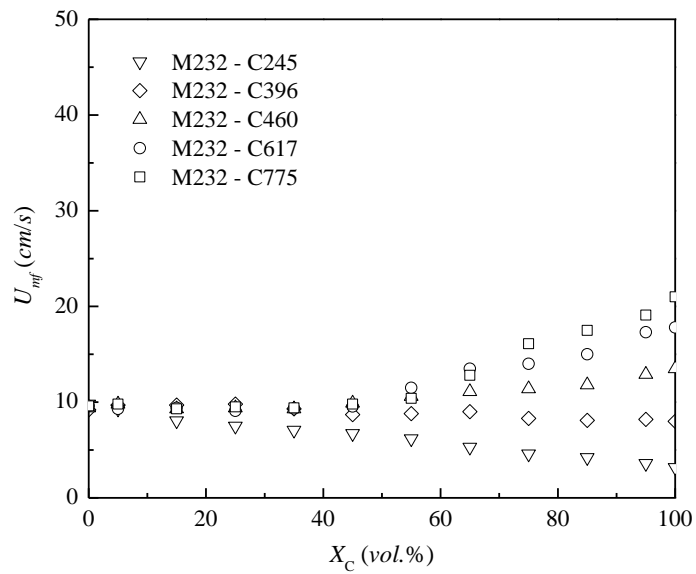


Figure 3.5 The minimum fluidization velocity of binary mixtures of magnetite and coal particles.

3.3.2 Comparison of the correlations for binary mixtures

A number of investigators have carried out experiments involving the gas-solid fluidization of binary mixtures, and details of the experimentally determined minimum fluidization velocities are shown in Table 3.2. The available experimental data in the literature includes both size-difference and density-difference binary systems with the minimum fluidization velocity ranging from 0.1 to 145 *cm/s*. Based on the experimental data in the literature and the current work listed in Table 3.2, the comparison of different correlations for predicting the minimum fluidization velocity of binary systems is shown in Table 3.3.

Five different correlations are used to estimate the minimum fluidization velocity of binary mixtures of solid particles in all cases. As shown in Table 3.3, the correlation proposed by Goossens et al. (Goossens *et al.*, 1971), which treats the binary mixture as the mono-component particle system by introducing the effective particle size and density concepts ignores the significant variation of bed voidage in binary systems. Since the bed voidage is the key factor affecting the incipient fluidization of binary mixtures, this approach may be deficient for such estimation, especially in the case of large particle size ratio of binary mixtures. Besides, the Goossens equation can be applied in the laminar flow region only (Chyang *et al.*, 1989; Goossens *et al.*, 1971). The other four equations listed in Table 3.3 are all empirical correlations which require the knowledge of the minimum fluidization velocity of each particle component in binary systems. The advantages of empirical correlations are very simple and considerably accurate for the limited experimental data, but the validity of these correlations is uncertain when apply to other binary systems. Therefore, in order to obtain a universally applicable correlation, a large amount of binary mixtures covering various solid materials and different particle compositions have been employed to test the validity of these correlations in this work.

Based on 150 data points in the present work and 221 data points listed in Table 3.2, the Cheung equation has been shown to be the most suitable one for the prediction among the correlations listed in Table 3.3, which gives the overall standard deviations of 11.27% and 22.62% for the experimental data in this work and in the literature, respectively. As pointed out by Cheung et al., the minimum fluidization velocity of solid mixtures shows an exponential trend with the mixture composition when the incipient fluidization velocity of each component is known, which should

be more reasonable and reliable for binary systems. Moreover, the Cheung equation has also been recognized as a good correlation for estimating the minimum fluidization velocity of various binary systems by many researchers (Asif, 2014; Carsky *et al.*, 1987; Chyang *et al.*, 1989; Formisani, 1991; Kumoro *et al.*, 2014; Rao *et al.*, 2001; Turrado, *et al.*, 2018). However, the correlation proposed by Cheung *et al.* has some limitations, and it could be further improved, because the ratio of particle sizes cannot be greater than 3 and the exponent 2 in the correlation was found by fitting the limited experimental data (Cheung *et al.*, 1974).

Table 3.2. Literature summary of the minimum fluidization velocity of binary mixtures.

Reference	Bed cross-section (cm)	Material	ρ_p (kg/m ³)	d_p (um)	U_{mf} (cm/s)	Range of Ar	Range of Re_{mf}
Lockett <i>et al.</i> (1973)	3.5	FCC	1150	45~95	0.23~0.27	4.4~25.4	0.007~0.019
Cheung <i>et al.</i> (1974)	14	Glass powder	2520	195~461	2.5~15	737~9736	0.35~4.98
		Bronze	8540	388~550	39~51	19678~56052	10.9~20.2
		Ballotini	2520	271~642	8~36.5	1978~26296	1.56~16.89
Rowe <i>et al.</i> (1975)	-	Catalyst	1150	29~81	0.1~0.5	1.1~24.3	0.002~0.029
Chen <i>et al.</i> (1975)	10	Dolomite	2800	338~1125	11.5~78	4283~157436	2.8~63.3
		Char	702	718	38	10233	7.76
		Copper shot	8900	163~254	9.2~18.2	1520~5754	1.08~3.33
Chiba <i>et al.</i> (1979)	5	Glass bead	2520	115~385	1.6~14.4	151~5671	0.13~3.99
		Hollow char	1080	775	22.5	19811	12.57
		Silica balloons	190	359	0.79	344.5	0.21
		Glass bead	2520	45.4~84.3	13.9~45	9.3~59.5	0.45~2.73
Noda <i>et al.</i> (1986)	16	Sand	2600	45.4~139	16.9~76	9.6~275.4	0.55~7.61
		Rubber	1450	283	114	1296	23.25
		Soya bean	1220	785	145	23261	82.03
Formisani <i>et al.</i> (1991)	10.1	Glass bead	2530	153~483	2.4~21.2	357~11242	0.24~6.8
Marzocchella <i>et al.</i> (2000)	12	Silica sand	2600	125	1.7	200	0.15
		Glass bead	2540	500	22	12521	7.92
		Silica sand	2600	125~500	2.2~19	200~12817	0.2
Olivieri <i>et al.</i> (2004)	12	Silica gel	600	375	3.2	1246	0.87
		Polypropylene	900	500	11	4432	3.96
		Glass bead	2540	500	23	12521	8.29
Formisani <i>et al.</i> (2008)	10	Glass bead	2480	154~612	2.5~32.5	357~22418	0.28~14.33
		Molecular sieves	1460	624~800	21.5~35.5	13984~29468	9.67~20.47

Asif <i>et al.</i> (2010)	6	Steel shots	7600	243~439	17.5~46	25366	14.55
		Ceramic spheres	3760	701	44	51086	22.23
		Sand	2664	550	3.6	17479	1.43
		Plastic particles	1761	2550	26.5	1151254	48.7
Formisani <i>et al.</i> (2011)	10	Glass bead	2480	172~593	2.8~30.8	357~24571	0.24~14.78
		Ceramic spheres	3760	605	43.3	32841	18.88
Paudel <i>et al.</i> (2013)	14.5	Steel shots	7600	243	17.3	4302~25366	3.03~15.09
		Sand	2630	241	7.4	1448	1.28
		Walnut shell	1200	856	55.3	29665	34.11
Kumoro <i>et al.</i> (2014)	10	River sand	2630	241	9	1452~4142	1.56~4.54
		Corn cob	1080	1040	62	47876	46.47

Table 3.3. Summary of the error analysis of various correlations for binary systems.

Reference	Correlation	St. Dev. % - this work	St. Dev. % - literature	Notes
Goossens <i>et al.</i> , (1971)	$U_{mf} = 0.00061 \bar{Ar} \times \mu / (\rho_g \bar{d})$	14.63	39.22	$\bar{Ar} = \rho_g (\bar{\rho}_p - \rho_g) g \bar{d}_p^3 / \mu^2$
Otero <i>et al.</i> , (1971)	$U_{mf} = [x_p U_p + (1 - x_p) U_F]$	30.05	107.49	x_p is the volumetric fraction of larger component
Cheung <i>et al.</i> , (1974)	$U_{mf} = U_F (U_p / U_F)^{x_p^2}$	11.27	22.62	The exponent 2 was found by fitting limited experimental data
Chiba <i>et al.</i> , (1979)	$U_{mf} = U_F (\bar{\rho} / \rho_F) (\bar{d} / d_F)^2$	19.07	40.92	without the knowledge of U_p
Obata <i>et al.</i> , (1982)	$U_{mf} = (w_F / U_F + w_p / U_p)^{-1}$	18.08	32.53	w is the weight fraction of mono-component

3.3.3 Modify the Cheung equation with the experimental data

Compared with the other correlations listed in Table 3.3, the Cheung equation has shown to provide more accurate estimation of minimum fluidization velocity of binary systems in almost all cases. However, there is ample evidence, provided by some researchers (Chyang *et al.*, 1989; Turrado, *et al.*, 2018; Uchida *et al.*, 1983), that the exponent number in the Cheung equation should be an adjustable parameter instead of the constant 2. By analyzing the force balance of binary gas-solid fluidization, the corresponding minimum fluidization velocity not only depends on the properties of solid particles but also sensitive to the bed void fraction which has not yet been included in the original Cheung equation (Asif, 2012; Stovall *et al.*, 1986; Yu *et al.*, 1991). Since the exponent number in the original equation was found by fitting limited number of experimental data, the Cheung equation can be further improved by extensively fitting the recent experimental data and involving the bed voidage effect. For these reasons, the extended Cheung equation is therefore proposed as follow,

$$U_{mf} = U_F (U_P / U_F)^{x_p^n} \quad (3.7)$$

where n is the adjustable parameter which depends on the bed voidage of binary systems at the incipient fluidization state. It is generally known that the ratio of particle sizes is the main factor that affects the bed voidage of solid mixtures, and it is hereby to study the relation between the adjustable parameter n and the particle size ratio.

The relation between the parameter n and the particle size ratio (d_p/d_f) for the M-S mixtures is shown in Figure 3.6 together with the predicting curve calculated by Equation (3.7). The n value was obtained by fitting Equation (3.7) with the experimental data. It can be seen that the n value increases from 0.8 to 2.3 with the increase of particle size ratio (d_p/d_f) from 1.1 to 3.5. A similar trend was also observed for the literature data, as can be seen from Figure 3.7. An examination of all the available data reveals that the calculated n values generally increases with increasing particle size ratio of binary mixtures, and the published data precisely allow to establish a correlation for evaluating the particle size ratio effect. Based on almost all the available experimental data, the adjustable parameter n can be calculated from

$$n = 1.26 \times (d_p / d_f)^{0.53} \quad (3.8)$$

Such particle size ratio is the basic parameter for characterizing a binary mixture, and can be easily obtained from the properties of solid particles. It should be mentioned that the minimum fluidization velocity of each component can be accurately estimated by the popular Ergun-type correlations for single particles, such as Wen and Yu equation (Wen *et al.*, 1966) with the knowledge of average particle size and density. Substituting the Equation (3.8) into the Equation (3.7) and combining with the Wen and Yu equation for single particles, the following correlation for predicting the minimum fluidization velocity of binary mixtures can be obtained.

$$U_{mf} = U_F (U_P / U_F)^{x_p} \quad (3.9)$$

where U_P and U_F can be calculated from the correlation proposed by Wen and Yu (Wen *et al.*, 1966). The Wen and Yu equation is defined as,

$$Re_{mf} = (33.7^2 + 0.0408Ar)^{0.5} - 33.7 \quad (3.10)$$

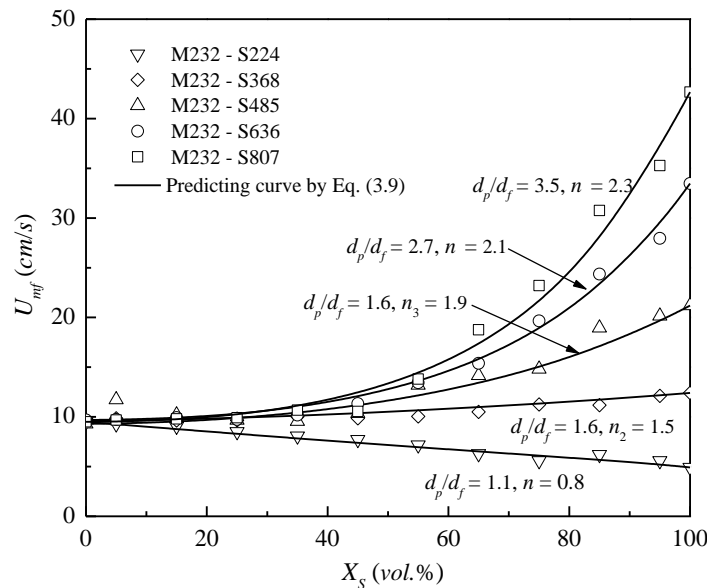


Figure 3.6 Comparison of the U_{mf} calculated by Equation (3.9) with the experimental data in the present work.

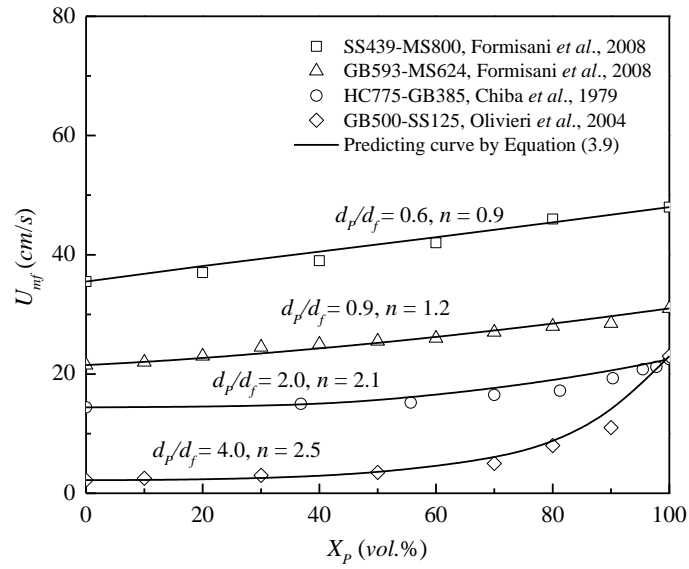


Figure 3.7 Comparison of the U_{mf} calculated by Equation (3.9) with the experimental data in the literature.

3.3.4 Error analysis of the proposed correlation

A comparison of the minimum fluidization velocity of binary mixtures calculated using the proposed Equation (3.9) with almost all the available experimental data is shown in Figure 3.8. It can be seen that this correlation gives an overall standard deviation of 7.14% based on 150 data points with the minimum fluidization velocity ranging from 3.6 to 35.3 cm/s in the present work. Moreover, an overall standard deviation of 17.85% was obtained by this correlation based on 221 data points with the minimum fluidization velocity ranging from 0.13 to 57.5 cm/s in the literature. The difference between the values of the above standard deviations is mainly due to the literature experimental data covers more than twenty different types of materials with a wider particle size/density ranging from 29 to 2250 $\mu m/600$ to 8900 kg/m^3 , while only four different types of materials with the particle size/density ranging from 215 to 808 $\mu m/1300$ to 4600 kg/m^3 were considered in this work. For the sake of comparison, the Cheung equation has been tested and has been found to only give the overall standard deviations of 11.27% and 22.62% for these 150 and 221 data points, respectively, which is less accurate than that of Equation (3.9). Since the Cheung equation has already been deemed to be a good correlation for the prediction, the proposed Equation (3.9) shows better accuracy, and is to be preferred as a better method for estimating the minimum fluidization velocity of binary systems.

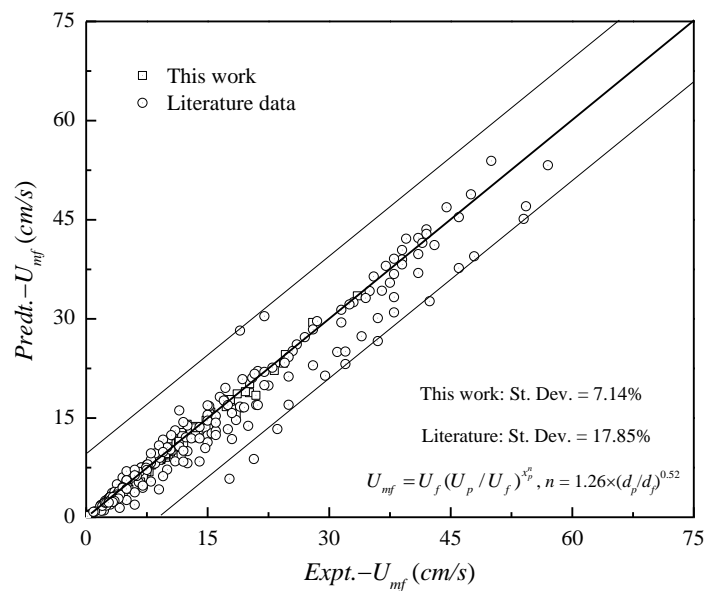


Figure 3.8 Comparison of the U_{mf} calculated by Equation (3.9) with all available experimental data.

3.4 Conclusion

Knowledge of the minimum fluidization velocity of binary mixtures is crucial for design and operation of Air Dense Medium Fluidized Beds for dry coal beneficiation. Minimum fluidization velocities of magnetite mixed with sand/gangue/coal particles were experimentally investigated. It was observed that, when the volume fraction of magnetite is above 50%, addition of sand/gangue/coal particles that is coarser than (or equal to) magnetite particles did not appreciably change the minimum fluidization velocity of binary mixtures, which may be exploited in the optimization of energy consumption for the ADMFB operation. On the contrary, the minimum fluidization velocity of binary mixtures varied significantly when the volume fraction of magnetite was below 50%. A new equation was derived for estimating the minimum fluidization velocity of binary mixtures by extending the correlation proposed by Cheung *et al.*, which required the additional knowledge of particle size ratio (d_p/d_f). Such particle size ratio is the basic parameter for characterizing a binary mixture. Almost all the available experimental data were used to test the validity of this correlation, and it gave an overall standard deviations of 17.85% and 7.14% for the experimental data in the literature and the present work, respectively. Therefore, the proposed correlation based on the Cheung equation is to be preferred as a better method for estimating the minimum fluidization velocity of binary mixtures of solid particles for ADMFB and other similar fluidized bed applications.

Nomenclature

Ar	Archimedes number, <i>dimensionless</i>
\overline{Ar}	Archimedes number of binary mixture, <i>dimensionless</i>
\overline{d}	effective particle diameter of binary mixture, <i>m</i>
d_F	diameter of particles with lower minimum fluidization velocity, <i>m</i>
d_p	diameter of particles with higher minimum fluidization velocity, <i>m</i>
n	adjustable parameter, <i>dimensionless</i>
ΔP	pressure drop of the fluidized bed, <i>Pa</i>
Re_{mf}	Reynolds number at minimum fluidization state, <i>dimensionless</i>
\overline{Re}_{mf}	Reynolds number of binary mixture at minimum fluidization state, <i>dimensionless</i>
U_g	superficial gas velocity, <i>m/s</i>
U_{if}	incipient fluidization velocity, <i>m/s</i>
U_{mf}	minimum fluidization velocity, <i>m/s</i>
U_{tf}	total fluidization velocity, <i>m/s</i>
w_F	weight fraction of particles with lower minimum fluidization velocity, %
w_p	weight fraction of particles with higher minimum fluidization velocity, %
x_F	volumetric ratio of particles with lower minimum fluidization velocity, %
x_p	volumetric ratio of particles with higher minimum fluidization velocity, %

Greek letters

μ	gas viscosity, <i>kg/(m.s)</i>
$\overline{\rho}$	effective particle density of binary mixture, <i>kg/m³</i>
ρ_F	density of particles with lower minimum fluidization velocity, <i>kg/m³</i>
ρ_g	gas density, <i>kg/m³</i>
ρ_p	density of particles with higher minimum fluidization velocity, <i>kg/m³</i>

Acknowledgements

The authors are grateful to the financial support by Natural Science and Engineering Research Council of Canada (NSERC), China Scholarship Council (CSC), and National Natural Science Foundation of China.

References

- Asif M., 2010. Minimum fluidization velocities of binary-solid mixtures: model comparison. *Int. J. Chem. Mol. Nucl. Mater. Metall. Eng.* 4, 243-247.
- Asif M., 2011. Effect of volume-contraction on incipient fluidization of binary-solid mixtures. *Particuology*. 9, 101-106.
- Asif M., 2012. Volume-change of mixing at incipient fluidization of binary solid mixtures: Experimental data and predictive models. *Powder Technol.* 217, 361-368.
- Carsky M., Pata J., Vesely V., Hartman M., 1987. Binary system fluidized bed equilibrium. *Powder Technol.* 51, 237-242.
- Chen J. L. P., Keairns D. L., 1974. Particle segregation in a fluidized bed. *Can. J. Chem. Eng.* 53, 395-402.
- Chen Q. R., Yang Y. F., 2003. Development of dry beneficiation of coal in China. *Coal prep.* 23, 3-12.
- Cheung L., Nienow A. W., Rowe P. N., 1974. Minimum fluidization velocity of a binary mixture of different sized particles. *Chem. Eng. Sci.* 29, 1301-1303.
- Chiba S., Chiba T., Nienow A. W., Kobayashi H., 1979. The minimum fluidization velocity, bed expansion and pressure-drop profile of binary particle mixtures. *Powder Technol.* 22, 255-269.
- Choung J., Mark C., Xu Z., 2006. Fine coal beneficiation using an air dense medium fluidized bed. *Coal Prep.* 26, 1-15.
- Chyang C. S., Kuo C. C., Chen M. Y., 1989. Minimum fluidization velocity of binary mixtures. *Can. J. Chem. Eng.* 67, 344-347.
- Dwari R. K., Rao K. H., 2007. Dry beneficiation of coal – a review. *Miner. Process. Extra. Metall. Rev.* 28, 177-234.
- Ergun S., 1952. Fluid flow through packed columns. *Chem. Eng. Prog.* 48, 89-94.
- Firdaus M., Oshea J. P., Oshitani J., Franks G. V., 2012. Beneficiation of coarse coal ore in an air-fluidized bed dry dense-medium separator. *Int. J. Coal Prep. Util.* 32, 276-289.

Formisani B., 1991. Packing and fluidization properties of binary mixtures of spherical particles. *Powder Technol.* 66, 259-264.

Formisani B., Girmonte R., Longo T., 2008. The fluidization process of binary mixtures of solids: Development of the approach based on the fluidization velocity interval. *Powder Technol.* 185, 97-108.

Formisani B., Girmonte R., Vivacqua V., 2011. Fluidization of mixtures of two solids differing in density or size. *AIChE J.* 57, 2325-2333.

Formisani B., Girmonte R., Vivacqua V., 2013. Fluidization of mixtures of two solids: A unified model of the transition to the fluidized state. *AIChE J.* 59, 729-735.

Franks G. V., Forbes E., Oshitani J., Batterham R. J., 2015. Economic, water and energy evaluation of early rejection of gangue from copper ores using a dry sand fluidised bed separator, *Int. J. Miner. Process.* 137, 43-51.

Goossens W. R. A., Dumont G. L., Spaepen G. L., 1971. Fluidization of binary mixtures in the laminar flow region. *Chem. Eng. Progr. Symp. Ser.* 67, 38-45.

Jena H. M., Roy G. K., Biswal K. C., 2008. Studies on pressure drop and minimum fluidization velocity of gas-solid fluidization of homogeneous well-mixed ternary mixtures in un-promoted and promoted square bed. 145, 16-24.

Kumoro A. C., Nasution D. A., Cifriadi A., Purbasari A., Falaah A. F., 2014. A new correlation for the prediction of minimum fluidization of sand and irregularly shape biomass mixtures in a bubbling fluidized bed. *Int. J. Appl. Eng. Res.* 21561-21573.

Li Z., Kobayashi N., Nisjimura A., Hasatani M., 2005. A method to predict the minimum fluidization velocity of binary mixtures based on particle packing properties. *Chem. Eng. Comm.* 192, 918-932.

Lockett M. J., Gunnarsson G., 1973. The delayed bubbling of gas fluidised beds. *Chem. Eng. Sci.* 28, 666-668.

Marzocchella A., Salatino P., Pastena V.D., Lirer L., 2000. Transient fluidization and segregation of binary mixtures of particles. *AIChE J.* 46, 2175-2182.

- Mohanta S., Chakraborty S., Meikap B. C., 2011. Influence of coal feed size on the performance of air dense medium fluidized bed separator used for coal beneficiation. *Ind. Eng. Chem. Res.* 50, 10865-10871.
- Mohanta S., Daram A. B., Chakraborty S., Meikap B. C., 2012. Characteristics of minimum fluidization velocity for magnetite powder used in an air dense medium fluidized bed for coal beneficiation. *Part. Part. Syst. Charact.* 29, 228-237.
- Mohanta S., Rao C. S., Daram A. B., Chakraborty S., Meikap B. C., 2013. Air dense medium fluidized bed for dry beneficiation of coal: technological challenges for future. *Part. Sci. Technol.* 31, 16-27.
- Noda K., Uchida S., Makino T., Kamo H., 1986. Minimum fluidization velocity of binary mixture of particles with large size ratio. *Powder Technol.* 46, 149-154.
- Obata E., Watanabe H., Endo N., 1982. Measurement of size and size distribution of particles by fluidization. *J. Chem. Eng. Japan.* 15, 23-28.
- Olivier G., Marzocchella A., Salatino P., 2004. Segregation of fluidized binary mixtures of granular solids. *AIChE. J.* 50, 3095-3106.
- Oshitani J., Isei Y. H., Yoshida M., Gotoh K., Franks G. V., 2012. Influence of air bubble size on float-sink of spheres in a gas-solid fluidized bed. *Adv. Powder Technol.* 23, 120-123.
- Oshitani J., Kawahito T., Yoshida M., Gotoh K., Franks G. V., 2011. The influence of the density of a gas-solid fluidized bed on the dry dense medium separation of lump iron ore. *Miner. Eng.* 24, 70-76.
- Otero A. R., Corolla J., 1971. Fluidization of mixtures of solids of distinct characteristics. 1. Fluidization velocities. *Anales de la RSEFQ.* 67, 1207-1219.
- Paudel B., Feng Z. G., 2013. Prediction of minimum fluidization velocity for binary mixtures of biomass and inert particles. *Powder Technol.* 237, 134-140.
- Rao T. R., Rheemarasetti J. V. R., 2001. Minimum fluidization velocities of mixtures of biomass and sands. *Energy.* 26, 633-644.
- Reina J., Velo E., Puigianer L., 2000. Predicting the minimum fluidization velocity of polydisperse mixtures of scrap-wood particles. 111, 245-251.

- Rincon J., Guardiola J., Romero A., Ramos G., 1994. Predicting the minimum fluidization velocity of multicomponent systems. *J. Chem. Eng. Japan.* 27, 177-181.
- Rowe P. N., Nienow A.W., 1975. Minimum fluidization velocity of multi-component particle mixtures. *Chem. Eng. Sci.* 30, 1365-1369.
- Sahu A. K., Biswal S. K., Parida A., 2009. Development of air dense medium fluidized bed technology for dry beneficiation of coal – a review. *Int. J. Coal Prep. Util.* 29, 216-241.
- Sekito T., Matsuto T., Tanaka N., 2006. Application of a gas-solid fluidized bed separator for shredded municipal bulky solid waste separation, *Waste Manage.* 26, 1422-1429.
- Stovall T., Larrard D. F., Buil M., 1986. Linear packing density model of grain mixtures. *Powder Technol.* 48, 1-12.
- Tang L. G., Zhao Y. M., Luo Z. F., Liang C. C., Chen Z. Q., Xing H. B., 2009. The effect of fine coal particles on the performance of gas-solid fluidized beds. *Int. J. Coal Prep. Util.* 29, 265-278.
- Turrado S., Fernandez J. R., Abanades J. C., 2018. Determination of the solid concentration in a binary mixture from pressure drop measurements. *Powder Technol.* 338, 608-613.
- Uchida S., Yamada H., Tada I., 1983. Minimum fluidization velocity of binary mixture. *J. Chinese Inst. Chem. Eng.* 14, 257-264.
- Vaid R. P., Gupta P. S., 1978. Minimum fluidization velocities in beds of mixed solids. *Can. J. Chem. Eng.* 56, 292-296.
- Wei L. B., Chen Q. R., Zhao Y. M., 2003. Formation of double-density fluidized bed and application in dry coal beneficiation. *Coal Prep.* 23, 21-32.
- Weintraub M., Deurbrouck A. W., Thomas R. H., 1979. Dry-cleaning coal in a fluidized bed medium, *RI-PMTC*, 4, 12-15.
- Wen C. Y., Yu Y. H., 1966. A generalized method for predicting the minimum fluidization velocity. *AIChE J.* 12, 610-612.
- Yoshida M., Oshitani J., Ono K., Ishizashi M., Gotoh K., 2008. Control of apparent specific gravity in binary particle systems of gas-solid fluidized bed. *Kona Powder Part. J.* 26, 227-237.

Yoshida M; Nakatsukasa S., Nanba M., Gotoh K., Zushi T., Kubo Y., Oshitani J., 2010. Decrease of Cl contents in waste plastics using a gas-solid fluidized bed separator, *Adv. Powder Technol.* 21, 69-74.

Yu A. B., Standish N., 1991. Estimation of the porosity of particle mixtures by a linear-mixture packing model. *Ind. Eng. Chem. Res.* 36, 1372-1385.

Zaltman A., Feller R., Mizrach A., Schmilovitch Z., 1983. Separation potatoes from clods and stones in a fluidized bed medium, *Trans. ASAE.* 26, 987-990.

Zhao Y. M., Liu J. T., Wei X. Y., Luo Z. F., Chen Q. R., Song S. L., 2011. New progress in the processing and efficient utilization of coal. *Miner. Sci. Technol.* 21, 547-552.

Zhao Y. M., Tang L. G., Luo Z. F., Liang C. C., Xing H. B., Duan C. L., Song S. L., 2012. Fluidization Characteristics of a fine magnetite powder fluidized bed for density-based dry separation of coal. *Sep. Sci. Technol.* 47, 2256-2261.

CHAPTER 4

MINIMUM FLUIDIZATION VELOCITY GROWTH DUE TO BED INVENTORY INCREASES IN AN AIR DENSE MEDIUM FLUIDIZED BED

Minimum fluidization velocity is one of the most important fluidization characteristics when applying Air Dense Medium Fluidized Bed (ADMFB) to dry coal beneficiation. Measurements were carried out for magnetite particles (150 – 300 μm) and binary mixtures of magnetite mixed with sand/gangue/coal particles (300 – 425 μm) to determine the influence of bed inventory on the characteristics at incipient fluidization state. The experimental results showed that minimum fluidization velocities of both single and binary mixtures of solid particles increase with increasing bed mass, which has not properly accomplished by the existing equations. The correlation proposed by Wen and Yu has been modified to predict the minimum fluidization velocity as a function of bed inventory. It only requires the knowledge of Archimedes number and the pressure drop of fluidized bed. This correlation is in reasonable agreement with almost all available data in the literature and the present work.

4.1 Introduction

Air Dense Medium Fluidized Bed technology, which utilizes the liquid-like flow behavior of gas-solid fluidized bed to achieve the coal dry beneficiation, was firstly proposed by T. Fraser et al (Fraser *et al.*, 1925; Fraser, 1926). The raw coal constituents can be effectively separated according to their densities in a particular fluidized bed separator. This method has the inherent advantage of functioning without process water (Douglass *et al.*, 1966; Iohn, 1971; Chen *et al.*, 2003; Houwelingen *et al.*, 2004), which provides an efficient way for dry coal cleaning in arid and prolonged cold areas. Furthermore, this technology is widely applicable, and it has already extended to iron/copper ore beneficiation (Oshitani *et al.*, 2013; Oshitani *et al.*, 2013; Franks *et al.*, 2013; Franks *et al.*, 2015), agricultural products cleaning (Zaltman *et al.*, 1983; Zaltzman *et al.*, 1985; Zaltzman *et al.*, 1987), municipal solid waste classification (Sekito *et al.*, 2006; Sekito *et al.*, 2006; Yoshida *et al.*, 2010), etc. The separation performance of ADMFB is strongly

dependent on the uniformity and dynamic stability of gas-solid fluidized bed. Therefore, for an efficient separation, many factors related to the overall design and operation of this fluidized bed should be carefully investigated.

Minimum fluidization velocity (U_{mf}) is recognized as one of the most important parameters when characterizing an ADMFB, especially for proper design of the air supply system and control of the separation process. Since the fluidized bed separator is horizontally placed to extend the residence time of coal separation process, the accurate estimation of minimum fluidization velocity becomes increasingly important for the ADMFB operation due to the large bed cross-section area. Moreover, an accurate prediction of the minimum fluidization velocity is also essential for the theoretical understanding of the fluidization hydrodynamics in various fluidized bed operations. In the past decades, a number of correlations (Wen and Yu, 1966; Richardson and Jeronimo, 1979; Phillai and Rao, 1971) have been proposed to predict the minimum fluidization velocity, which are almost all derived from the generalized Ergun-like equation (Ergun, 1952) that obtained from the integrating analysis of force balance and pressure drop relations. However, these correlations fail to incorporate the influence of bed inventory on the incipient fluidization, which is deemed to be of great importance for industrial scale fluidized bed operations, such as ADMFB and many other chemical reactors. In general, minimum fluidization velocity of the same material has been considered to be constant in the existing correlations (Wen and Yu, 1966; Richardson and Jeronimo, 1979; Phillai and Rao, 1971). As a matter of fact, the minimum fluidization velocity increases with the increasing of bed mass (Delebarre, 2004). The greater the Archimedes number (e.g., the greater the particle size or density), the greater the effect of bed inventory on the minimum fluidization velocity (Delebarre *et al.*, 2004). It may be explained by the gas expansion phenomenon that delays the incipient fluidization of fluidized bed (Delebarre *et al.*, 2004; Kusakabe *et al.*, 1989; Delebarre *et al.*, 2002). In recent years, researchers (Granfield and Geldart, 1974; Denloye, 1982; Thonglimp *et al.*, 1984; Tannous *et al.*, 1994; Gunn and Hilal, 1997; Caicedo *et al.*, 2002; Delebarre *et al.*, 2004; Rao *et al.*, 2010) have carried out many experiments in dealing with the bed inventory influence on fluidization characteristics, which allow to estimate precisely the relevance of minimum fluidization velocity.

Comprehensive analyses of experimental data conducted in the present work as well as in the literature show that the minimum fluidization velocities of both monodispersed and binary mixture of solid particles are highly dependent on the bed pressure drop, which indicates the weight of bed inventory per unit cross-sectional area of the fluidized bed. An attempt has been made to develop a suitable correlation for predicting the minimum fluidization velocity considering the bed inventory effect. A new correlation based on *Wen and Yu* equation (Wen and Yu, 1966) has been proposed considering the available data. The calculated results using the proposed equation have been compared with almost all the available experimental data.

4.2 Theory

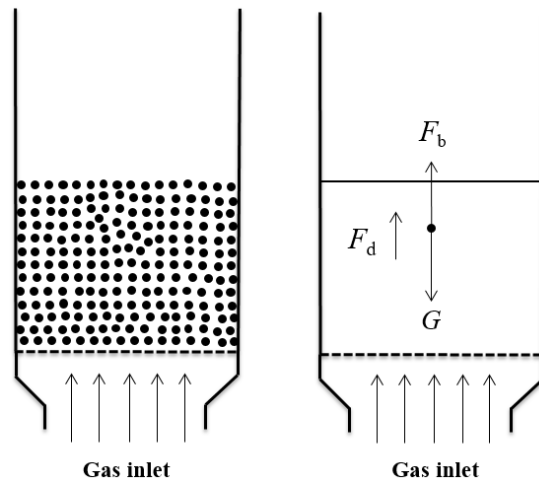


Figure 4.1 The schematic diagram of the minimum fluidization state.

The minimum fluidization velocity, in a gas-solid fluidized bed, represents the transition velocity between the fixed and fluidized states, as shown in Figure 4.1. At the transition point, the pressure drop across the fluidized bed appears to be equal to the apparent weight of the solid particles per unit area of the cross-section, which can be written as

$$\Delta P = W_{bed} / A = gH_{mf}(1 - \varepsilon)(\rho_p - \rho_g) \quad (4.1)$$

The pressure drop through a porous fluidized bed can also be obtained from a force balance on the continuous phase

$$\Delta P = \sum F / (\varepsilon A) \quad (4.2)$$

where ΣF is the sum of the forces acting on the continuous phase. In a gas-solid fluidized bed, the ΣF is composed of the gas weight and the friction of solids on the gas flow. As is known that the friction of solids on the gas flow is equivalent to the friction of gas flow on the solid particles in the opposite direction. Thus, the forces acting on the continuous phase can be given by

$$\Sigma F = \rho_g g \varepsilon V - \Delta F \quad (4.3)$$

where ΔF is the frictional pressure drop. The frictional pressure drop on the solid results from the combination of skin friction (F_s) and form drag (F_f) (Ergun, 1952), where

$$F_s = k_1 \mu U_g \Delta S / (\varepsilon D_h) \quad (4.4)$$

$$F_f = k_2 U_g^2 \Delta S / \varepsilon^2 \quad (4.5)$$

Generally, the gas weight is small indeed and can almost be neglected in comparison with the frictional pressure drop. Then, the total pressure drop per unit bed height can be given as

$$-\Delta P / H = [k_1 \mu U_g \Delta S / (\varepsilon D_h) + k_2 U_g^2 \Delta S / \varepsilon^2] / (\varepsilon A H) \quad (4.6)$$

where the specific solid surface (ΔS) is defined by

$$\Delta S = 6(1 - \varepsilon) A H / (\psi d_p) \quad (4.7)$$

and the hydraulic diameter (D_h) is defined by

$$D_h = (2/3) \psi d_p \varepsilon / (1 - \varepsilon) \quad (4.8)$$

Substituting the specific solid surface and hydraulic diameter into Equation (4.6), the frictional pressure drop equation, thus, can be deduced to

$$-\Delta P / H = k'_1 \mu U_{mf} (1 - \varepsilon)^2 / (\varepsilon^3 \psi^2 d_p^2) + k'_2 \rho_g U_{mf}^2 (1 - \varepsilon) / (\varepsilon^2 \psi d_p) \quad (4.9)$$

where k'_1 and k'_2 are empirical constants. Ergun has fitted this correlation with the help of 640 experiments that carried out with various gases and solids introducing two constants whose values are 150 and 1.75, which is one of the most widely used equations for predicting the

minimum fluidization. By introducing the Reynolds number (Re_{mf}) and Archimedes number (Ar), the Ergun equation then becomes

$$Ar = 150Re_{mf}(1 - \varepsilon)/(\psi^2\varepsilon^3) + 1.75Re_{mf}^2/(\psi\varepsilon^3) \quad (4.10)$$

where

$$Ar = \rho_g(\rho_p - \rho_g)gd_p^3/\mu^2 \quad (4.11)$$

$$Re_{mf} = \rho_g d_p U_{mf}/\mu \quad (4.12)$$

Despite the availability of the Ergun equation, it is still often difficult to accurately predict the minimum fluidization velocity, which can be attributed to the uncertainty associated with the bed voidage at the minimum fluidization state. Even a small error in its specification could result in a significant error. Therefore, proceeding from the fundamental Equation (4.10), several researchers have proposed particular simplified forms, replacing the shape factor (ψ) and bed voidage at minimum fluidization (ε) by numerical values. By rearranging the Equation (4.10) leads to

$$Re_{mf} = -C_1 + (C_1^2 + C_2 Ar)^{0.5} \quad (4.13)$$

where

$$C_1 = 42.86(1 - \varepsilon)/\psi \quad C_2 = 0.571\psi\varepsilon^3 \quad (4.14)$$

Various values have been proposed for the empirical constants (C_1/C_2) by many investigators (Davies and Richardson, 1966; Richardson et al., 1979; Thonglimp et al., 1984.), and the corresponding correlations have been established. Among these, the Wen and Yu correlation introducing the constants of 33.7 and 0.0408 for C_1 and C_2 is the most commonly used correlation. However, these correlations considering the two coefficients as constants all neglect the effects of bed inventory on the fluidization characteristics. Thus, for more accurate and reliable prediction of minimum fluidization velocity, a comprehensive correlation is proposed as

$$Re_{mf} = [-C_1 + (C_1^2 + C_2 Ar)^{0.5}] \times f(\Delta P) \quad (4.15)$$

where $f(\Delta P)$ is the influence of bed inventory on incipient fluidization, which has been experimentally determined in the present work.

4.3 Experimental

4.3.1 Experimental setup

Experiments were conducted in three cylindrical fluidized beds at ambient condition, as shown in Figure 4.2. The experimental setup consists of mainly four parts: (1) air supply including an air filter, a roots blower, and a tank; (2) fluidized bed columns with the inner diameters of 101.6, 152.4 and 203.2 mm. (3) *U*-shaped monometer for pressure-drop measurement; (4) dust collection device. After being filtered, the ambient air was sent to fluidize the solids in the column through the air chamber and perforated distributor. The distributor is made of two plastic perforated plates with filter cloth in between, and the orifice diameter is 1.5 mm with the total open area of 11%. In order to investigate the fluidization characteristics of the fluidized bed, the *U*-shaped piezometric pipes were connected to the axial pressure taps on the side of the column. Fine dust generated during fluidization in the experiment was collected by the dust collector device.

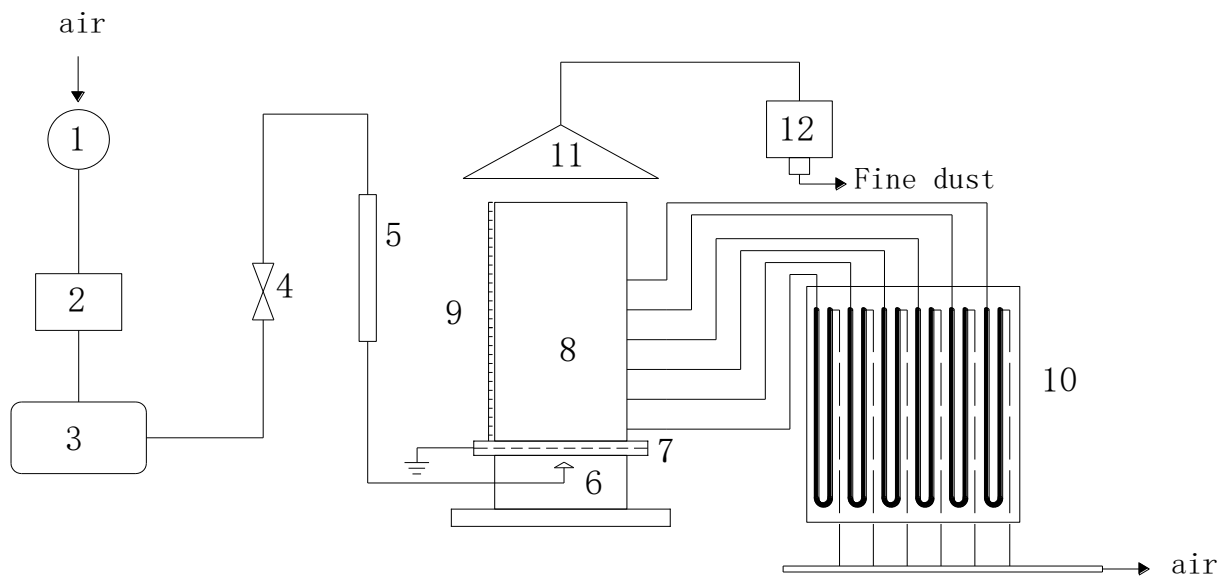


Figure 4.2 The schematic diagram of experimental apparatus: 1. Air filter; 2. Roots blower; 3. Tank; 4. Valve; 5. Rotameter; 6. Air chamber; 7. Bed distributor; 8. Fluidized bed column; 9. Ruler; 10. *U*-shaped manometers; 11. Dust cover; 12. Dust collector.

4.3.2 Experimental materials

Measurements were made to study the variation in minimum fluidization velocity with increasing bed inventory for the medium particles in the ADMFB system. Magnetite, sand, gangue, and coal powders were used in these experiments. The magnetite powder (150 – 300 μm) was found to be the appropriate core materials in ADMFB (Iohn, 1971; Chen and Wei, 2003). The three other materials with the same volume fraction of 25% were added separately to form binary mixtures for the bed density adjustment (Weintraub *et al.*, 1979; Beeckmans *et al.*, 1982; Yoshida *et al.*, 2008; Luo and Chen, 2001; Tang *et al.*, 2009). These added materials with the size range of 300 – 425 μm were chosen to balance the density difference with magnetite powder during fluidization. For convenience, the three types of binary mixtures are named as: MS mixture (magnetite 150 – 300 μm , vol. 75% with sand 300 – 425 μm , vol. 25%), MG mixture (magnetite 150 – 300 μm , vol. 75% with gangue 300 – 425 μm , vol. 25%), MC mixture (magnetite 150 – 300 μm , vol. 75% with coal 300 – 425 μm , vol. 25%). The properties of the experimental materials and binary mixtures are shown in Tables 4.1 and 4.2, respectively.

Table 4.1. The properties of experimental materials.

Particle properties	Magnetite	Sand	Gangue	Coal
Particle size range (μm)	150 – 300	300 – 425	300 – 425	300 – 425
Mean particle diameter (μm)	221	351	386	366
Particle true density (kg/m^3)	4600	2530	2060	1425
Aerated bulk density (kg/m^3)	2630	1510	1250	875
Angle of repose ($^\circ$)	36.1	34.5	39.5	40.3
Avalanche angle ($^\circ$)	42.5	41.1	42.9	43.8

Table 4.2. The properties of binary mixtures of solid particles.

Particle properties	MS mixture	MG mixture	MC mixture
Particle size range (μm)	150 – 425	150 – 425	150 – 425
Mean particle diameter (μm)	266	275	263
Particle true density (kg/m^3)	3980	3890	3770
Aerated bulk density (kg/m^3)	2280	2180	2090
Angle of repose ($^\circ$)	35.6	37.5	39.3
Avalanche angle ($^\circ$)	41.5	42.3	43.9

4.4 Results and discussion

4.4.1 The effect of bed inventory on the minimum fluidization

Minimum fluidization velocity in gas-solid fluidized beds is generally determined using the graph of bed pressure drop against superficial gas velocity (Phillai and Rao, 1971). It has also been customary to use Reynolds number to represent the incipient fluidization where its definition is given in Equation (4.12). In the present work, different weighed amount of solids were charged to vary the pressure drop of fluidized bed ranging from 1 *kPa* to 7 *kPa*, and the plots of Reynolds number against the bed pressure drop in three different fluidized beds are illustrated in Figure 4.3.

It can be seen that the magnetite powder as well as the MS/MG/MC mixtures all demonstrate an increasing trend of Reynolds number with increasing bed pressure drop. This rising Reynolds number indicates an increasing minimum fluidization velocity for the same material as the bed inventory increases. The same tendency for magnetite powder has also been claimed elsewhere (Sahu *et al.*, 2011; Sahu *et al.*, 2013). Some authors (Granfield and Geldart, 1974; Denloye, 1982) have attributed this to the increase of the ratio in pressure drop to particle weight per unit area of the bed cross-section. Others (Delebarre, 2002; Delebarre, 2004; Kusakabe *et al.*, 1989; Delebarre *et al.*, 2002) explained that it may be due to the gas expansion phenomenon, which delays the fluidization of particles at the bottom of bed whereas the upper part is already fluidized. For the design and operation purposes, it is very important to calculate the minimum fluidization velocity as a function of the bed inventory effect, thus avoiding experimental measurements.

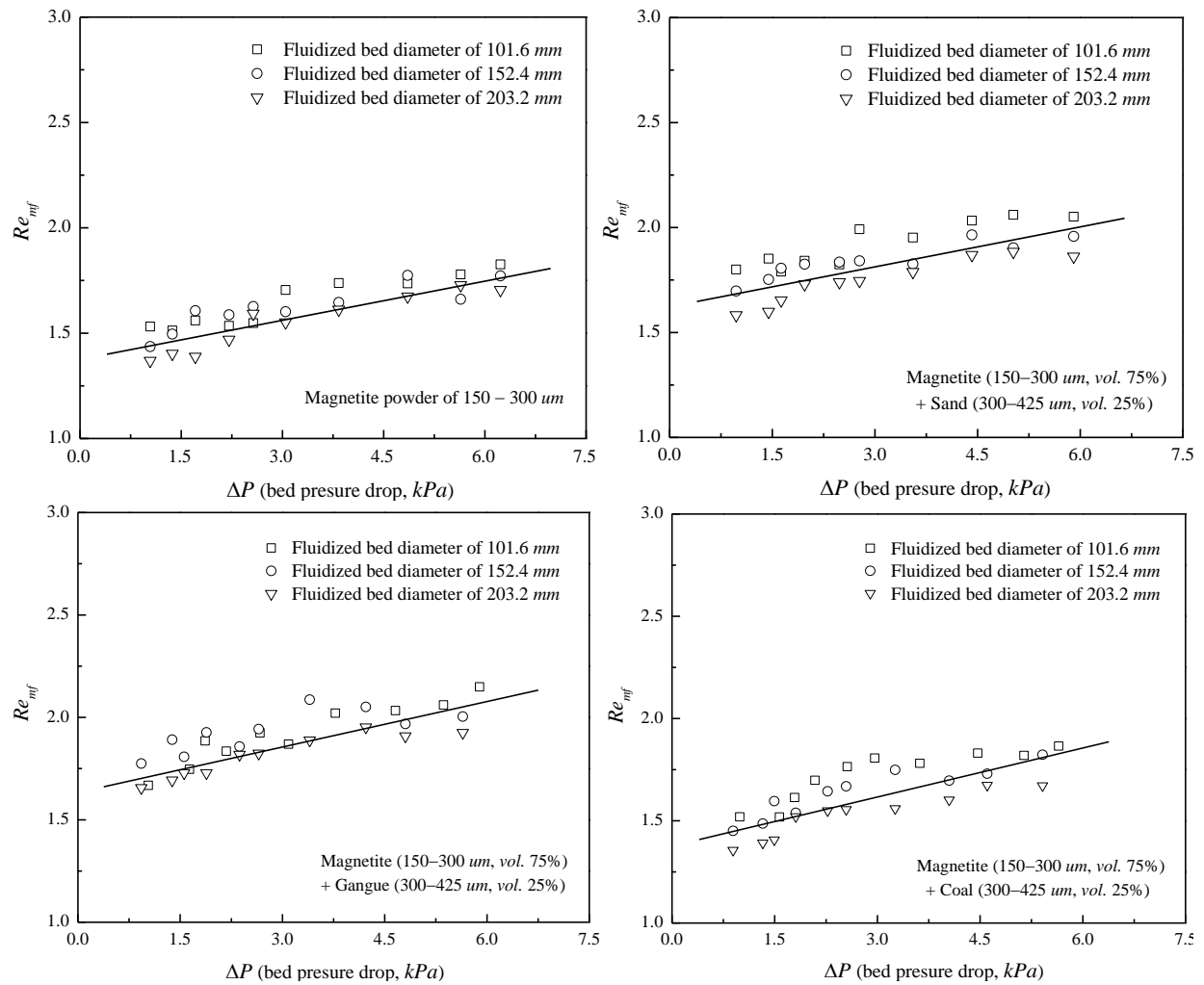


Figure 4.3 Dependence of Reynolds number on the bed pressure drop.

4.4.2 The correlation for estimating minimum fluidization velocity

The influences of bed inventory on fluidization characteristics have been extensively studied (Granfield and Geldart, 1974; Denloye, 1982; Thonglimp *et al.*, 1984; Tannous *et al.*, 1994; Gunn and Hilal, 1997; Caicedo *et al.*, 2002, Delebarre *et al.*, 2004; Rao *et al.*, 2010; Tang *et al.*, 2009; Sahu *et al.*, 2011), and Table 4. 3 shows the experimental details. An analysis of almost all available data reveals that the minimum fluidization velocity steadily increases with increasing bed mass. The increasing of bed inventory will lead to higher pressure drop at the bottom region, which may delay the overall minimum fluidization of fluidized bed. Then, the variation ratio of Reynolds numbers is employed, and is defined by

$$\varphi = (Re_{mf} - Re'_{mf})/Re'_{mf} \quad (4.16)$$

where Re_{mf} and Re'_{mf} are the actual and reference Reynolds numbers, respectively. The relationship between the variation ratio of Reynolds number and the bed pressure drop is presented in Figure 4.4 together with the curve calculated using non-linear fitting method. Such fitting results can be described by a simple empirical expression

$$\ln(\varphi) = -14.45\Delta P^{-0.3} \quad (4.17)$$

Substituting Equation (4.16) into the Equation (4.17) and combining with Wen and Yu equation (Wen and Yu, 1966), the following correlation for predicting the minimum fluidization velocity considering the influence of bed inventory has been obtained

$$Re_{mf} = [(33.7^2 + 0.0408Ar)^{0.5} - 33.7]/[1 - \exp(-14.45\Delta P^{-0.3})] \quad (4.18)$$

The Reynolds number at the static bed height of 5 *cm* was used as the reference Reynolds number for each experiment, as this is the lowest bed height away from the bubble jet zone. Moreover, the experimental data of binary mixtures were excluded in the calculation of the correlation.

Table 4.3. Literature summary of minimum fluidization velocity in the case of bed inventory.

Reference	Cross-section (cm)	Particle properties			Bed height (cm)	U_{mf} (cm/s)	Ar	Re_{mf}	
		Type	ρ_p (kg/m ³)	d_p (um)					
Granfield <i>et al.</i> , 1974	61×2	Alumina	1150	1520	5~30	51~64	159166	47.1~70.1	
	15			670		47		120.9	
Denloye <i>et al.</i> , 1982	15	Sand	2600	1020	5~30	40~45	110903	29.4~33.8	
				670		37~42		29652	17.9~20.3
Thonglimp <i>et al.</i> , 1984	5~19.4	Glass bead	2500	900	2~60	42~60	71871	27.2~38.9	
				1425		83~88		285279	85.2~90.4
				2125		105~122		946024	161~184
Caicedo <i>et al.</i> , 2002	20×1.2	Glass ballotini	2550	375	2~60	16~38	3452	3.7~8.9	
				595		34~90		21183	14.6~38.6
				89		8.6~34.4		1.5~2.8	56
Delebarre <i>et al.</i> , 2002	19.2	Sand	2640	183	6.5~26.1	5~6.5	638	0.66~0.86	
		Spent cracking catalyst	1550	77	11.1~44.4	1.4~2.6	28	0.08~0.14	
	9.6×9.6	Alumina	2000	89	8.6~17.4	1.2~1.8	56	0.08~0.12	
	9.6×9.7	Sand	2640	183	6.5~13.2	5.6~6	638	0.74~0.79	
	9.6×9.8	Spent cracking catalyst	1550	77	11.1~22.4	1.4~2.2	28	0.08~0.12	
			Glass	2500	116		1.8~4.2	154	0.15~0.35
			Glass	2500	231		3.9~7.2	1215	0.65~1.20
			Glass	2500	275		5.8~8.8	2050	1.15~1.75
			Glass	2500	385		9.6~13.3	5626	2.65~3.70
			Glass	2500	462		14.1~18.3	9722	4.70~6.10
1.6	Glass	2500	550		16.9~21.4	16403	6.70~8.50		
		Polystyrene	1250	275		3.5~8.3	1025	0.70~1.65	
		Polystyrene	1250	328	1.4~9.9	4.2~7.2	1739	1.00~1.70	
		Glass	2500	116		1.7~2.5	154	0.14~0.21	
		Glass	2500	231		4.1~6.6	1215	0.68~1.10	
		Glass	2500	275		5.9~7.1	2050	1.16~1.40	
		Glass	2500	385		9.4~10.5	5626	2.60~2.90	
		Glass	2500	462		13.5~15.3	9722	4.50~5.10	
		Glass	2500	550		19.2~20.4	16403	7.60~8.10	
		Polystyrene	1250	275		3.3~4.04	1025	0.65~0.80	
Polystyrene	1250	328	4.0~5.3	1739		0.95~1.25			
Sahu <i>et al.</i> ,	8.9×8.9	Magnetite	4700	7.26		7~43.8	1.2~4.2	220	0.06~0.19

2011	15.4×5				7~48	1.8~3.1	220	0.09~0.16
Present work	10.16	Magnetite	4600	232	5~30	8.7~10.4	2266	1.46~1.81
	15.24					8.9~9.9		1.50~1.69
	20.32					8.4~9.6		1.39~1.62
	10.16	Magnetite and sand	3980	266	5~30	9.4~10.7	3301	1.87~2.14
	15.24					8.9~10.2		1.76~2.03
	20.32					8.3~9.7		1.64~1.96
	10.16	Magnetite and gangue	3980	275	5~30	8.4~10.8	3226	1.67~2.16
	15.24					8.9~10.4		1.78~2.01
	20.32					8.4~9.7		1.66~1.96
	10.16	Magnetite and coal	3770	263	5~30	8.0~9.8	3126	1.59~1.96
	15.24					7.7~9.6		1.52~1.91
	20.32					7.2~8.8		1.42~1.75

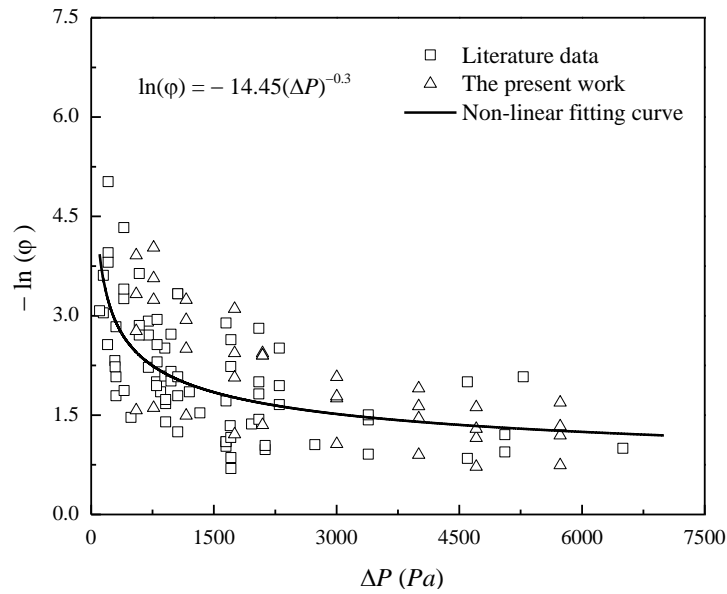


Figure 4.4 Relations between the variation ratio of Reynolds number and bed pressure drop.

4.4.3 Error analysis of the correlation for minimum fluidization velocity

The error analysis of the proposed correlation for minimum fluidization velocity with the available data in literature and the present work is shown in Figure 4.5. As can be seen that the Equation (4.18) gives an overall R -squared value of 0.91 based on 191 experimental data points in the superficial gas velocity range of 0.01 to 1.35 m/s , which shows a good agreement. For the sake of comparison, Wen and Yu equation has also been tested against the same 191 data points, and found to only give an average R -squared of 0.86. Hence, the proposed correlation has the advantage of being considerably simpler with greater accuracy over the Wen and Yu equation, and is to be preferred as a better method of prediction. Moreover, the experimental data of binary mixtures in the present work were included in the comparison for validation of Equation (4.18), and an average R -squared of 0.93 based on 120 points have been obtained. It is noted that, for binary mixtures, the combination of the Wen and Yu equation and the correlation by Cheung *et al.* (Cheung *et al.*, 1974) was used to calculate the theoretical minimum fluidization velocity. Therefore, the proposed correlation is of wide application, which can be used to accurately predict the minimum fluidization velocity for both monodispersed and binary mixture of solid particles as a function of bed inventory.

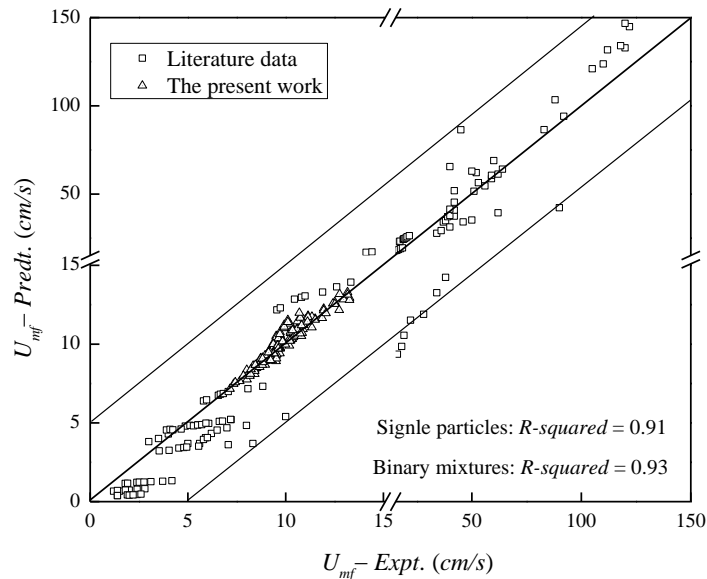


Figure 4.5 Error analysis of the proposed correlation for the available experimental data.

4.4.4 Comparison with the experimental data

A comparison of the minimum fluidization velocities calculated using Equation (4.18) with the literature data and the experimental data of the present work are shown in Figure 4.6. As can be observed that the bed inventory does have a diverse influence on the incipient fluidization of fluidized beds. The calculated minimum fluidization velocity by Equation (4.18) is able to describe the above trend and is in good agreement with experimental data in all cases. Therefore, the estimation of minimum fluidization velocity when considering the bed inventory influence is possible, and the proposed correlation based on Wen and Yu equation is clearly shown to give a reasonable prediction.

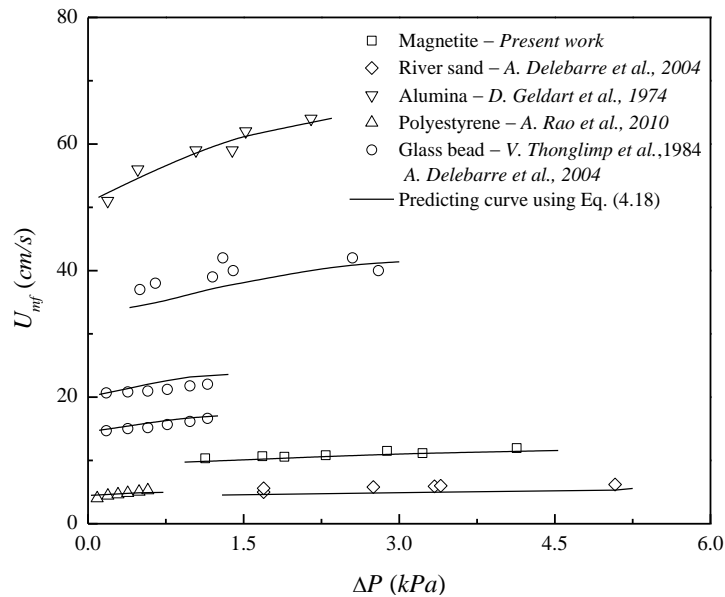


Figure 4.6 Comparison of the U_{mf} calculated using Equation (4.18) with the experimental data.

4.5 Conclusion

Knowledge of the minimum fluidization velocity is crucial if the behavior of an Air Dense Medium Fluidized Bed is to be properly analyzed. It is observed that the measured minimum fluidization velocities increased with increasing bed inventory regardless of the type of solid particles used. A correlation has been derived for predicting the minimum fluidization velocity considering the bed inventory influence by extending the Wen and Yu equation

$$Re_{mf} = [(33.7^2 + 0.0408Ar)^{0.5} - 33.7]/[1 - \exp(-14.45\Delta P^{-0.3})]$$

It only requires the knowledge of Archimedes number (Ar) and the bed pressure drop (ΔP), which can be easily obtained from the calculation of the particle bulk density and the static bed height before fluidization. This extended Wen and Yu equation is further shown to well predict the minimum fluidization velocity reported by previous researchers and can be used to estimate the minimum fluidization velocity for both single and binary mixture of solid particles for all practical purposes.

Nomenclature

A	cross-sectional area of the fluidized bed, m^2
Ar	Archimedes number of particle, kg/m
C_1	constant, <i>dimensionless</i>
C_2	constant, <i>dimensionless</i>
d_p	mean diameter of solid particles, m
D_h	hydraulic diameter of solid particles, m
F_s	skin friction, N
F_f	form drag, N
ΣF	sum of the forces acting on the continuous phase, N
ΔF	frictional pressure drop of fluidized bed, N
g	gravitational acceleration, m/s^2
H_{mf}	fluidized bed height at minimum fluidization state, m
k_1	constant, <i>dimensionless</i>
k_2	constant, <i>dimensionless</i>
k_1'	empirical constant, <i>dimensionless</i>
k_2'	empirical constant, <i>dimensionless</i>
ΔP	total pressure drop of the fluidized bed, Pa
Re_{mf}	actual Reynolds number with increasing bed inventory, <i>dimensionless</i>
Re_{mf}'	Reynolds number calculated by predicting equation, <i>dimensionless</i>
ΔS	specific solid surface, m^2
U_g	superficial gas velocity, m/s
U_{mf}	minimum fluidization velocity, m/s

V	volume of the fluidized bed, m^3
W_{bed}	weight of the loaded particles, kg

Greek letters

ε	voidage of the fluidized bed, <i>dimensionless</i>
ρ_g	density of the gas flow, kg/m^3
μ	viscosity of the gas flow, $Pa.s$
ψ	shape factor of particle, <i>dimensionless</i>
φ	variation of the ratio of Reynolds numbers, <i>dimensionless</i>

Acknowledgements

The authors are grateful to the financial support by Natural Science and Engineering Research Council of Canada (NSERC), China Scholarship Council (CSC), and National Natural Science Foundation of China.

References

- Beeckmans J. M., Butcher S. G., Goransson M., 1982. Coal cleaning by counter-current fluidized cascade, *Can. Min. Metall. Bullet.* 75, 184-191.
- Caicedo G. R., Ruiz M. G., Marques J. J. P., Soler J. G., 2002. Minimum fluidization velocities for gas-solid 2D beds, *Chem. Eng. Process.* 41, 761-764.
- Chen Q. R., Wei L. B., 2003. Coal dry beneficiation technology in China: The state-of-the-art, *China Particuol.* 1, 52-56.
- Cheung L., Niewnow A. W., Rowe P. N., 1974. Minimum fluidization velocity of a binary mixture of different sized particles. *Chem. Eng. Sci.* 29, 1301-1303.
- Davies L., Richardson J. F., 1966. Gas interchange between bubbles and continuous phase in a fluidized bed, *Trans. Inst. Chem. Eng.* 44, 293-298.
- Delebarre A., 2002. Does the minimum fluidization exist? *J. Fluids Eng.* 124, 595-600.
- Delebarre A., Levik E., Morales J-M., 2002. Does the minimum fluidization characterized a powder? in: *Processing of the World Congress on Particle Technology*, Vol. 4, Paper No. 401, Sydney, Australia, July 21-25.
- Delebarre A., Morales J. M., Ramos L., 2004. Influence of the bed mass on its fluidization characteristics, *Chem. Eng. J.* 98, 81-88.
- Denloye A. O., 1982. Bed expansion in a fluidized bed of large particles, *J. Powder Bulk Tech.* 6, 11-18.
- Douglass E., Walsh T., 1966. New type of dry, heavy-medium, gravity separator, *Trans. Inst. Min. Metall.* 75, 226-232.
- Ergun S., 1952. Fluid flow through packed columns, *Chem. Eng. Prog.* 48, 89-94.
- Franks G. V., Firdaus M., Oshitani J., 2013. Copper ore density separations by float/sink in a dry sand fluidised bed dense medium, *Int. J. Miner. Process.* 121, 12-20.
- Franks G. V., Forbes E., Oshitani J., Batterham R. J., 2015. Economic, water and energy evaluation of early rejection of gangue from copper ores using a dry sand fluidised bed separator, *Int. J. Miner. Process.* 137, 43-51.

Fraser T., 1926. Artificial storm of air-sand floats coal on its upper surface, leaving refuse to sink, *Coal Age*. 29, 325-327.

Fraser T., Yancey H. F., 1925. Process of separating loosely mixed materials, U. S. Patent. No. 1, 534, 846.

Granfield R. R., Geldart D., 1974. Large particle fluidization, *Chem. Eng. Sci.* 29, 935-947.

Gunn D. J., Hilal N., 1997. The expansion of gas fluidized beds in bubbling fluidisation, *Chem. Eng. Sci.* 52, 2811-2822.

Houwelingen van. J. A., de Jong T. P. R., 2004. Dry cleaning of coal: Review, fundamentals and opportunities, *Geol. Belgi.* 7, 335-343.

Iohn P., 1971. Fluidized bed heavy medium separation – A modern dry separation procedure, *Aufbereitung – Technik.* 3, 140-146.

Kusakabe K., Kuriyama T., Morooka S., 1989. Fluidization of fine particles at reduced pressure, *Powder Technol.* 58, 125-130.

Luo Z. F., Chen Q. R., 2001. Effect of fine coal accumulation on dense phase fluidized bed performance, *Int. J. Min. Pro.* 63, 217-224.

Oshitani J., Kajimoto S., Yoshida M., Franks G. V., Kubo Y., Nakatsukasa S., 2013. Continuous float-sink density separation of lump iron ore using a dry sand fluidized bed dense medium, *Adv. Powder Technol.* 24, 468-472.

Oshitani J., Ohnishi M., Yoshida M., Franks G. V., Kubo Y., Nakatsukasa S., 2013. Dry separation of particulate iron ore using density-segregation in a gas-solid fluidized bed, *Adv. Powder Technol.* 24, 554-559.

Phillai B. C., Rao M. R., 1971. Pressure drop and minimum fluidization velocities in air-fluidized beds, *Ind. J. Tech.* 9, 77-86.

Rao A., Curtis J. S., Hancock B. C., Wassgren C., 2010. The effect of column diameter and bed height on minimum fluidization velocity, *AIChE J.* 56, 2304-2311.

Richardson J. F., Jeronimo M. A. da S., 1979. Velocity-voidage relations for sedimentation and fluidization, *Chem. Eng. Sci.* 34, 1419-1422.

- Sahu A. K., Tripathy A., Biswal S. K., Parida A., 2011. Stability study of an air dense medium fluidized bed separator for beneficiation of high-ash Indian coal, *Int. J. Coal Prep. Utili.* 31, 127-148.
- Sahu A. K., Tripathy A., Biswal S. K., 2013. Study on particle dynamics in different cross sectional shapes of air dense medium fluidized bed separator, *Fuel.* 111, 472-477.
- Sekito T., Matsuto T., Tanaka N., 2006. Application of a gas-solid fluidized bed separator for shredded municipal bulky solid waste separation, *Waste Manage.* 26, 1422-1429.
- Sekito T., Tanaka N., Matsuto T., 2006. Batch separation shredded bulk waste by gas-solid fluidized at laboratory scale, *Waste Manage.* 26, 1246-1252.
- Tang L. G., Zhao Y. M., Luo Z. F., Liang C. C., Chen Z. Q., Xing H. B., 2009. The effect of fine coal particles on the performance of gas-solid fluidized beds, *Int. J. Coal Prep. Utili.* 29, 265-278.
- Tannous K., Hemati M., Laguerie C., 1994. Caracteristiques au minimum de fluidization et expansion des couches fluidisees de particules de la categorie D de Geldart. *Powder Technol.* 84, 55-72.
- Thonglimp V., Hiquily N., Laguerie C., 1984. Vitese minimale de fluidization et expansion des couches fluidisees par un gaz, *Powder Technol.* 38, 233-253.
- Weintraub M., Deurbrouck A. W., Thomas R. H., 1979. Dry-cleaning coal in a fluidized bed medium, *RI-PMTC*, 4, 12-15.
- Wen C. Y., Yu Y. H., 1966. Mechanics of fluidization, *Chem. Eng. Progr. Symposium Ser.* 62, 100-111.
- Yoshida M., Nakatsukasa S., Nanba M., Gotoh K., Zushi T., Kubo Y., Oshitani J., 2010. Decrease of Cl contents in waste plastics using a gas-solid fluidized bed separator, *Adv. Powder Technol.* 21, 69-74.
- Yoshida M., Oshitani J., Ono K., Ishizashi M., Gotoh K., 2008. Control of apparent specific gravity in binary particles systems of gas-solid fluidized bed, *Kona Powder Part. J.* 26, 227-237.
- Zaltman A., Feller R., Mizrach A., Schmilovitch Z., 1983. Separation potatoes from clods and stones in a fluidized bed medium, *Trans. ASAE.* 26, 987-990.

Zaltzman A., Schmilovitch Z., Mizrach A., 1985. Separating flower bulbs from clods and stones in a fluidized bed, *Can. Agric. Eng.* 27, 63-67.

Zaltzman A., Verma B. P., Schmilovitch Z., 1987. Potential of quality sorting fruits and vegetables using fluidized bed medium, *Trans. ASAE.* 30, 823-831.

CHAPTER 5

ON THE TWO-PHASE THEORY OF FLUIDIZATION FOR GELDART GROUP B AND D PARTICLES

Fluidized bed expansion behavior was carefully investigated in terms of the two-phase theory of fluidization which predicts the distribution of gas flow in bubbling fluidized beds. The two-phase theory, which suggested that the bubble flow rate being equal to the excess gas flow above the incipient fluidization, has been proved to be an overestimation in most cases. While the two-phase theory has been modified by introducing a correction factor (Y), most previous studies were conducted for Geldart Group A powders. In the present work, the contribution to predict the parameter Y for Geldart Group B and D particles has been formulated based on almost all the available experimental data. The experimental results demonstrated that the Y value increases with decreasing particle size or density and increasing excess gas velocity. A new correlation has been developed to estimate the Y value for Geldart Group B and D particles

$$Y = 1.72Ar^{-0.133}(U_g - U_{mf})^{0.024}$$

with an overall standard deviation of 19%. It only requires the knowledge of Archimedes number and excess gas velocity. This correlation is in reasonable agreement with almost all the available data in literature and the present work.

5.1 Introduction

Bubbling gas-solid fluidized bed is commonly operated at relatively lower gas flow rate, characterized by the solid particles becoming individually suspended with interstitial gas flow and gas bubbles rising with coalescence (Kunii and Levenspiel, 1991; Wen, 2003). As the gas-solid contacting and gas residence time are usually different between the interstitial gas flow and bubble flow, the distribution of gas flow will play a critical role in the modelling and design of fluidized bed operations, especially for the gas-solid chemical reactions (Botero *et al.*, 2009; Modekurti *et al.*, 2013; Bakshi *et al.*, 2013), combustion and gasification (Radmanesh *et al.*, 2006; Geng and Che, 2011; Basu, 2006), solids mixing and drying (Tahmasebi *et al.*, 2012;

Kannan *et al.*, Sun *et al.*, 2005), fluidized bed separation (Wang *et al.*, 2013; Zhang *et al.*, 2017), etc. In general, it is considered that the bubbling fluidized bed is composed of the dense (emulsion) phase and bubble phase (Davidson and Clift, 1985; Geldart, 1986), and the comprehensive knowledge of the division of gas flow between these two phases is therefore crucial for the fluidized bed operations. The two-phase theory of fluidization (Toomey and Johnstone, 1952) suggested that all the gas flow in excess of that required for incipient fluidization is in the form of gas bubbles, which provides a possible way to analyze the distribution of gas flow. It is usually formulated as

$$G_b/A = U_g - U_{mf} \quad (5.1)$$

where G_b is the volumetric bubble flow rate, A is the cross-sectional area of fluidized bed, U_g is the superficial gas velocity, and U_{mf} is the minimum fluidization velocity. The two-phase theory implies that the bed voidage and the interstitial gas velocity in the dense phase remain almost the same as in the incipient fluidization state, which is of great importance for the modelling and operation purposes. Unfortunately, most of the experimental evidences (Nicklin, 1962; Turner, 1966; Davidson and Harrison, 1966; Grace and Clift, 1974; Hepbasli, 1982; Geldart, 2004) have demonstrated that the original two-phase theory is only approximately true and tends to overestimate the visible bubble flow in most cases.

There was considerable controversy over the reasons for the unreliable prediction of the original two-phase theory. Some authors (Grace and Clift, 2004; Botterill *et al.*, 1966; Lockett *et al.*, 1967; Geldart, 1968; Grace and Harrison, 1969; Geldart, 1970; Geldart and Granfield, 1974; Rowe *et al.*, 1978) have attributed the deficit of bubble flow to an increase in the interstitial gas flow in dense phase above that required for minimum fluidization. At the other extreme, a number of workers (Werther, 1978; Michael, 1982; Hillgardt and Werther, 1986) have ascribed this discrepancy to the through-flow of gas inside the bubble phase. Other investigators (Hepbasli, 1998; Geldart, 2004) claimed that the original two-phase theory postulate, even including through-flow in isolated bubbles, substantially over-predicted the visible bubble flow rate. Thus, many modifications to the two-phase theory of fluidization have been proposed in the literature, aiming to improve the accuracy and reliability for modelling and operation purposes.

The earlier form was known as n -type two-phase theory (Grace and Harrison, 1969), in the form of

$$G_b/A = U_g - U_{mf}(1 + n\delta) \quad (5.2)$$

where n is the through-flow coefficient, and δ is the fraction of the cross-sectional area occupied by gas bubbles. After then, they summarized the available data in the literature and gave an extensive compilation of the experimental value of n (Grace and Clift, 1974). Their results indicate that the factor n were reported to vary in the range of 8 ~ 140, respectively, which were shown to be too difficult to be estimated.

Another form was developed by several workers (Hillgardt and Werther, 1986; Fryer and Potter, 1976; Xavier *et al.*, 1978; Geldart and Keairns, 1975) as

$$G_b/A = Y(U_g - U_{mf}) \quad (5.3)$$

where Y is the correction factor. The parameter Y indicates the deviation of the visible bubble flow rate from the original two-phase theory, which was found to be usually below unity. The Y value for different types of powders of Geldart's classification have been described as (Martin, 2008)

$$0.8 < Y < 1.0 \quad \text{Group A powders}$$

$$0.6 < Y < 0.8 \quad \text{Group B powders}$$

$$0.25 < Y < 0.6 \quad \text{Group D powders}$$

It is noteworthy that normal fluidization is extremely difficult for Geldart Group C powders, and thus the corresponding Y value is commonly excluded. For Geldart Group A powders, a number of works (Dry *et al.*, 1983; Wang *et al.*, 2009; Hong *et al.*, 2016) have been conducted to investigate the gas flow distribution due to its importance for the chemical reactions. The results concluded that the range of the corresponding Y values is relatively narrow (0.8 – 1.0), and the numerical value of 0.85 was usually recommended (Martin, 2008). However, for Geldart Group B and D particles, there is no reasonable and suitable predicting equation.

Comprehensive analysis of almost all experimental data shows that the division of gas flow between the dense phase and bubble phase is highly dependent on the particle size, density and superficial gas velocity. An attempt has been made to develop a correlation for predicting the correction factor (Y) of two-phase theory for bubbling fluidized bed with Geldart Group B/D particles. Almost all available data on gas-solid systems have been correlated to validate this correlation, and the calculated results have been compared with the experimental data in literature and the present work.

5.2 Theory

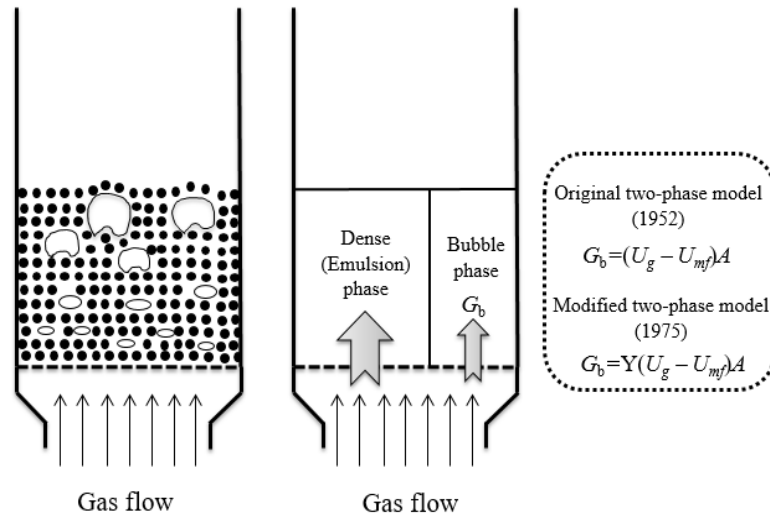


Figure 5.1 The schematic diagram of the two-phase theory of fluidization.

According to the modified two-phase theory (Geldart, 1975), the parameter Y indicates the deviation of the visible bubble flow rate from the original two-phase model, which can be obtained from the estimation of the fluidized bed expansion. Accordingly, the volume occupied by gas bubbles per bed cross-sectional area can be expressed as

$$dV_b = G_b dh / U_b \quad (5.4)$$

where V_b is the volume occupied by bubbles, dh is the differential height of fluidized bed, and U_b is the visible bubble flow rate. Thus, the total volume occupied by gas bubbles in the bed is

$$V_b = \int_0^H G_b dh / U_b = G_b H / \bar{U}_b \quad (5.5)$$

where \bar{U}_b is the average bubble flow rate, H is the fluidized bed height. The volumetric bubble flow rate (G_b) should be calculated from the modified two-phase theory,

$$G_b = Y(U_g - U_{mf})A \quad (5.6)$$

The important thing is to determine the average bubble flow rate, and it can be given by

$$\bar{U}_b = \int_0^H U_b dh / H \quad (5.7)$$

For freely bubbling beds, the bubble rise velocity is usually estimated from an equation proposed by Davidson et al. (Davidson and Harrison, 1963).

$$U_b = 0.71\sqrt{gD_e} + (U_g - U_{mf}) \quad (5.8)$$

where D_e is the diameter of an isolated bubble. Various correlations have been proposed for the estimation of mean bubble size in bubbling fluidized beds, among which Darton equation (Darton, 1977) is one of the most commonly used correlations considering the effects of bed height, gas distributor and gas velocity, and is defined as

$$D_e = 0.54(U_g - U_{mf})^{0.4} (h + 4A_D^{0.5})^{0.8} / g^{0.2} \quad (5.9)$$

Expansion of bubbling fluidized beds for Geldart Group B and D particles in general results from the volume occupied by gas bubbles, and total volume of bubbles can be written

$$V_b = (H - H_{mf})A \quad (5.10)$$

Submitting Equations (5.5) and (5.6) into Equation (5.10), the fluidized bed expansion leads to

$$(H - H_{mf})/H = Y(U_g - U_{mf})/\bar{U}_b \quad (5.11)$$

Combination of Equations (5.7), (5.8), (5.9) and (5.11), the parameter Y of the modified two-phase theory can be calculated from

$$Y = 0.93 \frac{H - H_{mf}}{H} \left[\frac{(H + 4A_D^{0.5})^{1.4} - (4A_D^{0.5})^{1.4}}{H(U_g - U_{mf})^{0.8}} + 1 \right] \quad (5.12)$$

5.3 Experimental

5.3.1 Experimental setup

Experiments were conducted in a fluidized bed at ambient conditions, as shown in Figure 5.2. The experimental setup consists of mainly four parts: (1) air supply including an air filter, a roots blower, and a tank; (2) fluidized bed column with inner diameter of 152.4 mm. (3) U-shaped monometers for pressure-drop measurement; (4) dust collection device. After being filtered, the ambient air was sent to fluidize the particles in the column through the air chamber and a perforated distributor. The distributor is made of two plastic perforated plates with filter cloth in between, and the orifice diameter is 1.5 mm with the total open area of 11%. To investigate the expansion of fluidized bed, a ruler is attached on the side of the column and the U-shaped piezometric pipes are connected to the axial pressure taps on the other side of the column. Fine dust generated during fluidization was collected by the dust collector device.

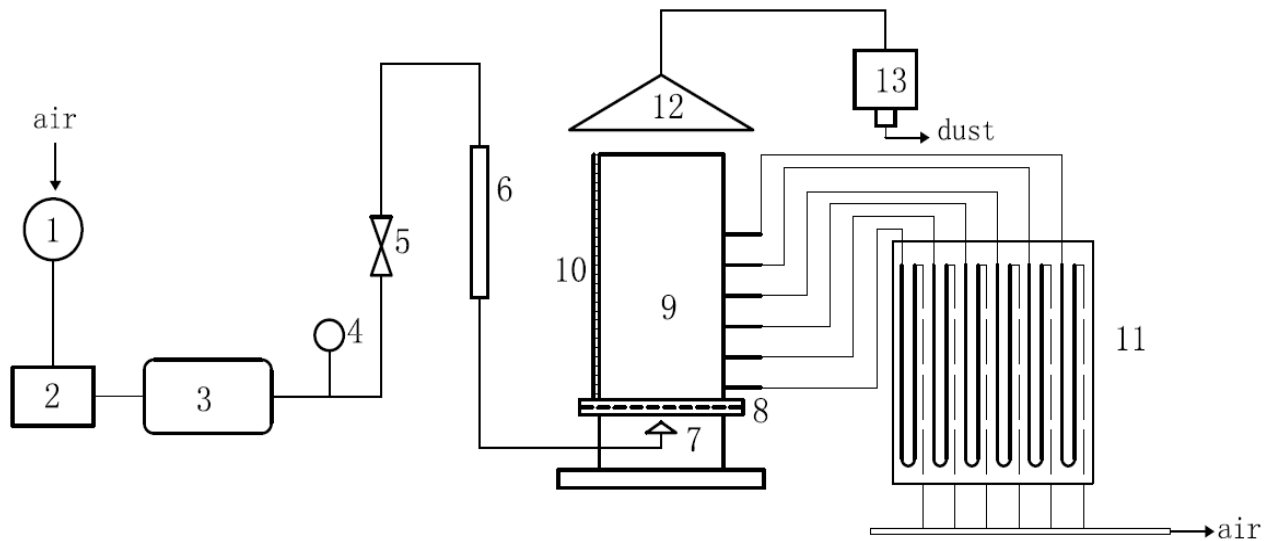


Figure 5.2 The schematic diagram of experimental apparatus: 1. Air filter; 2. Roots blower; 3. Tank; 4. Pressure gauge; 5. Gas valve; 6. Rotameter; 7. Air chamber; 8. Perforated distributor; 9. Fluidized bed column; 10. Ruler; 11. U-shaped manometer; 12. Dust cover; 13. Dust collector.

5.3.2 Experimental materials

Four types of solid materials have been employed in this work: magnetite, sand, gangue and glass beads. These samples were sieved into the following size fractions: 74 – 150 μm , 150 – 300 μm , 300 – 425 μm , 425 – 590 μm , 590 – 710 μm . The particle properties of the experimental materials of each size fraction are shown in Tables 5.1, 5.2, 5.3, and 5.4. It is noted that the solid particles with the angle of repose above 38 is considered cohesive. The gangue sample, which is the heavy product ($>1.85 \text{ g/cm}^3$) of the coal separation process, is collected from HuaiBei Coal Mine, Ltd., Anhui, China. It may be noteworthy that the magnetite particles of 590 – 710 μm was excluded in the present work due to its limited flowability.

Table 5.1. The particle properties of magnetite samples.

Particle size fraction (μm)	74 – 150	150 – 300	300 – 425	425 – 590
Mean particle size (μm)	121	213	348	457
Particle true density (kg/m^3)	4480	4650	4570	4540
Aerated bulk density (kg/m^3)	2460	2667	2687	2652
Archimedes number (Ar)	303	1715	7349	16533
Angle of repose ($^\circ$)	35.7	36.1	37.4	38.3

Table 5.2. The particle properties of glass bead samples.

Particle size fraction (μm)	74 – 150	150 – 300	300 – 425	425 – 590	590 – 710
Mean particle size (μm)	101	209	356	469	648
Particle true density (kg/m^3)	2550	2620	2650	2680	2640
Aerated bulk density (kg/m^3)	1560	1603	1611	1605	1612
Archimedes number (Ar)	100	912	4561	10547	27403
Angle of repose ($^\circ$)	32.5	33.1	34.3	34.6	35.2

Table 5.3. The particle properties of sand samples.

Particle size fraction (μm)	74 – 150	150 – 300	300 – 425	425 – 590	590 – 710
Mean particle size (μm)	113	224	368	475	636
Particle true density (kg/m^3)	2430	2530	2410	2510	2500
Particle bulk density (kg/m^3)	1493	1544	1610	1602	1593
Archimedes number (Ar)	134	1085	4581	10261	24534
Angle of repose ($^\circ$)	33.6	34.5	37.4	38.1	38.5

Table 5.4. The particle properties of gangue samples.

Particle size fraction (μm)	74 – 150	150 – 300	300 – 425	425 – 590	590 – 710
Mean particle size (μm)	118	215	372	486	625
Particle true density (kg/m^3)	2010	2050	2160	2120	2090
Particle bulk density (kg/m^3)	1180	1240	1290	1360	1330
Archimedes number (Ar)	126	777	4241	9282	19462
Angle of repose ($^\circ$)	41.8	41.3	41.5	42.8	43.3

5.4 Results and discussion

5.4.1 The effects of particle property and excess gas velocity

Measurements of the fluidized bed expansion have been carried out to determine the correction factor Y by using Equation (5.12). The pressure drop against distance above the distributor graph was employed to obtain the fluidized bed height at a certain superficial gas velocity. In the present work, the initial bed height was 20 cm and the excess gas velocity ranged from 0.5 cm/s to 4.5 cm/s. The Y value of magnetite, glass bead, river sand and gangue particles with the size range from 74 μm to 710 μm is reported as a function of the excess gas velocity in Figure 5.3.

As can be observed from Figure 5.3, Y value was found to decrease with the increasing particle size for the same material. This trend may be explained that the greater the particle size, the greater the interstitial gas velocity in the dense phase, which may results in more deficit of bubble flow in the fluidized bed (Davidson and Harrison, 1966; Hepbasli, 1998). It can also be observed from Figure 5.3 that Y value of different types of solids with same particle size

decreases slightly with increasing particle density. This can also be attributed to the increasing gas velocity required to fluidize solid particles in the dense phase. Moreover, it can be seen that there is an increase in Y value with the increasing of excess gas velocity, which can be attributed to the tendency of the gas flow moves more into the bubble phase. For the modelling and operation purposes, it is important to predict the Y value for the modified two-phase theory, thus avoiding the experimental measurements.

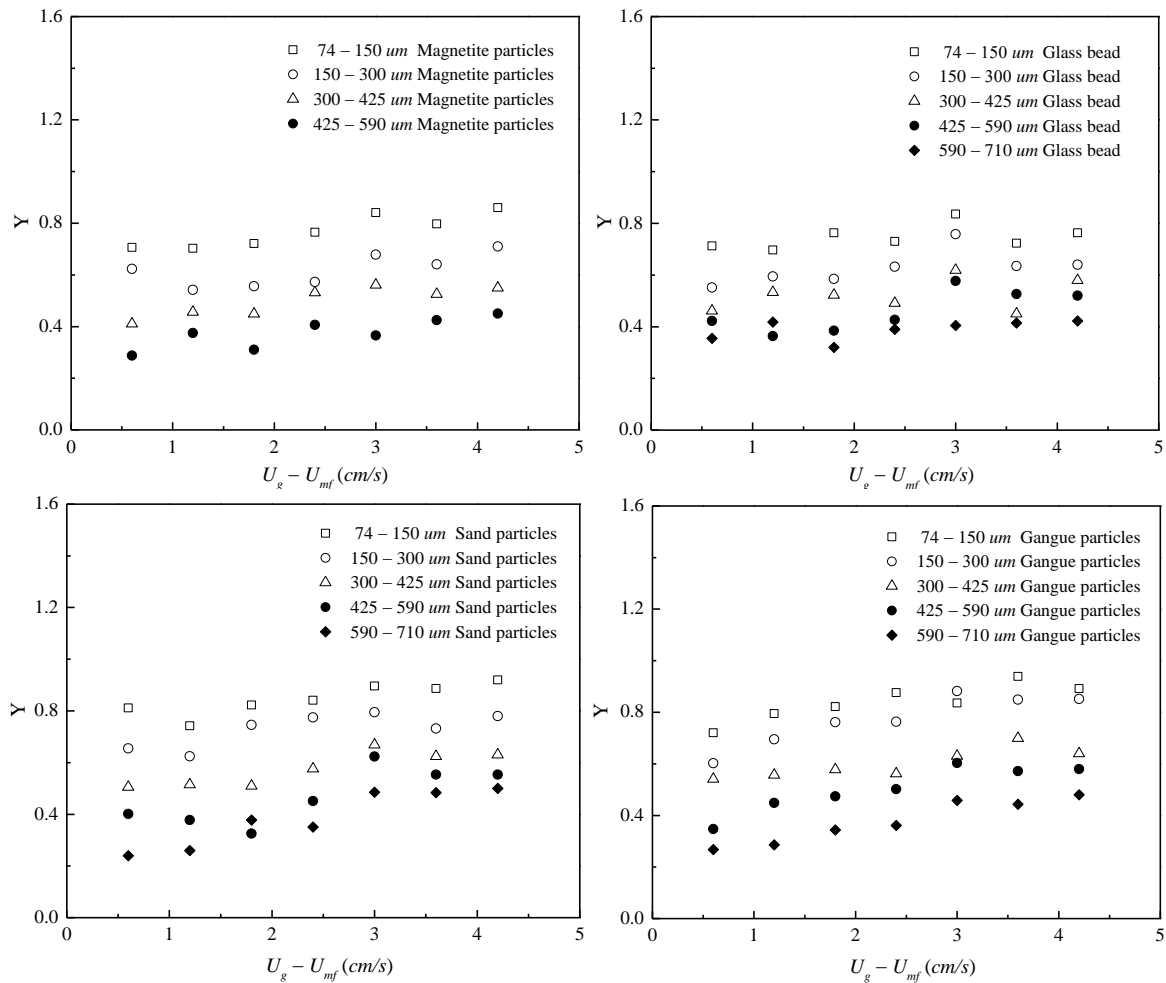


Figure 5.3 Plot of Y value against the excess gas velocity for different types of solid particles.

5.4.2 The correlation for estimating the correction factor Y

Experimental Y values of the present investigation have been summarized and plotted against Archimedes number and excess gas velocity in Figure 5.4. To consider the effect of particle properties in gas-solid fluidization systems, Archimedes number is employed and is defined by

$$Ar = \rho_g(\rho_p - \rho_g)gd_p^3/\mu^2 \quad (5.13)$$

As can be observed that the Y value was found to decrease with the increasing of Archimedes number. It can be explained that Archimedes number increases with the increasing of particle size or density, which may lead to an increase in interstitial gas velocity in the dense phase.

In recent years, many investigators (Hepbasli, 1998; Geldart, 2004; Rowe, *et al.*, 1978; Fryer and Potter, 1976; Xavier *et al.*, 1978; Morse, 1949; Johnson *et al.*, 1991; Tannous *et al.*, 1994; Gunn and Hilal, 1997) have carried out experiments which allow to estimate the parameter Y from the measurements of fluidized bed expansion, and the experimental details are shown in Table 5.5. The experimental data in literature and the present work, which covers the excess gas velocity below 1 m/s and Archimedes number ranges from 100 to 30000, are presented in Figure 5.5. An examination of almost all the available data reveals that the Y value regularly increases with decreasing Archimedes number and increasing excess gas velocity, and these published data precisely allow to develop a correlation for evaluating the parameter Y . Accordingly, the experimental results obtained have been fitted to the following expression

$$Y = 1.72Ar^{-0.133}(U_g - U_{mf})^{0.024} \quad (5.14)$$

where Ar is Archimedes number which is given in Equation (5.13) and the term $(U_g - U_{mf})$ represents the excess gas velocity. It should be mentioned that the proposed correlation can be only used for Geldart B and D particles in conventional fluidized beds at ambient operating conditions. Based on a similar approach by employing the original two-phase theory assumption (Toomey and Johnstone, 1952), the modified two-phase theory for Geldart B and D particles, then, can be written in the form of

$$G_b = 1.72Ar^{-0.133}(U_g - U_{mf})^{1.024}A \quad (5.15)$$

where G_b is the volumetric bubble flow rate and A is the cross-sectional area of fluidized bed.

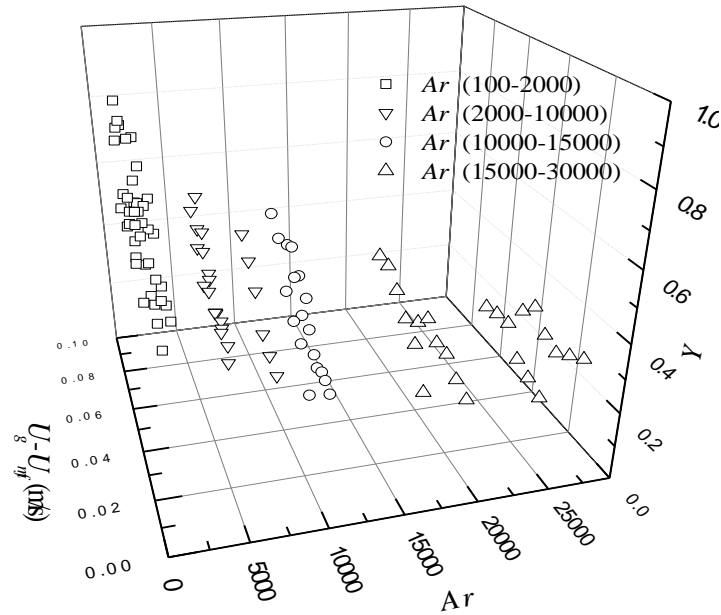


Figure 5.4 Effect of Archimedes number and excess gas velocity on parameter Y .

Table 5.5. Literature summary of experimental data on the correction factor (Y).

Reference	Bed cross-section (cm)	Bed height (cm)	Particles			U_{mf} (cm/s)	Ar	Re_{mf}	Y
			Type	ρ_p (kg/m ³)	d_p (um)				
Morse, 1949	6.35	71.12			569	25.26		10.36	0.29~0.60
	6.35	26.92			569	27.01	16566	11.08	0.10~0.80
	11.43	39.12			569	25.51		10.46	0.09~0.33
	6.35	63.5			452	18.29		5.96	0.38~0.62
	6.35	63.5			452	18.59	8304	6.06	0.16~0.83
	11.43	60.33			452	17.68		5.76	0.36~0.75
	6.35	63.5			285	7.92		1.63	0.54~1.22
	11.43	29.54			285	8.08	2082	1.66	0.12~0.44
	6.35	61.98	Glass bead	2355	155	2.13		0.24	0.56~1.54
	6.35	75.57			155	0.76		0.08	1.13~1.82
	6.35	26.67			155	2.84	335	0.32	0.81~1.22
	11.43	61.45			155	2.59		0.29	0.10~0.63
	11.43	30.45			155	2.44		0.27	0.58~0.82
	6.35	60.96			101	0.43		0.03	1.14~1.55
	6.35	79.76			101	1.52	93	0.11	0.35~1.75
11.43	56.52			101	1.52		0.11	0.90~1.18	
Geldart <i>et al.</i> , 1974	30.8	21.95	Fine sand (narrow)	2600	101	1.37	102	0.1	0.58~0.97

	30.8	19.4	Fine sand (wide)	2600	128	1.4	208	0.13	0.59~0.82
	30.8	20	Coarse sand	2600	275	5.6	2063	1.11	0.38~0.59
	22.9	11		2650	117	1.7			0.68~0.80
Flyer <i>et al.</i> , 1976	22.9	23	Sand with iron oxide	2650	117	1.7			0.73~0.80
	22.9	40		2650	117	1.7	162	0.14	0.74~0.80
	22.9	65		2650	117	1.7			0.73~0.79
		34	commercial silica base catalyst	2500	84	2.6		0.16	0.17~0.73
Xavier <i>et al.</i> , 1978	61	32		2500	158	2.6	376	0.3	0.28~0.98
		25			84	2.6		0.16	0.69~0.90
		32.7				2.9		0.12	0.17~0.48
Rowe <i>et al.</i> , 1978	28	33.5	Silica catalyst	2600	57	2.9	18	0.12	0.22~0.54
		34.8				2.9		0.12	0.17~0.53
		40			150	2		0.22	0.55~0.61
Johnsson <i>et al.</i> , 1991	68×7	40	Silica sand	2600	460	18	17418	5.97	0.33~0.45
		40			790	40		22.77	0.31~0.45
Tannous <i>et al.</i> , 1994	43.5	19.2	Polystyrene	1016	1840	60	241251	79.56	0.20~0.57
Gunn <i>et al.</i> , 1997	30	40	Diakon	1228	290	3.8	536	0.79	0.69~0.85
Hepbasli, 1998		17.17	Raw perlite	1836	593	20.33	14602	8.69	0.33~0.52
		10							
	61×61	17.17	Sand	2486	1233	62.8	177762	55.8	0.24~0.36
		10							

5.4.3 Comparison with the experimental data

A comparison of the Y values calculated by using Equation (5.14) with the available experimental data in literature and the present work is illustrated in Figure 5.6. As can be observed, this correlation gives an overall standard deviation of 19% based on 156 data points in the literature and 133 data points in the present work, and the corresponding overall R -squared is 0.86, which is in reasonable agreement with the experimental data. The proposed correlation only requires the knowledge of Archimedes number and the excess gas velocity, and it covers the widest Archimedes number range from 20 to 240000. Therefore, this correlation has the advantages of being considerably simpler with greater accuracy, and a more accurate and reliable method for estimating the parameter Y for the modified two-phase theory has been obtained. As a

result, it can be widely used to accurately predict the distribution of gas flow between the dense phase and bubble phase in a bubbling fluidized bed with Geldart Group B/D particles.

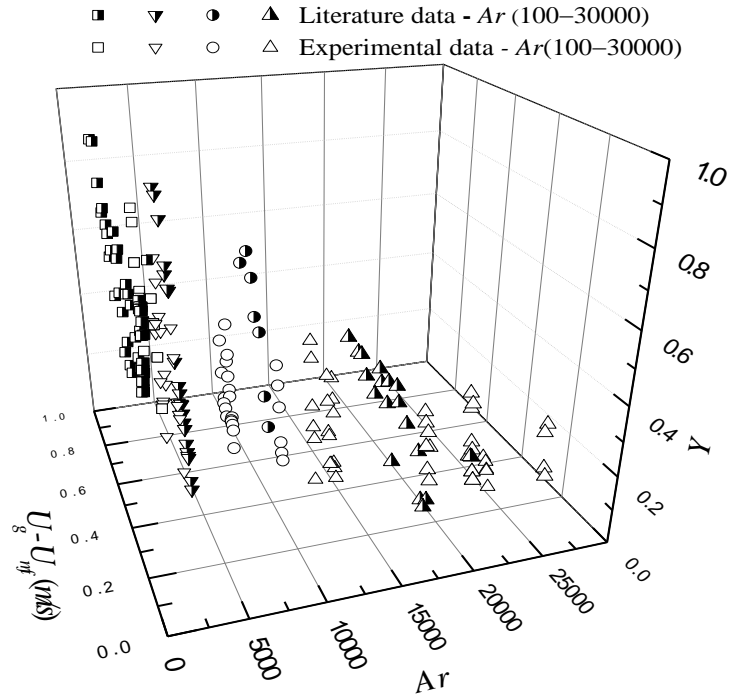


Figure 5.5 The summary of Y values of all available data in literature and the present work.

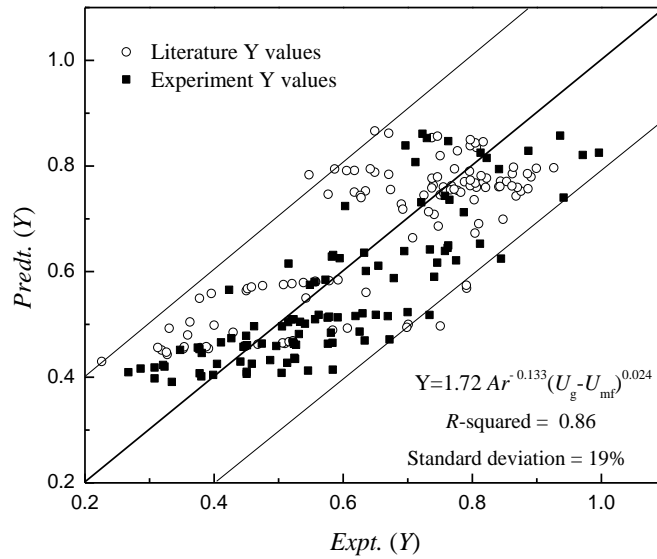


Figure 5.6 Comparison of Y values calculated using Equation (5.14) with all the available experimental data.

5.4.4 Further discussion of the correlation for correction factor Y

By plotting the calculated Y values using Equation (5.14) against Archimedes number and the excess gas velocity, a convenient graphical form for the proposed correlation has been constructed and shown in Figure 5.7. In this graph, Archimedes number varied from 100 to 30000 and the excess gas velocity ranged between 0.01 and 1 m/s . As can be observed that there is a sharp decrease in Y value from 0.9 to 0.5 with increasing Archimedes number from 100 to 5000. However, above 5000, the Y value was found to decrease slowly from 0.5 to 0.35 with further increasing Archimedes number from 5000 to 30000. Moreover, the excess gas velocity also affects the correction factor Y . To be exact, the Y value, in relatively low flow rates, increases slightly with increasing excess gas velocity. With this knowledge, the correction factor Y can be quickly estimated for Geldart Group B and D particles.

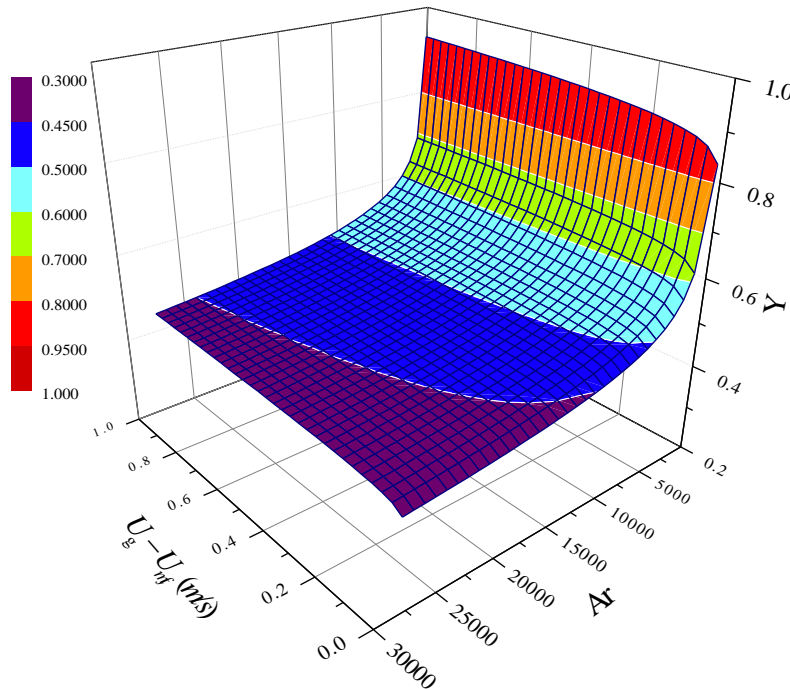


Figure 5.7 A generalized description of the proposed correlation for predicting the correction factor (Y).

5.5 Conclusion

The correction factor Y for the two-phase theory of fluidization was extensively studied for Geldart Group B and D particles. Experimental evidences indicate that the Y value increases with decreasing particle size or density and with increasing excess gas velocity. An equation has been derived to predict the parameter Y for Geldart Group B and D particles, and can be expressed as

$$Y = 1.72Ar^{-0.133}(U_g - U_{mf})^{0.024}$$

It only requires the knowledge of Archimedes number and the excess gas velocity, and gives an overall standard deviation of 19% for almost all available experimental data. Therefore, the proposed correlation has the advantages of being considerably simpler and more accurate. Furthermore, this correlation leads to a modified two-phase theory for Geldart Group B and D particles, and can be given by

$$G_b = 1.72Ar^{-0.133}(U_g - U_{mf})^{1.024}A$$

The above two correlations are shown to be as satisfactory for practical purposes, which can be used to accurately estimate the distribution of gas flow between the dense and bubble phases in the bubbling fluidized bed with Geldart Group B/D particles.

Nomenclature

A	cross-sectional area of the fluidized bed, m^2
A_D	area of single hole on the plate, m^2
Ar	Archimedes number, <i>dimensionless</i>
d_p	diameter of solid particle, m
D_e	diameter of isolated bubble, m
g	gravitational acceleration, m/s^2
G_b	volumetric bubble flow rate, m^3/s
H	fluidized bed height at operation condition, m
H_{mf}	fluidized bed height at minimum fluidization state, m
n	through-flow coefficient, <i>dimensionless</i>
Re_{mf}	Reynolds number at minimum fluidization state, <i>dimensionless</i>
U_b	visible bubble flow rate, m/s
\bar{U}_b	average bubble flow rate, m/s
U_g	superficial gas velocity, m/s
U_{mf}	minimum fluidization velocity, m/s
V_b	volume occupied by gas bubbles in fluidized bed, m^3
γ	correction factor, <i>dimensionless</i>

Greek letters

δ	fraction of the cross-sectional area occupied by gas bubbles, <i>dimensionless</i>
ρ_g	density of the gas flow, kg/m^3
ρ_p	density of the solid particle, kg/m^3
μ	viscosity of the gas flow, $Pa.s$

Acknowledgements

The authors are grateful to the financial support by Natural Science and Engineering Research Council of Canada (NSERC), China Scholarship Council (CSC), and National Natural Science Foundation of China.

References

- Bakshi A., Altantzis C., Glicksman L. R., Ghoniem A. F., 2017. Gas-flow distribution in bubbling fluidized beds: CFD-based analysis and impact of operating conditions. *Powder Technol.* 316, 500-511.
- Basu P., 2006. *Combustion and gasification in fluidized beds*. Boca, Ration.
- Botero A. M., Grace J. R., Lim C. J., Elnashaie S. S. E. H., Boyd T., 2009. Pure hydrogen generation in a fluidized bed membrane reactor: Application of the generalized comprehensive reactor model. *Chem. Eng. Sci.* 64, 3826-3846.
- Botterill J. S. M., George J. S., Bespord H., 1966. Bubble chains in gas fluidized beds. *Chem. Eng. Pro. Symp Ser.* 62, 7-15.
- Darton R. C., 1977. Bubble growth due to coalescence in fluidized beds. *Chem. Eng. Res. Des.* 55, 274-280.
- Davidson J. F., Harrison D., 1963. *Fluidised particles*. Cambridge Univ. Press.
- Davidson J. F., Harrison D., 1966. The behavior of a continuously bubbling fluidized bed. *Chem. Eng. Sci.* 21, 731-738.
- Davidson J. F., Clift R., Harrison D., 1985. *Fluidization: 2nd Edition*, London.
- Dry R. J., Judd M. R., Shingles T., 1983. Two-phase theory and fine powders. *Powder Technol.* 34, 213-223.
- Fryer C., Potter O. W., 1976. Experimental investigation of models for fluidized bed catalytic reactors. *AIChE J.* 22, 38-47.
- Geldart D., Keairns D. L., 1975. *Fluidization technology*. McGraw-Hill, New York. 1, 237.
- Geldart D., 2004. Expansion of gas fluidized beds. *Ind. Eng. Chem. Res.* 43, 5802-5809.
- Geldart D., 1986. *Gas fluidization technology*, Chichester, Toronto.
- Geldart D., Granfield R. R., 1974. Large particle fluidization. *Chem. Eng. Sci.* 29, 935-947.
- Geldart D., 1968. The expansion of bubbling fluidized beds. *Powder Technol.* 1, 355-368.

- Geldart D., 1970. The size and frequency of bubble in two- and three- dimensional gas-fluidised beds. *Powder Technol.* 4, 41-55.
- Geng Y. M., Che D. F., 2011. An extended DEM-CFD model for char combustion in a bubbling fluidized bed combustor of inert sand. *Chem. Eng. Sci.* 66, 207-219.
- Goyal A., Pushpavanam S., Voolapalli R. K., 2010. Modeling and simulation of co-gasification of coal and petcoke in a bubbling fluidized bed coal gasifier. *Fuel Process. Technol.* 91, 1296-1307.
- Grace J., Clift R., 1974. On the two-phase theory of fluidization. *Chem. Eng. Sci.* 29, 327-334.
- Grace J., Harrison D., 1969. The behavior of freely bubbling fluidized beds. *Chem. Eng. Sci.* 24, 497-508.
- Gunn D. J., Hilal N., 1997. The expansion of gas-fluidised beds in bubbling fluidization. *Chem. Eng. Sci.* 52, 2811-2822.
- Hepbasli A., 1998. Estimation of bed expansion in a freely-bubbling three-dimensional gas-fluidized bed. *Int. J. Energy Res.* 22, 1365-1380.
- Hillgardt K., Werther J., 1986. Local bubble gas hold-up and expansion of gas-solid fluidized beds. *Ger. Chem. Eng.* 9, 215-221.
- Hong K., Chen S., Wang W., Li J. H., 2016. Fine grid two-fluid modeling of fluidization of Geldart A particles. *Powder Technol.* 296, 2-16.
- Johnson F., Andersson S., Leckner B., 1991. Expansion of a freely bubbling fluidized bed. *Powder Technol.* 68, 117-123.
- Kannan C. S., Thomas P. P., Varma Y. B. G., 1995. Drying of solids in fluidized beds. *Ind. Eng. Chem. Res.* 34, 3068-3077.
- Kunii D., Levenspiel O., 1991. *Fluidization engineering: 2nd Edition.* United States.
- Lockett M. J., Davidson J. F., Harrison D., 1967. On the two-phase theory of fluidization. *Chem. Eng. Sci.* 22, 1059-1066.
- Martin R., 2008. *Introduction to particle technology, second edition.* West Sussex, England, Wiley.

- Modekurti S., Bhattacharyya D., Zitney S. E., 2013. Dynamic modeling and control studies of a two-stage bubbling fluidized bed adsorber-reactor for solid-sorbent CO₂ capture. *Ind. Eng. Chem. Res.* 52, 10250-10260.
- Michael H. P., Liangshih F., Thomas L. S., 1982. Reactant dynamics in catalytic fluidized bed reactors with flow reversal of gas in the emulsion phase. *Chem. Eng. Sci.* 37, 553-565.
- Morse R. D., 1949. Fluidization of granular solids - Fluid mechanics and quality. *Ind. Eng. Chem.* 41, 1104-1117.
- Nicklin D. J., 1962. Two-phase bubble flow. *Chem. Eng. Sci.* 17, 693-702.
- Radmanesh R., Chaouki J., Guy C., 2006. Biomass gasification in a bubbling fluidized bed reactor: Experiments and modeling. *AIChE J.* 52, 4258-4272.
- Rowe P. N., Santoro L., Yates J. G., 1978. The division of gas between bubble and interstitial phase in fluidized beds of fine powders. *Chem. Eng. Sci.* 33, 133-140.
- Sun Q. Q., Lu H. L., Liu W. T., He Y. R., Yang L. D., Gidaspow D., 2005. Simulation and experiment of segregating/mixing of rice husk-sand mixture in a bubbling fluidized bed. *Fuel.* 84, 1739-1748.
- Tahmasebi A., Yu J. L., Han Y. N., Li X. C., 2012. A study of chemical structure changes of Chinese lignite during fluidized bed drying in nitrogen and air. *Fuel Process. Technol.* 101, 85-93.
- Tannous K., Hemati M., Laguerie C., 1994. Caracteristiques au minimum de fluidization et expansion des couches fluidisees de particules de la categorie D de Geldart. *Powder Technol.* 80, 55-72.
- Toomey R. D., Johnstone H. F., 1952. Gaseous fluidization of solid particles. *Chem. Eng. Pro.* 48, 220-226.
- Turner J. C. R., 1966. On bubble flow in liquids and fluidized beds. *Chem. Eng. Sci.* 21, 971-974.
- Wang J. W., Van der Hoef M. A., Kuipers J. A. M., 2009. Why the two-fluid model fails to predict the bed expansion characteristics of Geldart A particles in gas-fluidized beds: A tentative answer. *Chem. Eng. Sci.* 64, 622-625.

Wang Q. G., Lu J. F., Yin W. D., Yang H. R., Wei L. B., 2013. Numerical study of gas-solid flow in a coal beneficiation fluidized bed using kinetic theory of granular flow. *Fuel Process. Technol.* 111, 29-41.

Wen C. Y., 2003. *Handbook of fluidization and fluid-particle system.* Basel, New York.

Werther J., 1978. Effect of gas distributor on the hydrodynamics of gas fluidized beds. *Ger. Chem. Eng.* 1, 166-174.

Xavier A. M., Lewis D. A., Davidson J. F., 1978. The expansion of bubbling fluidized beds. *Trans. Inst. Chem. Engrs.* 56, 274-280.

Zhang Y., Zhao Y. M., Lu L. Q., Ge W., Wang J. W., Duan C. L., 2017. Assessment of polydisperse drag model for the size segregation in a bubbling fluidized bed using discrete particle method. *Chem. Eng. Sci.* 160, 106-112.

CHAPTER 6

MIXING AND SEGREGATION BEHAVIOR IN AN AIR DENSE MEDIUM FLUIDIZED BED WITH BINARY MIXTURES FOR DRY COAL BENEFICIATION

Mixing and segregation behavior of binary medium particles in an Air Dense Medium Fluidized Bed (ADMFB) were studied for dry coal beneficiation. Magnetite mixed with coal/gangue/sand particles belonging to Geldart B/D group were tested individually for the bed density adjustment. The effects of design and operating parameters including particle density ratio, particle size ratio, mixture composition of solid particles, superficial gas velocity, and fluidized bed height on the solids mixing and segregation were examined. The results showed that segregation becomes more severe with the increasing density difference of solids mixtures. An increase in particle size ratio may also leads to partial segregation. Mixing and segregation of binary systems are almost independent of the lower excess gas velocity and the initial bed height when it is over 15 *cm*. Moreover, a mixing index was employed to evaluate the mixing and segregation performance, and the criteria for good mixing to achieve bed density adjustment were identified.

6.1 Introduction

Bubbling gas-solid fluidized beds composed of binary mixture of solid particles are widely applied in many industrial processes (Martin, 2008; Yang, 1999; Davidson and Harrison, 1985), such as the Air Dense Medium Fluidized Bed for dry coal beneficiation (Mohanta *et al.*, 2013; Sahu *et al.*, 2009). For a binary system, the inevitable particle mixing and segregation behavior have a significant influence on fluidization properties and have been extensively investigated by many researchers (Formisani *et al.*, 2013; Huang *et al.*, 2017; Joseph *et al.*, 2007; Turrado *et al.*, 2007; Olivier *et al.*, 2004). It is known that the mixing and segregation processes in a fluidized bed will determine the solids distribution in the axial and radial directions, which in turn influences the bed density distribution, bubble coalescence and growth, bed expansion, heat and mass transfer rates, etc. (Peng *et al.*, 2013; Rasul and Rudolph, 2000; Cui and Grace, 2007). Generally, the well mixing of solids mixture is required to ensure good separation properties and

uniform fluidization conditions for efficient dry coal beneficiation in an ADMFB (Oshitani *et al.*, 2011; Tang *et al.*, 2009; He *et al.*, 2013). However, the presence of binary mixtures with different physical properties (i.e. density, size, or shape) usually give rise to particle segregation, which may result in inefficient coal beneficiation performance. Therefore, a detailed knowledge of particle mixing and segregation behavior of binary systems is crucial for the application of ADMFB technology, as well as other similar fluidized bed processes.

In a bubbling fluidized bed of binary mixtures, the steady state of solids distribution results from a dynamic equilibrium between the competitive mechanisms of particle mixing and segregation processes (Rowe *et al.*, 1972). The bubbling behavior plays a very important role in mixing and segregation in the fluidized bed, which has been the emphasis in many research works (Donsi and Ferrari, 1988; Formisani *et al.*, 2011; Rowe and Nienow, 1976; Wirsum *et al.*, 2001). Fluidization of solid mixtures at relatively lower gas velocities typically leads to heterogeneous bubbling systems, characterized by gas bubbles forming just above the bed distributor or after the jetsam layer at the lower part of the bed (Hoffmann *et al.*, 1993; Luo *et al.*, 2013). The gas bubbles rise increasingly in the fluidized bed while bubble grow due to bubble coalescence and hydrostatic pressure reduction and then finally burst at the bed surface. The rising gas bubbles always gather solid particles in their wakes and carry them towards to the bed surface, meanwhile some particles in the wake region would spill over during transportation and other surrounding solids will be dragged into the bubble wake to fill the loss. This particle movement usually becomes more severe with the increasing bubble size and/or bubble rise velocity. On the contrary, solid particles in the bubble-free region of a fluidized bed tend to descend slightly because of the ascendant solids in the wake regions of rising gas bubbles. Consequently, the overall convective circulation of solid particles in the bubbling fluidized bed is achieved, which is of significant importance for the mixing and segregation pattern of binary systems.

In general, the particle mixing and segregation processes may coexist during gas-solid fluidization, which gives rise to a complex solids distribution profile (Chen and Keairns, 1975; Girimonte *et al.*, 2018; Rao *et al.*, 2011). Fluidization of binary mixtures of similar particle properties always show uniform fluidization and good mixing performance. However, the partial or complete segregation of binary mixtures may appear when a fluidized bed consists of different particle sizes and/or densities. As pointed out by many researchers (Naimer *et al.*, 1982; Olaofe

et al., 2013; Formisani *et al.*, 2014; Gidaspow *et al.*, 2013; Maio *et al.*, 2013), the segregation behavior of solid particles differing in size or density is an intrinsic feature of such fluidization systems, and it is enhanced as the differences in size and density of particles increase. In principle, the mechanism of the segregation process is that solid particles are subjected to an imbalance of forces during gas-solid fluidization, particularly the gravity and drag forces (Zamankan, 1995; Fan and Fox, 2008; Azizi *et al.*, 2010, Chao *et al.*, 2012). For a binary system of dissimilar particles, the denser or larger particles that tend to concentrate at the bottom of fluidized bed are referred to as jetsam, while the lighter or smaller particles that show the opposite tendency are termed as flotsam (Rowe *et al.*, 1972). The appearance of the segregation phenomenon is dominant at lower gas velocities, and the degree of segregation can be reduced or even eliminated by increasing gas velocity. A remarkable research effort has been made to improve the understanding of the mechanisms and transient of particle mixing and segregation (Maio *et al.*, 2013; Gibilaro and Rowe, 1974; Carsky *et al.*, 1987; Gilbertson and Eames, 2001; Mostafazadeh *et al.*, 2013; Chiba *et al.*, 1982), but a widely accepted theory to describe this phenomenon has not been yet developed. The apparent complexity of this problem is attributed to the large number of factors that may affect the distribution of solid particles, such as the particle properties, mixture composition, operating conditions, fluidized bed structure, etc. It is still somewhat obscure how these factors affect the particle mixing and segregation processes.

In the present work, comprehensive analyses of axial solids distribution of binary mixtures of medium particles in an ADMFB were carried out to address the issues of mixing and segregation behavior. The design and operating parameters which may affect the axial solids distribution of medium particles were examined, including particle density ratio, particle size ratio, mixture composition, operating gas velocity, and initial bed height. Furthermore, the mixing index was employed to clearly exhibit the mixing and segregation pattern, and the appropriate operating conditions to achieve bed density adjustment for dry coal beneficiation in an ADMFB were investigated experimentally.

6.2 Experimental

6.2.1 Experimental setup

All the experiments were carried out in a gas-solid fluidized bed, and the schematic diagram of the experimental setup is shown in Figure 6.1. The experimental apparatus comprises a fluidized bed made from plexiglas column with an internal diameter of 150 mm and a height of 500 mm. A perforated distributor with an open area of 11% and orifice diameter of 1.5 mm was used and a fabric cloth was fixed to the distributor plate to avoid particles from falling through the perforated distributor. Ambient air was introduced through an air filter, roots blower, and pressure tank to fluidize the solid mixtures at the bottom of the bed column. A gas valve and calibrated rotameter were used to control the air flow rate. A ruler was attached on the column wall to measure the bed height of solid mixtures. The pressure drop of fluidizing particles was tested by *U*-shaped monometers to determine the minimum fluidization velocity. Fine dust generated during gas-solid fluidization was removed by the dust collection device.

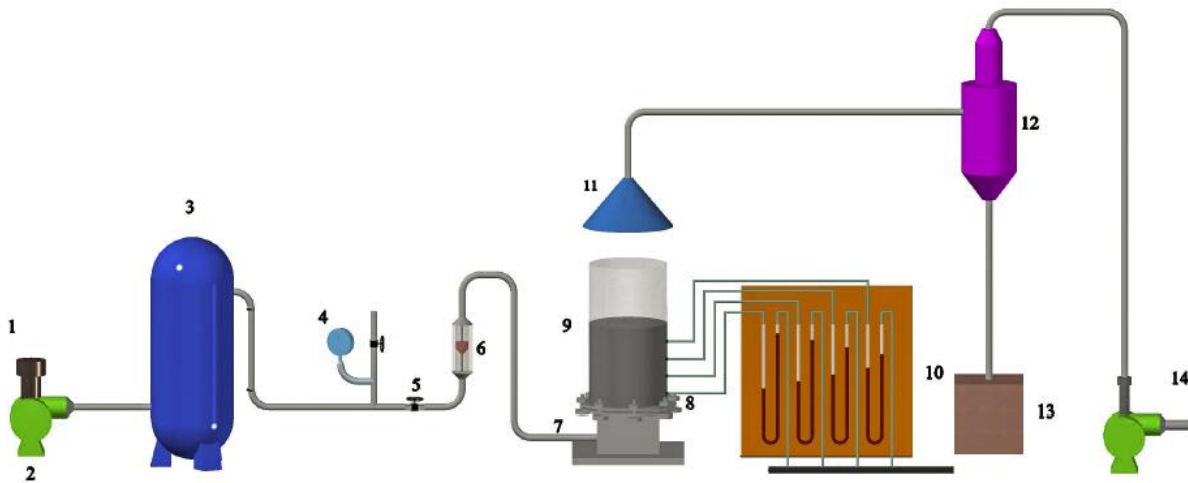


Figure 6.1 The schematic diagram of experimental apparatus: 1. Air filter; 2. Roots blower; 3. Pressure tank; 4. Pressure gauge; 5. Gas valve; 6. Rotameter; 7. Air chamber; 8. Bed distributor; 9. Fluidized bed column; 10. *U*-shaped manometer; 11. Dust cover; 12. Cyclone; 13. Dust collector; 14. Roots blower.

6.2.2 Experimental materials

Binary mixtures of magnetite and sand/gangue/coal particles were tested individually as the medium particles in an ADMFB. The 150 – 300 μm magnetite particles with a density of 4600 kg/m^3 were employed as the core medium material, and three other types of solid materials were added separately to form various binary mixtures. The particle densities of sand/gangue/coal particles are 2650, 2100, and 1300 kg/m^3 , respectively. The size ranges of each solid material are 150 – 300, 300 – 425, 425 – 590, 590 – 710 and 710 – 850 μm , respectively. The minimum fluidization velocity of both binary mixtures and single particles were determined by the pressure-drop-velocity method. For convenience, the three types of binary mixtures are referred to as: M-S mixtures (magnetite mixed with sand particles), M-G mixtures (magnetite mixed with gangue particles), and M-C mixtures (magnetite mixed with coal particles). The particle properties of experimental materials are displayed in Table 6.1.

Table 6.1. The properties of experimental materials.

Material	Size range (μm)	Mean size (μm)	Density (kg/m^3)	U_{mf} (cm/s)	Ar	Re_{mf}	Notation
Magnetite	150-300	232	4600	9.5	2266	1.6	M232
Sand	150-300	224	2650	4.9	1175	0.8	S224
Sand	300-425	368	2650	12.4	5208	3.3	S368
Sand	425-590	485	2650	20.2	11923	7.1	S485
Sand	590-710	636	2650	33.5	26885	15.4	S636
Sand	710-850	807	2650	39.7	54924	23.1	S807
Gangue	150-300	215	2100	4.0	823	0.6	G215
Gangue	300-425	372	2100	10.9	4263	2.9	G372
Gangue	425-590	486	2100	18.7	9505	6.5	G486
Gangue	590-710	625	2100	24.6	20216	11.1	G625
Gangue	710-850	808	2100	34.1	43681	19.9	G808
Coal	150-300	245	1300	3.2	754	0.6	C245
Coal	300-425	396	1300	8.0	3182	2.3	C396
Coal	425-590	460	1300	13.5	4988	4.5	C460
Coal	590-710	617	1300	17.8	12036	7.9	C617
Coal	710-850	795	1300	20.3	25747	11.6	C795

6.2.3 Mixing and segregation evaluation

Particle mixing and segregation of binary mixtures in a fluidized bed can be quantitatively evaluated by the axial distribution of solid particles through sampling and analysis. A simple measuring method was used for all the subsequent experiments. Weighted quantities of the particulate components are fluidized at a given gas velocity for an hour before shutting off the air supply abruptly. The solid particles in the fluidized bed, now at rest, are divided into several horizontal layers with equal bed height, and samples from each layer is collected and analyzed for their properties by measuring the weight of the different components. The separation of solids mixture can be achieved by using the magnet recovery method. Furthermore, a dimensionless mixing index (I_m) can be used to evaluate the mixing and segregation behavior of binary mixtures in fluidized beds, and the definition is given by (Chiba *et al.*, 1980)

$$I_m = \frac{\int_{h_{\bar{M}}}^H M_h dh}{\bar{M} \times (H - h_{\bar{M}})} \quad (6.1)$$

where M_h is the mass ratio of denser component at the bed height h above the base; \bar{M} is the average mass ratio of denser component; H is the total fluidized bed height; and $h_{\bar{M}}$ is the bed height at the average mass ratio of denser component. It can be inferred from Equation (6.1) that when the binary mixtures are perfectly mixed in the fluidized bed, I_m value is equal to 1. The increasing I_m value represents severity of the mixtures segregation with denser component distributed at the upper part of the bed, whereas the decreasing M value means severe segregation, where the denser component concentrated at the bottom of fluidized bed.

6.3 Results and discussion

6.3.1 Effect of particle density ratio

The particle density of medium materials is the most significant factor affecting the adjustment of fluidized bed density for efficient coal beneficiation in binary ADMFB systems. Ideally, the large density difference of the two types of solid particles are required for wide range control of the bed density (Oshitani *et al.*, 2011; Tang *et al.*, 2009; He *et al.*, 2013). However, fluidizing of binary mixtures of solid particles with significant density difference may give rise to non-uniform axial solids distribution, which may make the bed density adjustment challenging. Since the solids distribution in the fluidized bed is related to particle density difference, the effect of particle density on the mixing and segregation behavior is best described in terms of particle density ratio. In this work, the influence of particle density ratio on the mixing and segregation behavior of the binary systems is investigated by using binary mixtures of 150 – 300 μm magnetite and 300 – 425 μm sand/gangue/coal particles with equal volume fractions. The larger particle size of less dense component was chosen to balance the density difference with magnetite particles during fluidization. Experiments were performed at the initial bed height of 20 cm and excess gas velocity of 4 cm/s , and the results for three different types of binary mixtures are shown in Figure 6.2.

It can be observed that the M232-S368 mixture does not show any segregation appreciably, except for a few partial segregations at the bottom of fluidized bed, which can be explained by the bubble jet effect. However, significant particle segregation occurs to the M232-C396 mixture, where the upper part of fluidized bed contains mostly coal particles and therefore magnetite particles almost all concentrate at the lower part of bed. Furthermore, the M232-G372 mixture exhibits partial segregation performance. To be exact, the concentration of gangue particles slightly increases with the increasing bed height, whereas the concentration of magnetite particles decreases. It is hereby concluded that the increasing density difference will enhance the particle segregation and inhibit mixing behavior for binary mixtures. This is reasonable for the gas-solid fluidization of binary systems. In general, solid particles of less density are more active than that of heavier ones under the same fluidization conditions, and a large difference in particle densities will give a non-uniform axial solids distribution, since the axial distribution of solid

mixtures results from a dynamic equilibrium between the competing processes of particle mixing and segregation (Formisani *et al.*, 2011; Rowe and Nienow, 1976).

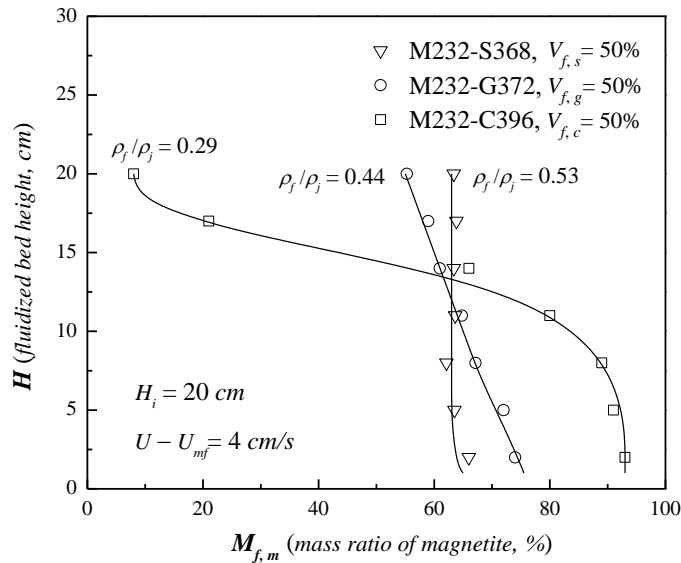


Figure 6.2 The effect of particle density ratio on axial solids distribution of binary mixtures.

6.3.2 Effect of particle size ratio

Particle size ratio of a binary mixture is an important factor in the selection of medium particles in an ADMFB system, especially for achieving uniform and stable fluidization for efficient coal beneficiation. In addition, the size range of medium materials which determines the production cost of medium particles is of great significance for industrial practices (Mohanta *et al.*, 2013; Sahu *et al.*, 2009). In the present work, the relations between particle size ratio and axial solids distribution for M-S, M-G, and M-C binary mixtures are shown in Figures 6.3, 6.4, and 6.5, respectively. For the sake of comparison, mixture compositions of *vol.* 25% and *vol.* 85% were chosen. As can be seen from Figure 6.3 (a) that M-S mixtures containing *vol.* 25% of sand particles exhibit good mixing behavior when the particle size ratio is below 2.1. However, above 2.1, the M-S mixtures show some partial segregation with relatively fewer sand particles at the lower part of fluidized bed, which may be due to the decreasing drag force effect per unit particle weight with the increasing size of sand particles, which will lead to an unbalance of forces during fluidization. From Figure 6.3 (b), it can be observed that significant segregation occurs to the M-S mixtures with *vol.* 85% of sand particles when the particle size ratio is over 3.5. This

can be explained by a decrease in the buoyancy force caused by the increasing ratio of lighter component (sand particles) in the fluidized bed.

It can be observed from Figure 6.4 (a) that, like the M-S mixtures, partial segregation occurs to the M-G mixtures containing *vol.* 25% of gangue particles at the larger size ratio. Moreover, a similar significant segregation was observed from Figure 6.4 (b) for the M-G mixtures with *vol.* 85% of gangue particles when the particle size ratio was above 2.7, which is comparably less than that of M-S mixtures. The particle segregation of M-G mixtures occurs earlier than that of M-S mixtures with the decrease in particle size ratio, which can be attributed to the gangue particles being less dense than the sand particles, and the decrease in particle density will require less drag force to balance the gravity of solid particles per unit volume in the fluidized bed (Girimonte *et al.*, 2018; Rao *et al.*, 2011). As can be seen from Figure 6.5 (a) and (b), the axial solids distribution of M-C mixtures is not very sensitive to the particle size ratio of magnetite and coal materials. To be exact, the slight partial segregation occurs to all of the M-C mixtures containing *vol.* 25% of coal particles at various particle size ratios, and only a few more coal particles with relatively less density will segregate to the upper part of bed. This can be attributed to the large density difference between the magnetite and coal particles, which gives rise to the severe segregation, and this particle segregation may overcome the mixing caused by bubbling behavior in the fluidized bed. Furthermore, the complete segregation phenomenon appears to the M-C mixtures with *vol.* 85% of coal particles at various particle size ratios, and most of the coal particles segregate at the top of fluidized bed and therefore the magnetite particles mostly concentrate at the bottom part. It can also be explained by the decreasing buoyancy force with the increase of fine coal content, and the denser component tends to sink in the fluidized bed.

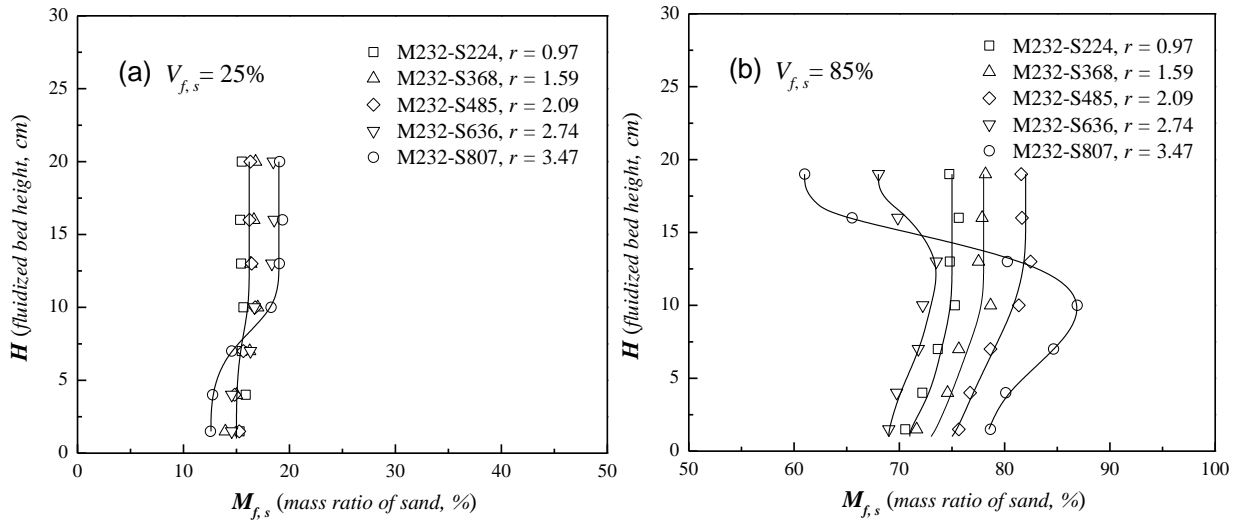


Figure 6.3 The effects of particle size ratio on the axial solids distribution of M-S mixtures at lower and higher volume fractions.

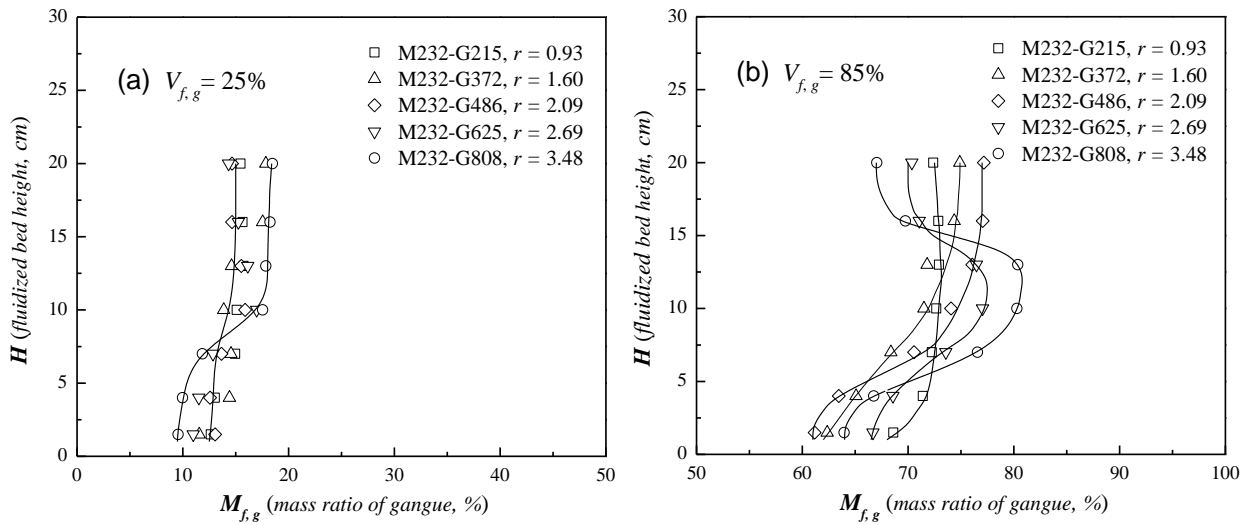


Figure 6.4 The effects of particle size ratio on the axial solids distribution for M-G mixtures at lower and higher volume fractions.

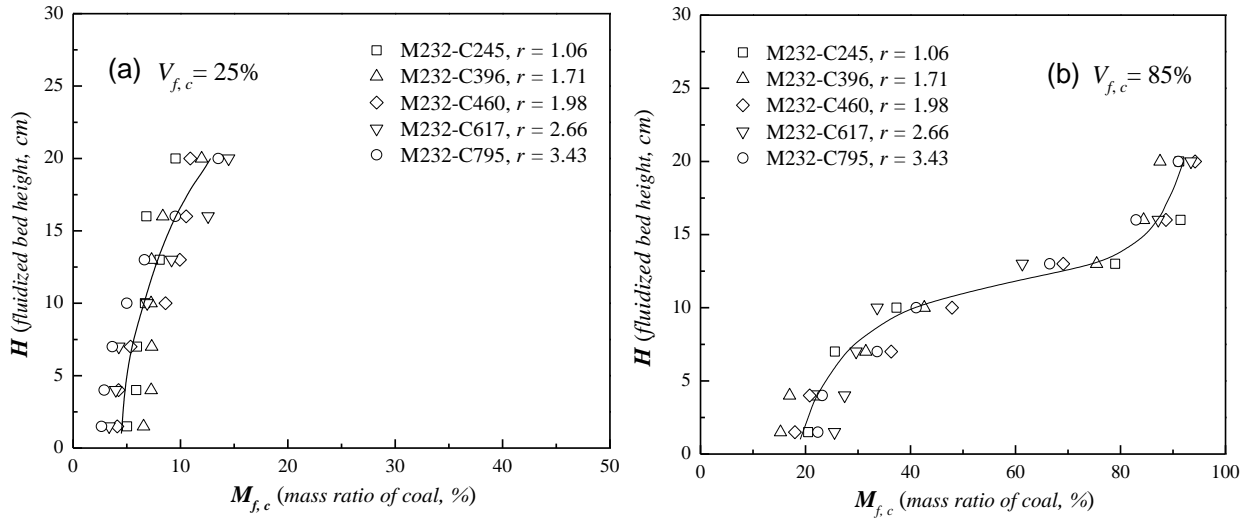


Figure 6.5 The effects of particle size ratio on the axial solids distribution for M-C mixtures at lower and higher volume fractions.

6.3.3 Effect of mixture composition

The mixture composition of binary mixtures of medium particles plays an important role in determining the control of bed density in the ADMFB system for efficient dry coal beneficiation. In this study, the effects of binary mixture composition on the axial solids distribution of M232-S368, M232-G372, and M232-C396 mixtures are shown in Figures 6.6, 6.7, and 6.8, respectively. It can be seen from Figure 6 that an increase in the volume fraction of sand particles does not cause any significant change in the mixing and segregation of M232-S368 mixtures, and all of M232-S368 mixtures exhibit slight partial segregation at the bottom of the fluidized bed and the well mixing state at the upper part. This may be due to the two types of solid particles have nearly the same aerodynamic properties, which may require similar fluidization conditions and will result in good mixing during the fluidization, and the minimal segregation of M232-S368 mixtures at the bottom part of bed can also be explained with the bubble jet effect.

As can be observed from Figure 6.7 that significant partial segregation happens to all of the M232-G372 mixtures, and the increasing volume fraction of gangue particles will enhance the partial segregation of solid mixtures. This can be explained by an increase in interstitial gas

velocity in the fluidization system, since the minimum fluidization velocity of M232-G372 mixtures will increase when the mass fraction of gangue particles increases. Gangue particles with relatively less density will become more active than the magnetite particles with the increase of interstitial gas velocity, which may result in more severe segregation of solid mixtures during fluidization. From Figure 6.8, it can be observed that the fluidization state of M232-C396 mixtures will transit from mixing to segregation state with the increasing fraction of coal particles. In details, the M232-C396 mixture exhibits particle mixing behavior when the fraction of coal particles is *vol.*25%, except for a few more coal particles concentrated at the top of fluidized bed. However, above *vol.*25%, complete segregation occurs to the binary systems with most of the coal particles concentrated at upper part of the bed and therefore most of the magnetite particles remain at the lower part.

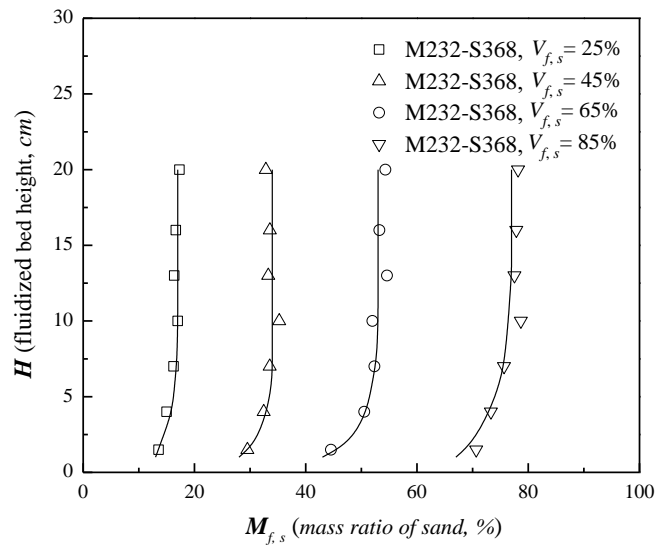


Figure 6.6 Axial solids distribution of fluidized bed with M232-S368 mixtures at different mixture compositions.

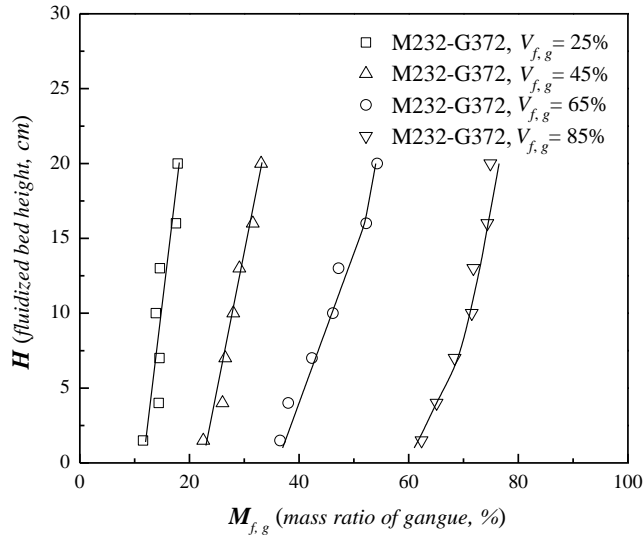


Figure 6.7 Axial solids distribution of fluidized bed with M232-G372 mixtures at different mixture compositions.

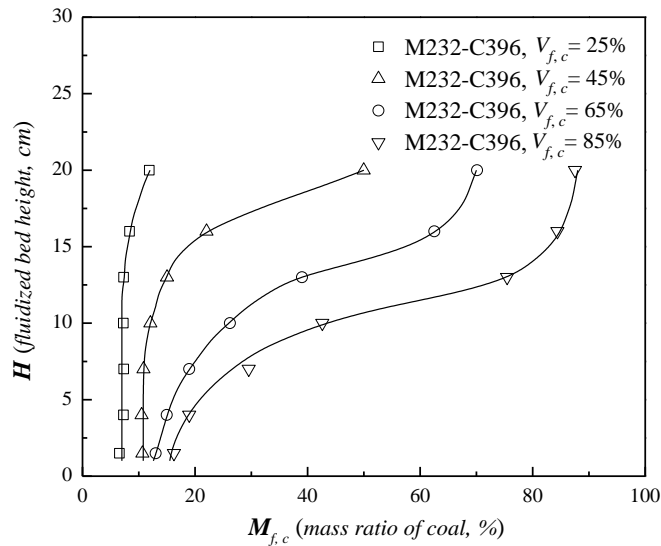


Figure 6.8 Axial solids distribution of fluidized bed with M232-C396 mixtures at different mixture compositions.

6.3.4 Effect of superficial gas velocity

Superficial gas velocity is one of the most important and complex factors affecting the particle movement and bubbling behavior (Formisani *et al.*, 2011; Wirsum *et al.*, 2001), which in return affects the solid mixing and segregation of binary mixtures in the ADMFB system. Since the rate

of gas bubbling is proportional to excess gas velocity ($U - U_{mf}$), the effect of superficial gas velocity on the particle mixing and segregation behavior shall be described in terms of excess gas velocity. With the increase of excess gas velocity examined from ranges of 2 to 8 *cm/s*, it can be observed that binary mixtures of magnetite and sand/gangue/coal particles could exhibit different solids distribution pattern, as shown in Figures 6.9, 6.10, and 6.11, respectively.

It is found from Figure 6.9 that the M232-S368 mixture exhibits a strong level of particle mixing and its axial solids distribution is relatively less sensitive to the changes in excess gas velocity. On the contrary, the M232-G372 mixture shows that partial solids segregation and an increase in excess gas velocity can improve the particle mixing of M232-G372 mixture system, as can be seen from Figure 6.10. This observation is similar to reports in previous investigations (Rowe and Nienow, 1976; Girimonte *et al.*, 2018; Sahoo and Roy, 2005). It can be explained by an increase in excess gas velocity, which facilitates the formation of larger and faster gas bubbles that will pick up more solids in their wakes from the bottom to top of the bed, which results in severe solids circulation and a higher degree of particle mixing in the fluidized bed. From Figure 6.11, it can be observed that the M232-C396 mixture system is completely segregated and the axial solids distribution is almost independent of excess gas velocity at a relatively lower range. This may be due to the significant density differences between magnetite and coal materials in the M232-C396 mixture, which leads to a drastic segregation process during fluidization, and this severe particle segregation could overcome the particle mixing caused by the increase of excess gas velocity.

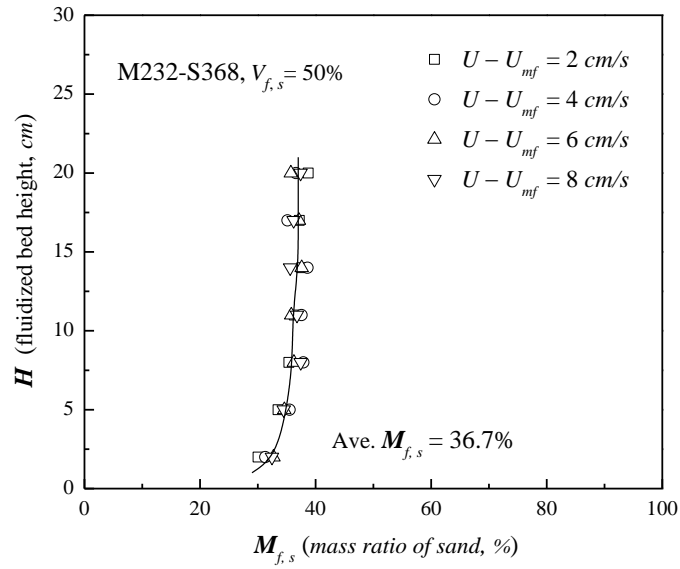


Figure 6.9 Axial solids distribution of fluidized bed with M232-S368 mixtures at various excess gas velocities ($U - U_{mf}$).

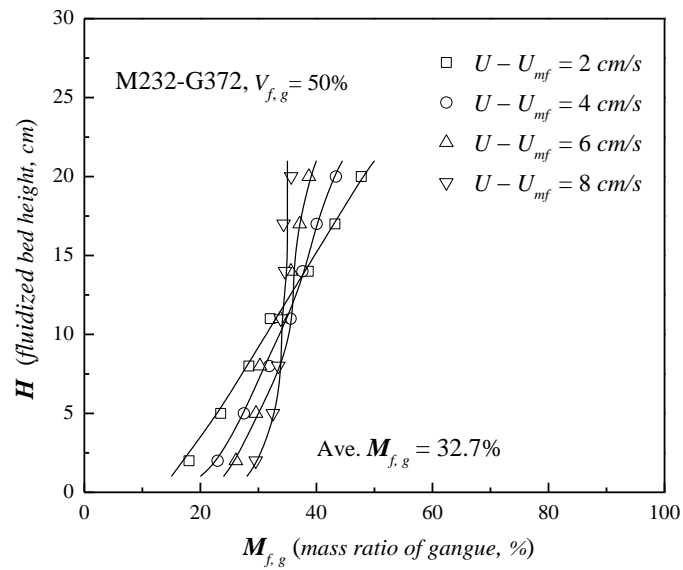


Figure 6.10 Axial solids distribution of fluidized bed with M232-G372 mixtures at various excess gas velocities ($U - U_{mf}$).

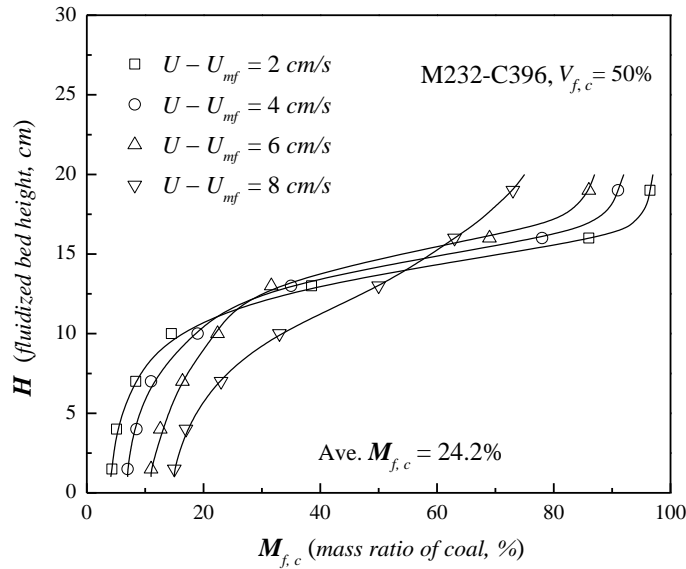


Figure 6.11 Axial solids distribution of fluidized bed with M232-C396 mixtures at various excess gas velocities ($U - U_{mf}$).

6.3.5 Effect of fluidized bed height

It is known that fluidized bed height determining the effective sorting space also has a significant influence on the separation performance and processing capacity of dry coal beneficiation in the ADMFB. In addition, the deep bed height is required for the effective beneficiation of super coarse coal ores of larger than 50 mm (Chen and Yang, 2003). Thus, the effects of initial bed height on axial distribution of M232-S368, M232-G372 and M232-C396 mixtures particles were examined, and the corresponding results are shown in Figures 6.12, 6.13 and 6.14, respectively. The initial bed height has some negative effects on the segregation behavior of M232-G372 and M232-C396 mixtures, as shown in Figures 6.13 and 6.14. It can be concluded that the particle mixing and segregation in the ADMFB, regardless of the types of solid mixtures, is relatively less sensitive to the changes in initial bed height than in particle properties and excess gas velocity, which is very important for the design and operation purposes. This can be explained by an increase in initial bed height, which facilitates the formation of larger bubbles, will give rise to a relatively higher degree of mixing at a given fluidizing velocity. However, the effect of large bubble diameter caused by increasing initial bed height on solids mixing is not as profound as particle properties and gas velocity.

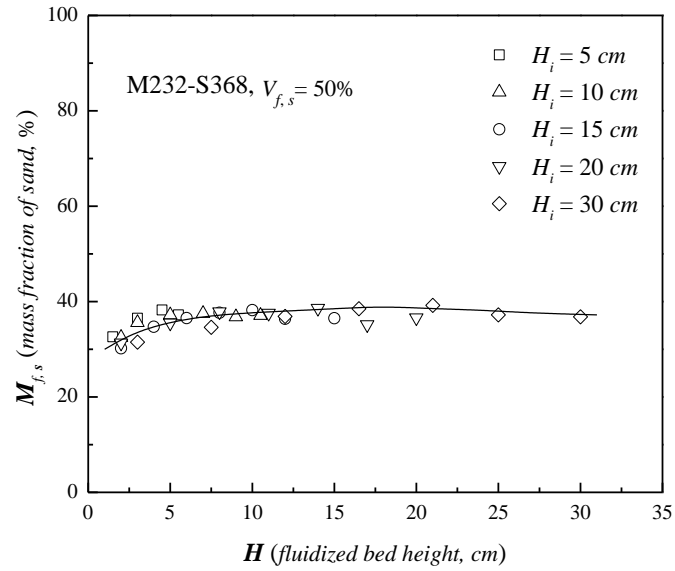


Figure 6.12 Axial solids distribution of fluidized bed with M232-S368 mixtures at different initial bed heights.

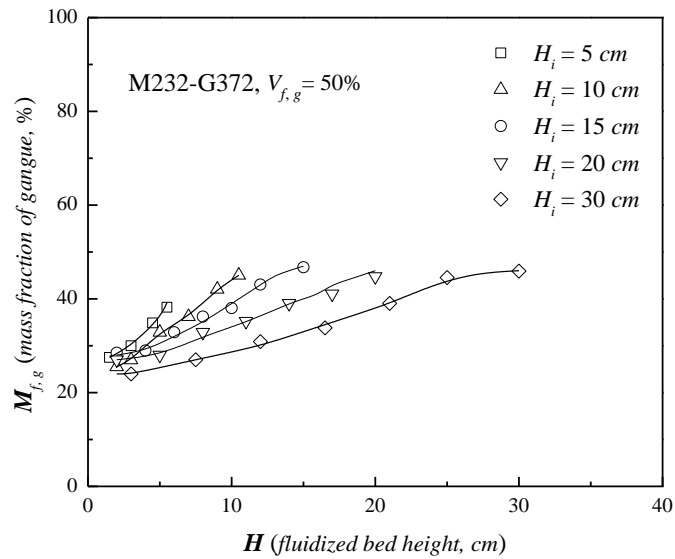


Figure 6.13 Axial solids distribution of fluidized bed with M232-G372 mixtures at different initial bed heights.

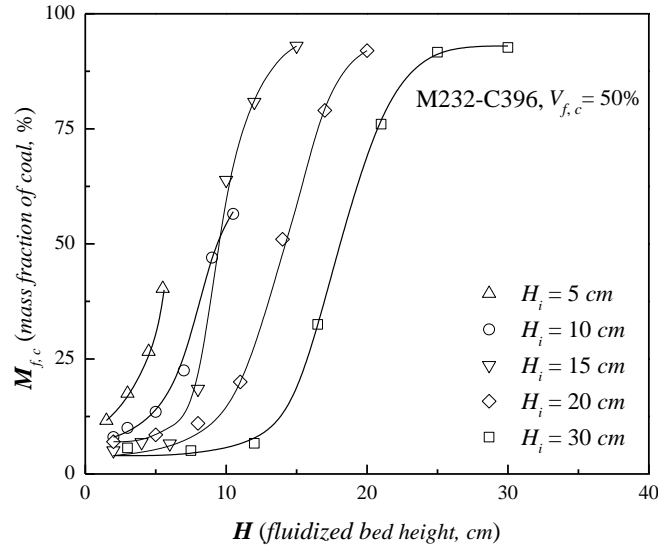


Figure 6.14 Axial solids distribution of fluidized bed with M232-C396 mixtures at different initial bed heights.

6.3.6 Mixing index of binary mixtures

When a binary solids mixture is fluidized, the mixing and segregation processes may coexist during fluidization, and the mixing index is therefore developed to estimate the degree of particle mixing and segregation (Naimer et al., 1982; Chiba et al., 1980; Sahoo and Roy, 2005; Marzocchella et al., 2000). The calculated values of the mixing index (I_m) by Eq. (6.1) for binary mixtures of magnetite and coal/gangue/sand particles are shown in Figures 6.15, 6.16 and 6.17, respectively. It is observed that practically perfect mixing of solids mixtures appears at lower mass fractions of lighter particles (coal/gangue/sand), which is the desired conditions for the adjustment of bed density in the ADMFB systems (Oshitani *et al.*, 2011; Tang *et al.*, 2009; He *et al.*, 2013). However, an increase in mass fraction of coal particles will lead to obvious decrease of I_m value below 1, indicating the significant segregation with the denser component (magnetite) as the jetsam, as shown in Figure 6.15. As can be seen from Figure 6.16 that the values of I_m are almost all marginally smaller than 1 with an increase of gangue particles, which reveals that partial segregation occurs with more magnetite particles distributed at the lower part of the bed. From Figure 6.17, it can be seen that good solids mixing exists until the mass fraction of sand particles reaches 60%, afterwards the particle segregation will turn out for the M-S mixtures.

The effects of excess gas velocity and initial bed height on the mixing index are shown in Figures 6.18 and 6.19, respectively. It can be seen from Figure 6.18 that the mixing index of solids mixtures with similar aerodynamic properties is not very sensitive to the increase of excess gas velocity at relatively lower ranges. This tendency is of great importance for the wide operating range of gas velocity for the coal beneficiation processing in an ADMFB system. Moreover, an increase in initial bed height also does not cause any significant changes in the mixing index of these binary mixtures, while fluidized bed reaches the certain initial bed height of 15 cm. This is meaningful for the design and scale-up of the ADMFB system in industrial practices, as well as the efficient dry beneficiation of coarse coal ores larger than 50 mm.

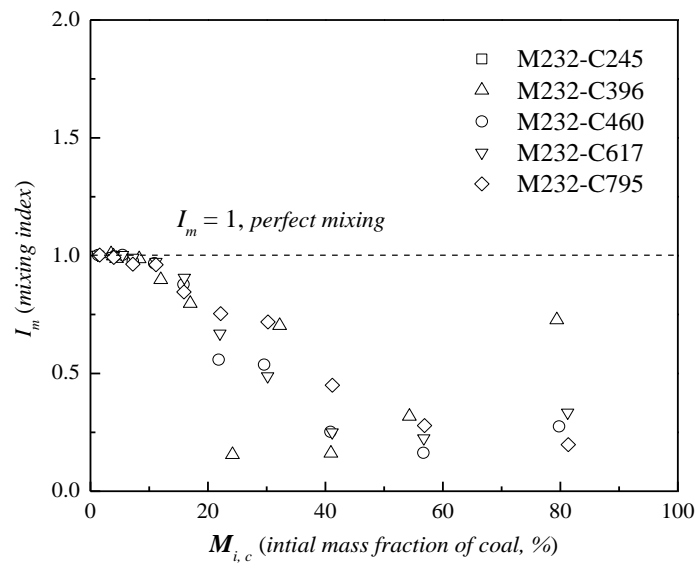


Figure 6.15 The mixing index (I_m) of binary mixtures of magnetite and coal particles.

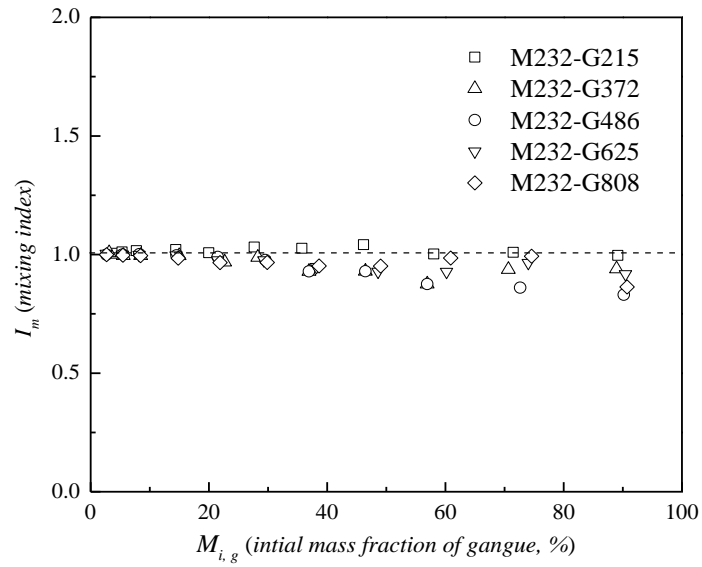


Figure 6.16 The mixing index (I_m) of binary mixtures of magnetite and gangue particles.

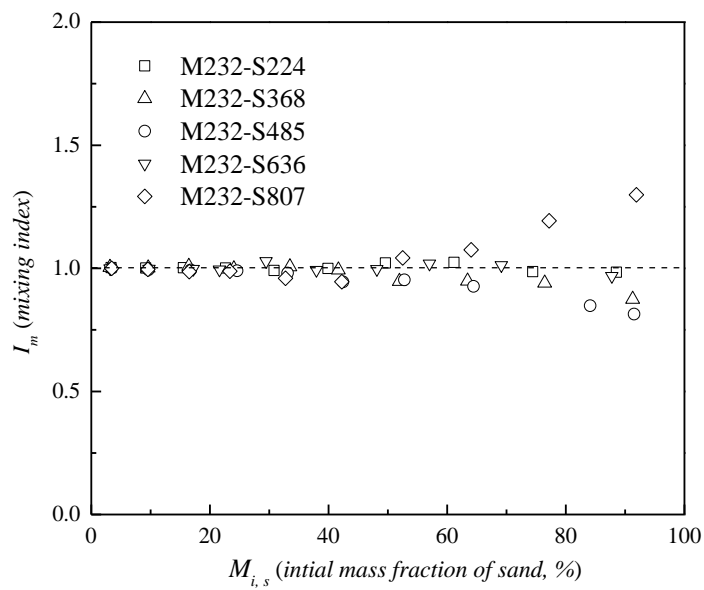


Figure 6.17 The mixing index (I_m) of binary mixtures of magnetite and sand particles.

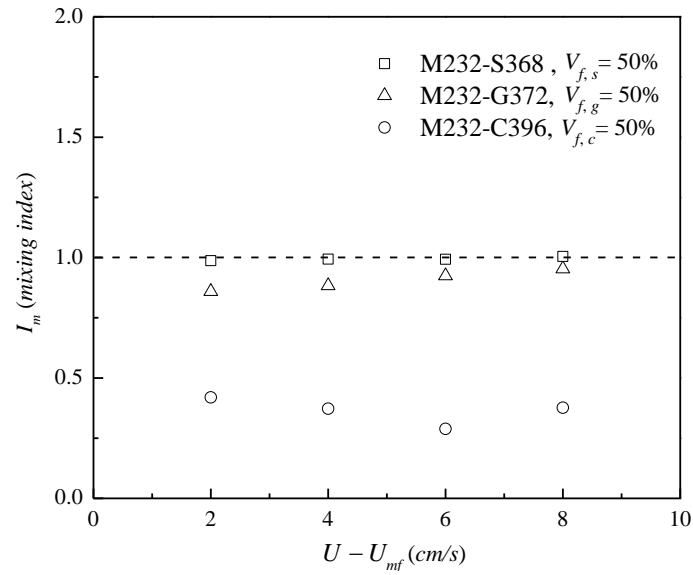


Figure 6.18 The effect of excess gas velocity on the mixing index (I_m).

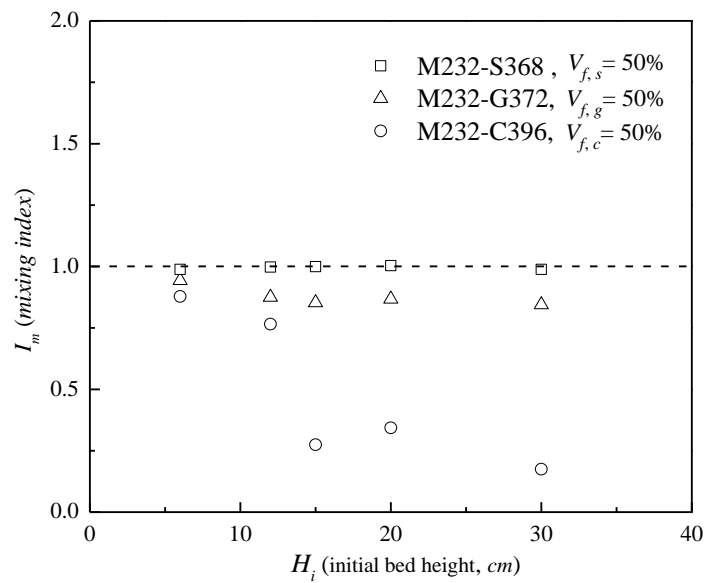


Figure 6.19 The effect of initial bed height on the mixing index (I_m).

6.4 Conclusion

The present work aims to evaluate the mixing and segregation behavior of binary mixtures of medium particles in an ADMFB for dry coal beneficiation, and the results were interpreted in terms of axial solids distribution. The experimental results demonstrated that particle segregation becomes more evident with the increase of particle density ratio. Particle mixing and segregation behavior of binary mixtures is less sensitive to the changes in particle size ratio than in particle density ratio. An increase in mass fraction of coal particles in the M-C mixtures will lead to the transition from the mixing to segregation state. Moreover, the increases of both the excess gas velocity in a relatively lower range and the initial bed height above 15 *cm* do not cause any significant variation in the mixing and segregation pattern of binary systems, which may give rise to broad conditions for the ADMFB operation. To achieve the adjustment of bed density, a lower mass fraction of fine coal particles (< 10%) which results in almost perfect mixing of binary medium particles is recommended as the fine coal particles will be generated automatically during coal beneficiation process. Magnetite mixed with gangue particles is the secondary consideration due to the occurrence of marginally partial segregation. Moreover, binary mixtures of magnetite and sand particles may exhibit a strong mixing performance, but the recovery and purification of sand particles will be an obstacle for efficient coal beneficiation in an ADMFB.

Nomenclature

h	fluidized bed height above the distributor, m
$h_{\bar{M}}$	bed height at the average mass ratio of denser component, m
H	total fluidized bed height, m
H_i	initial bed height, m
I_M	mixing index, <i>dimensionless</i>
$M_{f,c}$	mass fraction of coal particles, %
$M_{f,g}$	mass fraction of gangue particles, %
$M_{f,m}$	mass fraction of magnetite particles, %
$M_{f,s}$	mass fraction of sand particles, %
M_h	mass ratio of denser component at the bed height h , %
$M_{i,c}$	initial mass fraction of coal particles, %
$M_{i,g}$	initial mass fraction of gangue particles, %
$M_{i,s}$	initial mass fraction of sand particles, %
\bar{M}	average mass ratio of denser component, %
r	particle size ratio of binary mixture, <i>dimensionless</i>
U	superficial gas velocity, m/s
U_{mf}	minimum fluidization velocity, m/s
$V_{f,c}$	volume fraction of coal particles, %
$V_{f,g}$	volume fraction of gangue particles, %
$V_{f,s}$	volume fraction of sand particles, %

Acknowledgements

The authors are grateful to the financial support by Natural Science and Engineering Research Council of Canada (NSERC), China Scholarship Council (CSC), and National Natural Science Foundation of China.

References

- Azizi S., Hosseini S. H., Ahmadi G., Moraveji M., 2010. Numerical simulation of particle segregation in bubbling gas-fluidized beds. *Chem. Eng. Technol.* 33, 421-432.
- Babu M. P., Sai P. S. T., Krishnaiah K., 2017. Continuous segregation of binary heterogeneous solids in fluidized beds. *Particuology*. 35, 93-100.
- Carsky M., Pata J., Vesely V., Hartman M., 1987. Binary system fluidized bed equilibrium. *Powder Technol.* 51, 237-242.
- Chao Z. X., Wang Y. F., Jakobsen J. P., Fernandino M., Jakobsen H. A., 2012. Investigation of the particle-particle drag in a dense binary fluidized bed. *Powder Technol.* 224, 311-322.
- Chen J. L. P., Keairns D. L., 1975, Particle segregation in a fluidized bed. *Can. J. Chem. Eng.* 53, 395-402.
- Chen Q. R., Yang Y. F., 2003, Development of dry beneficiation of coal in China. *Coal Prep.* 23, 3-12.
- Chiba S., Nienow A. W., Chiba T., Kobayashi H., 1980, Fluidised binary mixtures in which the denser component may be flotsam. *Powder Technol.* 26, 1-10.
- Cui H. P., Grace J. R., 2007. Fluidization of biomass particles: A review of experimental multiphase flow aspects. *Chem. Eng. Sci.* 62, 45-55.
- Davidson J. F., Clift R., Harrison D., 1985. *Fluidization: 2nd Edition.* London, England: Academic press.
- Donsi G., Ferrari G., 1988. On the segregation mechanism of percolating fines in coarse-particle fluidized beds. *Powder Technol.* 55, 153-158.
- Fan R., Fox R. O., 2008. Segregation in polydisperse fluidized beds: Validation of a multi-fluid model. *Chem. Eng. Sci.* 63, 272-285.
- Formisani B., Girimonte R., Vivacqua V., 2011. Fluidization of mixtures of two-solids differing in density or size. *AIChE J.* 57, 2325-2333.
- Formisani B., Girimonte R., Vivacqua V., 2013. Fluidization of mixtures of two solids: A unified model of the transition to the fluidized state. *AIChE J.* 59, 729-735.

- Formisani B., Girimonte R., Vivacqua V., 2014. The interaction between mixture components in the mechanism of binary fluidization. *Powder Technol.* 266, 228-235.
- Gibilaro L. G., Rowe P. N., 1974. A model for a segregation gas fluidised bed. *Chem. Eng. Sci.* 29, 1403-1412.
- Gidaspow D., Chaiwang P., 2013. Bubble free fluidization of a binary mixture of large particles. *Chem. Eng. Sci.* 97, 152-161.
- Gilbertson M. A., Eames I., 2001. Segregation patterns in gas-fluidized systems. *J. Fluid. Mech.* 433, 347-356.
- Girimonte R., Formisani B., Vivacqua V., 2018. The relationship between fluidization velocity and segregation in two-component gas fluidized beds: density - or size - segregating mixtures. *Chem. Eng. J.* 335, 63-73.
- He J. F., Zhao Y. M., He Y. Q., Luo Z. F., Duan C. L., 2013. Fluidization characteristics of the dense gas-solid fluidized bed separator based on the mixed-medium solids of magnetite and paigeite powder. *Inter. J. Coal Prep. Util.* 33, 225-241.
- Hoffmann A. C., Janssen L. P. B. M., Prins J., 1993. Particle segregation in fluidised binary mixtures. *Chem. Eng. Sci.* 48, 1583-1592.
- Huang J. K., Lu Y. J., Wang H., 2017. A new quantitative measurement method for mixing and segregation of binary-mixture fluidized bed by capacitance probe. *Chem. Eng. J.* 326, 99-108.
- Joseph G. G., Leboreiro J., Hrenya C. M., Stevens A. R., 2007. Experimental segregation profiles bubbling gas-fluidized beds. *AIChE J.* 53, 2804-2813.
- Luo Z. F., Tang L. G., Dai N. N., Zhao Y. M., 2013. The effect of a secondary gas-distribution layer on the fluidization characteristics fluidized bed used for dry coal beneficiation. *Inter. J. Miner. Process.* 118, 28-33.
- Maio F. P. D., Renzo A. D., Vivacqua V., 2013. Extension and validation of the particle segregation model for bubbling gas-fluidized beds of binary mixtures. *Chem. Eng. Sci.* 97, 139-151.
- Martin R., 2008. *Introduction to particle technology*, second edition. West Sussex, England: Wiley.

- Marzocchella A., Salatino P., Pastena V. D., Lirer L., 2000. Transient fluidization and segregation of binary mixtures of particles. *AIChE J.* 46, 2175-2182.
- Mohanta S., Rao C. S., Daram A. B., Chakraborty S., Meikap B. C., 2013. Air dense medium fluidized bed for dry beneficiation of coal: technological challenges for future. *Part. Sci. Technol.* 31, 16-27.
- Mostafazadeh M., Rahimzadeh H., Hamzei M., 2013. Numerical analysis of the mixing process in a gas-solid fluidized bed reactor. *Powder Technol.* 239, 422-433.
- Naimer N. S., Chiba T., Nienow A. W., 1982. Parameter estimation for a solids mixing/segregation model for gas fluidised beds. *Chem. Eng. Sci.* 37, 1047-1057.
- Olaofe O. O., Buist K. A., Deen N. G., Hoef M. A., Kuipers J. A. M., 2013. Segregation dynamics in dense polydisperse gas-fluidized beds. *Powder Technol.* 246, 695-706.
- Olivier G., Marzocchella A., Salatino P., 2004. Segregation of fluidized binary mixtures of granular solids. *AIChE J.* 50, 3095-3106.
- Oshitani J., Kawahito T., Yoshida M., Gotoh K., Franks G. V., 2011. The influence of the density of a gas-solid fluidized bed on the dry dense medium separation of lump iron ore. *Miner Eng.* 24, 70-76.
- Peng Z. B., Doroodchi E., Alghamdi Y., Moghtaderi B., 2013. Mixing and segregation of solid mixtures in bubbling fluidized beds under conditions pertinent to the fuel reactor of a chemical looping system. *Powder Technol.* 235, 823-837.
- Rao A., Curtis J. S, Hancock B. C., Wassgren C., 2011. Classifying the fluidization and segregation behavior of binary mixtures using particle size and density ratios. *AIChE J.* 57, 1446-1458.
- Rowe P. N., Nienow A. W., Agbim A. J., 1972. The mechanisms by which particles segregate in gas fluidised beds – binary systems of near – spherical particles. *Trans. Instn. Chem. Engrs.* 50, 310-323.
- Rasul M. G., Rudolph V., 2000. Fluidized bed combustion of Australian bagasse. *Fuel.* 179, 123-130.

- Rowe P. N., Nienow A. W., 1976. Particle mixing and segregation in gas fluidised beds. A review. *Powder Technol.* 15, 141-147.
- Sahu A. K., Biswal S. K., Parida A., 2009. Development of air dense medium fluidized bed technology for dry beneficiation of coal – a review. *Inter. J. Coal Prep. Util.* 29, 216-241.
- Sahoo A., Roy G. K., 2005. Mixing characteristic of homogeneous binary mixture of regular particles in a gas-solid fluidized bed. *Powder Technol.* 159, 150-154.
- Tang L. G., Zhao Y. M., Luo Z. F., Liang C. C., Chen Z. Q., Xing H. B., 2009. The effect of fine coal particles on the performance of gas-solid fluidized beds. *Inter. J. Coal Prep. Util.* 29, 265-278.
- Turrado S., Fernandez J. R., Abanades J. C., 2018. Determination of the solid concentration in a binary mixture from pressure drop measurements. *Powder Technol.* 338, 608-613.
- Wirsum M., Fett F., Iwanowa N., Lukjanow G., 2001. Particle mixing in bubbling fluidized beds of binary particle systems. *Powder Technol.* 120, 63-69.
- Yang W. C., 1999. *Fluidization, solid handling and processing: Industrial applications.* Noyes, Westwood.
- Zamankhan P., 1995. Kinetic theory of multicomponent dense mixtures of slightly inelastic spherical particles. *Phys. Rev. E.* 52, 4877-4891.

CHAPTER 7

THE DISTRIBUTION OF BED DENSITY IN AN AIR DENSE MEDIUM FLUIDIZED BED WITH GELDART GROUP B AND/OR D PARTICLES

The distribution of bed density in an Air Dense Medium Fluidized Bed (ADMFB) with single and binary mixtures of Geldart Group B and/or D particles has been studied both theoretically and experimentally. The influences of particle properties, superficial gas velocity, and mixture composition of solid particles on the bed density distribution were examined. The results showed that there is lower density region at the bottom of fluidized bed with single particles, whereas the bed density at the upper part remains almost consistent. The increasing excess gas velocity does not change this trend although decreasing the overall bed density, however the binary mixtures of solid particles can be utilized to balance this non-uniform distribution of fluidized bed density. Moreover, an equation has been derived to estimate the bed density distribution based on the modified two-phase theory, considering particle properties and fluidization characteristics. The proposed correlation successfully accounts for predicting the distribution of bed density in an ADMFB involving both single and binary mixtures of Geldart Group B/D particles.

7.1 Introduction

Bubbling gas-solid fluidized beds composed of single or binary mixtures of solid particles are widely applied to various industrial processes, including gas-solid reactions, combustion and gasification, mixing, drying, mineral dry processing, etc. (Modekurti, *et al.*, 2013; Radmanesh, *et al.*, 2006; Geng and Che, 2001; Tahmasebi, *et al.*, 2013; Sun *et al.*, 2005). One of the main practical advantages of bubbling fluidized bed is connected with the relatively stable density of fluidization system (Davidson *et al.*, 1985; Kunii and Levenspiel, 1991). Therefore, it is natural to utilize this fluidized bed technology for dry coal beneficiation, which enables the dry separation between the coal products according to their density differences towards the fluidized bed density (Mohanta *et al.*, 2013; Sahu *et al.*, 2009; Zhang *et al.*, 2014; Zhao *et al.*, 2011). This dry separation method is named as Air Dense Medium Fluidized Bed (ADMFB) (Chen and Wei,

2003) which is capable of floating the clean coal with relative less density than the fluidized bed, whereas the heavier one (gangue) sinks to the bottom of the bed and thus can be rejected. The ADMFB technology has the inherent advantages of without using water, lower construction and processing costs, and comparable separation efficiency over the conventional wet processes, which is deemed to be the desired method for coal beneficiation in water-deficient, permafrost, and prolonged cold weather areas (Dwari and Rao, 2007; Houwelingen and Jong; 2004). Moreover, the ADFMB is an advanced and universally applicable technology, which has already been extended to other industries, including iron/copper ore beneficiation (Oshitani *et al.*, 2010; Oshitani *et al.*, 2013; Franks *et al.*, 2013; Franks *et al.*, 2015), agricultural products cleaning (Zaltzman *et al.*, 1983; Zaltzman *et al.*, 1985; Zaltzman *et al.*, 1987), municipal solid waste classification (Sekito *et al.*, 2006; Sekito *et al.*, 2006), etc.

Since the ADMFB is a physical and gravity-based process, a detailed knowledge of the uniformity and stability of fluidized bed density is of great importance for its application, especially for improving the efficiency and accuracy of dry coal separation (Sahu *et al.*, 2011; Firdaus *et al.*, 2012). The density of fluidized bed is defined as the mass of solid particles per unit volume of the suspension (Zinov'ev, 1976), which is highly affected by the hydrodynamics of gas-solid fluidization system. As is known that the ADMFB is generally in the bubbling fluidization regime, characterized by rising gas bubbles and gas-driven moving particles. According to the two-phase theory of fluidization (Toomey and Johnstone, 1952), all the gas flow in excess of that required for incipient fluidization is in the form of gas bubbles, and a bubbling fluidized bed can be composed of the dense (emulsion) phase and bubbles phase. The dense phase consisting of suspended solid particles and interstitial gas flow remains almost consistent as the incipient fluidization state, and the bubble phase consisting of rising gas bubbles of various sizes and velocities is essentially free from solid particles. Hence, the density of fluidized bed can be determined by the mixture composition of these two phases, and the bubbling behavior and its associated effects have a significant influence on the bed density of an ADMFB, which have been investigated extensively by many researchers (Oshitani *et al.*, 2011; Azimi *et al.*, 2013; Schmilovitch *et al.*, 1992; He *et al.*, 2002; Chikerema and Moys, 2012). In details, typical gas bubbles are initially very small forming at the bottom region, just above the bed distributor, move upward and then burst finally at the upper surface (Davidson *et al.*, 1985;

Kunii and Levenspiel, 1991). While gas bubbles travel through the fluidized bed, the bubble size usually increases as the bed height increases mainly due to the coalescence behavior (Mori and Wen, 1975; Darton *et al.*, 1977), and the rise velocity of gas bubbles growth with the increase of bubble size which can be attributed to an increase in buoyancy force with the increase of bubble volume (Rippin and Davidson, 1967; Davies and Taylor, 1950). Consequently, the distribution of gas bubbles in the fluidized bed is apparently non-uniform, which will change the solid concentration in the axial direction of the bed. As the density of fluidized bed is determined by the dispersed solid particles and gas bubbles, the uniformity and stability of bed density is therefore affected obviously by the fluidization characteristics, e.g. bubbling behavior, which require to be further investigated.

Understandably, if a fluidized bed is to be utilized as a means of density separation process, the knowledge of the influences of particle properties and mixture composition on the uniformity and stability of bed density is crucial. Early experimental studies attempting to utilize the ADMFB with single particles, e.g. magnetite particles, mainly due to its good flowability and magnetic property which can lower the consumption of medium particles through the magnetic recovery process (Sahan, 1997; Luo and Chen, 2001; Mak *et al.*, 2008). However, the bed density of fluidizing single particles is almost consistent and is usually not the desired one. For efficient dry coal beneficiation, the adjustable bed density is more preferred in the ADMFB operation. In order to achieve the bed density adjustment, various types of binary mixtures of solid particles have been processed as medium materials (Yoshida *et al.*, 2008; Oshitani *et al.*, 2013; Luo and Chen, 2001; Wei *et al.*, 2003), which have also been extensively studied in the fields of iron/copper ore separation and agricultural products cleaning. Although the binary fluidization system can manipulate freely the bed density by changing the mixture composition of solid particles, the uniformity and stability of bed density of binary fluidized beds cannot be guaranteed due to the complex fluidization and inevitable segregation behavior (Row *et al.*, 1972; Gilbertson and Eames, 2001). An understanding of the effects of particle properties and mixture composition of solid particles on the bed density distribution in the ADMFB is therefore of considerable importance. For design and operation purposes, it is also necessary to calculate the bed density distribution in the ADMFB with single and binary mixtures of solid particles, thus avoiding experimental measurements.

It is the purpose of the present work to determine the distribution of bed density in an ADMFB with the Geldart Group B and/or D particles both theoretically and experimentally. An equation has been derived to evaluate how the process variables affect the distribution of fluidized bed density. Experiments were performed on several size fractions of four solid particles with various binary mixtures, involving magnetite, river sand, glass bead and fine coal particles. The process variables which affect the axial density distribution from the proposed model can be summarized as particle size, particle density, particle composition, and excess gas velocity. The proposed model has been verified with experimental data obtained in the present work involving both single and binary mixtures of Geldart Group B and/or D particles.

7.2 Theory

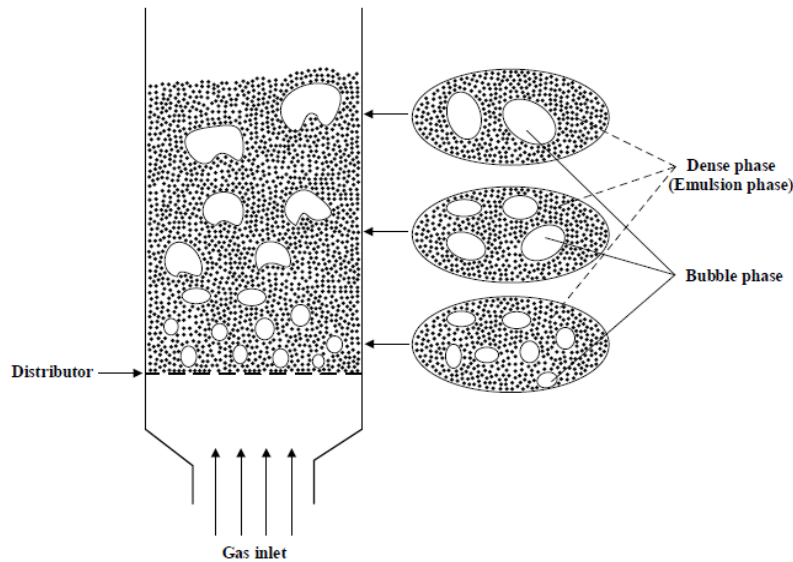


Figure 7.1 The schematic diagram of an Air Dense Medium Fluidized Bed.

In general, Air Dense Medium Fluidized Bed system is in the bubbling fluidization regime, characterized by rising gas bubbles and disordered moving particles. Based on the two-phase theory of fluidization (Toomey and Johnstone, 1952), an ADMFB can be considered to be composed of dense (emulsion) phase and bubble phase, as shown in Fig. 7.1. If ignoring the volume of solids dispersed in the gas bubbles, the density of fluidized bed at a certain level of bed height can be given by

$$\rho_{bed} = \rho_b A_b / A + \rho_d A_d / A \quad (7.1)$$

where ρ_b and ρ_d are the densities of bubble phase and dense phase, respectively, A_b and A_d are the bed cross-sectional areas occupied by bubble phase and dense phase. As is known that the density of bubble phase is very close to gas density, and the density of dense phase can be taken as (Davidson *et al.*, 1985)

$$\rho_d = \rho_p(1 - \varepsilon_{mf}) + \rho_g \varepsilon_{mf} \quad (7.2)$$

where ε_{mf} is the bed voidage at minimum fluidization state, ρ_g and ρ_p are the densities of gas and solid particles, respectively. The bed cross-sectional area (A) can be given as

$$A = A_b + A_d \quad (7.3)$$

To calculate the distribution of bed density, it is important to determine the bed cross-sectional area occupied by gas bubbles at a certain level (A_b), which can be obtained from

$$A_b = G_b / U_b \quad (7.4)$$

where G_b is the volumetric bubble flowrate, U_b is the rise velocity of gas bubbles.

Combining of Eqs. (7.1), (7.2), (7.3) and (7.4), the correlation for estimating the distribution of bed density in an ADMFB leads to

$$\rho_{bed} = (1 - \varepsilon_{mf})(\rho_p - \rho_g)[1 - G_b / (AU_b)] + \rho_g \quad (7.5)$$

It should be mentioned that the behavior of gas-fluidized system is closely dependent on the properties of solid particles, which needs to be carefully considered in the estimation of bed density. According to the Geldart's particle classification (Geldart, 1973), there are four different types of solid particles, which termed as Geldart A, B, C and D Groups. It is noteworthy that all the cohesive powder, which are very difficult to be fluidized at normal condition, belong to Group C powders. Fluidized beds of Group A powders exhibit a particulate expansion before bubbling occurs, which will results in unpredictable bed voidage of dense phase during fluidization. Therefore, the Geldart Group B and D particles containing most of the coarse and dense particles are usually employed as the medium material in the ADMFB system. And then,

the investigation of fluidized bed density for both single and binary mixtures of Geldart B and/or D particles is carried out in this work.

As described by the two-phase theory of fluidization, all the gas flow in excess of that required for incipient fluidization is in the form of gas bubbles in the bubbling fluidized bed. However, there is ample experimental evidence (Turner, 1966; Grace and Clift, 1974; Hilligard and Werther, 1986; Hepbasli, 1998) which demonstrates that the original two-phase theory tends to overestimate the bubble flow rate in most cases. Thus, the modified two-phase theory (Hilligard and Werther, 1986) has been developed by introducing the correction factor Y , defined by

$$G_b = Y(U_g - U_{mf})A \quad (7.6)$$

where G_b is the volumetric bubble flow rate, U_g and U_{mf} are the superficial gas velocities at operating condition and minimum fluidization, respectively. The parameter Y represents the deviation of the visible bubble flow rate from the original two-phase theory assumption, which was found to be generally below unity. For Geldart Group B and D particles, a reasonable correlation (Eq.(5.14)) has been proposed in the earlier work as follows

$$Y = 1.72Ar^{-0.133}(U_g - U_{mf})^{0.024} \quad (7.7)$$

where Ar is the Archimedes number. Practically, Archimedes number increases with the increasing of particle size or density, which is defined as

$$Ar = \rho_g(\rho_p - \rho_g)gd_p^3/\mu^2 \quad (7.8)$$

In order to determine the bed cross-sectional area occupied by bubbles, knowledge of the bubble rise velocity is needed. In general, the bubble rise velocity through a fluidized bed is related to the bubble size, and it is usually estimated by the relationship proposed by Davidson and Harrison (Davidson and Harrison, 1963)

$$U_b = 0.71\sqrt{gD_e} + (U_g - U_{mf}) \quad (7.9)$$

where D_e is the volume-equivalent bubble diameter. Various correlations have been developed to evaluate this bubble diameter, and Darton equation (Darton *et al.*, 1977)] is one of the commonly used correlations

$$D_e = 0.54(U_g - U_{mf})^{0.4}(h + 4A_D^{0.5})^{0.8}/g^{0.2} \quad (7.10)$$

where h is the bed height above the distributor, A_D is the area of each orifice in perforated plate distributor and is equal to zero for a porous plate distributor.

By submitting the Eqs. (7.6), (7.7), (7.9), (7.10) into Eq. (7.11), the distribution of bed density in an Air Dense Medium Fluidized Bed with Geldart B and/or D particles can be expressed by

$$\rho_{bed} = (1 - \varepsilon_{mf})(\rho_p - \rho_g) \left[1 - \frac{1.72Ar^{-0.133}(U_g - U_{mf})^{0.024}}{1 + 1.3(h + 4A_D^{0.5})(U_g - U_{mf})^{-0.8}} \right] + \rho_g \quad (7.11)$$

It can be observed from Eq. (7.11) that the process variables which affect the bed density distribution can be summarized as the properties of solid particles, mixture composition, excess gas velocity, and fluidized bed height, which have been experimentally investigated in this work. For a rapid estimation, we have assumed approximately $\varepsilon_{mf} = 0.45$ for Geldart Group B and D particles, and the gas density could almost be neglected due to the large difference when compared with the particle density.

7.3 Experimental

7.3.1 Experimental apparatus

All experiments were conducted in a cylindrical fluidized bed of 152 mm in diameter at ambient conditions, as shown in Figure 7.2. After being filtered and compressed, the surrounding air was sent to fluidize the solid particles in the bed column through a perforated distributor. The air flowrate was controlled by a valve and measured by a rotameter. The diameter of each orifice on the distributor plate is 1.5 mm and the total open area is 11%. To investigate the axial distribution of bed pressure, *U*-shaped manometers were employed. The piezometric pipes of manometers are connected to the pressure taps along the bed column with the interval of 5 cm. First pressure tap is located at 1 cm above the distributor, which is designed to prevent the effects of bubble jets. Fine dust generated during particle fluidization was gathered by the dust collection device. It is noteworthy that the axial density distribution of bubbling fluidized bed was obtained and calculated from the time-averaged pressure drop.

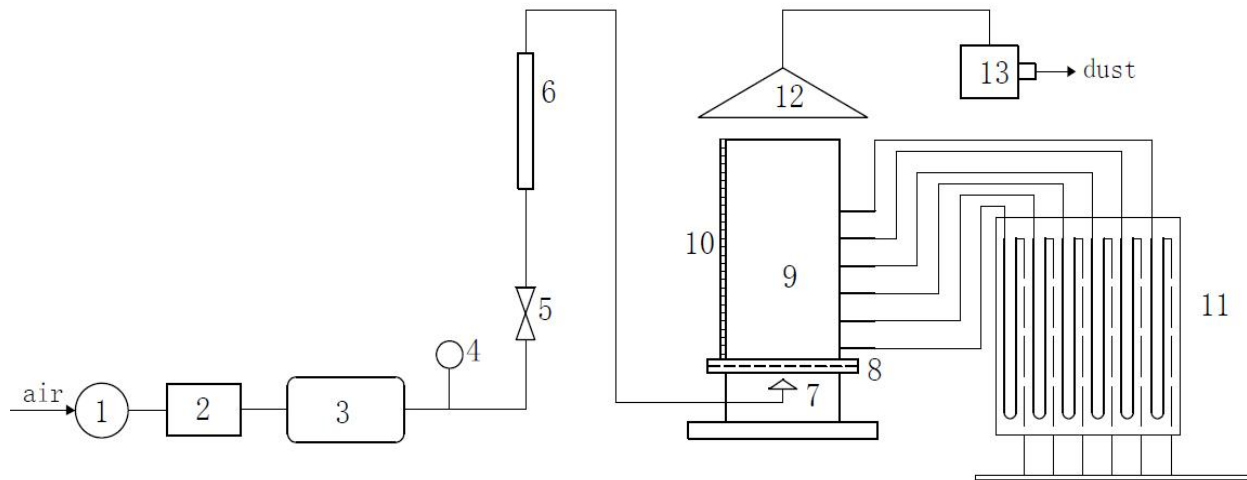


Figure 7.2 The schematic diagram of experimental apparatus: 1. Air filter; 2. Roots blower; 3. Tank; 4. Pressure gauge; 5. Gas valve; 6. Rotameter; 7. Air chamber; 8. Bed distributor; 9. Plexiglas column; 10. Rule; 11. *U*-shaped manometer; 12. Dust cover; 13. Dust collector.

7.3.2 Experimental materials

Magnetite, glass bead, river sand and coal particles with the size range from 150 to 710 μm were used as the bed materials. These samples were classified into the specific size fractions of 150 – 300 μm , 300 – 425 μm , 425 – 590 μm , and 590 – 710 μm by screening. The properties of these experimental materials are shown in Tables 7.1, 7.2, 7.3 and 7.4. Hosokawa Powder Tester was employed to measure the aerated bulk density and angle of repose. BT-2900 Particle Image Analysis system was used to test the mean particle diameter. The particle true density was measured by the Archimedean immersion method, and the minimum fluidization velocity of each material was determined using the graph of bed pressure drop against decreasing gas velocity. It is noteworthy that the solid particles of smaller than 150 μm were excluded in this study as they may belong to Geldart A/C Group.

Table 7.1. The particle properties of magnetite samples.

Size range (μm)	Mean size (μm)	True density (kg/m^3)	Bulk density (kg/m^3)	AOR ($^\circ$)	Ar (kg/m)	U_{mf} (cm/s)	Notation
150 – 300	232	4650	2667	36.1	2215	9.1	M232
300 – 425	348	4570	2687	37.4	7348	16.2	M348
425 – 590	457	4540	2652	38.3	16533	34.5	M457
590 – 710	651	4590	2560	38.8	48317	71.0	M651

Table 7.2. The particle properties of glass bead samples.

Size range (μm)	Mean size (μm)	True density (kg/m^3)	Bulk density (kg/m^3)	AOR ($^\circ$)	Ar (kg/m)	U_{mf} (cm/s)	Notation
150 – 300	209	2620	1630	33.1	912	6.9	G209
300 – 425	356	2650	1611	34.3	4561	12.3	G356
425 – 590	469	2680	1605	34.6	10547	18.5	G469
590 – 710	648	2640	1612	35.2	27403	23.3	G648

Table 7.3. The particle properties of river sand samples.

Size range (μm)	Mean size (μm)	True density (kg/m^3)	Bulk density (kg/m^3)	AOR ($^\circ$)	Ar (kg/m)	U_{mf} (cm/s)	Notation
150 – 300	224	2530	1544	34.5	1085	5.8	S224
300 – 425	368	2410	1610	37.4	4581	14.9	S368
425 – 590	475	2510	1602	38.1	10261	19.8	S475
590 – 710	636	2500	1593	39.3	24534	30.3	S636

Table 7.4. The particle properties of fine coal samples.

Size range (μm)	Mean size (μm)	True density (kg/m^3)	Bulk density (kg/m^3)	AOR ($^\circ$)	Ar (kg/m)	U_{mf} (cm/s)	Notation
150 – 300	236	1507	874	35.3	755	2.8	C236
300 – 425	361	1545	896	37.1	2771	6.5	C361
425 – 590	479	1476	856	39.5	6147	13.5	C479
590 – 710	633	1465	845	40.6	14168	17.8	C633

7.4 Results and discussion

7.4.1 Effect of particle size and density

The distribution of bed density of an ADMFB with various size fractions of different single particles within Geldart B and D Group are shown in Figure 7.3 together with the predicting curve calculated by Eq. (7.11). It should be mentioned that the predicting curve is based on the particle size range of 150 – 300 μm for each material as the density difference of same material with different particle sizes is very small indeed. As can be observed from Figure 7.3 that for all the 16 different types of solid particles, there is always a lower bed density region at the bottom of fluidized bed, whereas the bed density at the upper part of bed remains almost unchanged. The same trend has also been claimed elsewhere (Granfield and Geldart, 1974; Korolev and Syromyatnikov, 1971; Ruzicka, 2006), which can be ascribed solely to the bubbling behavior of the fluidized bed. According to the two-phase theory, the bubbling fluidized bed is composed of gas bubbles (bubble phase) and suspended solid particles with interstitial gas flow (dense phase). The gas bubbles formed at the bottom area of fluidized bed, very close to the distributor, rise and

travel through the bed, growing due to bubble coalescence. Therefore, the retention of volumetric bubble flow at the lower part of fluidized bed is more than that at the upper part as the bubble rise velocity increases with increasing bubble size. The more the retention of volumetric bubble flow, the less the solid particle concentration, which will result in a lower bed density at the lower part of fluidized bed. Moreover, this tendency of lower bed density at the bottom of fluidized bed has been successfully predicted by the proposed model in this work.

It can also be observed from Figure 7.3 that the distribution of bed density is almost independent of the size range of solid particles of the same material, but the tendency of decreasing bed density at the bottom of fluidized bed becomes more evident with the increase of particle density of different materials. This can be explained that the bed voidage in dense phase maintains almost the same for Geldart Group B and D particles (Geldart, 1973), and the bubbling behavior primarily relates to the excess gas velocity, both of them regardless of particle size and density. However, the bed density at the bottom part will decrease due to decreasing ratio of solid particles caused by increasing bubble volume. Therefore, the greater particle density of material will result in more decrease of bed density at the bottom of fluidized bed.

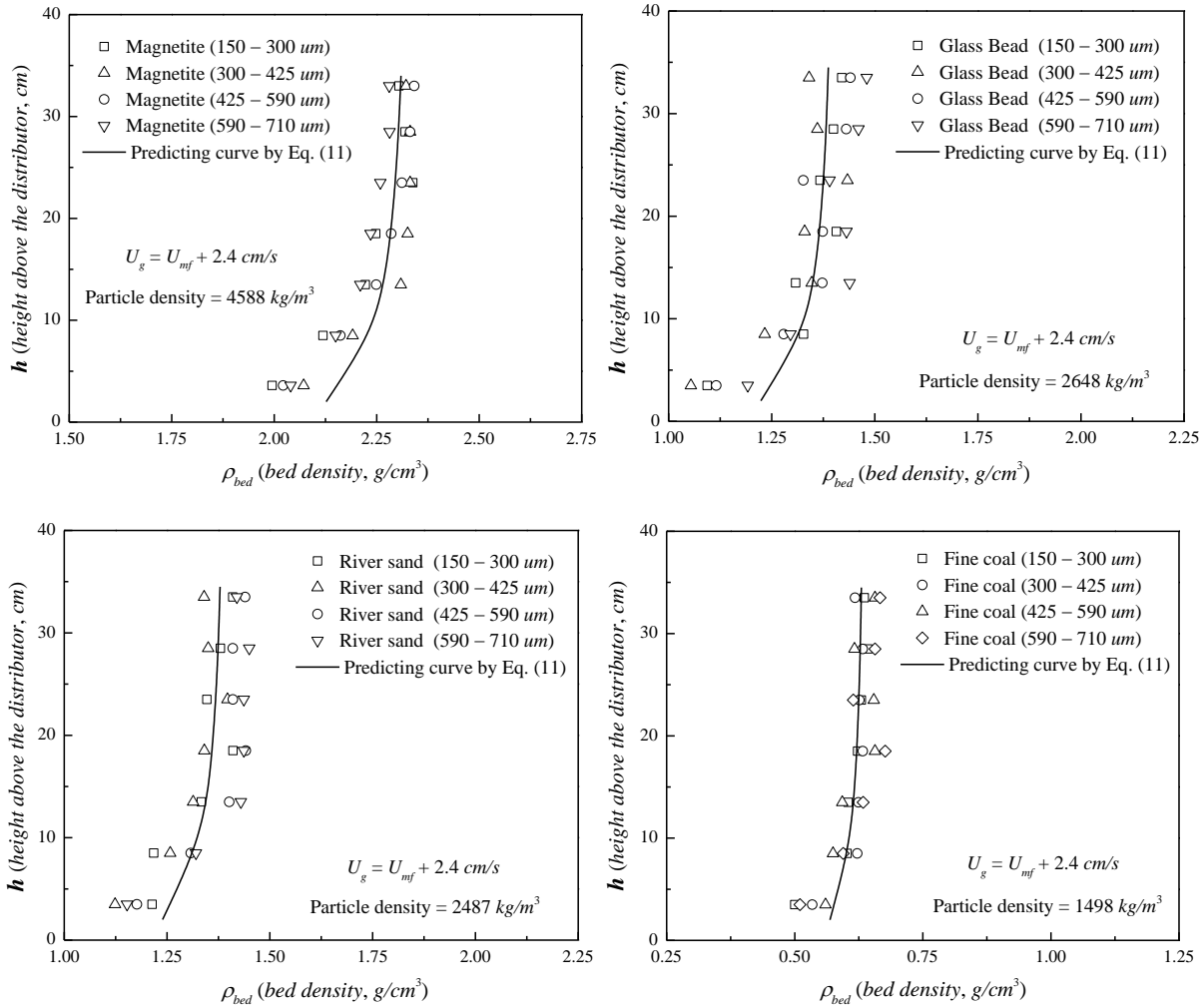


Figure 7.3 The distribution of bed density for different single particles of various size fractions.

7.4.2 Effect of excess gas velocity

The operating gas velocity playing an important role in determining both the performance of gas-solid fluidization and the efficiency of dry coal beneficiation can be generally expressed in terms of the excess gas velocity, which indicates the superficial gas velocity over than the minimum fluidization velocity. The influences of excess gas velocity on the distribution of bed density in an ADMFB with typical Geldart Group B and D particles are shown in Figures 7.4 and 7.5, respectively, and compared to the calculated data using the Eq. (7.11). It can be seen that both the Geldart Group B and D particles demonstrate a decreasing trend of bed density with increasing excess gas velocity, and the decrement of bed density under the same excess gas velocity increases with increasing particle density. This is reasonable that the increasing excess

gas velocity generally gives rise to an increase in the volume of gas bubbles; as a result, the bed density decreases due to the expansion of fluidized bed. Furthermore, the influence of excess gas velocity was found to have definite effects on the axial distribution of bed density, which may be due to the relatively stable bubbling behavior in the gas-solid fluidized bed. It should be noted that the measured bed densities with varying degrees of excess gas velocity are in fairly good agreement with the results predicted from the proposed Eq. (7.11). Although some scattering can be observed, which may be attributed to the heterogeneous bubbling behavior, the proposed model has been verified as acceptable and applicable to describe the relations between the bed density distribution and excess gas velocity.

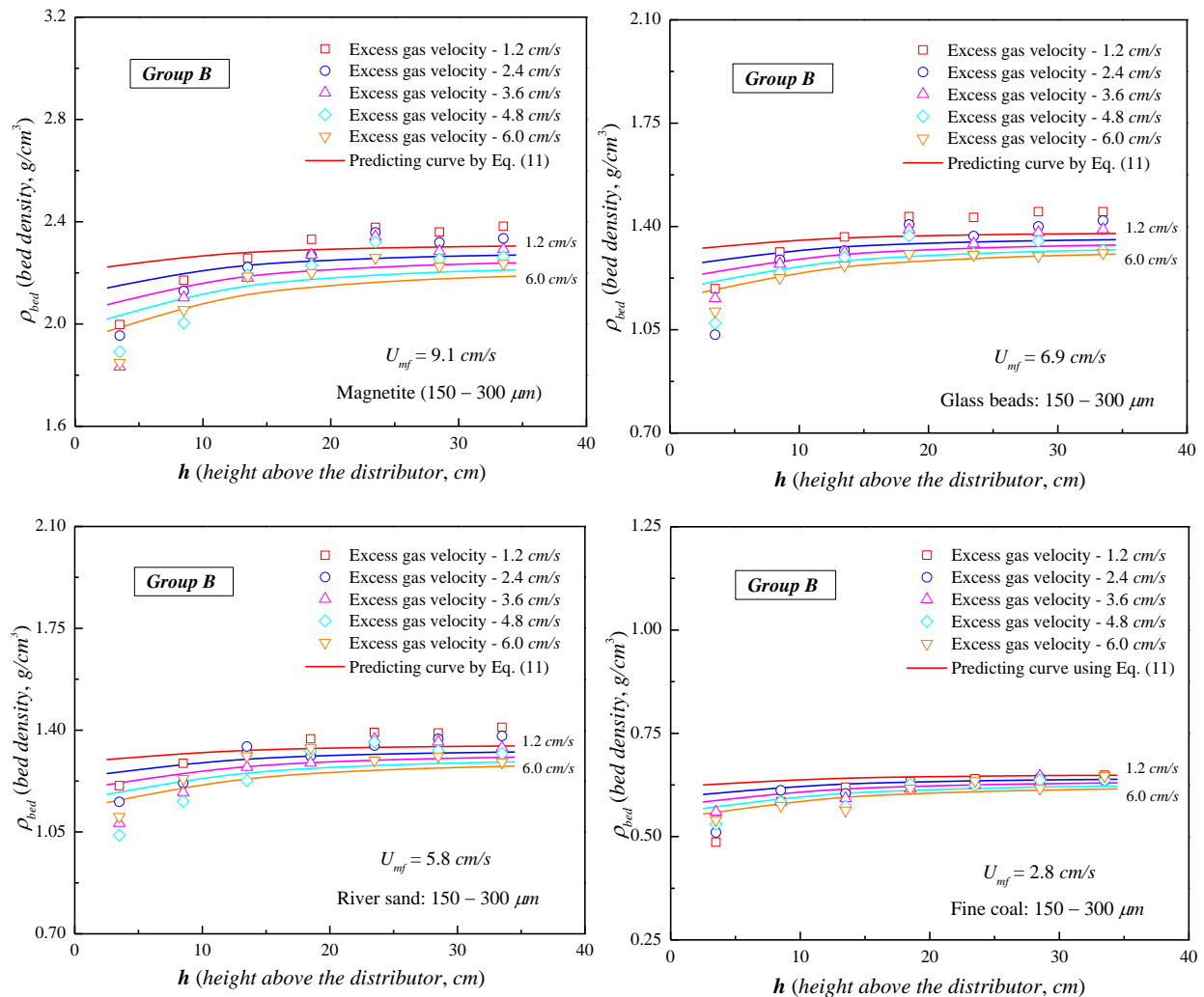


Figure 7.4 The distribution of bed density for Geldart Group B particles at various excess gas velocities.

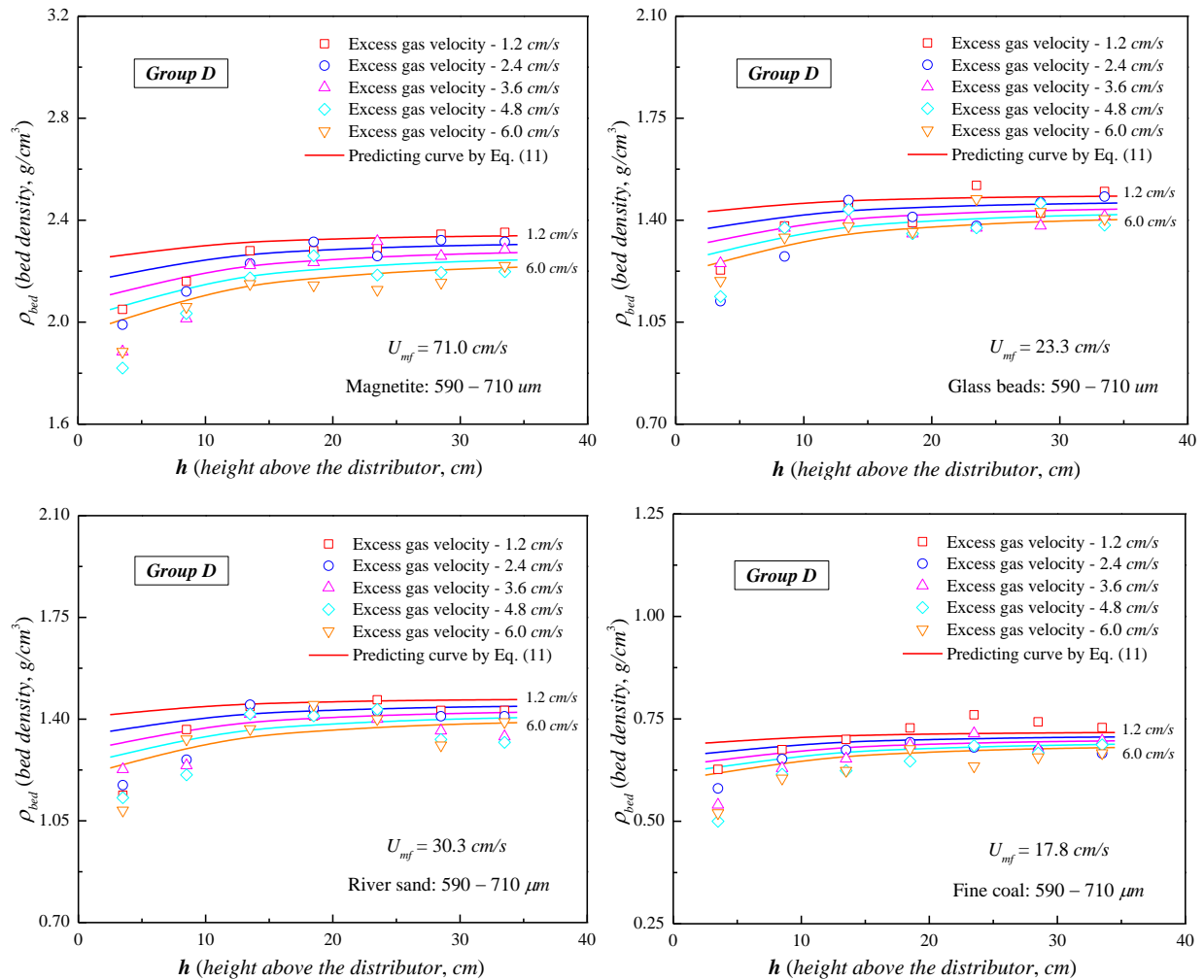


Figure 7.5 The distribution of bed density for Geldart Group D particles at various excess gas velocities.

7.4.3 Effect of mixture composition

In order to control the bed density for efficient separation, different types of binary mixtures have been used as medium particles in the ADMFB system. In this study, binary mixtures of magnetite and sand/coal particles of various mixture compositions have been tested in an ADMFB for dry coal beneficiation. The mass distributions of magnetite mixed with sand/coal particles in the axial direction of fluidized bed are shown in Figures 7.6 and 7.7, respectively. It can be observed from Figure 7.6 that binary mixtures of magnetite and sand particles almost all demonstrate a uniform distribution of solid particles in the bed, and only the ratio of sand

particles at the bottom region is relatively less than that of the upper part of the bed. This can be explained by magnetite and sand particles have similar aerodynamic properties which will lead to good mixing performance during fluidization, and the slight partial segregation at the bottom of fluidized bed can be attributed to the bubble jets effect. However, for binary mixtures of magnetite and fine coal particles, the severe particle segregation behavior occurs, as can be seen clearly in Figure 7.7. In details, there is a significant trend of increased fine coal content at the upper part of fluidized bed with the increasing bed height, and this tendency becomes more evident with the increase of fine coal content in the feed material. This can be due to the large density difference between the magnetite and fine coal particles.

The measured bed densities together with predicting curves for ADMFB with magnetite mixed with sand/coal particles are illustrated in Figures 7.8 and 7.9, respectively. It is noteworthy that all the predicting curves are based on the mass distributions of binary mixtures shown in Figures 7.6 and 7.7. As can be seen in Figure 7.8, the distributions of bed density for magnetite mixed with sand particles are almost uniform in the axial direction. The tendency of lower bed density at the bottom of fluidized bed with single particles is almost overcome by the binary fluidization system, which can be explained by an increase in mass ratio of magnetite particles at the bottom region due to the bubble jets effect and density difference. For the binary mixtures of magnetite and coal particles, the non-uniform distribution of bed density appears, and this performance becomes more significant with the increase of fine coal content, as can be seen in Figure 7.9. It can be attributed to the severe particle segregation behavior during fluidization mainly caused by the large density difference between these two types of solid particles. However, for the fine coal content of *wt.*8%, a relatively uniform distribution of bed density surprisingly exists, which may be due to the solid back-mixing and gas bubbling behavior in the fluidized bed. This phenomenon is of great importance for the bed density adjustment in ADMFB for dry coal beneficiation since the fine coal particles will be generated automatically during the coal transportation and separation processes. In conclusion, the distribution of bed density for the ADMFB with binary mixtures of solid particles is mainly dependent on the axial solid distribution and bubbling behavior, and the experimental data for binary mixtures is in good agreement with the Eq. (7.11).

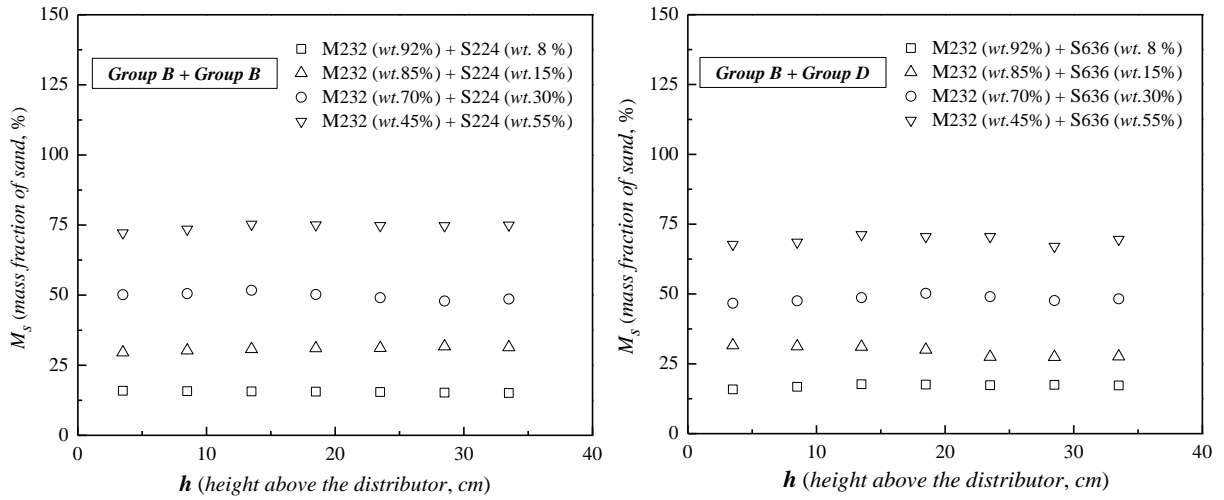


Figure 7.6 Axial mass distribution of fluidized beds with binary mixtures of magnetite and sand particles.

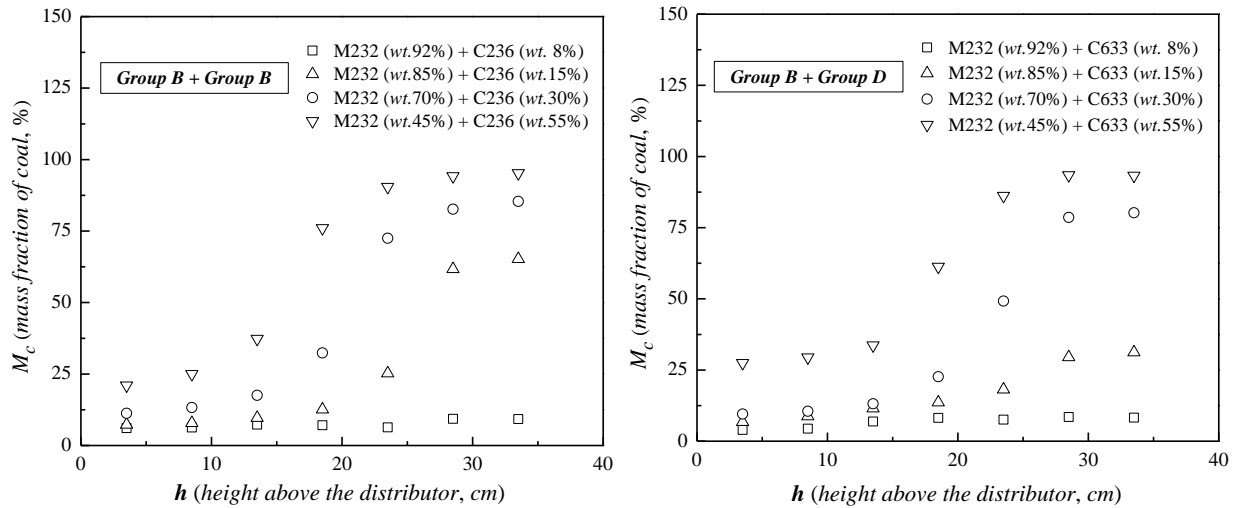


Figure 7.7 Axial mass distribution of fluidized beds with binary mixtures of magnetite and coal particles.

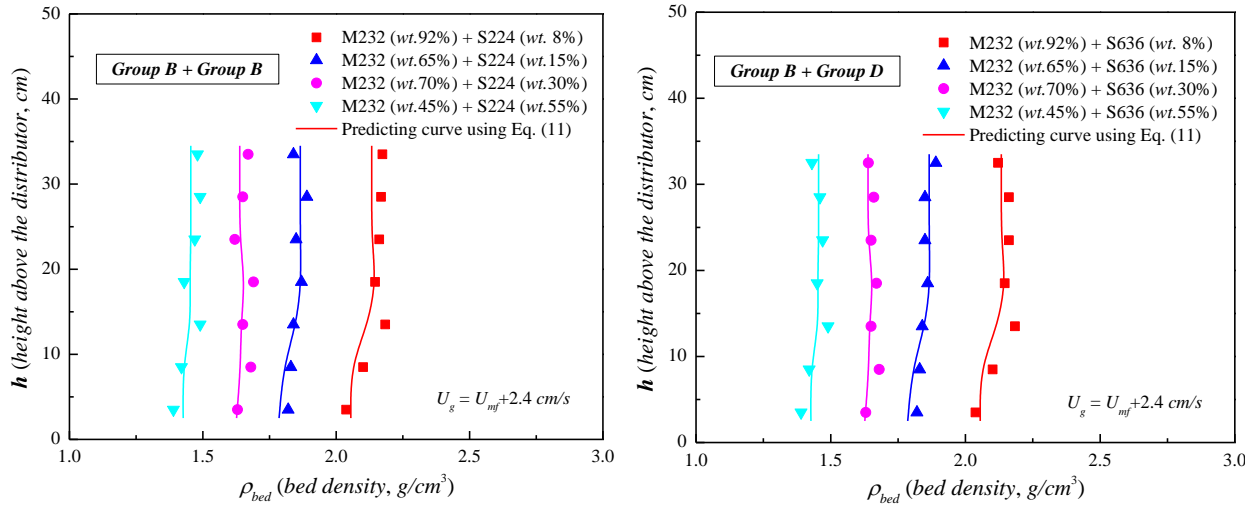


Figure 7.8 Effect of mixture composition on the bed density distribution for binary mixtures of magnetite and sand particles.

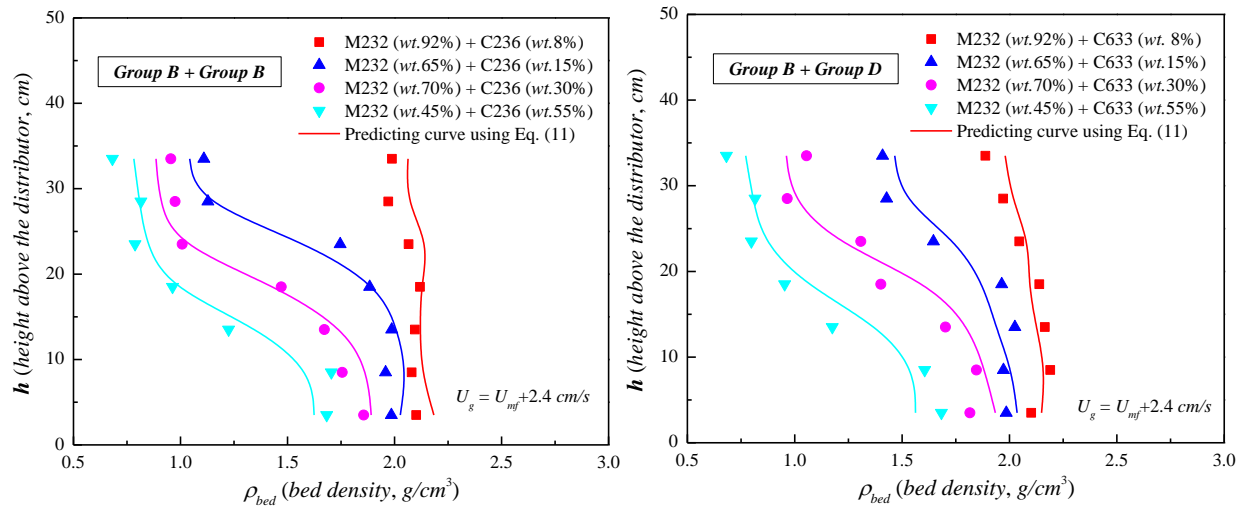


Figure 7.9 Effect of mixture composition on the bed density distribution for binary mixtures of magnetite and coal particles.

7.4.4 Comparison with the experimental data

In order to examine the validity and applicability of Eq. (7.11), the error analysis of the proposed correlation with the available experimental data was carried out. The comparison of the axial bed densities of ADMFB with single and binary mixtures of solid particles calculated using Eq. (7.11) with experimental data of this work are shown in Figures 7.10 and 7.11, respectively. As can be observed that, for different types of single particles, this correlation gives an overall standard deviation of $\pm 8.1\%$ based on 640 experimental data, which shows a good predicting performance. For various binary mixtures of solid particles, an average standard deviation of $\pm 8.5\%$ is obtained based on 160 data points tested, which indicates a good agreement. Hence, the proposed correlation has the advantages of comparably reliable and greater accuracy, and is to be preferred as an acceptable and practical method for predicting the bed density distribution of the ADMFB. Moreover, it is of wide application which can be used to accurately predict the axial distribution of fluidized bed density for both single and binary mixtures of solid particles. Although a few scattering may be observed in this correlation, a more accurate and reliable way for calculating the axial distribution of bed density for ADMFB is seen to exist.

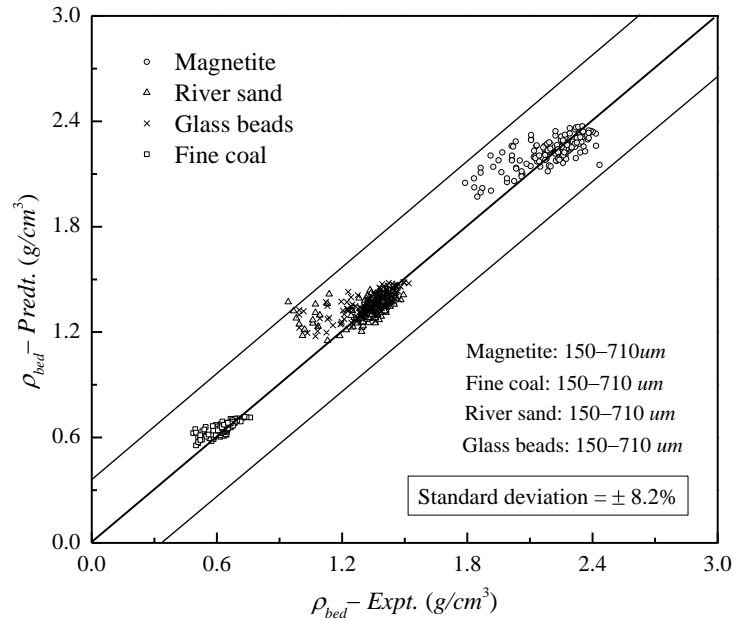


Figure 7.10 Comparison of fluidized bed densities with various single particles calculated by Eq. (7.11) with the experimental data.

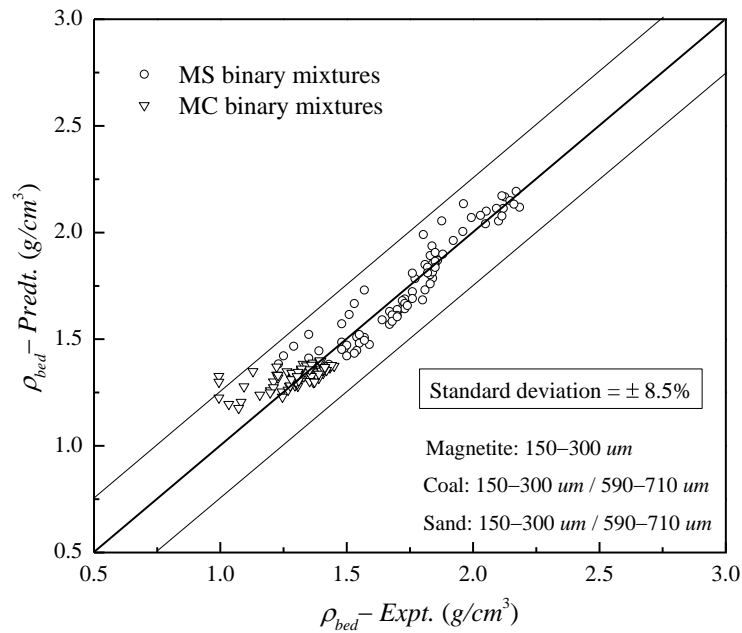


Figure 7.11 Comparison of fluidized bed densities with various binary mixtures of solid particles calculated by Eq. (7.11) with the experimental data.

7.5 Conclusion

Knowledge of the distribution of bed density is crucial for the Air Dense Medium Fluidized Bed operation. Experimental evidences reveal that a comparable lower density is obtained at the bottom of fluidized bed with various single particles, whereas the bed density at the upper part remains almost consistent. The average bed density decreases with the increasing of excess gas velocity, but the influence of excess gas velocity was found to have definite effects on the tendency of axial density distribution. Moreover, the particle composition of binary mixtures have a significant influence on the axial density distribution due to the variation of axial particle distribution of mixture solid particles. An equation has been derived to predict the bed density distribution in the ADMFB based on the modified two-phase theory, and can be estimated by

$$\rho_{bed} = (1 - \varepsilon_{mf})(\rho_p - \rho_g) \left[1 - \frac{1.72Ar^{-0.133}(U_g - U_{mf})^{0.024}}{1 + 1.3(h + 4A_D^{0.5})(U_g - U_{mf})^{-0.8}} \right] + \rho_g$$

and it requires knowledge of the excess gas velocity, and properties of solid particles and gas. The proposed equation has been verified by various single and binary mixtures of Geldart Group B and/or D particles at different excess gas velocities.

Nomenclature

A	cross-sectional area of the fluidized bed, m^2
A_b	bed cross-sectional area occupied by bubble phase, m^2
A_d	bed cross-sectional area occupied by dense phase, m^2
A_D	area of each orifice in perforated plate distributor, m^2
Ar	Archimedes number of particle, kg/m
d_p	mean diameter of solid particles, m
D_e	volume-equivalent bubble diameter, m
G_b	volumetric bubble flow rate, m^3/s
g	gravitational acceleration, m/s^2
h	height above the bed distributor, m
U_b	rise velocity of gas bubbles, m/s
U_g	superficial gas velocity, m/s
U_{mf}	minimum fluidization velocity, m/s
Y	correction factor for modified two-phase theory, <i>dimensionless</i>

Greek letters

μ	viscosity of gas fluid, $Pa.s$
ε_{mf}	bed voidage at minimum fluidization state, <i>dimensionless</i>
ρ_{bed}	density of fluidized bed, kg/m^3
ρ_b	density of bubble phase, kg/m^3
ρ_d	density of dense phase, kg/m^3
ρ_g	density of gas fluid, kg/m^3
ρ_p	density of solid particles, kg/m^3

Acknowledgements

The authors are grateful to the financial support by Natural Science and Engineering Research Council of Canada (NSERC), China Scholarship Council (CSC), and National Natural Science Foundation of China.

References

- Azimi E., Karimipour S., Rahman M., Szymanski J., Gupta R., 2013. Evaluation of the performance of air dense medium fluidized bed (ADMFB) for low-ash coal beneficiation. Part 1: Effect of operating conditions. *Energy Fuels*. 27, 5595-5606.
- Chen Q. R., Wei L. B., 2003. Coal dry beneficiation technology in China: The state – of – the – art. *China Part. 1*, 52-56.
- Chikerema P., Moys M., 2012. Effects of particle size, shape, and density on the performance of an air fluidized bed in dry coal beneficiation. *Inter. J. Coal Prep. Util.* 32, 80-94.
- Cranfield R. R., Geldart D., 1974. Large particle fluidization. *Chem. Eng. Sci.* 29, 935-947.
- Darton R. C., Lanauze R. D., Davidson J. F., Harrison D., 1977. Bubble growth due to coalescence in fluidised beds. *Trans. Inst. Chem. Eng.* 55, 274-280.
- Davidson J. F., Clift R., Harrison D., *Fluidization: 2nd Edition*, London, England, Academic press, 1985.
- Davidson J. F., Harrison D., 1963. *Fluidised particles*. Cambridge Univer. Press. London and New York.
- Davies R. M., Taylor G. I., 1950. The mechanics of large bubbles rising through extended liquids and through liquids in tubes. *Proc. R. Soc. A.* 200, 375-390.
- Dwari R. K., Rao K. H., 2007. Dry beneficiation of coal – a review. *Miner. Process. Extr. Metall. Rev.* 28, 177-234.
- Firdaus M., O Shea J. P., Oshitani J., Franks G. V., 2012. Beneficiation of coarse coal ore in an air-fluidized bed dry dense-medium separator. *Int. J. Coal Prep. Util.* 32, 276-289.
- Franks G. V., Firdaus M., Oshitani J., 2013. Copper ore density separations by float/sink in a dry sand fluidised bed dense medium. *Int. J. Miner. Process.* 121, 12-20.
- Franks G. V., Forbes E., Oshitani J., Batterham R. J., 2015. Economic, water and energy evaluation of early rejection of gangue from copper ores using a dry sand fluidised bed separator. *Int. J. Miner. Process.* 137, 43-51.

- Fu Z. J., Zhu J., Barghi S., Zhao Y. M., Luo Z. F., Duan C. L., 2019. On the two-phase theory of fluidization for Geldart B and D particles. *Powder Technol.* In press.
- Geldart D., 1973. Types of gas fluidization. *Powder Technol.* 7, 285-292.
- Geng Y. M., Che D. F., 2001. An extended DEM-CFD model for char combustion in a bubbling fluidized bed combustor of inert sand. *Chem. Eng. Sci.* 66, 207-219.
- Gilbertson M. A., Eames I., 2001. Segregation patterns in gas-fluidized systems. *J. Fluid. Mech.* 433, 347-356.
- Grace J. R., Clift R., 1974. On the two-phase theory of fluidization. *Chem. Eng. Sci.* 29, 327-334.
- Hepbasli A., 1998. Estimation of bed expansions in a freely-bubbling three-dimensional gas-fluidized bed. *Int. J. Energy Res.* 22, 1365-1380.
- He Y., Zhao Y., Chen Q., Luo Z., Yang Y., 2002. Development of the density distribution model in a gas-solid phase fluidized bed for dry coal separation. *J. S. Afr. Inst. Min. Metall.* 10, 429-434.
- Hillgard K., Werther J., 1986. Local bubble gas hold-up and expansion of gas/solid fluidized beds. *German. Chem. Eng.* 9, 215-221.
- Korolev V. N., Syromyatnikov N. I., 1971. Structure of a fixed and a fluidized bed of granular material near an immersed surface (wall). *J. Eng. Phys.* 21, 1475-1478.
- Kunii D., Levenspiel O., *Fluidization engineering: 2nd Edition*, United States, Butterworth-Heinemann, 1991.
- Luo Z. F., Chen Q. R., 2001. Dry beneficiation technology of coal with an air dense-medium fluidized bed. *Int. J. Miner. Process.* 63, 167-175.
- Luo Z. F., Chen Q. R., 2001. Effect of fine coal accumulation on dense phase fluidized bed performance. *Int. J. Miner. Process.* 63, 217-224.
- Mak C., Choung J., Beauchamp R., Kelly D. J. A., Xu Z., 2008. Potential of air dense medium fluidized bed separation of mineral matter for mercury rejection from Alberta sub-bituminous coal. *Int. J. Coal Prep. Util.* 28, 115-132.

Modekurti S., Bhattacharyya D., Zitney S. E., 2013. Dynamic modeling and control studies of a two-stage bubbling fluidized bed absorber-reactor for solid sorbent CO₂ capture. *Ind. Eng. Chem. Res.* 52, 10250-10260.

Mohanta S., Rao C. S., Daram A. B., Chakraborty S., Meikap B. C., 2013. Air dense medium fluidized bed for dry beneficiation of coal: technological challenges for future. *Part. Sci. Technol.* 31, 16-27.

Mori S., Wen C. Y., 1975. Estimation of bubble diameter in gaseous fluidized beds. *AIChE J.* 21, 109-115.

Oshitani J., Franks G. V., Griffin M., 2010. Dry dense medium separation of iron ore using a gas-solid fluidized bed. *Adv. Powder Technol.* 21, 573-577.

Oshitani J., Kajimoto S., Yoshida M., Franks G. V., Kubo Y., Nakatsukasa S., 2013. Continuous float-sink density separation of lump iron ore using a dry sand fluidized bed dense medium. *Adv. Powder Technol.* 24, 468-472.

Oshitani J., Kawahito T., Yoshida M., Gotoh K., Franks G. V., 2011. The influence of the density of a gas-solid fluidized bed on the dry dense medium separation of lump iron ore. *Miner. Eng.* 24, 70-76.

Oshitani J., Kawahito T., Yoshida M., Gotoh K., Franks G. V., 2013. Improvement of dry float-sink separation of smaller sized spheres by reducing the fluidized bed height. *Adv. Powder Technol.* 23, 27-30.

Radmanesh R., Chaouki J., Guy C., 2006. Biomass gasification in a bubbling fluidized bed reactor: Experiments and modeling. *AIChE J.* 52, 4258-4272.

Rippin D. W. T., Davidson J. F., 1967. Free streamline theory for a large gas bubbles in a liquid. *Chem. Eng. Sci.* 22, 217-228.

Rowe P. N., Nienow A. W., Agbim A. J., 1972. The mechanisms by which particles segregate in gas fluidised beds – binary systems of near-spherical particles. *Trans. Instn. Chem. Engrs.* 50, 310-323.

Ruzicka M. C., 2006. On buoyancy in dispersion. *Chem. Eng. Sci.* 61, 2437-2446.

Sahan R. A., 1997. Coal cleaning performance in an air fluidized bed. *Energy Sources*. 19, 475-492.

Sahu A. K., Biswal S. K., Parida A., 2009. Development of air dense medium fluidized bed technology for dry beneficiation of coal – A review. *Int. J. Coal Prep. Util.* 29, 216-241.

Sahu A. K., Tripathy A., Biswal S. K., Parida A., 2011. Stability study of an air dense medium fluidized bed separator for beneficiation of high-ash Indian coal. *Int. J. Coal Prep. Util.* 31, 127-148.

Schmilovitch Z., Zaltzman A., Wolf D., Verma B. P., 1992. Apparent density variations in a fluidized bed. *Trans. ASAE*. 35, 11-16.

Sekito T., Matsuto T., Tanaka N., 2006. Application of a gas-solid fluidized bed separator for shredded municipal bulky solid waste separation. *Waste Manage.* 26, 1422-1429.

Sekito T., Tanaka N., Matsuto T., 2006. Batch separation shredded bulk waste by gas-solid fluidized bed at laboratory scale. *Waste Manage.* 26, 1246-1252.

Sun Q. Q., Lu H. L., Liu W. T., He Y. R., Yang L. D., Gidaspow D., 2005. Simulation and experiment of segregating/mixing of rice husk-sand mixture in a bubbling fluidized bed. *Fuel*. 84, 1739-1748.

Tahmasebi A., Yu J. L., Han Y. N., Li X. C., 2012. A study of chemical structure changes of Chinese lignite during fluidized bed drying in nitrogen and air. *Fuel Process. Technol.* 101, 85-93.

Toomey R. D., Johnstone H. F., 1952. Gaseous fluidization of solid particles. *Chem. Eng. Pro.* 48, 220-226.

Turner J. C. R., 1966. On bubble flow in liquids and fluidised beds. *Chem. Eng. Sci.* 21, 971-974.

Wei L. B., Chen Q. R., Zhao Y. M., 2003. Formation of double-density fluidized bed and application in dry coal beneficiation. *Coal Prep.* 23, 21-32.

Yoshida M., Oshitani J., Ono K., Ishizashi M., Gotoh K., 2008. Control of apparent specific gravity in binary particle system of gas-solid fluidized bed. *KONA-Powder Part.* 26, 227-237.

Zaltzman A., Feller R., Mizrach A., Schmilovitch Z., 1983. Separating potatoes from clods and stones in a fluidized bed medium. *Trans. ASAE.* 26, 987-995.

Zaltzman A., Schmilovitch Z., Mizrach A., 1985. Separating flower bulbs from clods and stones in a fluidized bed. *Can. Agric. Eng.* 27, 63-67.

Zaltzman A., Verma B. P., Schmilovitch Z., 1987. Potential of quality sorting fruits and vegetables using fluidized bed medium. *Trans. ASAE.* 30, 823-831.

Zhang B., Zhao Y. M., Luo Z. F., Song S. L., Li G. M., Cheng S., 2014. Utilizing an air-dense medium fluidized bed dry separating system for preparing a low-ash coal. *Int. J. Coal Prep. Util.* 34, 285-295.

Zhao Y. M., Liu J. T., Wei X. Y., Luo Z. F., Chen Q. R., Song S. L., 2011. New progress in the processing and efficient utilization of coal. *Int. J. Min. Sci. Technol.* 21, 547-552.

Zinov'ev Y. I., 1976. Effective density of a fluidized bed. *J. Eng. Phys.* 31, 1279-1284.

van Houwelingen J. A., de Jong T. P. R., 2004. Dry cleaning of coal: Review, fundamentals and opportunities. *Geol. Belgica.* 7, 335-343.

CHAPTER 8

DRY COAL BENEFICIATION BY THE SEMI-INDUSTRIAL AIR DENSE MEDIUM FLUIDIZED BED WITH BINARY MIXTURES OF MAGNETITE AND FINE COAL PARTICLES

Air Dense Medium Fluidized Bed (ADMFB) is deemed to be one of the most efficient methods for dry coal beneficiation. In the present work, a semi-industrial ADMFB system in continuous operation was utilized to study the effects of operating gas velocity, feed coal size, and mixture composition of medium particles on the coal beneficiation in industrial practice. Binary mixtures of magnetite and fine coal particles were used as the medium material, and four different feed coal samples with the size ranges of $-50 + 25$, $-25 + 13$, $-13 + 6$, and $-6 + 2$ mm were tested individually. The experimental results showed that the influence of excess gas velocity on the dry coal separation is relatively small in the lower flow rates. The separation density and probable error increase with the decreasing of feed coal size, regardless of the type of feed coal. The separation density can be continually reduced by further increasing the fraction of fine coal in the medium material, with the compromise of the increased probable error. Moreover, the ash content and calorific value of $-50 + 6$ mm coarse coal can be effectively upgraded, but the beneficiation of $-6 + 2$ mm fine coal was less efficient.

8.1 Introduction

Coal is one of the most important and available energy sources, which plays a significant role in the economic development of many countries all around the world (BP statistical review, 2017). In general, raw coal needs removal of ash-forming (inorganics) impurities through the coal beneficiation process, which can upgrade the carbon concentration, reduce the environmental impact of emissions, and decrease the transportation weight and waste disposal expenses (Lockhart, 1984; Houwlingen *et al.*, 2004; Dwari and Rao, 2007). Air Dense Medium Fluidized Bed (ADMFB) is well known to be one of the most efficient methods for dry coal beneficiation, which utilizes the pseudo-fluid behavior of gas-solid fluidization to achieve the coal separation as per their densities (Sahu *et al.*, 2009; Mohanta *et al.*, 2013; Chen and Yang, 2003; Zhao *et al.*,

2011). In the ADMFB, the clean coal with comparatively less density will float on the top of the fluidized bed, whereas the gangue product with heavier density will settle towards the bottom. The fluidization characteristics and basic principles of the ADMFB can be found in the literature (Luo and Chen, 2001; Wei and Chen, 2003; Mohanta *et al.*, 2011; Chikerma and Moys, 2012). This technology has the advantages of excluding process water with comparable separation performance compared to the hydraulic methods (Sahan and Kozanoglu, 1997; Chen and Wei, 2003; Firdaus *et al.*, 2012), which provides an efficient way for coal beneficiation in arid and area with water shortage. Furthermore, the ADMFB technology is widely applicable and has already extended to the fields of iron/copper ore beneficiation (Oshitani *et al.*, 2013; Franks *et al.*, 2013; Franks *et al.*, 2015), agricultural products cleaning (Zaltman *et al.*, 1983; Zaltman *et al.*, 1985; Zaltman *et al.*, 1987), municipal solid waste classification (Sekito *et al.*, 2006; Sekito *et al.*, 2006; Yoshida *et al.*, 2010), etc.

The ADMFB method was proposed firstly by T. Fraser (Fraser, 1926) for dry coal beneficiation using sand particles as medium material, with the bed density ranging from 1.2 to 1.4 g/cm^3 , followed by elsewhere (Dotson, 1959; Lohn, 1971; Weintraub *et al.*, 1979; Zinov'ev, 1976; Mizrach *et al.*, 1984; Rios *et al.*, 1986) attempts to investigate its hydrodynamic characteristics and separation properties. Despite the advantages and practicality of this technology, challenges still remain when applied to industrial practice. As pointed out, the performance of coal beneficiation in ADMFB is highly dependent on fluidized bed conditions and feed coal properties (Chen and Yang, 2003; Luo and Chen, 2001; Mohanta *et al.*, 2011; Chikerma and Moys, 2012). The separation mechanism of the ADMFB is not exactly the same as hydraulic dense medium separation, mainly due to the upward gas bubbles and disorderly solids flow in the fluidized bed (Mohanta *et al.*, 2013; Mohanta *et al.*, 2011). It is hereby that the superficial gas velocity which gives rise to the bubbling behavior in the fluidized bed will play an important role in determining the coal beneficiation. Additionally, the feed coal objects with smaller size or with relatively less difference in specific gravity are difficult to separate because of significant fluctuations of bed density caused by the fluidization behavior (Chen and Yang, 2003; Mohanta *et al.*, 2011; Sahan and Kozanoglu, 1997). Therefore, the process variables such as operating gas velocity and feed coal properties should be carefully investigated, especially for industrial applications.

Since the ADMFB is a gravity-based separation method, it is therefore anticipated that the bed density is to be a critical parameter for dry coal beneficiation. As is known that the bed density of gas-solid fluidization is taken as that of the mass of solid particles per unit volume of suspension (Zinov'ev, 1976), and thus the particle properties and composition of medium materials are the key points for control the bed density. In order to obtain the desired bed density, various monodispersed and mixtures of solid particles have been processed as the medium material for bed density adjustment (Wei *et al.*, 2003; Firdaus *et al.*, 2012; Oshitani *et al.*, 2013; Franks *et al.*, 2013; Franks *et al.*, 2015; Zaltman *et al.*, 1983; Sekito *et al.*, 2006; Weintraub *et al.*, 1979; Luo and Chen, 2001, Luo *et al.*, 2010; Yoshida *et al.*, 2011; Zhao *et al.*, 2012). Among these, the binary mixtures of magnetite and fine coal particles are deemed to be the most appropriate and readily available medium materials (Sahu *et al.*, 2009; Mohanta *et al.*, 2013). Magnetite particles are chosen as they can be easily recycled using their magnetic property, thus avoiding medium particle loss. Fine coal particles are readily available, and a certain amount of fine coal will also be automatically generated during the coal separation process. Furthermore, the bed density of the ADMFB with the binary mixtures of magnetite and fine coal particles can be manipulated to be between 1.3 g/cm^3 and 2.2 g/cm^3 (Luo and Chen, 2001; Zhao *et al.*, 2012), which is the desirable condition for efficient coal beneficiation. A number of researchers (Lohn, 1971; Weintraub *et al.*, 1979; Luo and Chen, 2001, Zhao *et al.*, 2012; Tang *et al.*, 2009) have carried out experiments to investigate the separation properties of the ADMFB with binary mixtures. However, almost all these experiments were conducted in batch or continuous laboratory devices, and it has been rarely investigated and not further confirmed by industrial practices.

It is the purpose of the present work to determine the performance of coal beneficiation in the semi-industrial Air Dense Medium Fluidized Bed system with the binary mixtures of magnetite and fine coal particles. The influences of feed coal size, operating gas velocity, and particle composition of binary mixtures on the coal separation performance were experimentally studied with the continuous processing. Moreover, the variations of ash content and calorific value of the separated coal samples were also examined as part of the analysis. The experimental results of dry coal beneficiation in the semi-industrial ADMFB system were compared with the available data in the batch or continuous laboratory equipment stated in the literature.

8.2 Experimental

8.2.1 Air Dense Medium Fluidized Bed system

The schematic diagram of dry coal beneficiation in the Air Dense Medium Fluidized Bed is shown in Figure 8.1. Feed coal is introduced from the top of the fluidized bed separator. In the ADMFB, feed coal is separated according to their densities with respect to the density of the gas-solid fluidized bed. After separation, the clean coal with relative less density floats on the top surface of fluidized bed, whereas the gangue with higher density sinks to the bottom. Then, the separated coal products are transported to different sides of the fluidized bed and are discharged. During coal separation, the medium particles are continually added to the fluidized bed to maintain a stable fluidization condition, and the fine dust generated during operation is collected to prevent dust pollution.

All the experiments were conducted in a semi-industrial ADMFB system, as can be seen in Figure 8.2. The system consists of mainly five parts: (1) Air supply; (2) Fluidized bed separator. (3) Product transportation; (4) Medium particle recovery; (5) Dust collection. The size of the fluidized bed separator is: Length \times Width \times Depth = 10000 mm \times 350 mm \times 1200 mm. The processing capacity of this ADMFB system is 5 ~ 10 t/h. For separating each ton of feed coal, the power consumption and medium particle loss are 1.5 kw.h/t and 0.3 ~ 0.5 kg/t, respectively. Furthermore, the detailed flowsheet of the coal beneficiation process in the ADMFB can be found elsewhere (Luo and Chen, 2001).

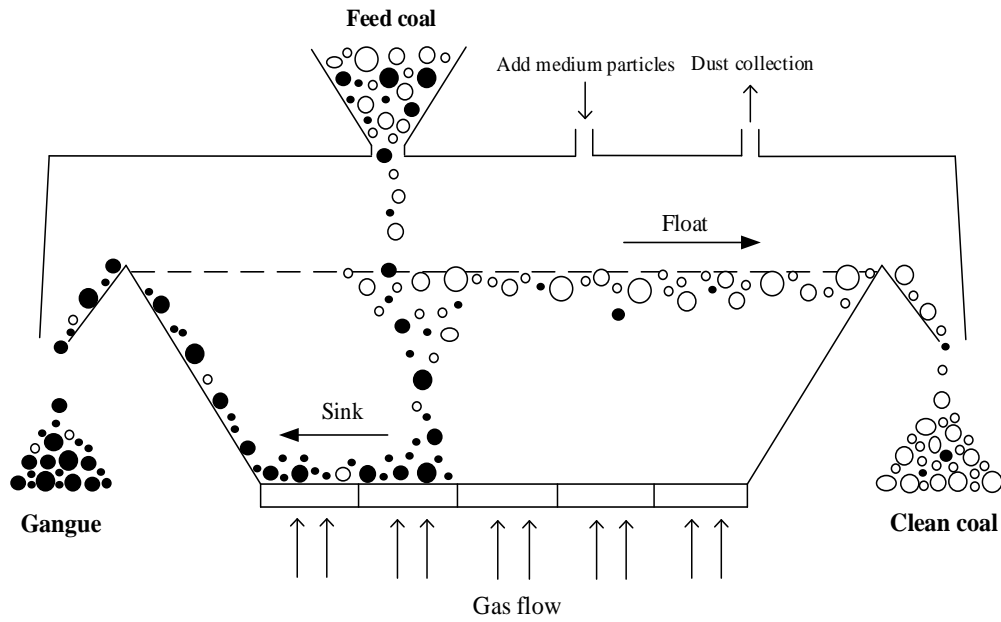


Figure 8.1 The schematic diagram of dry coal beneficiation process in Air Dense Medium Fluidized Bed system.



Figure 8.2 A semi-industrial Air Dense Medium Fluidized Bed system for dry coal beneficiation.

8.2.2 The properties of medium materials and feed coal samples

Binary mixtures of magnetite and fine coal particles were used as medium material in the semi-industrial ADMFB system. Magnetite particles were prepared from a sample of mineral magnetite obtained from Zhongtie Industry & Trade Co., Ltd. Fine coal particles were collected from Lijiahao Coal Mine, Ltd. Particle true densities of magnetite and fine coal are 4600 kg/m^3 and 1500 kg/m^3 , respectively. To avoid particle segregation during fluidization, the medium particles with relatively wide size distribution were used (Luo and Chen, 2001). Magnetite particles, which have been found to be the appropriate material in the ADMFB (Lockhart, 1984; Houwelingen *et al.*, 2004; Dwari *et al.*, 2007; Sahu *et al.*, 2009; Mohanta *et al.*, 2013; Chen and Yang, 2003), were considered as the core material. For the bed density adjustment, fine coal particles were mixed with magnetite in quantities to produce two types of binary mixtures with the fine coal content of *wt.*12.08% and *wt.*20.88%, respectively. For convenience, the two types of binary mixtures are named as binary medium A and B. The mass distribution of binary medium A and B are shown in Tables 8.1 and 8.2, respectively.

Four coal samples were collected from four different collieries namely Changcun, Lijiahao, Jiahe, and Hecaogou Coal Mine in China. All of these raw coals belong to bituminous coal. The properties of these coal samples are shown in Table 8.3. Each coal sample was subjected to crushing and until the coal size below 50 mm . The coal sample was then classified by screening into four different size fractions: $- 50 + 25$, $- 25 + 13$, $- 13 + 6$, and $- 6 + 2 \text{ mm}$. As many authors (Zaltman *et al.*, 1985; Zaltman *et al.*, 1987; Sekito *et al.*, 2006; Sekito *et al.*, 2006; Yoshida *et al.*, 2010; Fraser, 1926) suggested, ADMFB technology experiences many difficulties and complications for fine coal beneficiation, thus fine coal particles below 2 mm were excluded in the present work, which is also necessary to maintain a stable fine coal content in the medium material. The mass distribution and ash content of the classified coal product samples are shown in Table 8.4.

Table 8.1. The mass distribution of binary medium A.

Size fraction (<i>mm</i>)	Mass fraction of each particle (%)		Mass fraction of medium sample (%)		Mass fraction of each size fraction (%)	
	Magnetite	Fine coal	Magnetite	Fine coal	Magnetite	Fine coal
0.710 – 1.000	0.95	19.50	0.84	2.36	26.24	73.76
0.425 – 0.710	5.86	13.43	5.15	1.62	76.05	23.95
0.300 – 0.425	19.06	22.25	16.75	2.69	86.17	13.83
0.150 – 0.300	26.44	13.55	23.25	1.64	93.42	6.58
0.074 – 0.150	41.04	22.53	36.08	2.72	92.98	7.02
0.045 – 0.074	5.89	5.10	5.18	0.62	89.37	10.63
0 – 0.045	0.76	3.64	0.67	0.44	60.26	39.74
Total	100.00	100.00	87.92	12.08	87.92	12.08

Table 8.2. The mass distribution of binary medium B.

Size fraction (<i>mm</i>)	Mass fraction of each particle (%)		Mass fraction of medium sample (%)		Mass fraction of each size fraction (%)	
	Magnetite	Fine coal	Magnetite	Fine coal	Magnetite	Fine coal
0.710 – 1.000	0.82	23.23	0.65	4.85	11.80	88.20
0.425 – 0.710	5.70	12.90	4.51	2.69	62.61	37.39
0.300 – 0.425	19.17	17.14	15.17	3.58	80.91	19.09
0.150 – 0.300	27.56	20.72	21.81	4.33	83.44	16.56
0.074 – 0.150	40.39	17.79	31.96	3.71	89.59	10.41
0.045 – 0.074	5.45	5.53	4.31	1.16	78.88	21.12
0 – 0.045	0.90	2.68	0.72	0.56	56.13	43.87
Total	100	100	79.12	20.88	79.12	20.88

Table 8.3. The properties of coal samples.

Colliery	Ash content (%)	Calorific value (MJ/kg)	Sulfur content (%)	Coal type
Changcun Mine	19.06	28.86	0.56	Meager Lean coal
Lijiahao Mine	25.25	19.50	0.70	Non-caking coal
Jiahe Mine	31.55	24.15	1.28	Lean coal
Hecaogou Mine	34.26	21.77	0.88	Long flame coal

Table 8.4. Mass distribution and ash content of the classified coal samples.

Size fraction (mm)	Changcun mine		Lijiahao mine		Jiahe mine		Hecaogou mine	
	wt. %	ash (%)	wt. %	ash (%)	wt. %	ash (%)	wt. %	ash (%)
- 50 + 25	29.02	15.02	24.66	29.90	29.48	30.60	24.45	40.42
- 25 + 13	26.44	17.50	23.14	28.99	27.88	30.71	29.61	38.00
- 13 + 6	23.66	20.90	19.65	22.35	19.62	31.93	27.76	34.38
- 6 + 2	20.88	20.83	32.55	22.97	23.02	30.83	18.19	29.18
Total	100	18.28	100	25.95	100	30.94	100	35.98

8.2.3 Experimental procedure

Binary mixtures of magnetite and fine coal particles were loaded into the semi-industrial ADMFB system up to a static bed height of 40 cm. After being filtered, ambient air was compressed and sent to fluidize the medium particles through a porous plastic distributor. The air flowrate was adjusted by the gas valve and measured by a vortex flowmeter. About 5 ~ 10 min was allowed to reach to steady state for the coal beneficiation. After stable fluidization, raw coal was introduced to the ADMFB system and was separated based on the density difference. After separation, the clean coal and gangue were transported to different sides of the fluidized bed and discharged. Samples of clean coal and gangue products were collected and subjected to float-sink analysis, using a range of liquid density from 1.3 to 2.0 g/cm³ with the interval of 0.1 g/cm³. The partition curve was used to evaluate the performance of coal beneficiation by producing the separation density and probable error. The separation density corresponds to the density at partition coefficient of 50% (Mohanta *et al.*, 2011). The probable error which indicates the accuracy of gravity-based separation is defined by $E_p = (\rho_{75\%} - \rho_{25\%}) / 2$, where $\rho_{75\%}$ and $\rho_{25\%}$ are the densities at the partition coefficients of 75% and 25%, respectively (Luo and Chen, 2001). A perfect gravity-based separation results in a vertical partition curve with an E_p value equals to zero, and the increasing E_p generally represents the decreasing of separation accuracy. Moreover, the variation of ash content and calorific value of clean coal and gangue samples were determined as parts of the analysis.

8.3 Results and discussion

8.3.1 The effect of operating gas velocity

The operating gas velocity is commonly expressed in terms of excess gas velocity, which represents the superficial gas velocity over the minimum fluidization velocity. In the present work, the influence of excess gas velocity on the separation performance of Lijiahao coal were investigated in semi-industrial ADMFB with binary medium A. The partition curves of the sunk products after coal separation at various excess gas velocities are shown in Figure 8.3, and the corresponding separation density and probable error are plotted against the excess gas velocity in Figures 8.4 and 8.5, respectively. As can be observed that, for $-50 + 2 \text{ mm}$ Lijiahao coal, an increase in excess gas velocity from 2 to 8 cm/s does not cause significant change in the separation density and probable error. The results demonstrated that the effectiveness of coal separation in the ADMFB is not sensitive to the excess gas velocity in relatively low flow rates, which is important as the range of operating gas velocity is comparatively wide for a consistent coal separation performance, rather than an optimum operating gas velocity (Chen and Yang, 2003; Chen and Wei, 2003). According to the two-phase theory of fluidization (Toomey and Johnstone, 1952), almost all the gas flow in excess of that required for the incipient fluidization will go to the bubble phase, and the dense phase remains almost unchanged with the increasing of excess gas velocity. Meanwhile, the separation of immersed objects in a bubbling fluidized bed is primarily determined by the dense phase rather than the bubble phase (Korolev *et al.*, 1971; Nguyen and Grace, 1978; Rees *et al.*, 2005), so that the performance of coal beneficiation in the ADMFB remains almost unchanged with the increasing of excess gas velocity in relatively low flow rates is reasonable.

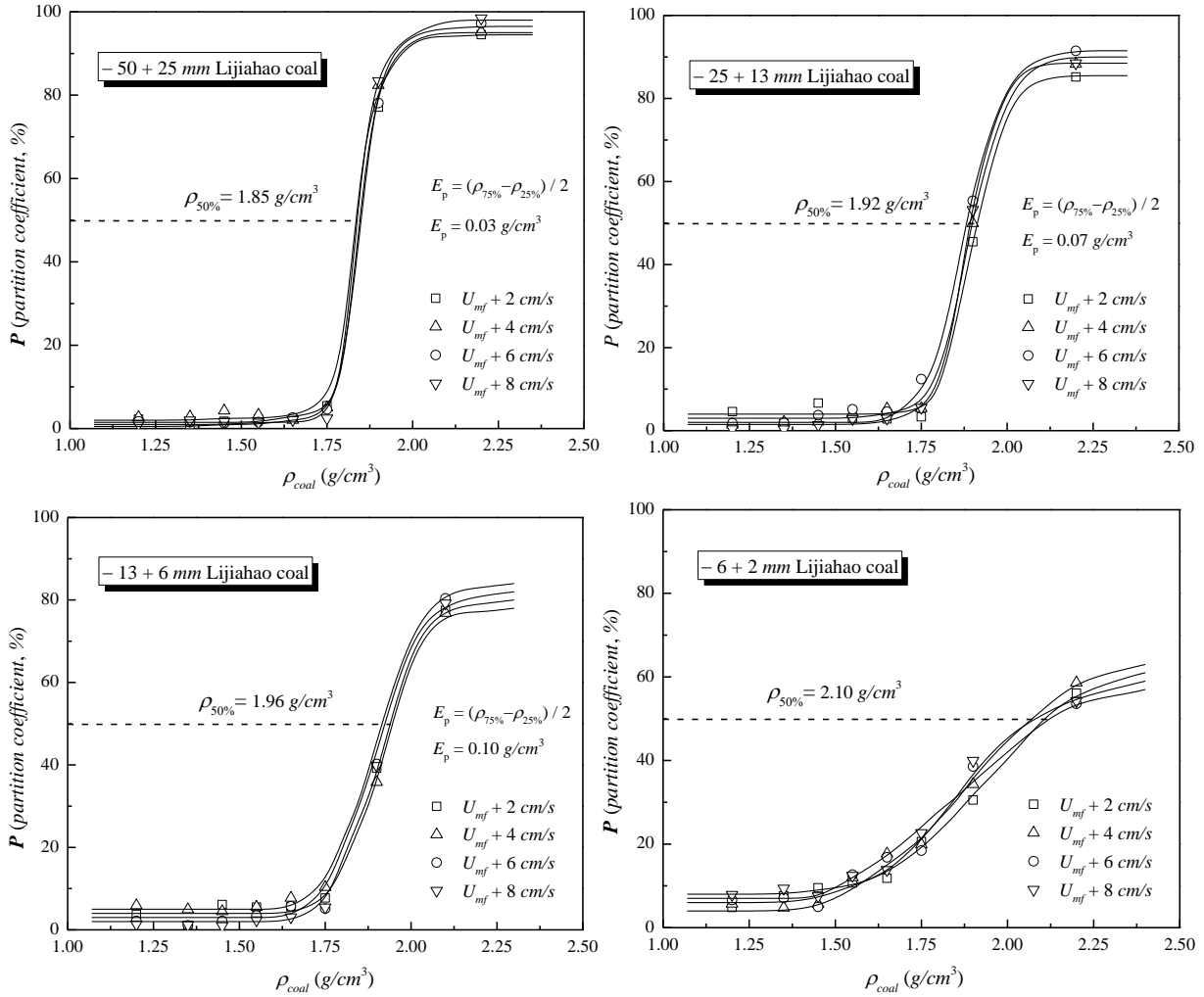


Figure 8.3 The partition curves of sunk products of Lijiahao coals at various excess gas velocities.

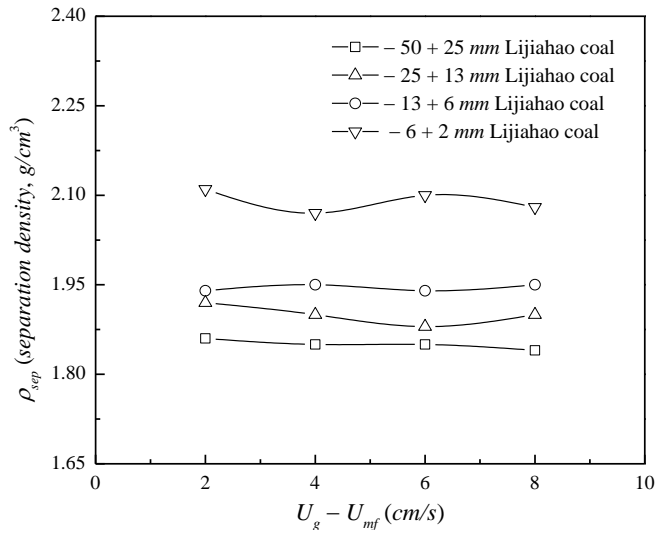
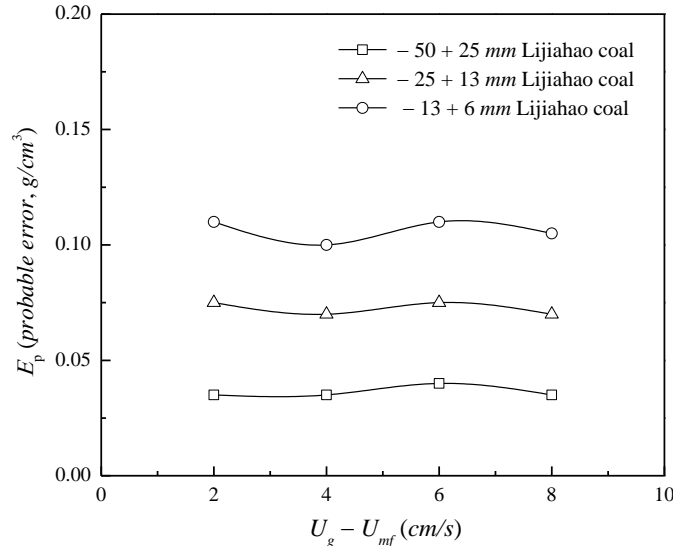


Figure 8.4 The effect of excess gas velocity on the separation density.**Figure 8.5** The effect of excess gas velocity on the probable error.

8.3.2 The effect of feed coal size

Experiments were performed individually with $-50 + 25$, $-25 + 13$, $-13 + 6$, and $-6 + 2$ mm size fractions of four different coal samples in a semi-industrial ADMFB with binary medium A, and the excess gas velocity was 4 cm/s. The partition curves of the sunk products after coal separation in ADMFB are shown in Figure 8.6, and the corresponding probable error and separation density are summarized as a function of feed coal size in Figure 8.7. As can be observed that there is an almost vertical partition curve for $-50 + 25$ mm coal with an E_p value approximately equal to 0.03 g/cm³, which shows an excellent separation performance. For $-25 + 13$ mm and $-13 + 6$ mm coal, the E_p values are around 0.07 g/cm³ and 0.10 g/cm³, respectively. However, for $-6 + 2$ mm coal, the E_p value was not obtained due to its partition coefficient of 75% being unavailable. Therefore, it can be concluded that the probable error increases with decreasing feed coal size, independent of the types of coal, indicating a decrease in degree of separation accuracy. The same tendency has also been claimed elsewhere in the bench or continuous laboratory apparatus (Zaltman *et al.*, 1987; Sekito *et al.*, 2006; Sekito *et al.*, 2006; Yoshida *et al.*, 2010). This may be due to the influence of rising gas bubbles: small coal particles may fall into the bubbles during beneficiation. Moreover, the separation density also shows an

increasing trend with the decreasing of feed coal size. In details, the separation densities of $-50 + 25$, $-25 + 13$, $-13 + 6$, and $-6 + 2$ mm feed coal particles are around 1.85, 1.90, 1.95, and 2.05 g/cm^3 , respectively. It should be mentioned that with an increase in separation density there will be more impurities (ash-forming matters) remain in the float products, which may lower the quality of clean coal.

The partition coefficients of the sunk products above 2.0 g/cm^3 and below 1.3 g/cm^3 are illustrated in Figure 8.8. It can be seen that the partition coefficient above 2.0 g/cm^3 decreases sharply with the decreasing of feed coal size, which leads to a significant increase in impure content in the float products. Furthermore, there is an increase of partition coefficient below 1.3 g/cm^3 with the decreasing of feed coal size, and thus the loss of clean coal in the sink products increases as the feed coal size decreases. This could be attributed to the bubbling behavior and back-mixing of medium particles in the ADMFB (Luo and Chen, 2001; Mohanta *et al.*, 2011), which may prevent the efficient separation of smaller coal particles. As a consequence, the efficiency of coal separation in ADMFB decreases with decreasing feed coal size, not only because of the probable error and separation density increase, but also due to the variation of partition coefficients above 2.0 g/cm^3 and below 1.3 g/cm^3 .

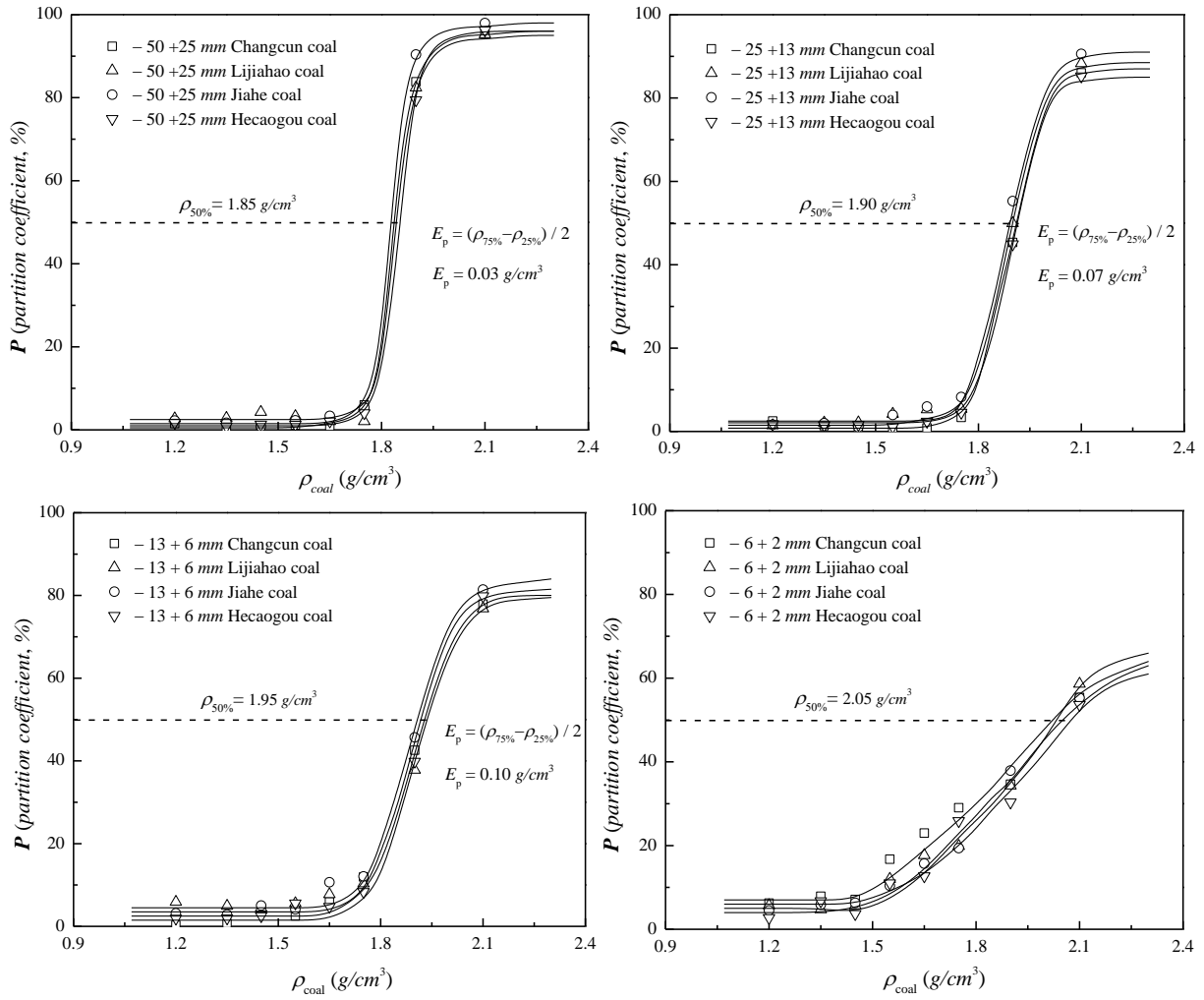


Figure 8.6 The effect of feed coal size on partition curves of sunk products.

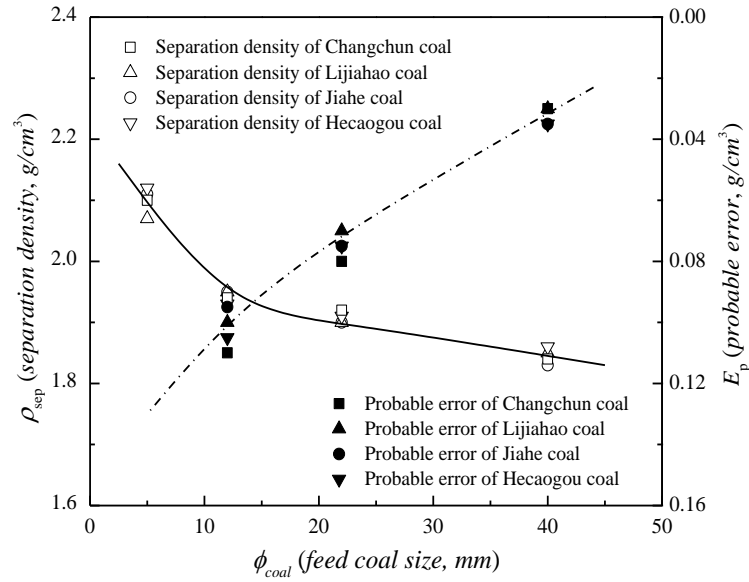


Figure 8.7 The effect of feed coal size on the separation density and probable error.

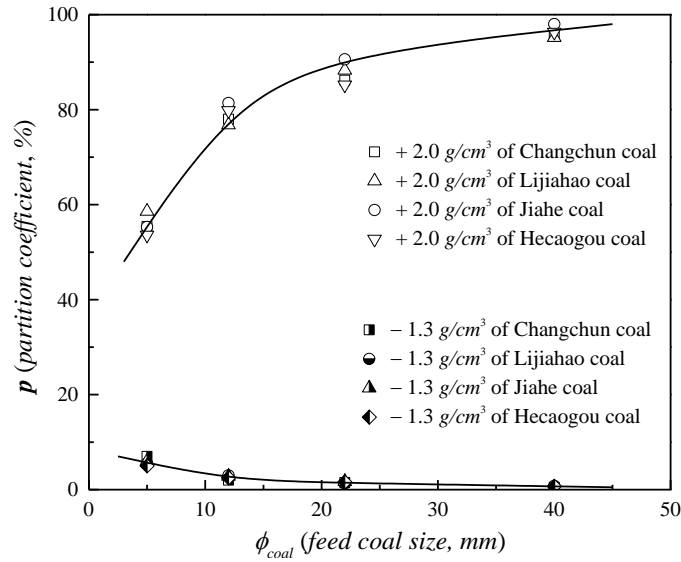


Figure 8.8 The partition coefficients of + 2.0 g/cm³ and - 1.3 g/cm³ coal as a function of feed coal size.

8.3.3 The effect of particle composition of binary mixtures

The particle composition of medium material is the key factor that influences the bed density, which may further affect the effectiveness of dry coal beneficiation in the ADMFB. In this study, the comparison of the separation performance of Hecaogou coal in the semi-industrial ADMFB with two types of binary medium samples was experimentally investigated. The partition curves of the sunk products after coal separation by the ADMFB with binary medium A and B are shown in Figure 8.9, and the corresponding separation density and probable error are summarized in Figure 8.10. As can be observed that the separation density decreases approximately 0.05 g/cm^3 using binary medium B comparing to binary medium A for all size fractions of Hecaogou coal, whereas the probable error increases by 0.03 g/cm^3 . This may be explained by an increase in non-uniform axial distribution of binary mixtures of solid particles with increasing fine coal content (Luo and Chen, 2001; Tang et al., 2009). It should be mentioned that the mass fractions of fine coal particles in binary medium A and B are 12.08% and 20.88%, respectively. Therefore, it can be concluded that the lower separation density can be achieved by further increasing the fraction of fine coal particles in the medium material, while compromising the increased probable error.

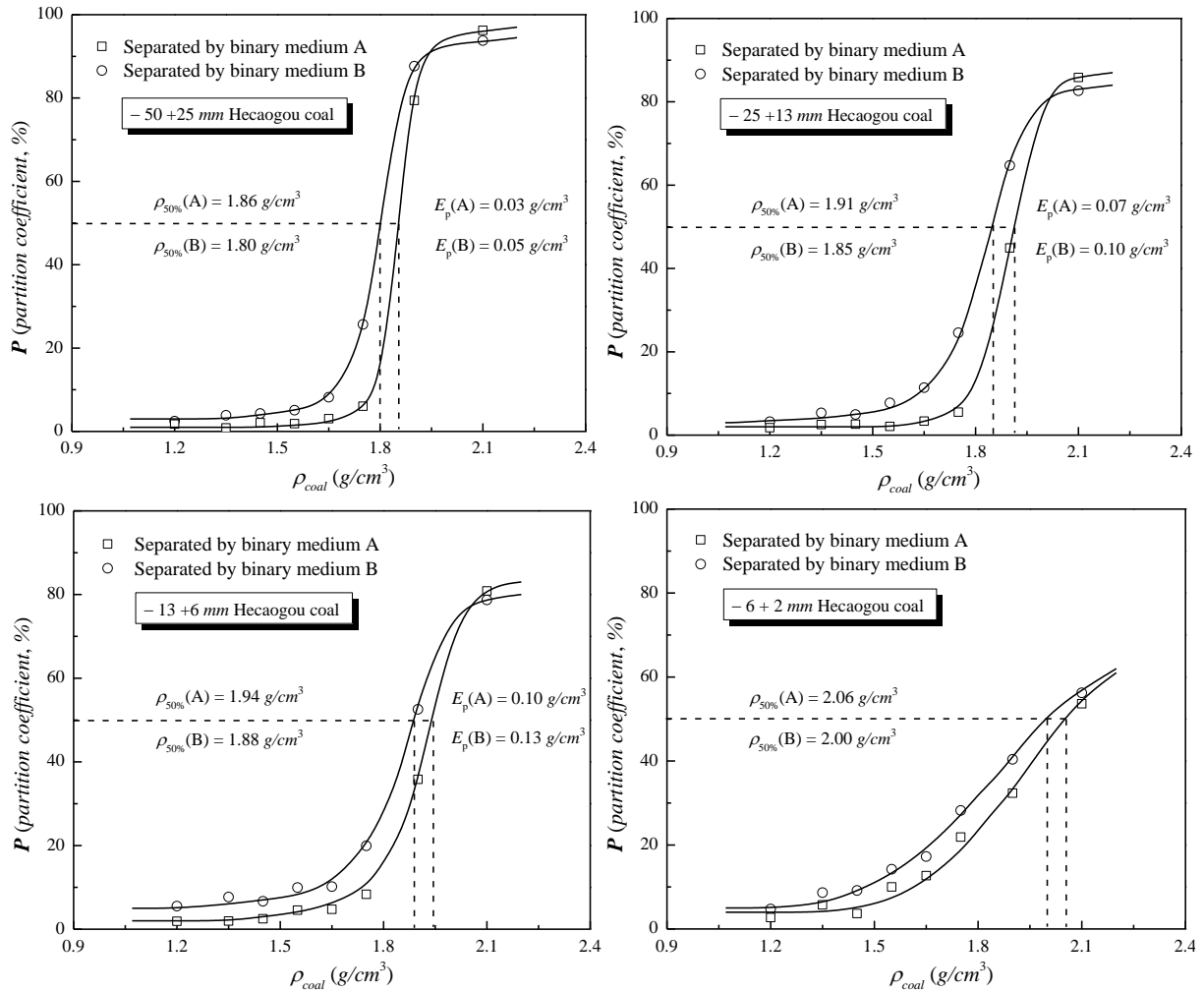


Figure 8.9 The partition curves of sunk products of Hecaogou coal by two types of binary mixtures of solid particles.

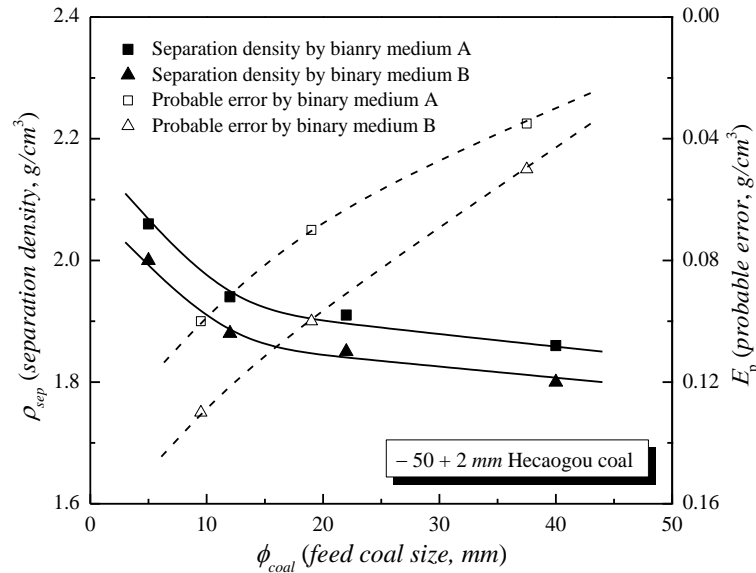


Figure 8.10 Comparison of the separation density and probable error by two types of binary mixtures of solid particles.

8.3.4 The performance of coal beneficiation in semi-industrial ADMFB

The ash content and calorific value are important criteria that reflect the quality of coal products and are generally used to evaluate the performance of the coal beneficiation process. Figure 8.11 shows the ash content variation of different coal samples after dry separation by the semi-industrial ADMFB. As can be observed that, for $-50 + 6$ mm coarse coal, there is a significant increase of ash content in the sink products; as a result, the ash content of float products decreases significantly. To be exact, higher ash contents, around 59.6 ~ 89.1%, can be achieved in the sink products of coarse coal. However, for $-6 + 2$ mm fine coal, the increase of ash content in sink products is comparatively less than that of coarse coal, and thus the decrement of ash content in the float products is very small. In detail, the ash contents of 39.8 ~ 46.8% are obtained in the sink products of fine coal. Moreover, it can also be seen from Fig. 8 that the decrement of ash content in the float products of Changcun and Lijiahao coals is less than that of Jiahe and Hecaogou coals, which may be explained with an increase in mass fraction of ash-forming matters in the Jiahe and Hecaogou coals.

Figure 8.12 shows the calorific concentration of different coal samples after dry separation by the semi-industrial ADMFB. For $-50 + 6$ mm coarse coal, the calorific value of the sink

products decreases dramatically, and a significant calorific concentration appears in the float products. For $-6 + 2$ mm fine coal, the decrement of calorific value in sink products is relatively less than that of the coarse coal, and thus the calorific value in float products is very close to raw coal. Furthermore, the calorific concentration in the float products of Changcun and Lijiahao coals is less than that of Jiahe and Hecaogou coals, which may also be explained by an increase in mass fraction of ash-forming matters in the Jiahe and Hecaogou coals. Consequently, efficient coal beneficiation can be achieved for $-50 + 6$ mm coarse coal in the semi-industrial ADMFB, whereas the beneficiation of $-6 + 2$ mm fine coal is relatively less efficient. This is reasonable; because the sharpness of partition curves of $-6 + 2$ mm fine coal is very small compared to that of $-50 + 6$ mm coarse coal as can be seen from Figure 8.6.

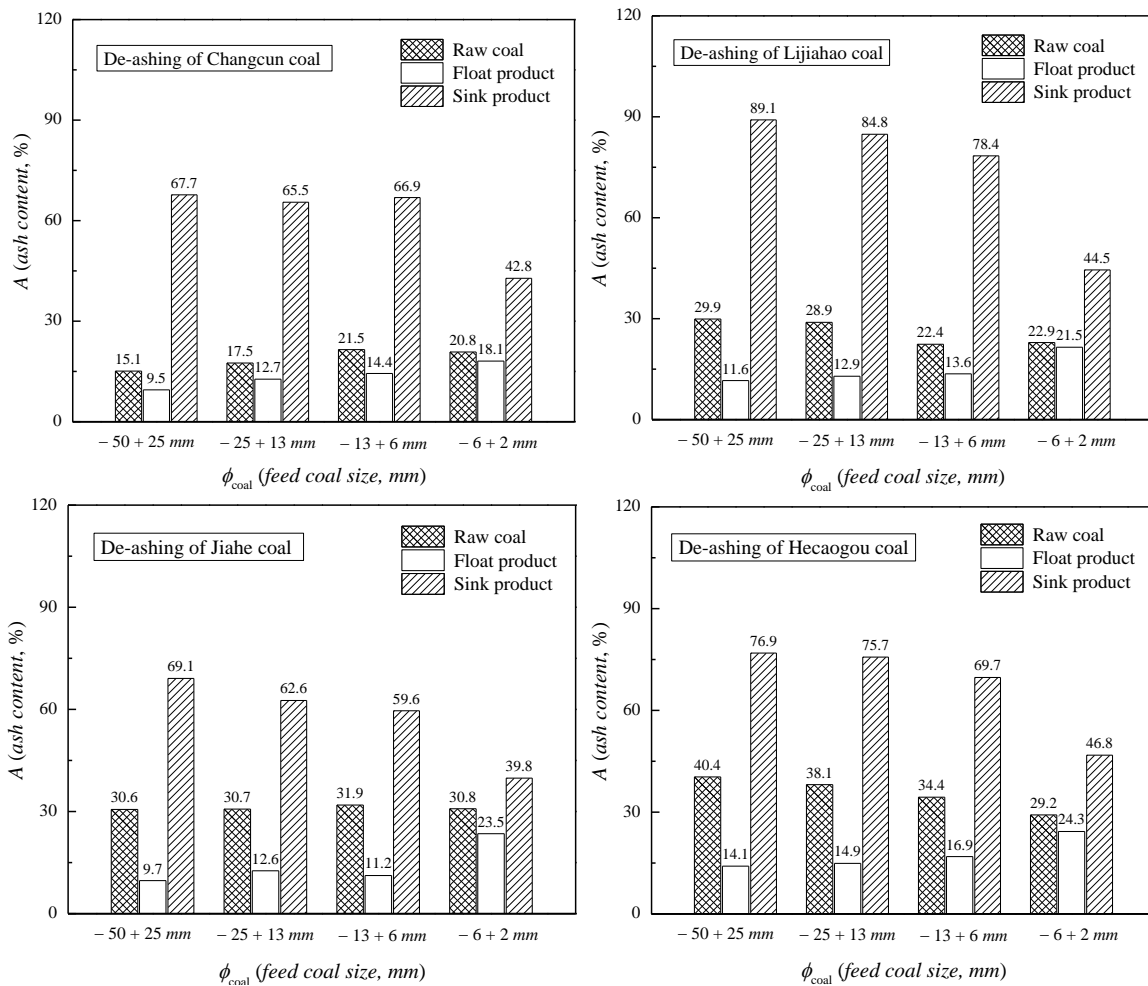


Figure 8.11 The variation of ash content of different feed coals with different coal size.

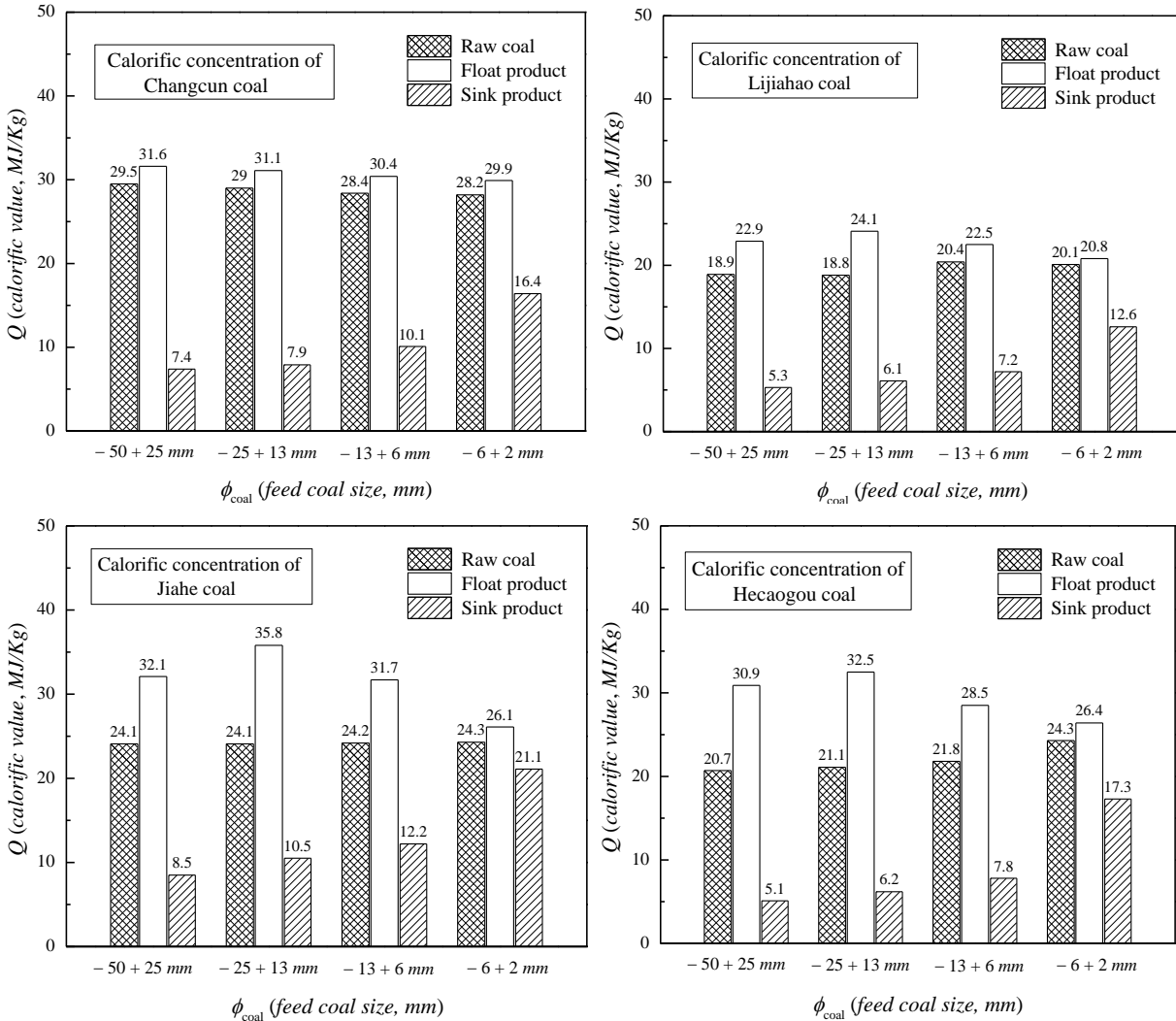


Figure 8.12 The variation of calorific value of different feed coals with different coal size.

8.3.5 Comparison with the literature data

Summary of data available in literature for dry coal beneficiation by the batch or continuous laboratory ADMFB is shown in Table 8.5 in comparison to the experimental results obtained from the present work by the semi-industrial ADMFB system. As can be observed that the effectiveness of coal separation in the semi-industrial ADMFB is almost consistent with those separation results in the literature. In detail, the general trend of decreasing separation efficiency (including the increasing of separation density and probable error) with decreasing feed coal size is verified (Firdaus et al., 2012; Oshitani et al., 2013; Franks et al., 2013; Franks et al., 2015). It is also confirmed that the separation density can be adjusted by varying the particle composition

of medium material (Luo and Chen, 2001; Tang et al., 2009). However, for the binary medium of magnetite and fine coal particles, the lower separation density can be achieved by further increasing the fraction of fine coal with the expense of the increased probable error. Additionally, the separation density in the semi-industrial ADMFB is relatively higher than that in the laboratory devices, which may be due to the influence of continuous coal separation processing. In conclusion, the sink coal products with extremely high ash content and low calorific value can be achieved by ADMFB; as a result, the quality of float coal products will be upgraded significantly, which leads to a good coal beneficiation performance.

Table 8.5 Literature summary of dry coal beneficiation by different Air Dense Medium Fluidized Bed systems.

Reference	Bed cross-section (cm)	Medium materials			Feed coal		H (cm)	ρ_{sep} (g/cm ³)	E_p (g/cm ³)	Ash separation performance	
		Type	ρ_p (kg/m ³)	d_p (um)	Type	d_p (mm)					
Choung J. <i>et al.</i> , 2006	4	Magnetite	4600	45~106	Sub-bituminous	3.35~5.6	5	1.50	0.03	Feed coal = 14%, 21% Clean coal = 6%, 7% Reject = 86%, 54%	
				45~75		1.00~3.35	2.6	-	-		
				45~53		0.42~1.00	2.6	1.77	0.10		
Oshitani J. <i>et al.</i> , 2004	30×22	Zircon	4650	90~250	Coal	20~45	20	1.55	0.05	Feed coal = 24.6%, Clean coal = 10% Reject = 60%	
		CaCO ₃	2680	300~425				1.47	0.04		
								1.42	0.05		
Firdaus M. <i>et al.</i> , 2012	29	Zircon	4700	238	Bituminous coal	10~14	15	1.46	0.19	Feed coal = 22% Clean coal = 9.94% Reject = 70%	
								14~20	1.59		0.01
								14~20	1.50		0.02
								20~25	1.55		0.02
Sahu A. K. <i>et al.</i> , 2011	150×10.8	Magnetite	4800	0.5~110	Noncoking	6~25	40.3	1.72	0.08	Feed coal = 40% Clean coal = 32~35% Reject = 48~61%	
								25~31	1.68		0.12
Azimi E. <i>et al.</i> , 2017	240×98	Silica	2600	355~500	Sub-bituminous	2.8~5.6	20	-	-	Feed coal = 31.29%, 30.14%, Clean coal = 20.37%, 22.09% Reject = 73.32%, 77.98%	
								5.6~13.2	20		-
Luo Z. F. <i>et al.</i> , 2001	500×200	Magnetite	4600	0~500	Coal	6~50	31.5	1.44	0.06	Feed coal = 45.57%, 39.11% Clean coal = 18.21%, 16.35% Reject = 63.81%, 67.5%	
		Fine coal	1500	0~1000				1.76	0.05		

8.4 Conclusion

Dry coal beneficiation by the semi-industrial ADMFB with binary medium of magnetite and fine coal particles was experimentally investigated for four different coals from Changcun, Lijiahao, Jiahe, and Hecaogou Coal Mines in China. The experimental results demonstrate that the performance of coal separation in the ADMFB is not sensitive to the excess gas velocity at the relatively low flow rates, and thus the range of operating gas velocity can be comparatively wide to maintain consistent coal beneficiation, rather than an optimal operating gas velocity. It is also found that the separation density and probable error increase with the decreasing of feed coal size, regardless the types of feed coal, indicating that the separation efficiency decreases as the feed coal size decreases. Moreover, the lower separation density in the ADMFB can be achieved by further increasing the fraction of fine coal particles in the medium materials, but with compromise of the decrease in separation accuracy. The separation results show that, for $-50 + 6$ mm coarse coal, there are considerable increase of ash content and decrease of calorific value in the sink coal products, and thus the quality of float coal products can be upgraded significantly, whereas the beneficiation of $-6 + 2$ mm fine coal is relatively less efficient.

Nomenclature

d_p	particle diameter, m
E_p	probable error, kg/m^3
H	fluidized bed height, m
P	partition coefficient, %
Q	calorific value, MJ/kg
U_g	superficial gas velocity, m/s
U_{mf}	minimum fluidization velocity, m/s
$wt.$	weight fraction, %

Greek letters

ρ_p	particle density, kg/m^3
ρ_{sep}	separation density, kg/m^3
ρ_{coal}	coal density, kg/m^3
$\rho_{50\%}$	density at the partition coefficient of 50%, kg/m^3
\emptyset_{coal}	feed coal size, m

Acknowledgements

The authors are grateful to the financial support by Natural Science and Engineering Research Council of Canada (NSERC), China Scholarship Council (CSC), and National Natural Science Foundation of China.

References

<http://www.bp.com/content/dam/bp/en/corporate/pdf/energy-economics/statistical-review-2017/bp-statistical-review-of-world-energy-2017-full-report>.

Azimi E., Karimipour S., Xu Z. H., Szymanski J., Gupta R., 2017. Statistical analysis of coal beneficiation performance in a continuous air dense medium fluidized bed separator. *Int. J. Coal Prep. Util.* 37, 12-32.

Chen Q. R., Wei L. B., 2003. Coal dry beneficiation technology in China: the state-of-the-art. *China Part. 1*, 52-56.

Chen Q. R., Yang Y. F., 2003. Development of dry beneficiation of coal in China. *Coal Prep.* 23, 3-12.

Chikerma P., Moys M., 2012. Effects of particle size, shape, and density on the performance of an air fluidized bed in dry coal beneficiation. *Int. J. Coal Prep. Util.* 32, 80-94.

Choung J., Mak C., Xu Z. H., 2006. Fine coal beneficiation using an air dense medium fluidized bed. *Coal Prep.* 26, 1-15.

Dotson J. M., 1959. Factors affecting density transients in a fluidized bed. *AIChE J.* 5, 169-174.

Dwari R. K., Hanumantha R. K., 2007. Dry beneficiation of coal – a review. *Miner. Process. Extr. Metall. Rev.* 28, 177-234.

Firdaus M., Oshea J. P., Oshitani J., Franks G. V., 2012. Beneficiation of coarse coal ore in an air-fluidized bed dry dense-medium separator. *Int. J. Coal Prep. Util.* 32, 276-289.

Franks G. V., Firdaus M., Oshitani J., 2013. Copper ore density separations by float/sink in a dry sand fluidized bed dense medium. *Int. J. Miner. Process.* 121, 12-20.

Franks G. V., Forbes E., Oshitani J., Batterham R. J., 2015. Economic, water and energy evaluation of early rejection of gangue from copper ores using a dry sand fluidized bed separator. *Int. J. Miner. Process.* 137, 43-51.

Fraser T., 1926. Artificial storm of air-sand floats coal on its upper surface, leaving refuse to sink. *Coal Age.* 29, 325-327.

- Korolev V. N., Syromyatnikov N. I., Tolmachev E. M., 1971. Structure of a fixed and a fluidized bed of granular material near an immersed surface (wall). *J. Eng. Phys.* 21, 1475-1478.
- Lockhart N. C., 1984. Dry beneficiation of coal. *Powder Technol.* 40, 17-42.
- Lohn P., 1971. Fluidized bed heavy medium separation – A modern dry separation procedure. *Aufbereitung. Technik.* 3, 140-147.
- Luo Z. F., Chen Q. R., 2001. Effect of fine coal accumulation on dense phase fluidized bed performance. *Int. J. Miner. Process.* 63, 217-224.
- Luo Z. F., Chen Q. R., 2001. Dry beneficiation technology of coal with an air dense-medium fluidized bed. *Int. J. Miner. Process.* 63, 167-175.
- Luo Z. F., Zhu J. F., Tang L. G., Zhao Y. M., Guo J., Zuo W., Chen S. L., 2010. Fluidization characteristics of magnetite powder after hydrophobic surface modification. *Int. J. Miner. Process.* 94, 166-171.
- Mizrach A., Zaltzman A., Manor G., Nir Z., 1984. Gravitational motion of spheres in a fluidized bed. *Trans. A. S. A. E.* 6, 1674-1678.
- Mohanta S., Chakraborty S., Meikap B. C., 2011, Influence of coal feed size on the performance of air dense medium fluidized bed separator used for coal beneficiation. *Ind. Eng. Chem. Res.* 50, 10855-10871.
- Mohanta S., Rao C. S., Daram A. B., Chakraborty S., Meikap B. C., 2013. Air dense medium fluidized bed for dry beneficiation of coal: technological challenges for future. *Part. Sci. Technol.* 31, 16-27.
- Nguyen T. H., Grace J. R., 1978. Forces on objects immersed in fluidized beds. *Powder Technol.* 19, 255-264.
- Oshitani J., Kajimoto S., Yoshida M., Franks G. V., Kubo Y., Nakatsukasa S., 2013. Continuous float-sink density separation of lump ore using a dry sand fluidized bed dense medium. *Adv. Powder Technol.* 4, 468-472.
- Oshitani J., Tani K., Takase K., Tanaka Z., 2004. Fluidized bed medium separation (FBMS) for dry coal cleaning. *J. Society. Powder Technol. Japan.* 41, 334-341.

- Rees A. C., Davidson J. F., Dennis J. S., Hayhurst A. N., 2005. The rise of a buoyant sphere in a gas-fluidized bed. *Chem. Eng. Sci.* 60, 1143-1153.
- Rios G. M., Tran K. D., Masson H., 1986. Free object motion in a gas fluidized bed. *Chem. Eng. Commun.* 47, 247-272.
- Sahan R. A., Kozanoglu B., 1997. Use of an air fluidized bed separator in a dry coal cleaning process. *Energy Comers. Mgmt.* 38, 269-286.
- Sahu A. K., Biswal S. K., Parida A., 2009. Development of air dense medium fluidized bed technology for dry beneficiation of coal – a review. *Int. J. Coal Prep. Util.* 29, 216-241.
- Sahu A. K., Biswal S. K., Parida A., 2011. Stability study of an air dense medium fluidized bed separator for beneficiation of high-ash Indian coal. *Int. J. Coal Prep. Util.* 31, 127-148.
- Sekito T., Matsuto T., Tanaka N., 2006. Application of a gas-solid fluidized bed separator for shredded municipal bulky solid waste separation. *Waste Manage.* 26, 1422-1429.
- Sekito T., Tanaka N., Matsuto T., 2006. Batch separation shredded bulk waste by gas-solid fluidized at laboratory scale. *Waste Manage.* 26, 1246-1252.
- Tang L. G., Zhao Y. M., Luo Z. F., Liang C. C., Chen Z. Q., Xing H. B., 2009. The effect of fine coal particles on the performance of gas-solid fluidized beds. *Int. J. Coal Prep. Util.* 29, 265-278.
- Toomey R. D., Johnstone H. F., 1952. Gaseous fluidization of solid particles. *Chem. Eng. Process.* 48, 220-226.
- Van Houwelingen J. A., De Jong T. P. R., 2004. Dry cleaning of coal: review, fundamentals and opportunities. *Geol. Belgica.* 7, 335-343.
- Wei L. B., Chen Q. R., Zhao Y. M., 2003. Formation of double-density fluidized bed and application in dry coal beneficiation. *Coal Prep.* 23, 21-32.
- Weintraub M., Deurbrouck A. W., Thomas R. H., 1979. Dry-cleaning coal in a fluidized bed medium. *RI-PMTC-4-79.*
- Yoshida M., Nakatsukasa S., Nanba M., Gotoh K., Zushi T., Kubo Y., Oshitani J., 2010. Decrease of Cl contents in waste plastics using a gas-solid fluidized bed separator. *Adv. Powder Technol.* 21, 69-74.

Yoshida M., Oshitani J., Tani K., Gotoh K., 2011. Fluidized bed medium separation (FBMS) using the particles with different hydrophilic and hydrophobic properties. *Adv. Powder Technol.* 22, 108-114.

Zaltman A., Feller R., Mizrach A., Schmilovitch Z., 1983. Separation potatoes from clods and stones in a fluidized bed medium. *Trans. A. S. A. E.* 26, 987-990.

Zaltman A., Schmilovitch Z., Mizrach A., 1985. Separating flower bulbs from clods and stones in a fluidized bed. *Can. Agric. Eng.* 27, 63-67.

Zaltman A., Verma B. P., Schmilovitch Z., 1987. Potential of quality sorting fruits and vegetables using fluidized bed medium. *Trans. A. S. A. E.* 30, 823-831.

Zinov'ev Y. I., 1976. Effective density of a fluidized bed. *J. Eng. Phys.* 31, 1279-1284.

Zhao Y. M., Liu J. T., Wei X. Y., Luo Z. F., Chen Q. R., Song S. L., 2011. New progress in the processing and efficient utilization of coal. *Min. Sci. Technol.* 21, 547-552.

Zhao Y. M., Tang L. G., Luo Z. F., Liang C. C., Xing H. B., Duan C. L., Song S. L., 2012. Fluidization characteristics of a fine magnetite powder fluidized bed for density-based dry separation of coal. *Sep. Sci. Technol.* 47, 2256-2261.

CHAPTER 9

CONCLUSIONS AND RECOMMENDATIONS

As a newly developed method, the Air Dense Medium Fluidized Bed (ADMFB) with binary mixtures for efficient dry coal beneficiation has been proposed and investigated in this work. Based on the experimental results so far, conclusions for the present study and recommendations for the future work are addressed as following.

9.1 Conclusions

The fluidization characteristics of the Air Dense Medium Fluidized Bed system containing single or binary mixtures of solid particles for dry coal beneficiation have been studied theoretically and experimentally, with the consideration of minimum fluidization velocity, two-phase theory of fluidization, mixing and segregation behavior, and bed density distribution. The efficient coal dry beneficiation has been successfully verified in a semi-industrial ADMFB system with binary mixtures of magnetite and fine coal particles as medium materials.

Minimum fluidization velocities of binary mixtures of magnetite and sand/gangue/coal particles were tested individually. When the volume fraction of magnetite is above 50%, the addition of sand/gangue/coal particles that is coarser than (or equal to) magnetite particles would not appreciably change the minimum fluidization velocity of binary mixtures. On the contrary, the minimum fluidization velocities varied significantly when the volume fraction of magnetite was below 50%. A new equation (Eq. (3.9)) was derived for estimating the minimum fluidization velocity of binary mixtures by extending the correlation proposed by Cheung *et al.* This modified equation only requires the additional knowledge of particle size ratio which is a basic parameter for characterizing a binary mixture. Almost all available experimental data were used to test the validity of this modified correlation, and it gave an overall standard deviations of 17.85% and 7.14% for the experimental data in the literature and this work, respectively.

The influence of bed inventory on the minimum fluidization velocity was carefully studied in an ADMFB due to the consideration of industrial practices. It was found that the measured

minimum fluidization velocities increased with increasing bed inventory regardless of the type of solid particles used. A new correlation (Eq.(4.18)) was derived for predicting the minimum fluidization velocity considering the bed inventory effect by extending the Wen and Yu equation. The proposed correlation only requires the knowledge of Archimedes number (Ar) and the bed pressure drop (ΔP), which can be easily obtained from the calculation of the particle bulk density and the static bed height before fluidization. This extended Wen and Yu equation is shown to well predict the minimum fluidization velocity reported by previous researchers and can be used to estimate the minimum fluidization velocity for both single and binary mixtures of solid particles for all practical purposes.

The understanding of the two-phase theory is of great significance for the design and operation of ADMFB systems. In this work, the correction factor Y for the two-phase theory model was extensively studied for Geldart Group B and D particles which was generally used as medium particles in ADMFB systems. Experimental evidences indicated that the Y value increases with decreasing particle size or density and with the increase of excess gas velocity. An equation (Eq.(5.14)) was derived to predict the parameter Y for Geldart Group B and D particles. It requires the knowledge of Archimedes number (Ar) and the excess gas velocity ($U - U_{mf}$), and gives an overall standard deviation of 19% for almost all available experimental data. The proposed correlation could lead to a modified two-phase theory model (Eq. (5.15)), which can be used to accurately estimate the distribution of gas flow between the dense and bubble phases in the bubbling fluidized bed with Geldart Group B and D particles.

The evaluation of the mixing and segregation behavior for binary mixtures of medium particles in an ADMFB was carried out, and the results were interpreted in terms of axial solids distribution. It was observed that the particle segregation of binary mixtures becomes more evident with the increase of particle density ratio, and the mixing and segregation behavior is less sensitive to the changes in particle size ratio. Increasing both the excess gas velocity in a relatively lower range and the initial bed height above 15 *cm* did not cause any significant change in the mixing and segregation pattern for binary systems, which may give rise to broad conditions for the ADMFB operation. To achieve the bed density adjustment, a lower mass fraction of fine coal particles (< 10%) which will result in almost perfect mixing pattern is

recommended for raw coal dry beneficiation, due to the fine coal particles automatically being generated during the fluidized bed separation process.

The distributions of bed density in an ADMFB system with both single and binary mixtures of medium particles were theoretically and experimentally studied. The experimental evidences revealed that a comparable lower density was obtained at the bottom of fluidized bed with various types of single particles, whereas the bed density at the upper part remained almost consistent. The average bed density decreased with the increasing of excess gas velocity, but the influence of excess gas velocity was found to have definite effects on the tendency of axial density distribution. Moreover, the particle composition of binary mixtures was found to have a significant influence on the bed density distribution due to the variation of axial particle distribution of solid particles. An new equation (Eq.(7.11)) was derived to predict the distribution of bed density in the ADMFB based on the modified two-phase theory proposed in this work. The proposed correlation was verified successfully by various single and binary mixtures of Geldart Group B/D particles at different excess gas velocities.

Dry coal beneficiation performed by a semi-industrial ADMFB system with a binary medium of magnetite and fine coal particles was experimentally studied for four different types of raw coals from Changcun, Lijiahao, Jiahe, and Hecaogou Coal Mines in China. The results demonstrated that the performance of coal beneficiation in the ADMFB is not very sensitive to the excess gas velocity at the relatively low flow rates, and thus the range of operating gas velocity can be comparatively wide to maintain consistent coal beneficiation, rather than an optimal operating gas velocity. The separation density and probable error were found to increase with the decreasing of feed coal size, regardless the types of feed coal, indicating that the separation efficiency decreases as the feed coal size decreases. A lower separation density in the ADMFB could be achieved by further increasing the fine coal fraction in medium materials, but with compromise to the separation accuracy. Moreover, the semi-industrial results showed that, for 6 ~ 50 mm coarse coal, there were considerable increase of ash content and decrease of calorific value in gangue products, and thus the quality of clean coal products can be upgraded significantly, whereas the beneficiation of 2 ~ 6 mm fine coal was relatively less efficient. Finally, the newly developed technology of ADMFB with binary mixtures for efficient dry coal beneficiation has been successfully proposed and verified in this work.

9.2 Recommendations

This dissertation provides comprehensive experimental results and theoretical understanding on the newly developed technology of the Air Dense Medium Fluidized Bed with binary mixtures of medium particles for efficient dry coal beneficiation. However, there are still some areas where further research is required.

The current study only focuses on the ADMFB with lower bed heights (< 0.5 m), where the gas bubbling and solids movement are relatively stable. Future work can be extended to the ADMFB with a higher bed height to improve the separation efficiency and process capacity, as well as achieve the dry beneficiation of extra-large coal ores (> 50 mm).

Particle properties of medium materials have been shown to play a very important role in determining separation properties of ADMFB systems. Future work with more types of binary mixtures and varying particle size distribution are needed to broaden the knowledge of the particle property effects on the dry gravity separation.

The visualization techniques have been applied to many fluidized bed operations, where the solids distribution and bubbling behavior are relatively stable. In future works, high-speed cameras can be used to detect the mixing and segregation pattern of binary systems, as well as the behavior of coal separation in the ADMFB.

Since the ADMFB with a binary mixture is a general method for dry gravity separation with the advantage of free bed density adjustment, it can be further researched and exploited to various applications including:

- *Dry gravity separation of mineral ores, such as iron, copper, and so on.*
- *Municipal solid waste classification.*
- *Agriculture products cleaning.*
- *Chemical reaction processes optimization.*

Appendix A1. Curves for the improved Cheng Equation.

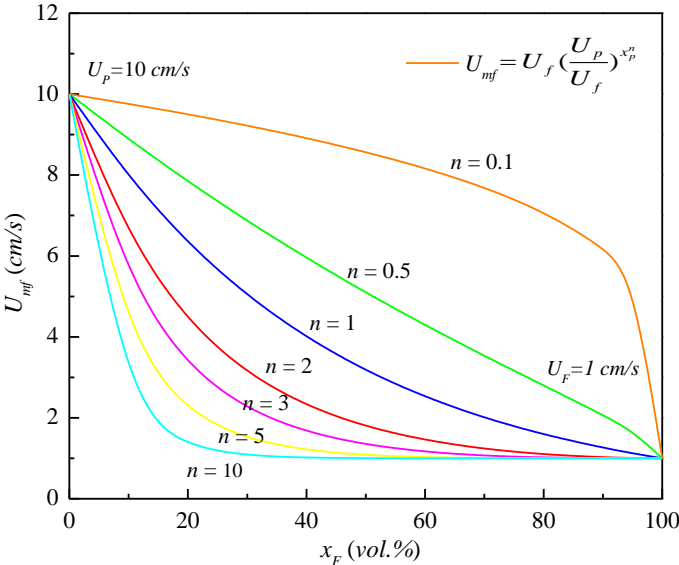


Figure (1). The example curves calculated by Cheng Equation with different n values.

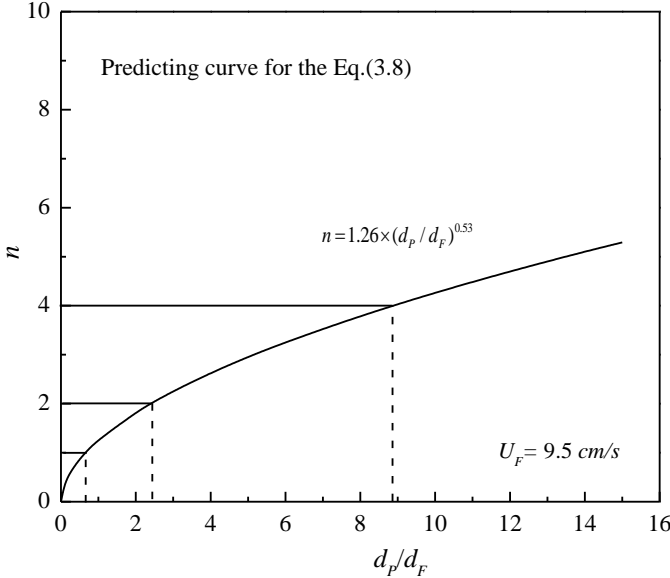


Figure (2). The calculated n value by Eq. (3.8) at different particle diameter ratios.

Appendix A2. Modified two-phase theory for binary mixtures.

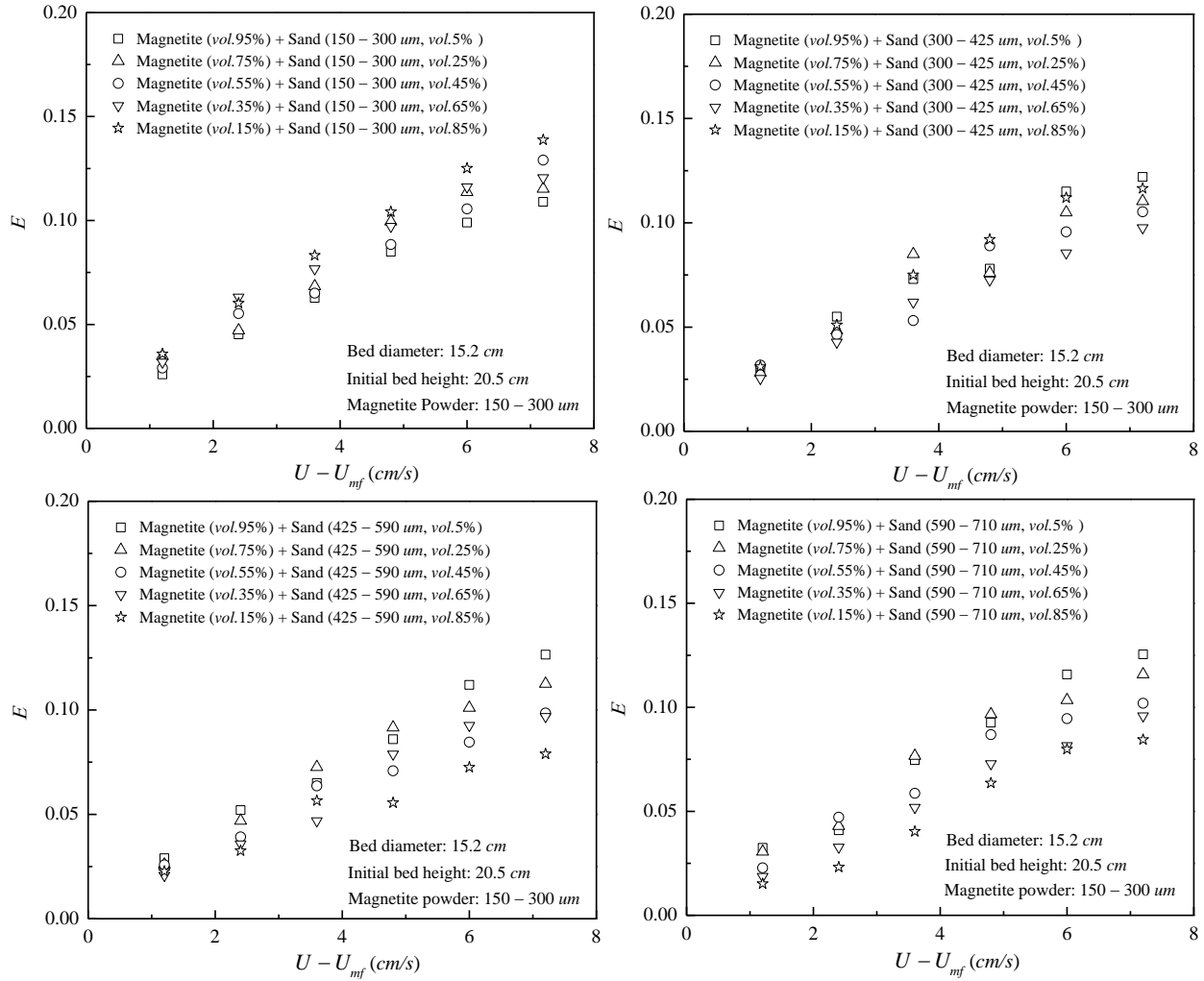


Figure (3). Fluidized bed expansions of MS binary mixtures at different excess gas velocities.

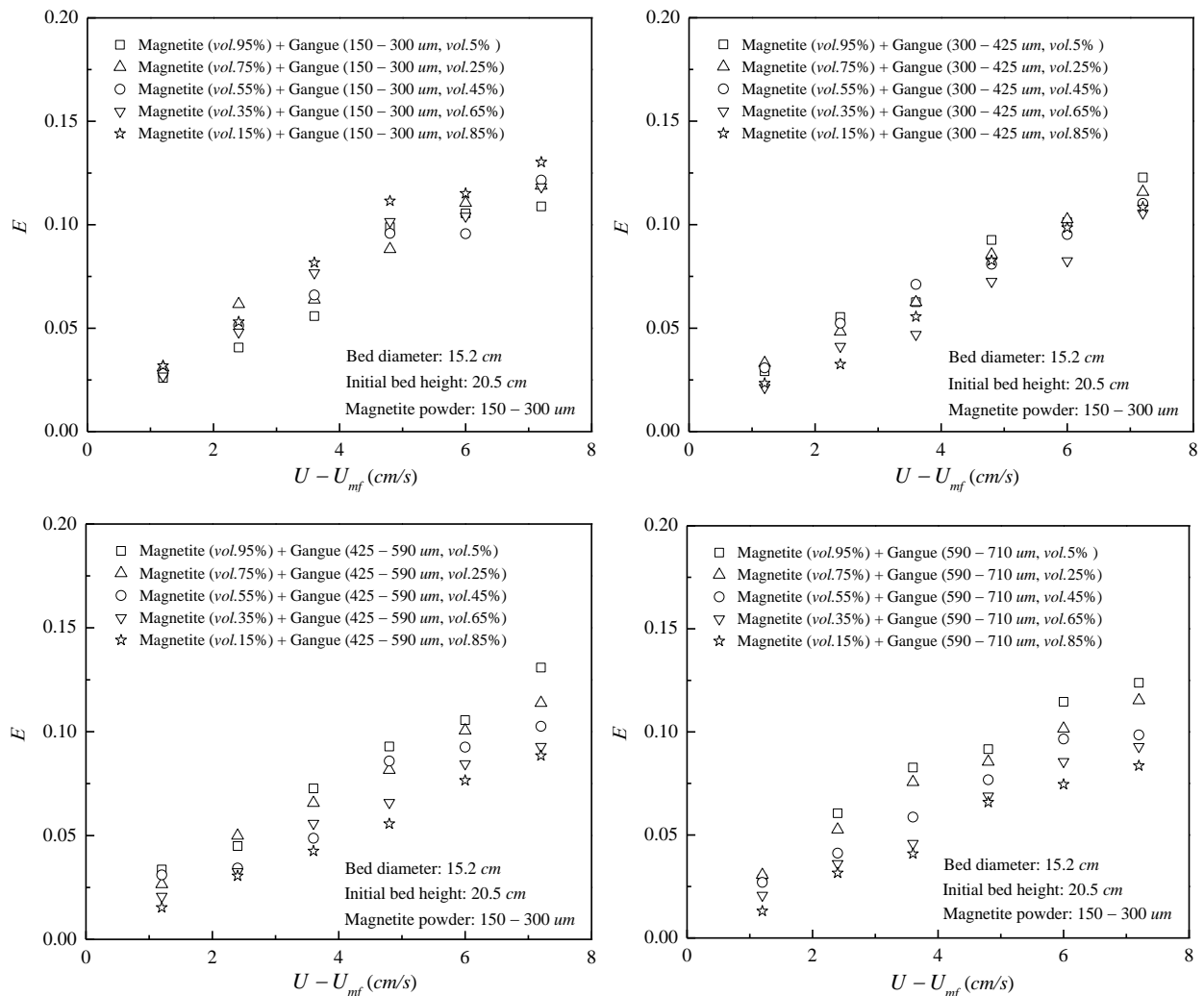


Figure (4). Fluidized bed expansions of MG binary mixtures at different excess gas velocities.

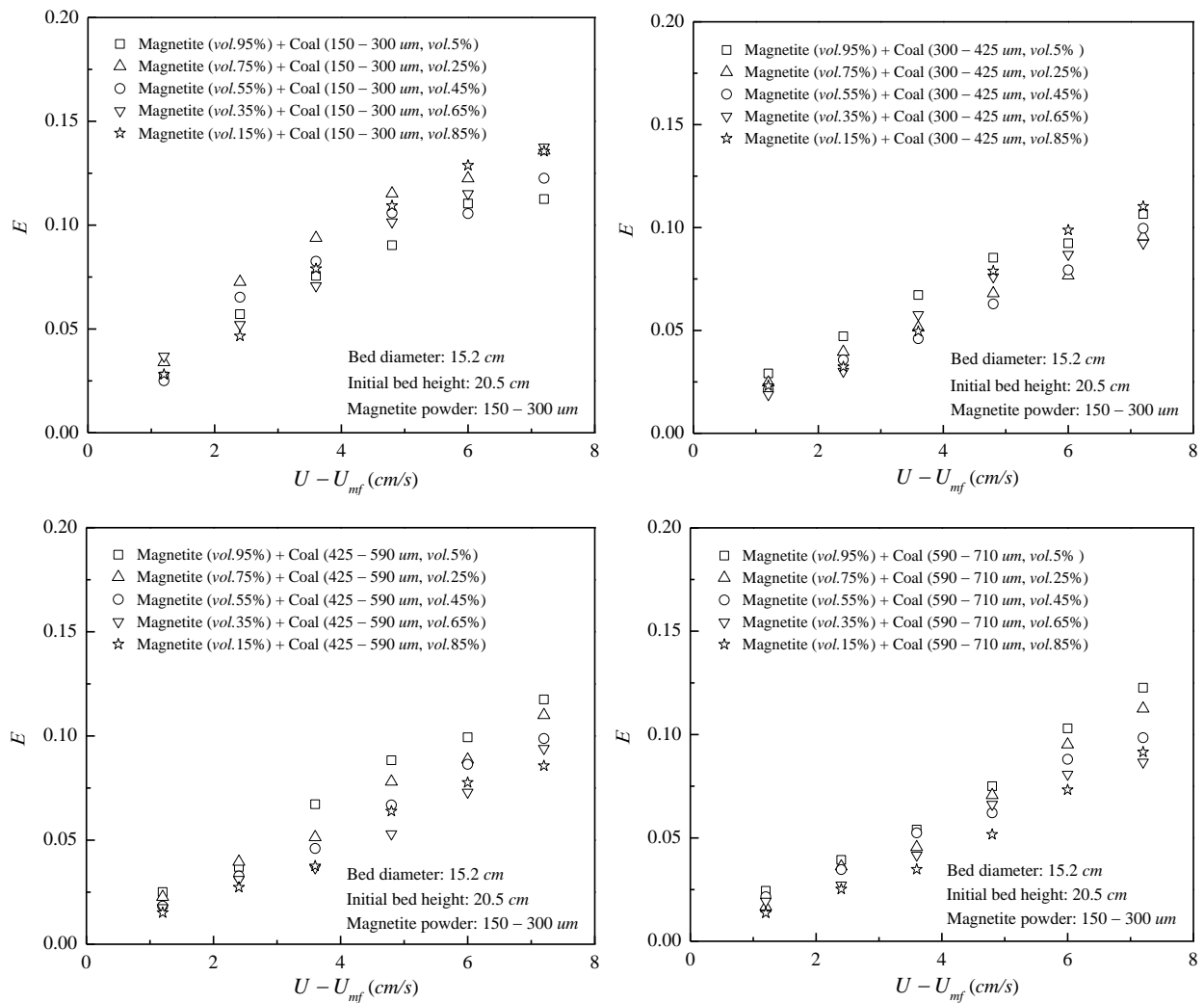


Figure (5). Fluidized bed expansions of MC binary mixtures at different excess gas velocities.

Table (1). Different equations for binary systems.

Eq. (1)	Eq. (2)	Eq. (3)	Eq. (4)
$\rho_m = (\sum (x_i / \rho_i))^{-1}$	$\rho_m = \sum (x_i \rho_i)$	$Re_i = d_i \rho_g U / \mu$	$Re_i = d_i \rho_g U / \mu$
$d_m = (\sum (x_i / d_i))^{-1}$	$d_m = (\sum (x_i / d_i))^{-1}$	$Ar_i = d_i^3 \rho_g (\rho_i - \rho_g) g / \mu^2$	$Ar_i = d_i^3 \rho_g (\rho_i - \rho_g) g / \mu^2$
$\overline{Ar} = d_m^3 \rho_g (\rho_m - \rho_g) g / \mu^2$	$\overline{Ar} = d_m^3 \rho_g (\rho_m - \rho_g) g / \mu^2$	$\overline{Ar} = \sum (x_i Ar_i)$	$\overline{Ar} = (\sum (x_i / Ar_i))^{-1}$
$\overline{Re} = d_m \rho_g U / \mu$	$\overline{Re} = d_m \rho_g U / \mu$	$\overline{Re} = \sum (x_i Re_i)$	$\overline{Re} = \sum (x_i Re_i)$

Table (2). Summary of error analysis of various equations for MS binary mixtures.

Formula	M232-S224	M232-S368	M232-S485	M232-S636	M232-S807
Eq. (1)	8.13	10.65	13.76	19.34	29.55
Eq. (2)	8.27	10.5	13.23	19.01	28.99
Eq. (3)	8.32	10.38	11.06	18.22	23.64
Eq. (4)	8.11	10.57	14.71	22.05	35.75

Table (3). Summary of error analysis of various equations for MG binary mixtures.

Formula	M232-G215	M232-G372	M232-G486	M232-G625	M232-G808
Eq. (1)	10.63	14.66	22.08	19.20	31.66
Eq. (2)	9.95	13.82	20.94	18.44	30.47
Eq. (3)	9.78	13.58	18.78	17.24	24.52
Eq. (4)	10.89	14.08	22.08	20.74	36.15

Table (4). Summary of error analysis of various equations for MC binary mixtures.

Formula	M232-C245	M232-C396	M232-C460	M232-C617	M232-C795
Eq. (1)	11.87	29.93	40.43	37.87	29.55
Eq. (2)	12.55	25.37	35.78	33.66	28.99
Eq. (3)	12.46	26.22	35.25	29.07	23.64
Eq. (4)	11.93	26.55	37.04	35.71	35.75

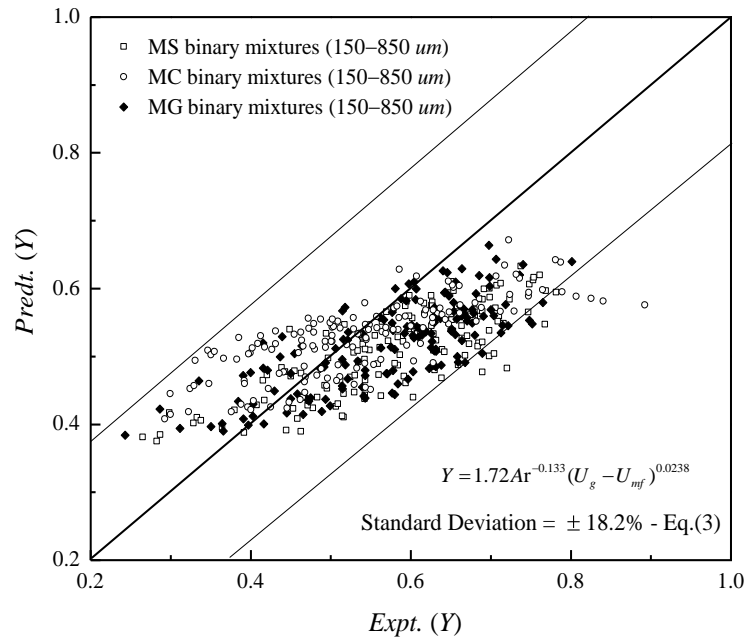


Figure (6). Error analysis of the modified two-phase theory model for binary mixtures of magnetite and sand/gangue/coal particles.

Appendix A3. Flow sheet of industrial ADMFB system.

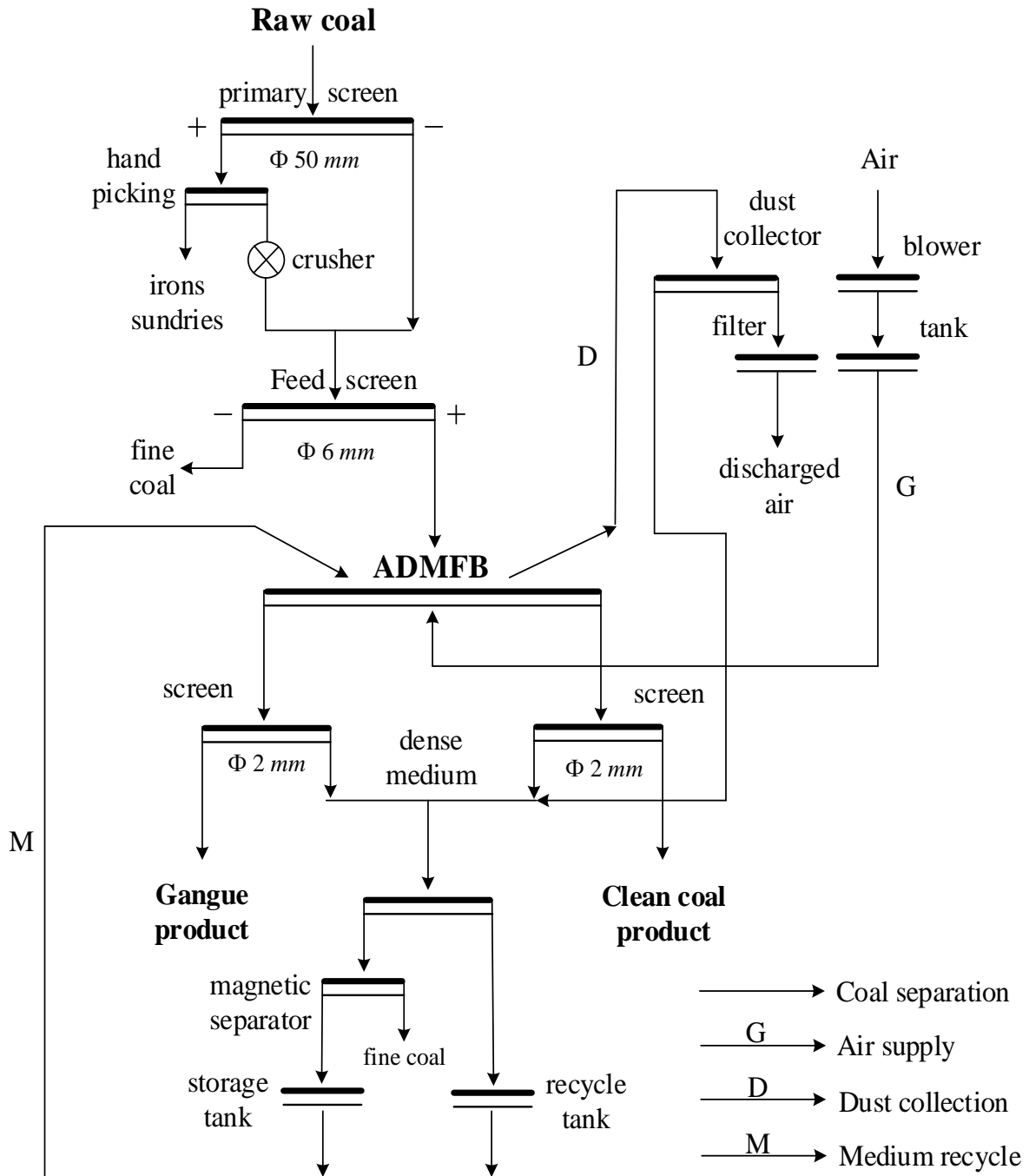


Figure (7). The flow sheet of Air Dense Medium Fluidized Bed for dry coal beneficiation.

Curriculum Vitae

- Name:** Zhijie Fu
- Place of Birth:** Sichuan, China
- Post-secondary Education and Degrees:** Chemical Engineering, University of Western Ontario
London, Ontario, Canada
2015-2019 Ph.D.
- Mineral Processing Engineering, China University of Mining and Technology, Xuzhou, Jiangsu, China
2011-2017 Ph.D.
- Mineral Processing Engineering, China University of Mining and Technology, Xuzhou, Jiangsu, China
2005-2009 B. E. Sc.
- Work Experience:** Research Assistant, Teaching Assistant, University of Western Ontario
2015-2019
- Mineral Engineer, Coal Geological Exploration & Designing Institute of Sichuan Province, China.
2009-2011
- Honors & Awards:** Graduate Student Scholarship, University of Western Ontario
2015-2019
- Chinese Government Scholarship, China
2014
- First Academic Scholarship, China University of Mining and Technology
2012
- Innovation Scholarship, China University of Mining and Technology
2009
- Publications:**
- Zhijie Fu, Jesse Zhu, Shahzad Barghi, Yuemin Zhao, Zhenfu Luo, Chenglong Duan. (2019). Minimum fluidization velocity growth due to bed inventory increase in an air dense medium fluidized bed. *Chemical Engineering Journal*, 359, 1372-1378.

- Zhijie Fu, Jesse Zhu, Shahzad Barghi, Yuemin Zhao, Zhenfu Luo, Chenglong Duan. (2019). Dry coal beneficiation by the semi-industrial air dense medium fluidized bed with binary mixtures of magnetite and fine coal particles. *Fuel*, 243, 509-518.
- Zhijie Fu, Jesse Zhu, Shahzad Barghi, Yuemin Zhao, Zhenfu Luo, Chenglong Duan, (2019). Minimum fluidization velocity of binary mixtures of medium particles in the air dense medium fluidized bed. *Chemical Engineering Science*, 207, 194-201.
- Zhijie Fu, Jesse Zhu, Shahzad Barghi, Yuemin Zhao, Zhenfu Luo, Chenglong Duan (2019). On the two-phase theory of fluidization for Geldart B and D particles. *Powder Technology*, 354, 64-70.
- Zhijie Fu, Jesse Zhu, Shahzad Barghi, Yuemin Zhao, Zhenfu Luo, Chenglong Duan. (2019). Mixing and segregation behavior in an air dense medium fluidized bed with binary mixtures for dry coal beneficiation. *Powder Technology*, POWTEC-S-19-1780. (Under Review)
- Zhijie Fu, Jesse Zhu, Shahzad Barghi, Yuemin Zhao, Zhenfu Luo, Chenglong Duan. (2019). The distribution of bed density in an air dense medium fluidized bed with Geldart Group B and/or D particles. *Minerals Engineering*, MINE-S-19-00585. (Under Review)
- Zhijie Fu, Jesse Zhu, Shahzad Barghi, Yuemin Zhao, Zhenfu Luo, Chenglong Duan. (2019). The two-phase theory of fluidization for binary mixtures of Geldart B/D particles. *Powder Technology*. (To be submitted)
- Zhijie Fu, Jesse Zhu, Shahzad Barghi, Yuemin Zhao, Zhenfu Luo, Chenglong Duan. (2019). On the separation density of the air dense medium fluidized bed for dry gravity separation. *Mineral Engineering*. (To be submitted)
- Zhijie Fu, Yuemin Zhao, Xuliang Yang, Chenglong Duan. (2017) Spontaneous segregation behavior in a vibrated gas-fluidized bed for fine lignite dry cleaning. *Separation Science and Technology*, 52, 2017-2028.
- Zhijie Fu, Yuemin Zhao, Xuliang Yang, Zhenfu Luo, Chenglong Duan. (2016) Fine coal beneficiation via air-dense medium fluidized beds with improved magnetite powders. *International Journal of Coal Preparation and Utilization*, 36, 55-68.